ENVIRONMENTAL IMPACTS RESULTING FROM GOLD MINING TAILINGS STORAGE FACILITIES WITHIN THE WEST RAND AREA IN SOUTH AFRICA

by

Gladness Mmadibakisha Chadi

Student No.: 38780593

submitted in accordance with the requirements for
the degree of

PHD ENVIRONMENTAL MANAGEMENT

in the
COLLEGE OF AGRICULTURE & ENVIRONMENTAL SCIENCES
DEPARTMENT OF ENVIRONMENTAL SCIENCES

at the

UNIVERSITY OF SOUTH AFRICA

Supervisor: Prof. Linda Lunga Sibali

August 2022

DECLARATION

I **Gladness Mmadibakisha Chadi** (Student no: 38780593) hereby declare that the dissertation/thesis title**: Environmental Impacts Resulting from Gold Mining Tailings Storage Facilities Within the West Rand Area in South Africa**, which I hereby submit for the degree of PhD in Environmental Management in the college of Agriculture and Environmental Sciences Department of Environmental Sciences in the University of South Africa, is my own work and has not previously been submitted by me for a degree at this or any other institution.

I declare that the above dissertation is my own work and that all the sources that I have used or quoted have been indicated and acknowledged by means of complete references.

I further declare that I submitted the dissertation to originality checking software and that it falls within the accepted requirements for originality.

I further declare that I have not previously submitted this work, or part of it, for examination at Unisa for another qualification or at any other higher education institution.

Student signature:  Date: 08 March 2022

ACKNOWLEDGEMENTS

First and foremost, I would like to thank God Almighty for letting me through all the difficulties.

To my family, close and extended for their continuous support and understanding. Your prayers gave me strength and kept me going to achieve my childhood dream.

I could not have completed this work without the unwavering support of my supervisor Prof. Linda Lunga Sibali, who has made this work possible through prayers, valuable knowledge, motivation, consistent encouragement and immense knowledge.

I would like to express my appreciation to my previous supervisor Prof. Shadung John Moja for his guidance during the inception of this study.

DEDICATION

This dissertation thesis work is dedicated to my mother **O'lucky 'Olga' Chadi**. Your prayers, love, teachings, undying support and encouragement kept me going. You have taught me to work hard for the things I aspire to achieve, and I can achieve anything in life.

ABSTRACT

Dust from gold mine tailings storage facilities (TSFs) have been noted to be of enormous challenge in the Republic of South Africa (RSA) owing to lack of successful rehabilitation of these structures. In the RSA, many of these communities such as Tudor Shaft Informal Settlement, Pennyville, Braamfischerville, Noordgesig,Diepkloof, Riger Park, Geluksdaal, Riverlea and Stilfontein comprised of historically marginalised ethnic groups (mainly poor black people) living in government-funded houses, informal settlements and retirement homes.

Gold mining process produces waste through three main activities, namely mining, mineral processing and metallurgical extraction, releasing approximately 99% of extracted ore as waste into the environment. The disposal of mine waste, chiefly tailings, has of late, assumed an importance that transcends even the massive volumes of materials produced annually by mining operations. Aside from their significance in strictly engineering terms, TSFs receive intense regulatory attention and public scrutiny.

People living downwind of mine tailings are exposed to the potentially inhalable trace metal and metalloid-bearing dust particles. Active TSF dams rarely have dust problems compared to dormant dams. Wind erosion can transport environmental contaminants such as metals and metalloids, pesticides, and biological pathogens, all of which are typically associated with finer atmospheric particles and tropospheric aerosols. These pollutants get dispersed by wind and lighter dust sized particles persist long enough to pose problems in distant areas, resulting in trans-boundary pollution.

Several cases of dust emanating from tailings dams were previously lodged against mining houses in which mine dust exposures resulted in health impacts on the nearby communities. On windy days, windblown tailings material was reported billowing off the surface of the tailings thereby posing visibility impact within nearby roads.

Many pathological effects may result from gold mine TSFs dust exposures, depending on mineral content, shape, size, chemical composition, levels, and duration of exposure of the dust particle. Human health effects resulting from quartz exposure has been confirmed as one of the main health related concerns in the Witwatersrand gold TSFs dust. Due to their height in physical design structure as well as the colour of tailings material, TSF structures are highly visible from key viewpoints posing significant visual intrusion and blocking clear lines of sight and from unsightly new landmarks.

This study undertakes to assess the environmental risks of public exposure to the dust from gold mine tailings storage facilities within the Witwatersrand Basin. Both analytical and survey methods of dust deposition monitoring and experimental analyses will be employed to establish the precipitant dust and dust characteristic. This will further enable calculations of the extent of TSFs dust exposures of particulate matter.

Dust sampling was conducted as per the American Society for Testing and Materials (ASTM D1739 1970) Standard Method for Collection and Analysis of Dust Fallout" (settleable particulates deposition dust) and several instruments were used to obtain to reflected results. Results of one-way ANOVA Test as per Table 4.15 above shows

a correlation between TSF height and distance at which the particle travelled before reaching the ground confirmed a Welch P-value of 0.118, in which P-value > 0.005.

Main finding of this study with regards to health exposure perspective is that even though most learners (70%) reside in formal housing made up of bricks and cement, they get exposed to dust from mainly mine TSF and vehicular movement as they spend time playing outside. This was confirmed by a strong association between dust and time child spend outside playing.

Keywords: Environmental impacts, gold mine tailings storage facilities, dust, visual impacts, human health, West Rand area.

Contents

LIST OF FIGURES

LIST OF TABLES

LIST OF EQUATIONS

GLOSSARY

%	Percentage
° C	Degrees Celsius
µl	Micro litre
AAS	Atomic absorption spectroscopy
AGA	AngloGold Ashanti
AMD	Acid mine drainage:
ASTM	American Society for Testing and Materials (ASTM D1739 1970) Standard Method
ASGM	artisanal small-scale gold miners
ATSDR	Agency for Toxic Substance and Disease Registry
ATS	American Thoracic Society
CBD	Central Business District
CDCP	Centres for Disease Control and Prevention
CGR	Crown Gold Recovery
CGS	Council for Geosciences
CRSA	Constitution of the Republic of South Africa
COM (MCSA)	Chamber of Mines (now Minerals Council of South Africa)
DEM	Digital Elevation Models
DMR(DMRE)	Department of Mineral Resources
DRDLR	Department: Rural Development and Land Reform
DRD	Durban Roodepoort Deep
DTM	Digital Terrain Models
DWAF (DWS)	Department of Water Affairs and Forestry (now Department of Water and Sanitation)
EC	electrical conductivity
EF	enrichment factor
EIA	Environmental Impact Assessment
EMF	Environmental Management Framework
EMPR	Environmental Management Programme Reports
ERGO	East Rand Gold and Uranium Company
ERPM	East Rand Proprietary Mine
EU	European Union

FWR	Far West Rand
g	Gram
GC	Gas chromatography
GDACE	Gauteng Department of Agriculture, Conservation and Environment
GDARD	Gauteng Department of Agriculture and Rural Development
GIS,	Geographic Information System
GPS	Global Positioning System
h	Hour
HHRF	Human Health Risk Framework
HHRA	Human Health Risk Assessment
IARC	International Agency for Research on Cancer
IAEA	International Atomic Energy Agency
ICPMS	Inductively coupled plasma mass spectroscopy
ICPOES ICPOES	Inductively coupled plasma optical emission spectrometry
ICMM	International Council on Mining and Metals
ICRP	International Commission on Radiological Protection
IDP	Integrated Development Plan
I*geo*	geo-accumulation indices
ISAAC	International Study of Asthma and Allergies in Childhood
Km	Kilometre
KOSH	Klerksdorp, Orkney, Stillfontein and Hartbeesfontein
L	Litre
LHR	Lawyers for Human Rights
MCLM	Merafong City Local Municipality
mg g^{-1}	Milligrams per gram
mg kg^{-1}	Milligram per kilogram
mg mL^{-1}	Milligram per millilitre
mg/m^2/day	Milligrams per square metre per day
M	Metre
mm	Millimetre
M	Metre
M/S	Metre per second

MHSA	Mine Health and Safety Act (MHSA) (92 of 1996),
MPRDA	Minerals and Petroleum Resources Development Act 28 of 2002
MRD	Mine Residue Deposit
MS	Mass spectrometry
MW	Molecular weight
NAA	Neutron Activation Analysis
ND	Not detected
NDCR	National Dust Control Regulations
NEMA	National Environmental Management Act 107 of 1998
NEM: AQA	National Environmental Management: Air Quality Act 39 of 2004
NECSA	South African Nuclear Energy Corporation
NEMWA	National Environmental Management: Waste Act 59 of 2008
NIOSH	National Institute for Occupational Safety and Health
NNR	National Nuclear Regulator
NNRA	National Nuclear Regulator Act
NRC	National Research Council
NORMS	Naturally Occurring Radioactive Materials
NWA	National Water Act
RESRAD	Residual Radioactivity
RSA (SA)	Republic of South Africa
SANAS	South African National Accreditation Standard
SANS	South African National Standard
SEM	Scanning Electron Microscopy
SPSS	Statistical Package for Social Scientists
TENORMS	Technologically Enhanced NORMS
TSFs	tailings storage facilities
TB	tuberculosis
PTB	pulmonary tuberculosis
SoER	State of The Environment Report
PCBs	Polychlorinated biphenyls
PM	Particulate Matter

POPs	Persistent organic pollutants
ppb	Parts per billion
ppm	Parts per million
ppt	Parts per trillion
UK	United Kingdom
UNEP	United Nations Environmental Protection
USA	United States of America
USEPA	United States Environmental Protection Agency
VAC	Visual Absorption Capacity
VIA	Visual Impact Assessment/Analysis
WCA	Wonderfonteinspruit Catchment Area
WDL	Western Deep Levels
WeatherSA	South African Weather Services
WHO	World Health Organisation
WRC	Water Research Commission
WR	West Rand
WRDM	West Rand District Municipality
WRDAQMP	West Rand District Air Quality Management Plan
XRD	X-ray Diffraction
XRF	X-Ray Fluorescence
ZVI	zone of visual influence

CHAPTER 1

1. INTRODUCTION

1.1 Background

The gold-mining industry has been the basis of the economy and socio-economic development of the Republic of South Africa (RSA), which has led to improvements of the livelihoods of many both within and outside the country (Chamber of Mines, 2006). Unfortunately, in contrast to all the economic and social benefits derived from mining, there are several negative impacts on the environment that were brought about by gold mining (Downing, 2002; Bridge, 2004; Oelofse, 2010; White, 2013; Makua & Odeku, 2017). Gold mining has been identified as one of the main environmental pollution contributors, releasing significant amounts of toxic contaminants such as sulphates, chlorides, heavy metals, and Naturally Occurring Radioactive Materials (NORMS) (Sutton *et al*., 2006; Gauteng Department of Agriculture and Rural Development (GDARD, 2009); White, 2013; Liefferink, 2019) into various receptor environs (Sutton *et al*., 2006; GDARD, 2009).

Even though some contaminants occur naturally, the mining induced anthropogenic sources, could pose long-term adverse effects on the environment, including human health (Akabzaa, 2000; Fashola *et al.,* 2016). Dust from gold mine tailings storage facilities (TSFs) have been noted to be of enormous challenge in the RSA owing to lack of successful rehabilitation of these structures (Madalane, 2012; Dlamini & Xulu, 2019). This has resulted to numerous amendments of the legislation such as the Mineral Petroleum Resources Development Act (MPRDA) (Act 28 of 2004) as there were no clear regulatory guidance and thus satisfactory results in addressing the

impacts of dust on the immediate residential areas (Sutton *et al*., 2006; Krause & Snyman, 2014).

Many researches have revealed environmental impacts of mining-related activities and of mine TSFs as being severe, wide-ranging and long-term in nature (Sutton *et al.*, 2006; Coetzee *et al*., 2006; National Nuclear Regulator, 2007; Sutton & Weiersbye, 2007; Rademeyer, 2008; Turton, 2008; GDARD, 2009 & 2012; Wright *et al*., 2012; Maseki, 2013; Utembe *et al*., 2015, Winde, 2015; Yalala, 2015; Mathuthu *et al*., 2016; Kamunda, 2017; Poswa & Davies, 2017; Liefferink, 2019). In instances of mine closure, communities are often left exposed to polluted air, water and soil that were left unattended during active mine operations (Olalde, 2015). Residual and latent environmental impacts outlast the lifespan of a mine, resulting in a legacy that poses a daily threat to the health, safety, and well-being of communities. In recent years, high incidents of respiratory illnesses and skin diseases have been reported in mine-affected communities (Sutton & Weiersbye, 2007; Liefferink, 2011).

The trends have shown that towards the end of life of a mine, major mining operations, including TSFs are sold to junior miners, thereby diverting rehabilitation obligations to companies that frequently lack the capacity and experience to conduct large-scale rehabilitation (Sutton *et al*., 2006; Olalde, 2015). This results in increased derelict mines, posing constant threat to the health and safety of the community, specifically to children who may encounter toxic materials through ingestion and inhalation of contaminated dust material from mainly TSFs (Sutton & Weiersbye, 2007). The gold mine dumps and TSFs remain sources of air pollution as many of them are neither vegetated nor covered with dust suppressing materials. The Witwatersrand Mining

Basin of SA is the oldest mined area and the world's largest gold and uranium mining basin. It is formed by the Eastern Basin, the Central Rand Basin, the Western Basin, the Far Western Basin, the Klerksdorp, Orkney, Stillfontein and Hartbeesfontein (KOSH) Basins and the Free State gold mines (Liefferink, 2019). The Far West Rand Area or the West Wits Mines is formed by the mining operations (Western Deep Levels, Goldfields, Blyvooruizicht and Oberholzer Mines) based in the western part of the Witwatersrand Basin. Thus, the area is the world's uranium hotspot, with enhanced concentrations of uranium relative to average crustal rock which have led to concerns about mobilization of radioactive substances (Von Backström, 1976; Winde *et al*., 2004; National Nuclear Regulator (NNR), 2007; Winde, 2015; Kamunda, 2017). Since establishment of mining in the area, an estimated 1.6 million people reside in proximity to or downwind of these tailings' dumps (Sutton, 2007; DEA, 2009; Yalala, 2015).

In the Republic South Africa, many of these communities such as Tudor Shaft Informal Settlement, Pennyville, Braamfischerville, Noordgesig,Diepkloof, Riger Park, Geluksdaal, Riverlea and Stilfontein (Lottermoser, 2003; Duri, 2016), comprised of historically marginalised ethnic groups (mainly poor black people) living in government-funded houses, informal settlements and retirement homes (Ojelede *et al*., 2012; Nkosi *et al*., 2013; Wright *et al*., 2014; Nkosi *et al*, 2015). Evidence suggested that these mine residue stockpiles and TSFs are a dust nuisance to the local communities during episodes of high winds, and in dry and low vegetation cover conditions (Scorgie *et al*, 2002; Scorgie, 2006; GDARD, 2009; Ojelede *et al*., 2012; Maseki, 2013; Ojelede, 2015; Nkosi, 2018; Liefferink, 2019). The most affected within these communities are children and the elderly (Wright *et al*., 2014; Nkosi *et al.*, 2016; Nkosi, 2018) as their immune systems are too weak to fight against toxic attacks.

Human health risk assessment from TSF dust occur through multiple exposure pathways (i.e., inhalation, ingestion, and dermal contact) for local communities who complain of the general deterioration of their health and other environmental impacts (Sutton *et al*., 2006; GDARD, 2011 and 2012). These impacts are discussed under Section 1.4 below.

1.2 Dust Definition

According to DustWatch (2016), precipitant dust is defined as particulate with size ranging up to 100 µm in diameter, formed by the dust that falls. Dust particles settling from gravity are collected as dry deposition whereas dust collected from rainy conditions are collected as wet deposition. Summing up dry and wet deposition results in total precipitant dust. Occult deposition is hidden from measurements that determine wet and dry deposition, by fog, cloud-water, and mist interception according to the United States Environmental Protection Agency (USEPA, 1996a). While the coarse fraction of precipitant dust will be blown by mechanical disturbance or wind erosion, this lands on the ground within 1 km of the sources, the finer and lighter particulate dust get suspended in the atmosphere and can be blown significantly further away from the source (DustWatch, 2016; Liefferink, 2019).

Dust particulate matter (PM) sizes are categorised into three (3) classes, namely: (1) ultrafine particles, <0.1µm ($PM_{0.1}$), (2) fine particles, <1µm (PM_1), and (3) coarse particles, >1µm (PM_1). Particles >1µm (PM_1) are further categorised as: (a) respirable fraction, <2.5µm ($PM_{2.5}$), (b) inhalable fraction, <10µm (PM_{10}) (Yalala, 2015; DustWatch, 2016).

1.3 Environmental Impacts of Dust from Gold Mining Tailings Storage Facilities (TSFs)

1.3.1 Mine waste generation

Gold mining process produces waste through three main activities, namely mining, mineral processing and metallurgical extraction, releasing approximately 99% of extracted ore as waste into the environment (Oelofse *et al*., 2007; GDARD, 2009). Mineral processing or beneficiation involves physical separation and concentration of ore bearing mineral through physical, chemical, and microbiological techniques (Fashola *et.al.,* 2016). Tailings is waste material, loaded with heavy metals and is generated from gold extraction in a form of slurry. As per Fashola *et.al.* (2016), these often leach out into the environment in a form of surface water runoff, seepage or wind borne.

Approximately 200 000 tonnes of waste per tonne of gold is generated from gold mining and six billion tonnes of waste is deposited on TSFs as tailings slurry within the Witwatersrand Basin (Wymer, 2001; Mining Weekly 2003; Chevrel *et al*. 2003; Ojelede *et al.,* 2012). Furthermore, about 70% of solid waste is generated from mining industry of which 23% emanates from gold mining sector alone, making it the largest single source of waste and pollution in South Africa (Coakley, 1998; Department of Water Affairs and Forestry, 2001; AGA, 2004; Oelefse *et al*., 2007).

1.3.2 Land contamination

The disposal of mine waste, chiefly tailings, has of late, assumed an importance that transcends even the massive volumes of materials produced annually by mining operations (Sutton *et al*., 2006). Aside from their significance in strictly engineering

terms, TSFs receive intense regulatory attention and public scrutiny. The Department of Mineral Resources (DMR) recorded a list of 6,000 “derelict and ownerless” mines, which became the government’s problem over the years when the former owners disappeared (van Tonder *et al*., 2009; Olalde; 2015). Part of Gauteng’s safe land is inaccessible for commercial and agricultural purposes as these pockets of land are occupied by mine infrastructure such as TSFs, waste rock dumps and other immovable infrastructure (Bobbins & Trangoš, 2018)**.**

1.3.3 Air pollution

A study by Piechota *et al. (*2004) has cautioned that dust impacts from TSFs depend upon dust composition, application rates and interactions with other environmental components such as (1) surface and groundwater quality deterioration; (2) soil contamination; (3) toxicity to soil and water biota; (4) toxicity to humans during and after application; (5) air pollution; (6) accumulation in soils; (7) changes in hydrologic characteristics of the soils, and (8) impacts on native flora and fauna populations.

People living downwind of mine tailings are exposed to the potentially inhalable trace metal and metalloid-bearing dust particles (Kneen *et al.*, 2015; Von Oertzen, 2015; Liefferink, 2019). Active TSF dams rarely have dust problems compared to dormant dams. Wind erosion can transport environmental contaminants such as metals and metalloids, pesticides, and biological pathogens, all of which are typically associated with finer atmospheric particles and tropospheric aerosols (Csavina *et al.*, 2011; Yalala, 2015). These pollutants get dispersed by wind and lighter dust sized particles persist long enough to pose problems in distant areas, resulting in trans-boundary pollution (DEA, 2016; Yu *et al*., 2019).

Due to their designs, the establishment of large and steep sand dumps and TSFs from mining operation, without the necessary precautions, create optimal conditions for wind erosion (USEPA, 1994; Seiderer *et al*., 2016). Factors such as the height of the TSF dams, the texture of the tailing's material and the alignment of the TSFs with the prevailing winds increase the susceptibility of the sand dumps and slimes dams to wind erosion. Elevated dust deposition from TSFs is linked to strong winds and high wind speed increased with TSF height (Yalala, 2015; Liefferink, 2019).

Several cases of dust emanating from tailings dams were previously lodged against mining houses in which mine dust exposures resulted in health impacts on the nearby communities (Nkosi *et al.*, 2016). On windy days, windblown tailings material was reported billowing off the surface of the tailings thereby posing visibility impact within nearby roads (Kneen *et al*., 2015; Liefferink, 2019). Windows and doors had always to be kept closed as the dust landed on food, floor, and hard surfaces (Jazeera, 2019). According to Sutton *et al*. (2006), these problems have persisted for decades due to the lack of proper remediation strategies to combat pollution from the tailings (Sutton & Weiersbye, 2008). The TSFs sites have low pH and deficient in soil nutrients from deprived soil structure to support plant cover (Poswa & Davies, 2017).

Just only on the West Rand, 42.24 metric tons of tailings-piles dust were recorded, blowing into the air daily, some of it taken up by livestock and food crops (WRDM, 2013; Olalde; 2015). Poor quality air in a form of dust loaded with heavy metals of concern and radioactive material air impacts are mainly experienced through ingestion, inhalation, skin contact and biomagnification in the food chain, thus posing a threat to human health (Kneen *et al*., 2015; Poswa & Davies, 2017). Many of the

TSFs are neither vegetated nor rehabilitated making them prone to wind erosion (AGA, 2004; Oelofse *et al.,* 2007).

1.3.4 Soil contamination

TSFs are inhospitable environments for plant growth, and various combinations of leaching, liming, fertilization, and irrigation were used to facilitate the growth of a small suite of herbaceous, mostly pasture species (Govender, 2011; Seiderer *et al*., 2016; Van Deventer, 2011c; Van Deventer, 2012; Mathuthu *et al*., 2016; Schimmer & van Deventer, 2017). TSFs poor soil structure makes them nutrient deficient due to lack of organic matter which makes vegetation difficult to adapt and survive in some instances only surviving for a short period of time, exposing tailings soil to dust and rain erosion which loads the surrounding receptors (Yalala, 2015).

According to Van Deventer (2011c), the ideal electrical conductivity (EC) value for soils in South Africa should not exceed 360-400 mS/m and the presence of soluble salts and ions such as Cl^-, SO_4^{2-}, HCO_3^-, Na^+, Ca^{2+}, Mg^{2+}, NO_3^- and K^+ may damage vegetation by reducing the osmotic potential and may result in water deficiencies. High salinity and solidity in the soil can also contribute to the decrease in water quality and increase the solubilization of trace metal elements which can further have hostile effects on plant growth (Seiderer, 2011; Seiderer *et al*., 2016).

1.3.5 Impacts on vegetation

Wind erosion accounts for resource outflow from systems and hence, the rehabilitation effort can be compromised, wind can be more damaging to vegetation than water (AGA, 2011). Trees can contain up to 2-3 tons of dust. Particulate matter deposition

and effects on vegetation include (1) nitrate and sulphate and their associations in the form of acidic and acidifying deposition and (2) trace elements and heavy metals, including lead. Deposition dust may affect vegetation directly following deposition on foliar surfaces or indirectly by changing soil chemistry (Angus, 2005; O'Connor and Kuyler, 2007; Weiersbye & Witkowski, 2007). Most documented toxic effects of particles on vegetation are associated with their acidity, trace metal content, nutrient content, surfactant properties, or salinity (Grantz *et al.,* 2003).

1.3.6 Radiation exposure

Anthropogenic activities, such as mining, can result in mine waste with radiation above background levels in the environment, leading to major concern for radiation protection (Nour *et al*., 2005). According to GDARD (2012), in South Africa, on average the Witwatersrand gold-bearing ores contain almost four times the amount of uranium than gold, giving an estimated 430 000 tons of uranium and approximately 30 million tonnes of sulphur (GDARD, 2012; Winde, 2013).

Mining-induced radiation exposures can contaminate soils over a large area and other environmental contaminants (United States Environmental Protection Agency, 2008), This could lead to human health effects via different radiation exposure pathways, either external or internal (*i.e.*, ingestion and inhalation pathways) direct exposure from contamination in soil, inhalation of dust/radon, ingestion of plant foods, ingestion of water, and incidental ingestion of soil (Poswa and Davies, 2017).

Studies have detailed the level of radiation within the Witwatersrand and the Far West Rand, but the focus was mostly slanted towards surface and groundwater resources,

as well as sediments contamination (Winde, 2015), but too little data has been documented on radiation levels in dust particulate matter. Both potential acute and toxicity impacts of bioaccumulated pollutants, including human health effects were recorded for dust exposures near TSFs gold reclamation operations (Liefferink, 2019).

Mathuthu *et al.* (2016) investigated the radiological health risks associated with mine tailings within the Wonderfonteinspruit Catchment and established that water-independent pathway was the most significant contribution to the dose directly from soil sources, then followed by radon gas (direct and airborne) pathway. Episodes of radon gas and windblown dust from gold mine TSFs have been confirmed in the West Rand, dispersing emissions outwards from mine site over long distances (Liefferink, 2019). Radon gas, also known as a silent killer, as it has no smell, colour or taste, can remain radioactive in the environment for millions of years, causing cancer upon inhalation (Health24, 2016).

Contradictorily, the ingestion of dust and soil was found to the most common heavy metals and metalloids exposure pathway in children by a variety of researchers (De Miguel *et al.,* 1997; Rasmussen *et al.*, 2001; De Miguel *et al*., 2007; Nelson, 2013). One of the few studies conducted on the radiation exposure from gold mine TSF in the West Rand by the NNR in 2007 yet revealed that strong dust emissions from slimes dams occur during wind events due to the small particle size of the slurry slimes, with particulate matter being transported over relatively long distances to agricultural land in the surrounding environments (Liefferink, 2019).

1.3.7 Health impacts

Human health effects can be classified as acute, chronic, as well as accelerated, and air pollutants exposures may result in or cause increased mortality, or serious illness or pose potential health hazard based on clinical and/or epidemiological studies (Kampa & Castanas, 2008). Many pathological effects may result from gold mine TSFs dust exposures, depending on mineral content, shape, size, chemical composition, levels, and duration of exposure of the dust particle (Utembe *et al*., 2015; Lawyers for Human Rights, 2017).

Crystalline and amorphous form of silica commonly found as quartz, cristobalite and tridymite (NIOSH, 1994) are classified as Group 1 carcinogens (IARC, 2009) by the International Agency for Research on Cancer (IARC). Chronic occupational exposure to high levels of crystalline silica dust over prolonged periods has been found to cause lung cancer (Vida *et al.,* 2010) as well as pulmonary silicosis (Craighead, 1988), chronic obstructive pulmonary disease, chronic bronchitis, emphysema, small airways disease (Hnizdo & Vallyathan, 2003), tuberculosis/silicotuberculosis (Kootbodien *et al*., 2019), autoimmune diseases (*rheumatoid arthritis, scleroderma, systemic lupus erythematosus*) and kidney disease (Steenland Vupputuri *et al.*, 2012).

Human health effects resulting from quartz exposure has been confirmed as one of the main health related concerns in the Witwatersrand gold TSFs dust (Nkosi *et al*., 2015; Liefferink, 2019). Studies have further shown that children residing in close proximities of mine TSFs in South Africa experienced upper respiratory infection related symptoms such as wheezing chest with runny nose, congested nasal passages and postnasal drip, and high prevalence of asthma within such areas as

compared to less cases predominant mining areas (Nkosi & Voyi, 2016; Nkosi *et al*., 2017). This was found to be consistent with related studies conducted around the similar topic within South Africa and other countries such as Europe and Australia (Nkosi *et al*., 2017). Furthermore, high asthma rates in elderly people in South Africa were found to be higher than United States and Australia (Nkosi, 2018).

1.3.8 Metals exposure and toxicity

Recent technological developments and increased energy production marked the resultant high metal toxicity exposures with more contamination of the environment. Chemicals demands in both developed and developing countries lack comprehensive laws in protecting the health of their workers and residents (Kumpiene *et al*., 2017; Kootbodien *et al.*, 2019).

Three important formations of chemicals exist within the surrounding environment, namely metals (iron, copper, mercury, and zinc), nonmetals (hydrogen, carbon, and halogens) and metalloids. Metals form an important and essential part of the environment as they play numerous crucial roles including immense role in the rapid developments of healthcare, technological, construction and other sectors of the industries. Metals such as iron, copper, zinc, and molybdenum are essential for human biological processes and enzymatic reactions. Yet, upon high level exposures they could potentially present health risks and hazards within the environment due to acute toxic characteristics (Morakinyo *et al.*, 2017).

Heavy metals, such as cadmium and mercury, conversely, may pose more toxic threats on human health even at lower concentrations while other heavy metals such

as molybdenum, selenium, and zinc are essential for normal human physiology and not toxic to the human body at lower concentrations. Light metals such as beryllium can however be as toxic as heavy metals (Fashola *et al*., 2016).

1.3.9 Visual Impacts

Due to their height in physical design structure as well as the colour of tailings material, TSF structures are highly visible from key viewpoints posing significant visual intrusion and blocking clear lines of sight and from unsightly new landmarks. Countryside character can be detrimentally and permanently impacted on by TSFs both individually and cumulatively (GDARD, 2012). The severity of this impact therefore needs careful consideration during planning stages of mining activities. Historic impacts of these structures should be considered from the outset to determine the level of extent on the surrounding environment (GDACE, 2006; Rademeyer, 2007, GDARD, 2012).

Findings by Rösner and van Schalkwyk (1999) confirmed that TSF topsoil is contaminated with heavy metals, resulting in high acidification of localised soils. This poses threats to desirable future land use on previously TSF deposited land, as only acid-tolerant plants can be grown in acidic soils. Exposed soils can be vulnerable to erosion during high and dry windy conditions making TSFs even more visible.

1.3.10 Economic impacts of gold mine tailings storage facilities

While mining has historically made a key contribution to the South African economy (Chamber of Mines, 2011), mine waste, however, now also represents a considerable economic cost. Currently, the South African government has inherited 6 000 ownerless and derelict mines (Van Schie, 2012 and Baartjes & Gouden, n.d.) and this has direct implications as a tax burden on the broader economy from the rehabilitation point of

view. In this instance, the costs of dealing with mine waste and acid mine drainage (AMD) on public financial resources. This will decrease funding from much-needed support for agricultural and industrial production, tourism promotion, power generation, and a host of other essential economic infrastructure investments to the benefit of the local communities. To make matters worse, the environmental impacts associated with mine waste are most likely to contribute to an increased burden on public healthcare, which again falls as a major cost to the fiscus (Kearney, 2012).

1.4 Legal Challenges of Gold Mine Tailings Storage Facilities

The South African environmental legislation has been found to be one of the most effective and advanced laws in protecting its natural resources and in ensuring that human basic rights to a healthy environment are provisioned to the citizens as part of its corporate social responsibility and custodianship of the environment. However, the government had to deal with interdepartmental conflicts of interests between addressing the environmental damage caused by mining activities versus promotion of economic development. This has been found to contravene the requirements of various sectoral pieces of legislations, namely National Water Act (NWA), National Environmental Management Act (NEMA), Mineral and Petroleum Resources Development Act (MPRDA), National Nuclear Regulatory Act (NNRA) and The Constitution of the Republic of South Africa (CRSA) (Van Eeden *et al*., 2009).

Prior to 1991, South Africa had little legislation specifically directed towards environmental protection from mining impacts, although recommendations and statutes existed only for the structures and abandonment of tailings dams (James, 1964; James & Mrost 1965; Chamber of Mines of South Africa, 1968 and 1979; Blight

1969). Mines did not have a legal obligation to prevent dust pollution until the promulgation of the Atmospheric Pollution Prevention Act 45 (1965), amended in 1973. The main legal challenges relating to mine residues, including TSFs dust mitigation which resulted in the status quo in terms of dust exposure and consequent effects on the environment remain one of the mining biggest environmental challenges.

1.4.1 The Constitution of the Republic of South Africa

The Constitution of the Republic of South Africa (CRSA) Act No. 108 (of 1996a) imposes the basic right to an environment that is not harmful to health and well-being. Even though these requirements are clearly outlined, studies have, however revealed that the constitutional rights of communities affected by mine pollution are often infringed (Olalde, 2015; Mpanza *et al*., 2020). Practical means of limiting human exposure to harm were either not adequately dealt with in current legislations (Sutton and Weiersbye, 2007, van Tonder, 2008).

In South Africa and prior to 1998, environmental issues relating to mining were regulated and managed in terms of the Minerals Act (50 of 1991) and no extensive environmental assessments were conducted to predict impacts prior to establishments of TSFs for the protection of the natural environment. No stringent requirements for conducting far-reaching environmental studies to investigate and specifically determine the impacts of pollution from TSFs on the receiving environment resulting from existing historic mining activities (Mhlongo & Amponsah-Dacosta, 2016).

1.4.2 Mineral and Petroleum Resources Development Act

Historically in South Africa (SA), the disposal of mine residues deposits (MRD) stockpiles, i.e. waste rock dumps, TSFs, cyanided sand and slime, surplus mine water and discarded solutions, presented little difficulty in the early days of gold mining as there was no legislation constraining them (Tyrer, 2005; Sutton & Weiersbye, 2007). Most of South African mines are over fifty (50) years old and their establishments were carried out in the absence of ecological aspects considerations and with little legislation enforcement. As part of a mine activities project's lifecycle, the Environmental Management Programme Reports (EMPRs) contents lacked environmental risk management and was not an all-inclusive of stakeholders affected by mining activities (van Tonder, 2008).

Long-term health impacts on the communities residing and exposed to pollution sources were for instance, completely excluded in the financial provision for mine closure (Lawyers for Human Rights, 2017). Ownerless TSFs are mainly problematic as they are left unrehabilitated by previous owners, leaving nearby communities with consequential human health and environmental impacts (Olalde, 2015; Lawyers for Human Rights, 2017). Proper mitigations could potentially avoid or reduce health risks, but current mining closure legislation only came into effect between the 1970s and 1990s (Olalde, 2015; Liefferink, 2019). This remains a legacy that communities living in close proximities to the mines will potentially incur life-threatening, and long-term exposure to environmental hazards even beyond mine closure. In many instances, communities were perceived to be anti-mining when voicing their concerns on issues relating to human health and safety, loss of land due to mine pollution (Sutton and Weiersbye, 2007; Lawyers for Human Rights, 2017).

Public perception studies with regards to mine dust exposures have been reported in Mexico (Catalan-Vasquez *et al.,*2012), Tanzania (Kitula, 2006), Ghana (Garvin *et al*., 2009) and Australia (Higginbotham *et al*., 2010). However, only a few studies were conducted in South Africa, especially with regards to public's experiences and perception in relation to mine dust exposures (Wright *e t al.,* 2014). Only a handful of publications in articles, journals and news on issues relating to complaints from the public were documented (Olalde, 2015). The study by *Wright et al.,* (2014), was however, not TSF dust specific and lacked enough analytical component in support of the issues at hand. Furthermore, data collection only focused on one day's questionnaire administration which might not necessarily be a true representation of the views of the entire population within the study area.

Sutton and Weiersbye (2007) revealed several challenges pertaining to the MPRDA requirement for gold mining. Amongst others, they argued that there was eminent lack of proper determination and quantification of financial provision for latent and residual impacts for naturally occurring metals (NORMS) as they can be recycled throughout mineral processing, eventually found in the gold MRD such as TSFs. The latent impacts on biota, including humans, of bioaccumulation and exposure to elevated levels of metals and NORMs are established in the international scientific literature revealing consequent human health related catastrophes from mining activities (e.g., silicosis). This has been a learning curve to justify application of precautionary principles in managing other related latent impacts (Kootbodien *et al*., 2019).

1.4.3 National Environmental Management: Waste Act 59 of 2008 (NEMWA)

The National Environmental Management: Waste Act 59 of 2008 (NEMWA) aimed at promoting cleaner production, waste minimization, reuse, recycling, and waste treatment, with disposal being the last option in the management of waste, including MRDs. These were excluded under Section 4 (1) (b) of the NEMWA as these were regulated under MPRDA, but no environmental aspects of TSFs were catered for under both legislations' provisions (Sutton *et al*., 2006).

1.4.4 Mine Health and Safety Act

The Mine Health and Safety Act (MHSA) (92 of 1996), of South Africa governs the hazards and risks associated with mine worker's exposures to high concentration of dust, noxious fumes, and harmful gases (Utembe *et al*., 2015). At the time of this study non-occupational limits for crystalline silica for residential areas close to TSFs sites were not yet established in South Africa compared to international non-occupational limits (Andraos *et al*., 2018). Cases of silicosis were found to have long and progressive latency period of up to 20 years (Rees and Murray, 2007) and studies revealed that the disease may develop only after dust exposure has ceased (Lara, 2018; Thomas *et al.*, 2019). This then suggested that accurate estimations of the health risk require both current and ex mine employees (Nelson, 2012).

1.4.5 National Nuclear Radiation Act

Naturally Occurring Radioactive Materials (NORMs) such as ^{238}U, ^{232}Th, and ^{40}K posed human exposure to ionizing radiation (Ziajahromi *et al*., 2014; Winde, 2015; Mathuthu *et al*., 2016). These are disposed in TSFs as slurry or wet tailings material, leaving more troubling, legacy of environmental contamination from the many years of mining (Winde, 2015). Direct exposure from contamination in soil, inhalation of

dust/radon, ingestion of plant foods, ingestion of water, and incidental ingestion of soil has led to promulgation of regulations on public protection from these sources as they can pose serious health concerns (Liefferink, 2019). The NNR cautioned that radioactively deposition contaminated dust deposition on leaves of vegetables far exceeds inhalation doses within the Witwatersrand Basin, as the known radioactive hotspot (NNR, 2007; Liefferink, 2019). The uranium content in many gold mine tailings exceeded the exclusion limit for regulation by the National Nuclear Regulator (NNR, 2007; Mathuthu *et al*., 2016).

1.5 Problem Statement

Consequences of public exposures to dust from gold mine TSFs has been a burning issue over the years as documented in various studies (Maseki, 2013). Even though this has been the case, this study has identified several gaps in the current literature for the study area:

- The study area forms part of the Merafong City Local Municipality (MCLM) of the West Rand District Municipality (WRDM), hosting the highest number of gold mines TSFs. Even though the WRDM has its Air Quality Management Framework and Management Plan in place, no comprehensive air quality data was documented for MCLM as mining companies have their own individual in-house information. The reasoning from the WRDM confirmed that due to the study area not being a priority area in terms of air pollutants of national interest, no detailed air quality monitoring studies are being conducted/required. Thus, no dedicated monitoring station is currently available for the MCLM and the study area.

- There has been little focus by previous studies on public perceptions of the mining impacts resulting from tailings storage facilities. Only a few studies were conducted in South Africa, especially with regards to public's experiences and perception in relation to mine dust exposures (Wright *et al*., 2014). The study by Wright *et al.,* (2014), was however, not focused on TSF dust specific and lacked analytical component of the study in support of the issues raised by the public. Furthermore, data collection only focused on one day's questionnaire administration which might not necessarily be a representation of the views of the entire population within the study area. Whilst this study acknowledges complexities relating to this, the concern remains that issues of the current non-mining communities being exposed to mine dust and ex-mining employees who are still or may have been previously exposed are neither considered nor attention during the mines' decision-making processes.
- Not enough published reports on characterization of dust from mine dumps is available within the district and the local municipalities of the study area. Thus, the study area is not considered as one the priority areas in terms of the National Air Quality Management list of priority areas even though the area hosts the largest number of the gold mines TSF in the district.
- Public concerns have been raised relating to the dust emission from TSFs which include visibility and human health risk, but no clear link of this was confirmed, with reference to the area of study. Individual studies (radiological, water, soil, rehabilitation etc.,) are in place but no views from the public or involvement thereof were incorporated to assess their experiences.

- Previous studies only focused on the impacts around the mining operations (i.e., dust exposure), but little has been done to assess the potential risks within community areas in terms of exposure from the impact of TSFs. Mining companies mainly focussed on their onsite monitoring of impacts; however, studies have shown than offsite impacts are equally important.
- Visual impacts of mine TSF, with specific reference to the historic (i.e., the ones constructed prior to the environmental regulations) are not quantified and their severity on the receiving environment remain unknown.

1.6 Aim of the Study

This study undertakes to assess the environmental risks of public exposure to the dust from gold mine tailings storage facilities within the Witwatersrand Basin. Both analytical and survey methods of dust deposition monitoring and experimental analyses will be employed to establish the precipitant dust and dust characteristic. This will further enable calculations of the extent of TSFs dust exposures of particulate matter.

1.7 Research Objectives

The objectives of this study are to:

a) Establish the dust rates from the gold TSF sources to the nearby receptor environments.
b) Characterise the TSF dust collected at various sites in terms of morphology, particle size distribution, radiological, chemical, and mineralogical components.
c) Assess the perception of the public regarding the impacts of gold mine TSF dust based on their experience.

d) Assess the extent and degree of gold TSF dust contamination from selected heavy metals.
e) Determine the extent of TSF dust zones of influence using settling rates and deposition distance away from the source.
f) Determine the risks exposures sensitive receptors within close proximities of the mine TSFs.

1.8 Hypothesis

This research study hypothesized that:

There is high potential of dust exposure from gold mine TSFs into the surrounding environments which will pose significant detrimental human health and environmental risk to the surrounding environment.

Characterization of the settled dust in terms of size, mineralogy, morphology, and distribution from TSFs will make the study area to be part of the district air quality monitoring program as it hosts the largest gold mines in the district.

1.9 Novelty of The Study

The 2013 West Rand District Air Quality Management Plan does not include the air quality status for the Merafong Local Municipality, which is one of the local municipalities with the highest concentration of mining activities and the main contributor of particulate matter ($PM_{2.5}$ and PM_{10}) from mines TSFs in the district. This study will provide air quality data from the impact of TSFs in the surrounding environments of the municipality.

The characterisation and quantification of gold mine TSF dust in the WRDM generated in this study will be useful to the municipality and the public because most studies within the West Rand specifically made references to public radiation exposures relating to water and mine sediments through ingestion and physical contacts. Research on characterisation and human health exposure to TSFs dust particles is still rare around South Africa and the globe. As most environmental concerns were raised on the alleged impacts of TSF dust on community health, this study present among others, precipitant dust deposition rates, dust characteristic properties such as dust particle morphology (sizes, shapes, diameters), radioactive elements, mineralogical and chemical contents which have direct link to human health.

The results for the visual analysis from this study will assist the regulators to understand the current visual alterations since establishment of mines and related infrastructures from the public perception point of view of various types and scales of development, including different biophysical, social, economic and governance contexts. This will contribute towards the restoration and modifications of general sensitive landscape of the area upon mine closure. The results of this study will be instrumental in identifying the level of knowledge within mining-based communities, the public within the area, and be used as a starting point for engagement knowledge base in preparation for rehabilitation and closure of mines.

CHAPTER 2

2. LITERATURE REVIEW

This chapter aims to provide the general overview of environmental impacts of dust from gold mine TSFs, recent research, methods, instruments and techniques used to determine the characteristics of the dust. The resultant risks exposures by sensitive receptors and how these are determined by scientific research communities from local and global perspectives.

2.1 Air Pollution sources

Air pollution sources are classified into physical, chemical and biological, and secondly as natural (*biogenic)* and man-made (*anthropogenic*). Physical air pollution sources can be thermal pollution, natural or anthropogenic and this can alter the local climate, cause adverse effects, and deteriorate visibility. Natural sources of air pollution include volcanoes, which produce sulphur, chlorine, and particulates. Anthropogenic air pollution sources such as wildfires result in the production of smoke, carbon dioxide and carbon monoxide. Other natural air pollution sources include domestic animals such as cattle, which release methane, and pine trees, which release volatile organic compounds (VOCs) (DEA, 2011a).

The atmosphere is central in making life possible on earth, protects and supports life by absorption of dangerous solar radiation and warming the earth's surface thus regulating the temperatures (DEA,2010; Euronews, 2019). However, the anthropogenic release of pollutants into the atmosphere poses serious and life-threatening impacts (Hunter *et al*., 2002; DEA, 2010). Atmospheric emissions remain

the most harmful to human health and the environment as the impacts may originate from many different pathways (Fashola *et al.,* 2016).

Gaseous emissions result in chemical transformation to the national and regional climatic conditions posing hazards to human health, ecological and the functioning of the atmosphere on a global scale. Consequent global concerns relating to degraded air quality include climate change, stratospheric ozone depletion due to chloro-fluoro-carbons (CFC) emissions, and mercury emissions from coal combustion and cement production. General environmental degradation and the depletion of natural resources are also major challenges requiring urgent regulatory interventions (DEA, 2010).

Studies have shown that based on historical importance, concentration and overall effects on plants, humans and animals these environmentally persistent contaminants pose a potential risk to human health worldwide (Ione, 2006; Fang, 2013). Although natural processes can produce several environmental contaminants, significant amounts of contaminants are generated by anthropogenic activities like agricultural practices, vehicle emissions, industrial manufacturing, and mining operations (Barrie *et al*., 1992; Lacerda, 1997; Kolpin *et al*., 1998; Ritter *et al*., 2002; Driscoll *et al*., 2003; Volkamer *et al*., 2006).

Naturally, the gases in the atmosphere remained harmless to the environment and human life. Atmospheric pollution of natural origin is mainly contributed by volcanic eruptions, natural decomposition of organic matter and these are sources of less concern. However, the influence of mankind evolution and population growth pressures led to increased urbanization and industrialization, resulting in emissions of

toxic contaminants into the environment worldwide, causing modification of the air quality pushed above limits (Fashola *et al*., 2016).

Anthropogenic chemical pollution sources can be mobile or stationery and these are categorically sources from burning of fossil fuels, major industrial process and transportation. Point sources, which are either elevated or at ground-level include emissions from a combustion furnace, flue gas stack, etc. Line sources are emitted from vehicular traffic on a roadway whereas area sources are two-dimensional and include forest fires, landfill or emission from large spillages. Volume sources are three-dimensional, resulting from fugitive emissions from piping and from various heights from industrial infrastructures (Pandley, 2013). These anthropogenic chemical pollution sources pose main concerns as they remain borderless when released into the atmosphere and can lead to global impacts such as climate change. Of major concern is the threat to human life due to chemical exposures leading to illnesses and fatalities.

Even though most public exposure to air pollution are primarily linked to outdoor pollution, the most affected is still the poorest and most vulnerable populations including women and children in most cases (Smith, 2002; DEA, 2010; EPA, 2017). The incomplete combustion of the fossil fuels results in the release of high concentrations of some air pollutants associated with combustion into the living environment.

2.1.1 Dust sources

A few air pollution sources were identified within the study area (WRDM, 2013). Merafong City Local Municipality does not have ambient data; however, dust fallout monitoring data is restricted to the main mining areas in the region as each mine have their own monitoring points. Point and non-point sources of dust exist within the region, which comprise of the following:

2.1.1.1 Point sources

2.1.1.2 Commercial, Industrial and Residential Sectors

Sources and linked criteria of pollutants with the study area are entailed in the Table 2.1 below.

Table 2.1: Sources and linked criteria pollutants within the Study Area (WRDM, 2017/18)

SOURCE	**Criteria Pollutants**						
	SO_2	**NO_2**	**O_3**	**CO**	**PM_{10}**	**C_2H_4**	**Pb**
Brickworks (Corobrick Driefontein,einzger, West End, Wildebeeskuil)	x	x		x	x		
Cluster Holdings				x			
Carletonville Transport and Plant Hire	x	x		x			
Ernest Beeby (Kwik-Fit Carletonville)							
Fochville Abattoir							
Henque 2377 CC TA Water Ritw							
Hospitals (Fochvile, Western Deep Levels, Leslie Williams Private, Khutsong Medical Centre, Carletonville)	x	x		x	x		
Losberg Explosive Company	x	x		x	x		
Milton-Air Services							
Mines (Durban Roodeport Deep Gold, Harmony Elandsrand Gold, AngloGold Ashanti (now Harmony Gold), Goldfields (Now Sibanye), Blyvooruitzicht)							
Municipal (Carletonville, Fochville)	x	x		x	x		

2.1.1.3. Non-point sources

Residential sources emanate from activities within townships and informal settlements which include dust emissions, wood, coal, gas, paraffin, tyre and refuse burning thereby releasing pollutants such as CO, NO_2, SO_2, inhalable particulates and polycyclic aromatic hydrocarbons (Gondwana Environmental Solutions, 2006; Strategic Environmental Focus, 2010). In 2007, MCLM was the biggest consumer of coal and wood fuels, whilst Mogale City LM was the largest user of paraffin (WRDM, 2010).

2.1.1.3.1 Landfill sites

Few domestic landfill sites exist within the study area, but domestic waste is primarily deposed of at both the Merafong and Fochville Landfill sites, accommodating building rubble, garden refuse and household waste from mostly formal households of MCLM shown in Figure 2-1 below.

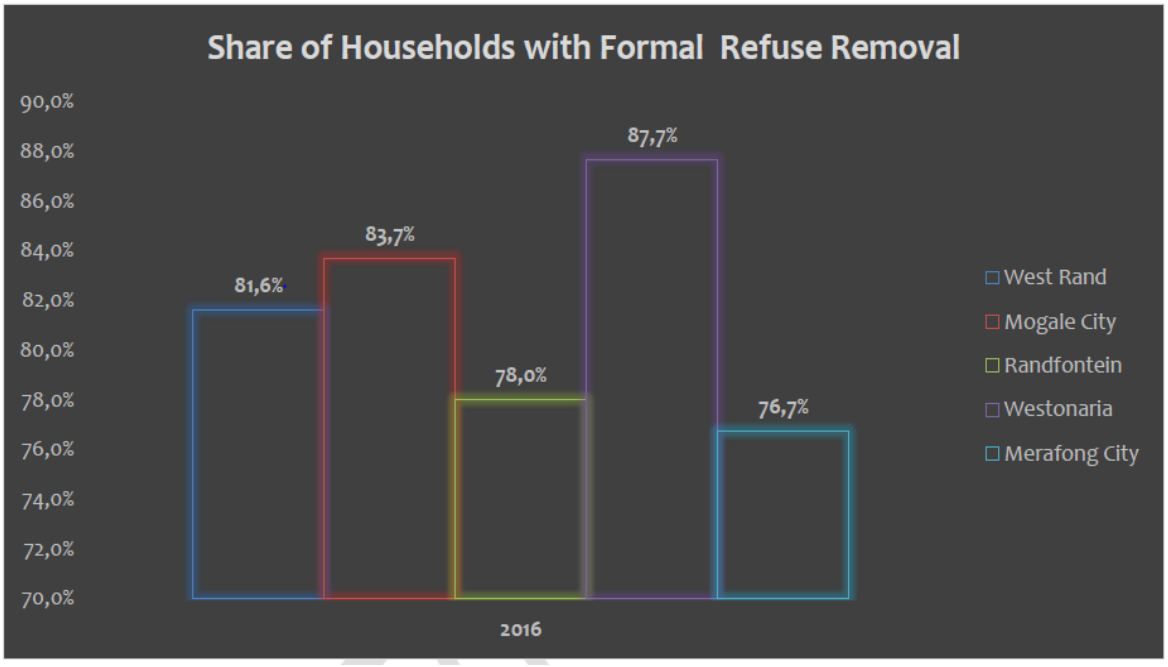

Figure 2-1: Population density of MCLM as compared to the WRDM (WRDM, 2017/18)

These emit greenhouse gases (GHGs), methane (CH_4) and carbon dioxide (CO2). Other landfill sites form part of the mines' operational areas managed and controlled by individual mining houses.

2.1.1.3.2 Agricultural Sector

Agricultural activities emit wind eroded dust, crop burning residue, chemical spraying, emission from manure, fertilizer and crop residue. These result in emission of CH_4, CO NO_2 and increased dust levels in the area (Gondwana Environmental Solutions, 2006). The emission factor of 0.2 kg/ha/hr (SKM, 2005) calculations confirmed that Merafong City Local Municipality (MCLM), which contained the largest surface area of (47%) contributed to the highest PM_{10} load per year (80045 tonnes per annum(t/a)) as compared to Westonaria (26%), Randfontein (20%) and Mogale City (7%) having PM_{10} loads of 4453, 34212 and 11512 tons per annum respectively (WRDM, 2010).

2.1.1.3.3 Mine Tailings Dams, including TSFs

Merafong City Local Municipality Area hosts the greatest number of TSF's within the WRDM region, with 23, followed by Mogale City (14), Westonaria (11) and Randfontein (2) (WRDM, 2011, Merafong IDP, 2018/2019). Even though most TSF's are active or being reclaimed and others dormant, many of these structures are not properly covered, and it has been reported that TSFs within the area result in significant dust liberation during windy conditions (WRDM, 2013).

2.1.1.4 Mobile Sources

2.1.1.4.1 Transportation

Mobile sources present the main atmospheric pollution within urban environment, contributing to atmospheric hydrocarbons, CO, NO_X, SO_2 and particulates (Gondwana Environmental Solutions, 2006). PM_{10} emissions from vehicular movement on dirt roads within the study area outweighed all the other contributors of PM_{10}. Criteria pollutants relating to petrol consumption has been found to be the most significant contributor to air pollution within the region. Furthermore, road transportation presented the most significant influencing factor of C_6H_6 emissions (WRDM, 2010). Recent studies confirmed the road transportation within one of the highly mining dominated hotspots as per Table 2.2 below.

Table 2.2: Roads dust contribution per type (AGA, 2016)

Source ID	**Silt content of road material**	**Average Vehicle Weight**	**No. of trips per day**	**Road Length**	**Width**	**Area of Road Segment**	**Estimated VKT**	**TSP Emissions**	**PM10 Emissions**
	%	(tons)		**(km)**	**(m)**	**(m^2)**	**(Km)**	**tpa**	**tpa**
Primary Road	11	2	43	22.42	9	201 799	44.93	17.76	5.34
Secondary Road	11	2	71	37.22	9	334 967	48.34	19.11	5.75
Tertiary Roads	11	2	20	8.05	9	72 488	10.23	4.04	1.22
TSF Roads	11	2	15	22.21	9	199 878	22.21	8.78	2.64

The above stated confirmed that wind erosion contributes the highest precipitant dust deposition (99%) from TSFs and the greatest $PM_{2.5}$ group contributor being point sources (79%) (AGA, 2016).

2.1.2 Environmental impacts from dust

The population growth, subsequent economic and industrial evolution have had a significant impact on urban and rural air quality of the world due to the use of chemicals. Studies have reported a 10-fold increase in the global output of chemicals worldwide (World Health Organization, 2010). Thus, elevated concentrations of toxic air pollutants like heavy metals and emissions from power generation, industrial sources, traffic and transport vehicles, mining and from anthropogenic activities have significantly contributed to reduced levels of clean air quality and deterioration of the environment. On the other hand, natural processes such as volcanic eruptions, forest fires, sea-salt emissions and biological processes have also contributed to deterioration of the air quality. Yet, the most significantly detrimental effects from emissions into the atmosphere are man-made or anthropogenic sources.

The main concern for both developed and developing countries is the pollution and impacts of chemicals and metals from anthropogenic sources, with the developed countries faced with air pollution in big cities and industrialized areas (Fashola *et al*., 2016). Metals such as iron, copper, zinc and molybdenum are essential in the biological functioning of the human system within certain concentrations while at higher concentration pose human health risk and environmental hazard. Studies have reported the relations between metal exposures and their adverse effects both in developing and developed countries. In the developed world, cognitive abilities of children have reduced from 40 µg/dL to the current <10 µg/dL due to lead exposures (Simeonov et al, 2011; Amodio *et al*., 2014). Ongoing research however recorded cognitive impairments due to lead exposure even at low exposures (American Academy of Paediatrics Committee on Environmental Health, 2005; Centre for

Disease Control and Prevention (CDC) Advisory Committee on Childhood Lead Poisoning Prevention, 2007). Fashola *et al.*, (2016) reported that in the developing world, there is still paucity of scientific data on the impacts of lead exposures to sensitive environmental groups

According to the United States Environmental Protection Agency (USEPA) and other environmental agencies, criteria pollutants posing major environment concerns include ozone (O_3), atmospheric PM (PM_{10}, $PM_{2.5}$), lead (Pb), carbon monoxide (CO), sulphur oxide (SO_2) and nitrogen oxides (NO_x). Heavy metals used in many anthropogenic sources are released into different environments such as water, vegetation, soil and air. Due to their chemical form and physical characteristics, heavy metals adhered onto atmospheric particles can travel long distance and have adverse effect on human health.

Fashola *et. al*., (2016) reported that approximately 1400 metric tons of mercury used by artisanal small-scale gold miners (ASGM) resulted in an annual average of 1000 metric tons of inorganic mercury emission into the environment of which one-third goes into the air and the balance mix with tailings, soil, and watercourses. Additional mercury got liberated in the reclamation of gold mine TSF's (Pacyna *et. al*., 2010). Mine dusts include solid airborne particles, often formed by operations, mainly grinding, crushing, milling, and sanding. Characteristics of dust such as particle size and chemical components differentiate between inhalable and respirable dusts and the nature of the hazards they present. Radioactive dusts are emitted from geogenic and anthropogenic sources. Geogenic radioactivity results from the presence of Earth's crust's radionuclides or from the interaction of cosmic radiation with

atmospheric gases. Anthropogenic radioactive emissions result from atomic energy industry, nuclear weapon explosions and plants, producing uranium and thorium (Maduna & Tomašić1, 2017).

A study by Piechota *et al. (*2002) has cautioned that dust impacts from TSF's depend upon dust composition, application rates and interactions with other environmental components. These include: (1) surface and groundwater quality deterioration; (2) soil contamination; (3) toxicity to soil and water biota; (4) toxicity to humans during and after application; (5) air pollution; (6) accumulation in soils; (7) changes in hydrologic characteristics of the soils, and (8) impacts on native flora and fauna populations.

Major transport pathways for contaminants in the environment include air, water, soils and biota as suggested by Csavina *et al*., (2012) and shown in Figure 2-1 below. The main transport pathway for air contaminants is initiated by direct transfer of up to 60 µm airborne particle size. Once suspended, these contaminants can be redistributed in the environment either from point sources or by dispersed sources swayed by increased land use activity and projected climate change (Csavina *et al*., 2012).

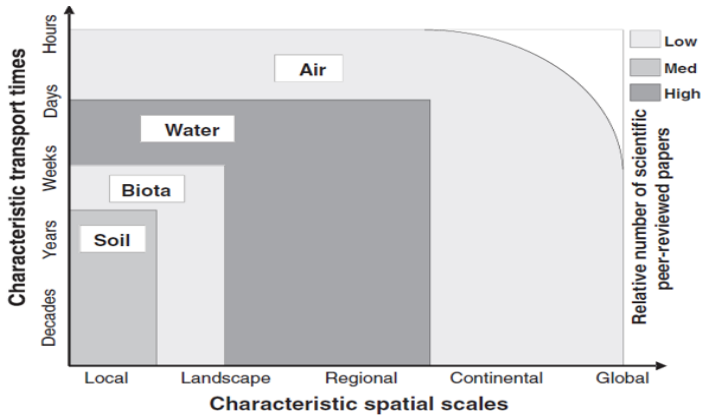

Figure 2-2: Illustration of contaminant exposure pathways media and spatial extent (Csavina *et al*., 2012)

2.1.2.1 Ambient air dust pollution

Ambient air quality is defined by the physical and chemical measure of pollutant concentrations in the ambient atmosphere to which the general population will be exposed. Industrialized countries have recorded serious deterioration of ambient air quality of mostly urban areas, exposing populations to pollutant levels above the recommended limits (UNEP 2002). The set limits as per World Health Organization's (WHO) and other international guidelines (WHO, 2000) suggested elevated outdoor air concentration which could result in adverse health and environmental effects.

2.1.2.2 Environmental impacts of TSF dust

Dust from active and dormant TSF and dams, through wind erosion, can transport environmental contaminants such as metals and metalloids, pesticides, and biological pathogens, all of which are typically associated with finer atmospheric particles and tropospheric aerosols (Pope *et al*., 1996; Griffin *et al.*, 2001; Csavina *et al.*, 2011; Yalala, 2015). These pollutants get dispersed by wind and lighter dust sized particles persist long enough to pose problems in distant areas, resulting in trans-boundary pollution (Hunter *et al*., 2002; DEA,2016).

The effect of prevailing winds in redistribution of contaminants could lead to soil accumulation of metals and metalloids a distance away from the source (Taylor *et al.*, 2010; Sanchez de la Campa *et al*., 2011). People living downwind of mine tailings were exposed to the potentially inhalable trace metal and metalloid-bearing particles.

The Witwatersrand Mining Basin of South Africa is the oldest mined area and the world's largest gold and uranium mining basin. It is formed by the Eastern Basin, the

Central Rand Basin, the Western Basin, the Far Western Basin, the Klerksdorp, Orkney, Stillfontein and Hartbeesfontein (KOSH) Basins and the Free State gold mines (Liefferink, 2019).

Yalala (2015) hinted that dust from tailings dams is a major contributor to poor quality ambient air in the Witwatersrand, especially from abandoned mine tailings (Annegarn *et al*.,1990; Annegarn, 2011). Gold TSF dust adversely affects amenities, human health and the environment of the Witwatersrand region. Dust deposition is primarily formed by coarse or settleable PM of more than 30 μm diameter and forms approximately 40% of dust from mine source materials. While settleable dust can impair visibility when it forms dust plumes, its nuisance effect has been noticed upon deposition on fabrics, buildings, vehicles, and water tanks (Oguntoke *et al.,* 2013).

2.1.2.3 Water contamination

Infiltration of water through sulphide-containing tailings material, leaching enormous volumes of Zn^{2+}, Ni^{+}, Pb^{2+}, As^{2+}, Cu^{2+} and sulphates into the stream and river ecosystem surface and underground water, resulting in AMD contamination (Edwards *et al*., 2000; Durkin and Herrmann, 2016). Studies have reported high sulphates, low pH, and high metal contents in ground water in the vicinity of TSF (Vega *et al*., 2004). According to Rafiei *et al*. (2010), pH value of 7.35 was recorded in gold mine tailings in Iran, whereas Mitileni *et al*. (2011) reported pH values of 3.25–6.28 in South Africa and Harish and David (2015) pH value of 3.48–8.12 in India. These highly acidic pH in acid mine drainage due to gold mine concur with findings from other studies by Naicker *et al.* (2003) and Tutu *et al*. (2008).

2.1.2.4 Land contamination

Gold mining activities in the Witwatersrand basin can result in contamination of the ecosystem (Kneen *et al*., 2015; Feshola *et al*., 2016; Kumpiene *et al*., 2017). So far, approximately 270 tailings storage facilities (TSFs) have been commissioned, covering an area of about 180 km^2 (Rösner *et al*., 2001). According to Sutton (2008), 88% of the mine residues deposits (MRD) including TSF's are found within 1000 m of formal residential areas, with 71% within 500 m buffer zone. In some cases, informal settlements, and industries like Selby and Booysens have been built on tailings footprints (Maseki, 2013).

A third (35%) of TSF's are located within 1000 m of agricultural land; with a quarter (23%) within 500 m. Impacts of dust from TSF's include acidification and salinization of soils, whereas impacts on crops include smothering, toxicity, and reduced yield. Some plant species accumulate metals to potentially toxic levels (Marschner, 1995), and plants on tailings and AMD have elevated metal contents (Weiersbye *et al*., 1999; Weiersbye & Witkowski; 2003).

2.1.2.5 Soil contamination

TSF's are inhospitable environments for plant growth, and various combinations of leaching, liming, fertilization and irrigation are used to facilitate the growth of a small suite of herbaceous, mostly pasture species (Sutton, 2008; Yalala, 2015). As per Halliday (1978), the grass cover can only be temporarily achieved, and the methods have been proven to be economically and ecologically unsustainable (Witkowski & Weiersbye, 1998a, b).

TSF's poor soil structure is nutrient deficient due to lack of organic matter, making vegetation unadaptable to the conditions for survival for long periods. Thus, tailings soil becomes exposed to wind and rain erosions, consequently loading the surrounding receptors (humans, animals, water and vegetation). Soils contaminated by AMD has a lower pH (4 - 6) and results in acidic to strongly acidic medium in soil profiles.

Most TSF localized topsoil is contaminated with increased levels of heavy metals such as cobalt, nickel, zinc and sulphur (Rösner & Schalkwayk, 1999). Hence, permanent soil degradation creates challenges in determining future land use, as only acid-tolerant plants can be grown in acidic soils. Heavy metals from contaminated soil are taken up by plants to humans and animals via food chain biomagnification. Evidence of severe risks for the agricultural and livestock industries have been recorded in the Witwatersrand area causing severe health problems and the degradation of ecosystems (Ochieng *et al*., 2010).

Although grassing and irrigation of tailings dam slopes significantly abates wind-borne erosion in the short term (Blight 1991), long-term erosion control and containment of water pollution from gold TSF by grassing was unsuccessful (Reichardt, 2012). Latest technologies such as phytoremediation of mitigating contamination have since been tested and implemented in some mines, presenting some work in progress.

2.1.2.6 Impacts on biodiversity

Particulate matter (PM) deposition and effects on vegetation include (1) nitrate and sulphate and their associations in the form of acidic and acidifying deposition and (2)

trace elements and heavy metals, including lead. TSFs contain amounts of sulphate, chloride, metal, and NORM which could potentially contaminate crops, soils, surface water and groundwater regimes (Philips, 2007). The areas located within or on land contaminated with TSF material can be evidenced by loss of biodiversity and disturbed ecosystem (Weiersbye & Witkowski, 2007).

Soils around the tailings have shown to have low organic matter (OM) content, highly acidic and have poor nutritional to the plants within the area (Ngole-Jeme & Fantke, 2017). Wind-blown dust originating from polluted soil disperse trace metals which get trapped on plant's leaves or be adsorbed by soil particles and taken up by the plants, thereby negatively affecting microbial activities. Arthropod, mammal and bird populations are also negatively affected. Arsenic (As) doses of 17 mg/kg to 48 mg/kg body weight (BW) were fatal to birds, whereas some mammals were negatively affected by As doses of 2.5 mg/kg BW after oral exposure from elevated levels of polluted soils (Migliorini *et al*., 2004; Gall *et al*., 2015, Ngole-Jeme & Fantke, 2017).

2.1.2.7 Socio-economic aspects

Studies of population growth projection for the Sub-Saharan Africa predict a 2.4% increase between 2000 and 2020, which is higher than other developing countries and developed world, at 1.3% and 0.1% respectively. This estimated that African cities will have an influx of 150 million residents in excess due to high rates of rural-out migration, with South African mining gold initiating a rapid population escalation since the discovery of gold in the 1890's (Kleen *et al*., 2015).

The 1950s marked an era of rapid socio-economic growth and urbanization of most part of the Witwatersrand Basin with rapid urbanization. Pre- 1994 in South Africa, no

policies and enforcements preventing human settlement development restrictions within a certain distance away from TSFs were in place. Human settlement practices by the apartheid regime and population growth post 1994 led to increased settlements encroachment within the TSF buffer zones, exposing inhabitants to greater risks than before (Ojelede, 2012). This led to intensifying human exposure to windblown mineral dust and public health concerns associated with exposure to airborne mineral quartz dust (Kneen *et al*., 2015).

In South Africa, most TSF complexes are not fenced making them accessible for uses such as children's informal playgrounds, recreation (quad-bikers) and as places of spiritual significance, thus exposing the public to the TSF dust heavily laden with toxic metals and metalloids (Sutton, 2008). Elevated concentrations of heavy metals such as Al, Co, Cu, Mn, Ni, U and Zn were also observed within very close proximity areas to active TSF's in the Witwatersrand (Tutu *et al*., 2008). Furthermore, ever increasing erosion and dust emissions, the increased hand-to-mouth activity through ingestion exhibited by young children have been commonly taking place posing them to particularly high risk of metal toxicity (Sutton *et al*., 2006).

Several complaints cases of dust exposures emanating from TSF impacting surrounding residential areas, and related health risks were previously lodged against mining houses (Lawyers for Human Rights, 2017; Liefferink, 2019). The Meadowlands Community and Environmental Group lodged a court case based on the dust emission from the nearby TSF's and the Riverlea community resulting in court interventions (Scorgie, 2006).

While dust episodes were constantly present in these areas during spring (August, September and October), the dust was mainly coarse, settleable particles which were not inhaled and remained primarily a nuisance. However, since 2002, advanced technologies linked to finer milling and generation of inhalable TSF dust transformed this nuisance into a health hazard. This called for an urgent need to invest in dust suppression, education to the locals on subsequent damaging effects and optional dust mitigation measures.

2.1.2.8 Visual impacts

The reduction in visibility caused by dust storms is a hazard to aviation, rail and road transport and many experiences were noted throughout the world. The severe pre-frontal storm of 7 November 1988 in South Australia, triggered road and airport closures across the Eyre Peninsula (Crooks and Cowan, 1993). In the United States (U.S), in November 1991, a series of collisions involving 164 vehicles occurred on Interstate 5 in the San Joaquin Valley in California (Pauley *et al*., 1996), while in Oregon a dust storm in September 1999 set off a chain reaction of 50 car crashes that killed eight people and injured more than 20 (State of Oregon, 2004). Studies have confirmed deserts, arid environments as perennial carriers of aeolian dust (Ojelede, 2012). These can be transported to reach distances of 10 000 km away from the source (Ojelede, 2012).

Volcanic eruptions result in thick haze fog of varied sized particulate matter, impacting on visibly observed in a form of floating dust, blowing dust, sand dust storm and severe sand dust storm (National Weather Bureau of China,1979; Yang *et al*., 2008). The varying horizontal visibility of floating dust (associated with light breeze), blowing dust

events, strong dust episodes and severe dust storm from <10km, 1km-10km, 500m-1 000 m and < 500m (Chen *et al.,* 2004).

Pinto *et al*. (2002) argued that quarries and TSF dusts can be visually intrusive from prominent landscape positions and their high colour contrasts making them highly noticeable from far-away distances. This could result in the loss of visual integrity on the natural landscape within nearby urban environments. TSFs occupy large extents of surrounding pieces of land are left un-rehabilitated and thereby permanently altering the visual landscape of the area due to their height and size (Sutton & Weiersbye, 2008).

Furthermore, their height in physical design structure as well as the colour of tailings material, TSFs are highly visible from key viewpoints posing significant visual intrusion and blocking clear lines of sight and from unsightly new landmarks. TSFs alter character of the countryside, individually and cumulatively, causing devastating visual effects. Severity of TSF during mining planning and historic impacts for existing structures on the surrounding environment need careful considerations (GDACE, 2006).

According to Greyling (2001), sensitivity of public perceptions and the potential for corporate social risk is usually directly linked to the sensitivity of the receiving environment. Potential impacts to areas with spiritual sense or “sense of place” as well as past environmental neglect by government or the proponent, or by other similar industry in the area.

TSFs dust may pose concerns as a nuisance and detrimentally influence the ecology and agricultural potential of a region. TSF dust deposition influenced by concentration of dust particles in the ambient air, their size distribution, the deposition rate and the geochemistry may have negative effects on the agriculture and ecology of an area. The meteorological and local microclimate conditions have also reportedly been changed by dust occurrence (GDARD, 2012).

In South Africa, a set of guidelines were published by government specifying precipitant dust deposition categories and limits that must be adhered to as shown in Table 2.3 below. Even though slight settleable precipitant dust deposition is barely visible to the naked eye, heavy and very heavy settleable precipitant deposition dust can be easily visible when the surface was not cleaned.

Table 2.3: Settleable precipitant deposition dust levels published by DEAT (1994)

Classification	**Settleable precipitant deposition dust (averaged over 1 month)**
Slight	Less than 250 mg/d/m^2
Moderate	250 to 500 mg/d/m^2
Heavy	500 to 1 200 mg/d/m^2
Very heavy	Greater than 1200 mg/d/m^2

This suggests that repeated levels more than 2000 mg/m^2/day will constitute legal offence (Olalde, 2015; Ngole-Jeme & Fantke, 2017) forming a layer of dust thick enough to allow a person to “write’ words in the dust surface with their finger. Numerous public complaints claiming health effects were previously lodged with local authorities and have since rekindled due to repossessing of TSFs within the area (Ojelede, 2015).

2.1.2.9 Radiation Impacts

Atmospheric aerosols play a vital role in the radiation budget of the Earth-atmosphere system by scattering and absorbing part of the incoming solar radiation and by modifying the cloud droplet size distribution, thereby changing the radiative properties and lifetime of clouds (Koren *et al.,* 2004). Direct scattering of solar radiation by dust aerosol particles may cause a change in the vertical temperature profile, cloud properties and precipitation.

Mining tailings storage facilities, as heavy mineral deposits, are often associated with naturally occurring radionuclides. Radionuclides such as uranium(U), thorium (Th) and radium (Ra) may form part of heavy minerals or be present as separate mineralized grains. Heavy mineral deposits exploitation activities lead to increased concentrations of naturally occurring radionuclides in the environment during transportation movements, thereby exposing humans (Sykora *et al.*, 2017; Dudu *et al*., 2019). Technologically Enhanced NORMS (TENORMs) are mainly anthropogenically induced from mining, burning of coal, etc., resulting in increased radionuclides (Dudu *et al*., 2019)

The typical background concentration of uranium in the earth's crust is 2-4 parts per million (grams per ton; g/t), whereas the overall average uranium grade of 1952-1988 production from the Carbon Leader Reef (CLR) on the Far West Rand was 145 g/t, with grade averages for other individual ore reefs in the West and far West Rand ranging between 51 g/t and 383 g/t (Coetzee *et al*., 2006). Since uranium was not extracted as a by-product of goldmining prior to the 1950s, nor at many Witwatersrand

gold mines outside the western region, the bulk of uranium from the mined reefs were left as TSF surface residue, (Coetzee *et al*., 2006).

Human exposure pathways to radiation emitted from mining and mineral processing activities according to the International Atomic Energy Agency (IAEA, 2002) include, a) atmospheric pathways through inhalation of airborne gases (e.g. radon and its progeny) and airborne radioactive particles, b) atmospheric and terrestrial pathways through ingestion of contaminated soil and foodstuff and external radiation; and; c) aquatic pathways in which there is ingestion of contaminated water, foods produced using contaminated irrigation water, fish, and other aquatic biota, food derived from animals drinking contaminated water, and from external radiation. The potential sources and mechanisms of contaminant releases include the atmospheric, surface water, groundwater and external (gamma radiation) pathways (Van der Blerk, 2015).

The individual dose limit for public radiation exposure in planned exposure situations is 1 mSv/year. In special circumstances, an effective dose up to 5 mSv in a single year if the average dose over five consecutive years does not exceed 1 mSv per year, can be applied. The International Commission on Radiological Protection (ICRP) recommends equivalent dose limits of 15 mSv in a year to the lens of the eye and 50 mSv in a year to the skin (Van der Blerk, 2015). South Africa has adopted the criteria of 1 mSv in a year for public protection as specified in Regulation No. 388 and consistent with the ICRP and IAEA recommendations for public exposure.

2.1.2.10 Health impacts

Indoor and outdoor air pollution has been ranked the world's 4th largest contributor in terms of the number of deaths by risk factor, as shown in Figure 2-3 below (Institute for Health Metrics and Evaluation (IHME), 2017). In 2017, air pollution was responsible for an estimated 5 million deaths globally, accounting to 9% (nearly 1-in-10) deaths, especially in low-income countries (Ritchie, 2017). Premature death estimation of 7 million people per year due to air pollution related diseases (strokes, respiratory illnesses and cancer) have been confirmed (WMO, 2018). This is due to air pollution exceedances above safe limits in most world's major cities (WHO, 1999).

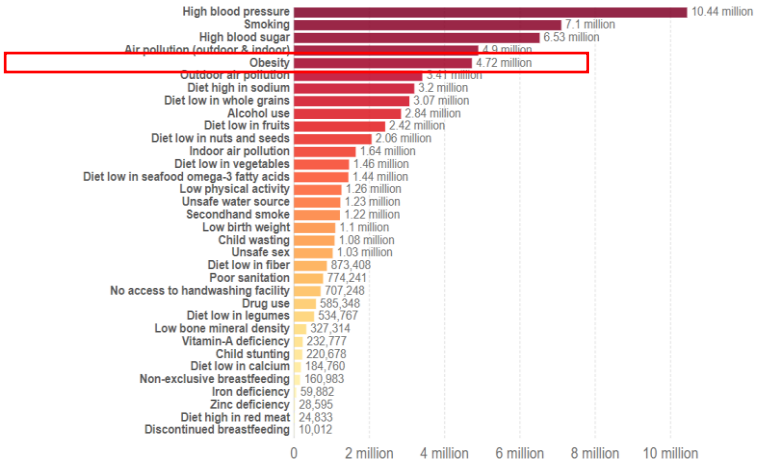

Figure 2-3: Total annual number of deaths by risk factor, measured across all age groups and both sexes World 2017 (Source: IHME, Global Burden of Disease)

The physiological effects of dust on human health are some of the major issues for any mining operation as certain types of dust can negatively affect working conditions (Petavratzi *et al.,* 2005). Long term exposure to excessive amounts of dust through inhalation, ingestion and dermal contact poses health risks on human health resulting from highly toxic chemicals, with high concentrations in TSF dusts (Newman, 2001; Sipes and Badger, 2001; Maseki, 2013). Such constituents include minerals and

chemicals like feldspar, quartz, silicates, sulphates and heavy minerals and cyanide species (Claqui, 1999, Aucamp, 2000; Rosner & van Schalkwyk, 2000; Rosner T., 2001; Naicker *et al*., 2003; Bakatula *et al*., 2008 Tutu *et al*., 2008). Silica, asbestos, clay minerals, highly radioactive material, and erionites are popularly highly toxic and linked human health effects (Fubini and Otero Areàn, 1999). This link is also shown in Table 2.4 below.

Table 2.4: Typical mineral-containing dust and linked health impacts

Minerals	**Sources of origin**	**Health effects**	**References**
Feldspar, quartz, clay minerals, cristobalite	Mining, industrial activities, eroded materials	Pulmonary fibrosis, silicosis, silicotuberculosis, cancer	Clausnitzer & Singer, 1999; Fubini & Otero Areàn, 1999; Smith & Lee, 2003; Plumlee & Ziegler, 2006
Asbestos (Amosite, crocidolite, tremolite, anthophyllite, actinolite, Chrysotile or white asbestos,	Mining, industrial and commercial products and activities, erosion	Asbestosis, lung cancer, pleural effusion, thickening plaques, mesothelioma	
Erionite	Mining, erosion	Asbestosis, lung cancer, mesothelioma	

The most sensitive and vulnerable groups are people with heart or lung diseases, especially children and the elderly either due to their compromised or developing immune systems (Maseki, 2013; Nkosi, 2017, Wright *et al.*, 2018). Children are particularly susceptible, showing symptoms of acute respiratory infections, like coughing, phlegm, bronchitis, which account for an estimated 1.3 million deaths each year in children under 5 years of age, where 43% occur in Africa (Walker *et al*., 2013). While elevated asthma cases were recorded within the period 1990 to 2012 in Africa, childhood respiratory infections became prevalent in HIV patients in South Africa

(Adeloye *et al.*, 2013; Annamalay *et al*., 2016). However, high health risk dust exposure cases and were recorded even the healthiest human beings with noted temporary symptoms due to high level exposures.

High exposures to heavy metals may pose damaged nervous system functioning, blood composition, lung functioning, kidney, liver and body tissues and organs (Occupational Safety and Health Information Centre (OSHIC), 1999). Symptoms such as headaches, anger, irritability, depression, asthma, multiple sclerosis and Parkinson's disease could occur due to heavy metals exposure (Fairbrother *et al*., 2007; Chapman, 2008). The Witwatersrand Basin's gold TSF's also contained quartz as per several studies and cases of silicosis were reported (Belle, 2005).

The effect reported during these storms included soiling, reduced visibility, irritation of the eyes, and ingestion of PM (Bullock, 2006). The size of PM affects distribution of dust, the depth of penetration and deposition in the respiratory system. The adverse health effects of $PM_{2.5}$ a respirable fraction of PM was recorded, which can easily be deposited in the alveoli of the lungs, negatively affecting the whole body. Whilst PM_{100} particles can be retained in the nasal cavities, $PM_{0.1}$ can deeply penetrate the respiratory system, alveoli and be absorbed by the body system (Yalala, 2015). Studies reported that trace metal absorption efficiency ranging from 60-80% result in the impairment of the physiological function of the lung based on bioavailability of toxic metals (Espinosa *et al*., 2001; Yalala, 2015).

2.2 Studies conducted in relation to the characterization of TSF dust

2.2.1 Dust deposition rates

Many studies explored the determination of concentration in settled particles, including comparative analysis of the atmospheric deposition rates in Central China and of the world (Gao *et al.,* 2017). These revealed that the annual dust deposition fluxes in China were ranked the highest in the world due to anthropogenic sources such as biofuel burning, heavy traffic, sand deposition and climatic contributions (Gao *et al*., 2017).

Comparative studies were conducted on site-specificity, seasonality, and daily variability of settleable particle concentrations between urban and harbour sites in Taiwan, which confirmed higher levels in harbours (Gao *et al*., 2017). Furthermore, deposition flux at a harbour site was 3 times higher in winter than in summer, which were similar findings by Soriano *et al*. (2012), for industrial sites in Spain. According to Querol *et al*., (2008), erosion and transport of common soil minerals by means of wind and African dust episodes are mostly reported in the Mediterranean.

In South Africa, patterns of dust deposition rates, meteorological influences, and relations to factors such as particle size distribution were published by various authors. These authors observed the spring months as the most critical periods for dust storm episodes or high dust periods in the Witwatersrand Basin, subject to weather events (Oguntoke *et al*., 2013). However, wind speed, humidity and precipitation influenced atmospheric aerosols in Japan (Chang *et al*., 2006). Similar recent study by Yassen (2000) established a direct link between precipitant dust fallout with rainfall, humidity, windspeed and temperature in Kuala Lampur, Malaysia. Other factors of influence

included type of monitoring equipment used, topography, vegetal cover, brittleness and hardness of the material, and speed and frequency of transport equipment (Mishra & Shambhu, 2010).

Dust from TSF posed a major contributor to poor quality ambient air in the Witwatersrand Basin, especially from abandoned structures (Mpanza *et al*., 2020). Periodical dust storms were reported during the months of late July to early October (spring months), where wind speeds exceeded 7 m s^{-1} were experienced (Ojelede *et al*., 2012). PM_{10} concentration with 2160 µg m^{-3} daily maximum with weekly average of 508 µg m^{-3} for the 7-day period (Ojelede *et al*., 2012) were recorded. These very high dust fallout depositions result in soiling, reduced visibility, irritation of the eyes, and ingestion of particulate matter, and could have adverse human health effects too (Yalala, 2015).

Subsequent increases in the incidences of wind erosion from TSFs in dust prone areas led to the development of set of regulations for precipitant dust deposition. Between August and October of 2007, exceedances of precipitant dust deposition beyond the ALERT level (2400 mg m^{-2} day^{-1}) on two sites and several exceedances (above 1200 mg m^{-2} day^{-1}) on other sites from the Durban Roodepoort Deep (DRD) TSF's were recorded (Annegarn, 2007; Yalala 2015). This data emphasized TSFs as significant sources of increased air pollution levels, the dispersion and distribution of toxic metals and metalloids contained within the dust. Cumulatively, dust concentration exceeding 5000 mg m^{-2} day^{-1} were reported for unrehabilitated TSFs (Mpanza *et al*., 2020).

The design nature of large and steep TSFs from gold mining operations, without the necessary precautions, created optimal conditions for wind erosion. Factors such as the height of the sand dumps and slimes dams, the texture of the TSF's material and the alignment of the TSF's with the prevailing winds increased the susceptibility of the TSF to wind erosion. direct correlation between the wind speed and the sand dumps height (Yalala, 2015).

In the Witwatersrand Basin region, studies of particle size distribution and characterization of mine dust were undertaken, even though determining factors on dust episodes occurrence and the resultant issues from public complaints lacked enough scientific backup (Ojelede *et al*., 2008). However, recent studies confirming that multiple occurrences of quartz rich inhalable dust and heavy metals in residential settings at levels that exceed occupational health standards represent in the mine dust (Kneen, 2015; Ojelede, 2015; Yalala, 2015).

2.2.2 Dust mechanics and movement

According to Lyles (1988), wind erosion occurs in four basic mechanisms, i.e., initiation, transport (suspension, saltation, and surface creep), abrasion, sorting and deposition of soil aggregates and primary particles. It is primarily influenced by atmospheric conditions (e.g., wind, precipitation and temperature), soil properties (e.g., soil texture, composition and aggregation), land-surface characteristics (e.g., topography, moisture, aerodynamic roughness length, vegetation and non-erodible elements) and land-use practice (e.g., farming, grazing and mining) (Shao, 2008).

For wind erosion to be generated, the threshold velocity should be exceeded by the wind speed in relation to gravity and the inter-particle cohesion that resists removal. While soil texture, soil moisture and vegetation cover influence the removal potential, the friction velocity or wind shear at the surface determine atmospheric flow conditions and surface aerodynamic properties. High wind shear at the surface must exceed the gravitational and cohesive forces upon them, resulting in either suspension or saltation of smaller and larger dust particles respectively by wind (Shao, 2008). Movement of particles include rolling along the surface by direct wind pressure for about 30 cm before starting to bounce off the ground, by pushing other soil particles within their vicinity (Marticorena, 2014).

2.2.3 Dust settling velocities

Studies of particle settling velocities presented an understanding of sediment transport and movement of the particle suspension, deposition, mixing and exchange processes (Zhiyao *et al*., 2008). Sánchez (2016) emphasized the understanding of the permanence time of heavy particles inside a 3D vortex as crucial in many areas of science and technology. Settling patterns of particles in different media were studied extensively, using mathematical equations considering shape, size and densities. Various numerical predictions and experimental studies (Kelessidis & Mpandelis, 2004; Shah *et al*., 2007) are available in literature to determine the drag force on a sphere in inelastic power-law fluids. This was achieved by using theoretical predictions of drag force in fluids as proposed by Tripathi et al. (2014) and Malhotra et al. (2014). Settling velocity of spherical particles or natural sediment particles in terms of the dimensionless grain size in a simpler form were expressed by different authors (Maggi, 2013).

2.2.4 Particulate Matter and particle size distribution composition

Global studies were conducted measuring PM composition, including source specific compositions and advanced measurements of individual particle characterization (Edgerton *et al*., 2006; EPA, 2006b; Ondov *et al*., 2006). Studies of particle size distribution have been published in many parts of the world. On average about 10% of the settled dusts having size <2 μm, about 80% having size between 2 and 50 μm, and 10% having size >50 μm were noted. Irrespective of dominance in small particles, due to their higher dry deposition velocities larger particles determine dry deposition rates (Gao *et al.*, 2017).

In China, PM_{10} and $PM_{2.5}$ monitoring mainly started at the end of the 20^{th} century, and most of these studies focused on the chemical compositions, i.e., elemental, major inorganic ions, and organic compounds constituents using tapered element oscillating microbalances model (TEOM) instrumentation (Ye *et al*., 2003; Guo *et al*., 2003)**.** Furthermore, Liu *et al. (*2014) employed this technique to read and quantify the PM_{10} and $PM_{2.5}$ concentrations and to investigate their concentration inter-relationships associations with gaseous pollutants (NO, NO_2, O_3, SO_2, and CO) and he then established those high concentrations of fine particles and ozone resulted in substantial and severe deterioration of air quality in Beijing due to high urbanization (Lui *et al*., 2014). This also established that both the traffic-related emissions and combustion sources were major contributors to the particulate, CO_x, NO_x, and that these were mainly dependent on the wind profile (Lui *et al*., 2014).

In South Africa, the gold mining industry has existed for over a century, particularly in the Witwatersrand Basin within which gold mining has taken place since 1881

containing the largest number of TSFs as waste deposit stockpiles. In the West Rand during wind events, strong dust emissions of small sized PM (<10) from gold mine TSFs is transported over long distances and deposited towards nearby agricultural land in the surroundings (Yalala, 2015). Thus, there is a need to monitoring the concentration of particulate matter in the surrounding environment.

2.2.5 Heavy metals

Comparative studies of dust deposition, fluxes, metal content and size distribution were investigated by many authors (Dudu *et al*., 2018; Nkosi, 2018; Mpanza *et al*., 2020). Fang *et al*. (2007) established that the average downward dry deposition fluxes of metallic elements (Fe, Zn, Mn, Cu, Pb, Cr, and Mg) were 218.0, 109.0, 194.3, 21.9, 56.0, 11.2, and 105.7 $\mu gm^{-2}\ d^{-1}$, respectively at Taichung Airport in central Taiwan. The results established that erosion of particles larger than 2.5 μm in size being influenced by high deposition velocities. The study recommended an overall estimation of the dry deposition determined by either coarse particle or total particle concentrations. Fang *et al*., (2007) further establish that average seasonal concentrations of Mn, Zn, Cr, Cu, and Pb in dry deposits were the highest in fall and winter and lowest in summer.

Studies were conducted to determine the influence of climatic conditions on heavy metal contamination in ambient air across various cities. These confirmed that the dry deposition for Izmir (Turkey) was 10–50 times higher for Cd, 4– 20 times higher for Pb, and 5–30 times higher for Zn than in Tokyo, Japan (Sakata and Marumoto, 2004; Muezzinoglu & Cizmecioglu, 2006). Elevated average total heavy metal

concentrations for Cr, Cd, Pb, Cu, Zn, and Ni in Izmir were higher than most sites around the world (Morselli *et al*., 2004; Sakata & Marumoto, 2004).

Similar fluxes of Cd, Cr, Cu, Ni, Pb, and V were detected in the Tokyo Bay area and in the Seine Estuary (Motelay-Massei *et al*., 2005) or the Pearl River Delta Wong *et al*. (2003) due to their highly industrial characters. However, these fluxes were much higher in Tokyo Bay than other aquatic regions in the US and Europe (Omodio *et al*., 2014). Sabin *et al*. (2006) showed that freeways presented a significant source of heavy metals (Cu, Pb and Zn) due to resuspension of road dust as vehicles at high speeds and from the tyre and brake from vehicles (Councell, 2004).

According to research conducted by the Desert Research Institute at the University of Nevada, an increase in vehicle speed of 10 miles per hour resulted in an increase in PM_{10} emissions of between 1.5 and 3 times. A similar study conducted by Flocchini *et al*. (1994) found a decrease in PM_{10} emissions of 42±35% with a speed reduction from 40 km/hr to 24 km/hr (Stevenson, 2004).

In South Africa, heavy metals, metalloids, alkali earth elements, and radionuclides have been found in the TSFs environment of the Witwatersrand Basin (Da Pelo *et al*., 2009). The total metal concentration in the Witwatersrand was reported to be in the range from 2 - 17 340 mg kg^{-1} (Tutu, 2005). Other studies confirmed that elements like As, Pb, Cd, Cr, Mn, Th, Zn and U occur in the gold mineral dust due to mining processes and chemicals used (Aucamp, 2000; Plumlee & Ziegler, 2006; Csavina *et al.,* 2012; Yalala, 2015). Immediate negative health effects of heavy metals exposures over 20 to 30 years include skin and lung cancer (Harada *et al*., 1997).

Studies of the state of surface and groundwater water pollution within TSFs localities over the years established useful baseline data of the Central Rand and the entire Witwatersrand Basin. Rand Water Board, Water Research Commission (WRC) and Crown Gold Recovery (CGR) joint study confirmed that the drainage systems on the East and Central Rand have been affected by salts-laden AMD (Tutu *et al*., 2011). The pH values ranging from 2 to 6.23 as observed by Nengovhela *et al*. (2006) but much lower than those reported by Tariq *et al.* (2016) within similar environments.

2.2.8 Land contamination

Gold mining TSFs occupy massive pieces of land which become sterile and useless post mining. According to Martin *et al.,* (2014), the number of abandoned mines is expected to increase worldwide, resulting in increased population and urban expansion. In the United States of America, 80% of an estimated 46,000 known abandoned mine sites require further investigation and/or remediation (Bureau of Land Management, 2013), whereas Australia registered more than 50,000 abandoned mines sites (Ministerial Council on Mineral and Petroleum Resources/Minerals Council of Australia, 2014). Mexico has recorded over 21.7 million hectares (ha) affected by mining activities whereas in China additional 2000 ha (Lottermoser, 2010) and 4000 Mt of tailings are stockpiled per year on new portions of land (Liao *et al*., 2007).

2.2.6 Toxicity of TSF dust exposure

2.2.6.1 Human health risk

Worldwide epidemiological studies have confirmed direct effects of short-term PM exposures with adverse health effects (e.g. decreased lung function and premature death in people with lung diseases) (Goldberg *et al*., 2013). Ambient PM may result in

a variety of human health deterioration like silicosis, pneumoconiosis, and increased risk of tuberculosis, lung cancer, scleroderma, and systemic lupus erythematous (James, 2011). The silica content of the gold mine TSF dust has been confirmed to result in the development of chronic bronchitis, emphysema, and air flow obstruction (American Thoracic Society (ATS), 1997; Wang *et al*., 1997). Cases of increased hospitalization, emergency room visits, and worst cases of mortality among patients of underlying respiratory ailments were recorded (Oguntoke *et al*., 2013).

For decades, epidemiological studies emphasized strongly on the health effects of PM_{10} exposures in terms of dose-response relationship on humans and have confirmed that the larger the dose passing into the body the more severe the outcome (WHO, 2000b). However, recent and advanced technology as well as instrumentation for monitoring fine and ultrafine particles revealed that $PM_{2.5}$ has become an emerging global concern. Increased patterns resulting from ever increasing population size, reliance on fossil fuel burning and transportation revealed new data requiring further investigations. For instance, epidemiological studies across Europe and the United States (US) have been undertaken with the object of linking $PM_{2.5}$ exposure and possible health risks (Martin *et al*., 2014). This led to policy developments and guidelines to set strict limits in controlling and managing the variables relating to health. Martin *et al*. (2014) established the link between arsenic exposures and health impacts in Australia. The study further advised that exposure to As and the long-term pulmonary bioavailability of As in PM requires serious consideration in health risk assessments. A study of paediatric blood lead levels in a lead mining area, Northern Cape Province in South Africa confirmed elevated mean blood lead levels (16 mg dL^{-}

^{1}) of children in lead mining communities than the levels in other rural area setup in other countries in the world (von Schirnding *et al*., 2003).

Studies of blood lead levels among children living in remote and isolated parts of the world, for example, the Himalayas and Papua New Guinea, had blood lead levels around 3–5 mg dL^{-1} (Piomelli *et al*., 1980; Poole *et al*., 1980). Epidemiological, as well as in vitro and in vivo studies showed adverse effects due to $PM_{2.5}$ exposures (normal ambient air and dust storms) on rats within two cities. The in vitro studies revealed a decrease in cell viability and an increase in damage to DNA of alveolar macrophages were found (Meng and Zhang, 2007). The same authors in in vivo studies established DNA damage to lung cells. These dose-dependent studies in vivo experiments revealed that oxidative and inflammation in human lung epithelial cells resulted from $PM_{2.5}$ exposures (Dagher *et al*., 2006).

Since 1960 South Africa has been responsive to the urgent needs to monitor and manage $PM_{2.5}$ exposures and the consequent health implications. The Department of Environmental Affairs and Tourism (DEAT, 2005) State of the Environment Outlook reported $PM_{2.5}$ as an emergent priority pollutant, however no supporting scientific data was available (DEAT, 2010).

The study by Morakinyo *et al*. (2017) investigated the extent of sub-10 µm PM exposures due to excessive high PM pollution levels in industrialized regions and urban areas of South Africa and that they contribute up to 30% of particulate pollution in the country. The study also linked PM exposures and respiratory, cardiovascular and cerebrovascular risks of children and elderly people living in the vicinities of the

sources of sub-10 µm PM and gaseous pollutants. Morakinyo *et al.*, (2017) recommended a comprehensive Human Health Risk Framework (HHRF) with proposed regulatory limits for public health, environmental and built infrastructure pollutants among industrialized and urbanized areas hosting activities of potential pollutants.

The link between silica dust exposures of mine workers and silicosis health risk within the global context was confirmed in many studies (Collins *et al*., 2005). Silica exists in nine different crystalline forms or polymorphs with the three main forms being quartz (the most common), tridymite and cristobalite. It also occurs in several cryptocrystalline forms. These include minerals such as quartz, feldspar, mica, amphibole, pyroxene, olivine, and a great variety of clay minerals, with differing toxicity levels (IARC), 1997). Some studies have been conducted implicating tuberculosis (TB) on immediate public exposures from industrial activities (Kootbodien *et al*., 2019). In India, elevated mean ambient PM_{10} silica concentrations were reported in areas near a pencil slate (41.1 gm^{-3}) and agate industry (57.2 gm^{-3}) compared to the control site 5 km away (3.5 gm^{-3}) as confirmed by Bhagia (2009).

Recent studies across the globe have raised concerns relating to the health impacts of PM_1 (GlobalCEH). These revealed an increased toxicity of PM_1, laden with 16 Polycyclic Aromatic Hydrocarbons (PAHs) compound, with average concentration of 160.16 ± 37.70 µg gm^{-3}) in India. Studies conducted in China revealed elevated risks for emergency hospitalization linked to an increase in PM_1 concentration. Similar studies in Turkey noted that even though of $PM_{2.5}$ and PM_1 were carriers of 23 elements (Na, Mg, Al, Si, P, S, Cl, K, Ca, Ti, V, Cr, Mn, Fe, Co, Cu, Zn, As, Rb, Sr, Y,

Mo, Ba), PM_1 concentrations were more prevalent in mass (GlobalCEH).

Even though comprehensive studies confirmed TB cases due to occupational silica exposure from gold TSFs in South Africa (Kootbodien *et al.,* 2019), recent studies reported elevated ambient PM_{10} and PM_4 crystalline silica levels in communities surrounding gold mine TSFs (Andraos *et al*., 2018). However, further study by Kootbodien *et al*. (2019) around this topic found no direct connection between pulmonary tuberculosis (PTB) risk association with occupational silica dust exposure on communities residing near the gold mine TSF within Gauteng.

An increased prevalence of respiratory disease was observed in people living near mining sites in both South Africa and Portugal, compared with a control group living further away (Nkosi *et al*., 2016). A few health analyses were carried out within the West Rand, Far West Rand and the North West Province, linking the health impacts on the nearby communities and gold mine TSF dust exposures. The resultant health issues included chronic respiratory diseases, with prevalence among adolescents of communities residing nearby (Nkosi *et al*., 2014) and elderly (Nkosi *et al*., 2015). Positive correlations between gold mine TSFs nearby communities and respiratory illness, exacerbated by smoking habits, low level of education and domestic use of gas or paraffin were thus established. This formed the basis of further epidemiological studies for communities living in close proximities to the mine TSFs.

Children residing in close proximities of mine TSF's in South Africa experienced upper respiratory infection related symptoms such as wheezing chest with runny nose, congested nasal passages and postnasal drip (Nkosi, 2018, Wright *et al.,* 2018), with

high prevalence of asthma within such areas as compared to less cases predominant mining areas. This concurred with related studies conducted around the similar topic within South Africa (Nkosi, 2018). However, no studies were conducted on adult asthma trends locally within South Africa and other developing countries for such comparisons.

The health risk exposure linked to these pollutants include cancer and non-cancer health complications associated with exposure to heavy metals via several ingestion- and dermal related pathways and via inhalation. This recommended toxicity characterization modelling in providing further insights, identifying and evaluating exposure reduction measures.

2.2.6.2 Radiation exposure

Studies showed that the U accumulation in the auriferous sediments was up to 1 000 mg kg^{-1} (0.1 %) and had 0.3 - 6 % (3 000 - > 60 000 mg kg^{-1}) in ore grades mined in Canada and Australia (McLean, 1994; Cole, 1998). Winde *et al*., (2004) determined the source of U in the aqueous and sediment media of Koekermoerspruit, in the Klerksdorp mining area in which sediments were sampled. The methods employed included determination of heavy metals by (ICP-MS) while for analyses of solid samples (AAS) was used. U concentration in water samples was determined by laser-phosphorescence at lower detection limit of 0.001 mg L^{-1}). The study revealed that transport of dissolved U from TSF presented major pathway for environmental contamination of stream water, groundwater, and sediments.

Studies have detailed the level of radiation within the Witwatersrand and the Far West Rand, but the focus was mostly slanted towards surface and groundwater resources, sediments but too little was documented on radiation levels in dust particulate matter (WRC, 2003). For instance, Tutu *et al*. (2005) established that there was mobilization of metals and U in the hydrological system of the Central Rand, Witwatersrand.

The Wonderfonteinspruit Catchment Area (WCA) has been identified a hotspot area of radioactive pollution within the Witwatersrand, posing serious threat to local communities due to high U exposures (WRC, 2009). Gold-bearing ores of the area contained almost ten times the amount of U than the gold, making it the most radioactive area in South Africa (GDARD, 2012). Since 2002, decanted water loaded with sulphates and radioactive material from Tweelopiespruit and Krugersdorp area resulted in increased contamination into the Rietspruit and Blaauwbankspruit channels (Liefferrink, 2011).

Inhalation of Rn-22 daughter nuclides from radon emissions pose potential significant radiation exposure on mining legacy sites and residential areas. Furthermore, ingestion exposures occur through consumption of contaminated crops as radiation contaminated dust is deposited on leaves of vegetable and forage plants, and from other related agricultural activities. Studies confirmed ingestion exposures being higher than inhalation and water pathways of contaminated TSF dust. However, direct impacts of radiological hazards of NORMS on the population could not be established by this study and this presented limited scientific information in the study area (GDARD, 2012).

In 2014 Kamunda *et al.*, (2014) assessed the risks from gold mine tailings in the Witwatersrand, South Africa due to radiological hazard exposures of NORMS. The study also revealed that high gamma activities from immobile daughter of the uranium decay series such as ^{226}Ra in gold TSFs potentially pos serious threats to the environmental media as suggested by other studies (Sutton & Weiersbye, 2008).

Further investigation relating to radiological health risk exposure gold TSF dust within WCA by Mathuthu *et al. (*2016) established that water-independent pathway was the most significant radiation dose from the soil structures, followed by radon (direct and airborne). Contradictorily, the ingestion of dust and soil is widely regarded as one of the key pathways by which children are exposed to heavy metals and metalloids from a variety of sources as suggested by other studies (Nelson, 2013).

Plants can uptake heavy metals (Michelot *et al.*, 1998) and U have been shown to concentrate metals (Moore & Adler 2000), from contaminated soil or the groundwater at a rate with 54% of the U being extracted from water within 4 min of contact time (Bhainsa & D'Souza 2001). Studies were also published on the review of transfer patterns through various pathways (Ribera *et al.*,1996). U accumulation in tobacco leaves (Arruda-Neto, 1989) in the form of snuff which were as high as 19.1 ppm (19.1 μg g^{-1}) in some Indian snuff samples (Lal *et al*., 1987).

Hamman (2012) determined the extent of mining related pollution in the Wonderfonteinspruit, sediment, water, soil, grass and cattle tissue samples were collected, analyzed and for comparisons polluted and non-polluted areas. Cattle tissue samples from the experimental and control group revealed that N, Zn, Se, Pb and U

concentrations were practically significant. The U concentration in the cattle samples from the experimental group was 126.75 times higher in the liver, 4,350 times higher in the kidney, 47.75 times higher in the spleen, 31.6 times higher in the muscle tissue, 60 times higher in the bone and 129 times higher in the hair than that of the cattle samples from the control group. Furthermore, high uranium levels were accumulated in tissues and muscle tissue samples (Hamman, 2012).

Similar levels were observed in spices and cereals, with the estimated value of 0.66 µg day $^{-1}$ of 238U found in human diet in China (Sharma *et al*. 1981; Lal *et al*. 1983; Giang *et al*. 2001), and 1.3 µg day $^{-1}$ of Eastern cities in the USA (Welford and Baird 1967) and in Europe. Even though the level of 0.05 g U/g creatinine was suggested as the approximate upper limit of the normal population distribution. However, U excretion levels in South African patients still lacked scientific evidence (McDiarmid *et al*. 2001).

The level of U concentrations in herbal remedies used within Gauteng, Limpopo, North West, and Mpumalanga Provinces of South Africa (Steenkamp *et al.,* 2005). This confirmed that the recent death of a child in Johannesburg from multiple metal-poisoning suspiciously from consuming herbal remedy and the ingested metals were typical of gold mine TSFs and found to be present in a range of herbal medicines (Steenkamp *et al.,* 2005). The study suggested that a patient taking the usual daily dose of one of these traditional remedies could ingest 10–60 µg and absorb 0.1– 4.8 µg. However, the biological implications of this in humans were unknown, an elemental and isotopic analysis to determine the nature and extent of U contamination was recommended (Steenkamp *et al.,* 2005). It was therefore revealed that windblown dust

from the air was the determining source of the high U contamination in the herbal remedies specimens as the tree barks served as dust collection point.

2.2.6.3 Contamination assessments

The enrichment factor (EF) method characterizes the magnitude of metal toxicity in environmental samples from a given site (Lee *et al*., 1997; Voutsa *et al*., 2002; Tokalio *et al*., 2003). EF distinguishes between naturally occurring and anthropogenic dust pollution sources (Chen *et al.*,2007).

Nowrouzi & Pourkhabbaz (2014) advised that enrichment factor (EF) and geo-accumulation index (Igeo)determine the level of metal contamination in different towns and villages like Laft Port and Khamir Port discharging their wastes into the Persian Gulf and Hara Biosphere Reserve. The results of the study, in which Fe was used to normalise metal contaminants reported strong to extremely contaminated sediments with Cd metal in Wadi Al-Arab Dam (Ghrefat & Yusuf, 2006). The sediments of Keratsini Harbour, Greece were heavily polluted in terms of Cd and Pb (Galanopoulou *et al*., 2009). The results of EF and *Igeo* for metals in this study concurred showed were directly proportional relationship with those studied by Praveena *et al*. (2007) and Ghrefat & Yusuf (2006).

The environmental impact of metals and the pollution level can be determined by the EF and Igeo, the former quantifies the anthropogenic pollution whereas the latter provides the metal contamination in sediment samples (Nowrouzi & Pourkhabbaz, 2014). The ER is a normalisation method proposed by Simex & Helz (1981) to assess the concentration of the metals as a ratio to another constituent of the sediments using

reference element for normalization. No standard has been published on specific element to be used as a reference (Rubio *et al*.,2000), however Al, Fe, Mn, total organic carbon and grain size, of which concentration remains anthropogenically unaltered (Ackerman, 1980). EFs can exaggerate some results as per some studies (Reimann & Caritat 2000).

Any crustal derived element of negligible enrichment can be used as the reference element for ER calculations of other elements (Adams *et al*. 1980). Also, most common elements used as reference are Sc, Al, Mn and Fe (Loska *et al*.,2003). Where the EF equates to the value of 1, this is an indication that the concentration in both tailings and crust are identical. However, if EF>1 then the metal concentration is higher in tailings than in the earth crust. While an EF<1 suggests a depletion of the element in tailings than in the crust.

According to Papadopoulos *et al.* (2014), assessment of gamma radiation dose from natural sources are important since natural radiation is the largest contributor to external dose of the world population (Dudu *et al*., 2018). Yalala (2015) characterized gold TSF dust within the Witwatersrand Basin to establish the mercury content, bioavailability and determine the associated health risks on the nearby communities such structures. The study focused on the areas of Johannesburg Central Business District (CBD) area, industrial areas of Aeroton, City Deep, Germiston, Selby, Springs, and the residential areas of Alberton, Boksburg, Centurion, Germiston, Greenside, Sandton and Springs.

2.2.6.4 Heavy metals bioavailability and bio-accessibility

Determination of heavy metals bioavailability unravels and quantifies ecological toxicity of trace elements-contaminated soils (TECSs), using the risk assessment of a contaminated site in relation to the ecosystems and human health. Oral metal bioavailability health risk assessment is determined by a) bio-accessibility, b) transport across the gastric and intestinal epithelia, and c) the first pass effect (Oomen *et al*., 2006). However, the human health risks related to TECSs determine the relative bioavailability since absolute bioavailability could not easily be experimented on humans due to ethical observation issues (USEPA, 2007).

The concept of assessing bioavailability and bio-accessibility of trace elements-contaminated soils (TECs) gained popularity in many parts of the world. Even though in Italy the concept was not practised in human health risk assessment, the bioavailability analyses were considered in site-specific risk assessment in France. In other EU countries (*e.g.*, UK, the Netherlands, Germany, and Switzerland), bioavailability was only recommended within the local context, with different applications within the country (Kumpiene *et al*., 2017). Bioavailability can be estimated from an experimental determination of bio-accessibility (*i.e.*, potential bioavailability for animals and humans). In Germany, the health risk from ingested soil is explicitly considered by the Federal Soil Protection Act as one critical exposure pathway (Kumpiene *et al*., 2017).

Even though there were no guidelines for evaluating bio-accessibility, the standard method of the German Institute for Standardisation DIN 19736 (DIN, 1998) was used for *in vitro* site-specific investigations. Studies noted that the total soil TEs were not

linked to pollutants from TECs but to TE bioavailability, and that phyto-technologies were useful in attenuating both human and other living organisms' exposures (Mench *et al*., 2010). The Swedish Environmental Protection Agency (SWEPA) guidelines set values for risk assessment and setting goals for remediation of contaminated sites in Sweden (SEPA, 1997,2009), based on toxicological and ecotoxicological reference values (Kumpiene *et al*., 2017).

2.2.6.5 Visual assessments

Theoretical paradigms of visual assessment research methodologies were studied and these include professional paradigm (Daniel & Vinning, 2003), formal aesthetic (Brett, 2009), ecological paradigm (Brett 2009), behavioural paradigm (Vinning & Steven 1986), psychophysical paradigm (Daniel ,1999), cognitive or psychological (Brett, 2009) and experiential paradigms (Zube *et al*, 1982).

Tviet *et al.(*2006) reviewed landscape aesthetics literature, suggesting that the visual character can be described by nine (9) key aspects: stewardship, disturbance, coherence, historicity, imageability, scale, complexity, naturalness and ephemera. Yet, the relationship between visual indicators preference remained unknown (Ode *et al*., 2008).

Public perception studies of dust exposures from various sources, have been reported in Mexico (Catalan-Vasquez *et al.,* 2012), Tanzania (Kitula, 2006), Ghana (Garvin *et al.*, 2009) and Australia (Higginbotham *et al*., 2010). However, only a few studies were conducted on public's experiences and perception of mine dust exposures in South Africa (Wright *et al*., 2014). Yet, some issues relating to complaints from the public

have been published in articles, journals and news (Liefferink, 2011; Olalde, 2015). The study by *Wright et al.,* (2014), was however, not TSF dust specific and lacked analytical component of the study in support of the issues raised by the public. Furthermore, data collection only focused on one day's questionnaire administration which might not necessarily be a representation of the views of the entire population within the study area.

2.2.7 Sampling Procedure

2.2.7.1 Active and passive dust monitors

Active and passive dust samplers have been popularly used in dust fallout monitoring devices both globally and locally. Passive dust monitors are preferred since they are simple to install, economical and are deployable at multiple sites for a wider view of dust deposition patterns of the area of interest (Kwata, 2014). These were also useful in measuring organic gases and vapours using diffusion and permeation to estimate sampling rates and air concentrations. Natural vegetation, leaves, tree rings bark and lichens have been used as passive samplers for measuring of ambient air metals concentrations in areas near mines, smelters and from traffic (BollhÖfer *et al*., 2006; Beamer *et al.,* 2014). This method is, however, more practical for outdoor than indoor dust deposition.

In America, multiple samplers have been widely used to characterize exposures and determine potential impacts in communities near contaminated mining sites as studied by Beamer *et al*. (2014). This method was successfully used in the Western United States to measure beryllium, manganese and arsenic concentrations from indoor and outdoor soil resuspension deposition. Its usefulness was evident in screening high-

risk communities near mines and in epidemiological studies lacking relative concentrations. Performances of this method was compared with traditional methods for different community areas to determine community dust exposure levels (Beamer *et al*., 2014; EPA, 2017).

Atmospheric dust fallout samplers have been widely used to measure the level of dust within the environment. The need to improve the health and environmental conditions, together with the ever-increasing technology advancement, a cost effective, yet efficient methods had to be developed both for the local and international situations. Dust fallout levels are regulated within legislation to ensure prevention of excessive precipitant dust emission in a year are within the set limit. Any maximum results above the residential or industrial action level are an indication that the area is dusty, and this requires action level to remediate and avoid the situation. Where the maximum results have not exceeded the industrial action level then the area can be acceptable (Loans, 2015; DustWatch, 2016).

Global review of the of national ambient air quality standards and for PM_{10} and SO_2 was documented in recent studies (Vahlsing & Smith, 2010). So far, no methods are available to for converting precipitant dust concentrations to Total Suspended Particulate (TSP) levels or to PM_{10} levels. Australia has the least commonly used method, whereas the United States of America (USA) does not have any air quality standards for PM larger than a d_{50} of 10 microns (PM_{10}) (Dustwatch, 2016).

Passive dust buckets (single or directional) monitors of specific size and diameter are mounted on a pole erected at the height of between 1 and 2m above the ground level

located strategically within a few meters from the pollution source. Single buckets, partly filled with capture medium (water), remain open to capture and accumulate precipitating dust from all directions. The water within the bucket assists in collecting and gravitating the dust to settle at the bottom of the bucket (Loans, 2015). However, this technique does not establish precipitant dust emanating from any given direction unless the bucket is closed to any dust from other directions (Loans, 2015).

Single buckets can therefore be subjected to inaccuracies due to wind turbulence within the buckets, lower air densities over the bucket and other environmental factors. Even though this presents a crude and nonspecific test method, single dust collection method can be useful for determining long-term trends (DustWatch,2016). Unlike the single bucket monitors, the directional unit has four buckets facing north, south, east, and west respectively, clamped onto a mounted pole. The export bucket monitors dust directly from targeted source by predominantly collecting precipitating dust fallout from the source. The directional dust bucket units have designed lids preventing the ground level dust of 3 m/s and above from contaminating the precipitant dust samples. This method can be reliable as its data is useful for legislative compliance purposes in instances where the dust collection unit is located at the direction of sensitive receptors from the source being monitored (DustWatch, 2016).

2.3 Review of Analytical Methods for TSF Dust Characterization

2.3.1 Dust deposition rates

South Africa has adopted the American Standard Test Method, (ASTM) D-1739 of 1998 "*Standard Method for Collection and Analysis for Dust Fall (Settleable particulates)",* as the recognized and convenient method for precipitant dust

measurement. This has since become legislative requirement that is well entrenched in the South African air quality legislation. This also sets out dust fall-out limits for implementing engineering solutions mitigate and avoid exceedances (DustWatch, 2016). The method enables dust control and establish settleable precipitant dust deposition rates in residential and non-residential areas as defined in Table 2.5 below.

Table 2.5: Acceptable precipitant dust deposition rates as measured (using ASTM D1739:1970 or equivalent) beyond the boundary of premises where dust is generated (DEA, 2013)

Restriction Areas	**Dust fall rate (mg/m2/day, 30 days average)**	**Permitted Frequency of exceeding dust fall rate**
Residential Area	D<600	Two within a year, not sequential months
Non-Residential Area	600 < D < 1200	Two within a year, not sequential months

2.3.1.1 Precipitant dust deposition rates technique

Passive methods collect dust fallout naturally through mass transfers, using single buckets and directional dust collectors prescribed by the American Society for Testing and Materials (ASTM D1739, 1970) Standard Method for Collection and Analysis of Dust Fallout. The ASTM D 1739 (1970) method is the recommended in South Africa (NDCR 827, 2013) and the results of the precipitant dust collected as per the South African National Management: Air Quality Act (Act 39 of 2004).

The Act specifies the regulated deposition rates limits for residential areas 600 mg/m^2 /day measured over a 30-day average and between 600 and 1200 mg/m^2 /day for non-residential areas. This study observed specifications of the South African National Standards (SANS) 1929 (2005) for precipitant dust measurements. To establish

possibilities of exposures from the TSF towards the surrounding communities, meteorological data (rainfall, windspeed, wind direction and temperature) at the Potchefstroom and Zuurbekom Weather Stations were obtained from the South African Weather Services (WeatherSA, 2019) the period 2015 to 2017.

Oguntoke *et al*. (2013) used the bucket collection technique for dust fallout monitoring as recommended by the American Society for Testing and Materials (ASTM D1739) to establish dust fallout data Crown-Gold dust monitoring project (CRUST) in Johannesburg, SA. This was useful in establishing that meteorology played no crucial role in the dust fallout of the study area. However, dust fallout resulted from activities like construction work within the vicinity of the areas, spontaneous dust emission due to equipment failure, and reprocessing of stabilized TSFs for fine gold extraction.

Variations were picked up from Ogutonke *et al*. (2013), in determining the mean wind speed levels and mean relative humidity in residential and non-residential sites which concurred with the findings in the GDARD report (GDARD, 2009) simulating the regional dust fallout pattern within Gauteng Province. The general pattern of dust fallout deposition rates across the monitored sites followed the order: spring > winter > summer > autumn. Summer is characterized by high wind speed, but its erosive effect is attenuated by heavy rainfall and strong vertical air mixing, whereas spring is typified by high dust fallout, high wind speeds with low rainfall. Spatial variations were, however noted by Petrilli (1962) and, Mishra & Shambhu (2010).

Even though Annegarn & Sithole (2002) and Annegarn *et al.* (1991) indicated the spring season as the “high dust period” in the Witwatersrand Basin, Fukagawa *et al*.

(2006) noted distinct atmospheric aerosol portrayed in Japan. High moisture content in atmospheric air constituted additional load carried by wind, hence reducing its speed and erosivity, but increased rainfall had less effect on average PM_{10} humidity (Giri *et al*., 2008).

2.3.2 Air quality models

Various models have been useful in determining the air pollutants concentrations and towards predicting and assessing impacts from a source on the surrounding sensitive receptors. Dispersion models compute ambient concentrations as a function of source configurations, emission strengths and meteorological characteristics. Thus, dispersion model provides a useful tool to ascertain the spatial and temporal patterns in the ground level concentrations arising from the emissions of various near sources and terrains (Mpanza *et al.,* 2020). Increasing reliance is placed on concentration estimates from models as the primary basis for environmental and health impact assessments, risk assessments and emission control requirements. The choice of suitable dispersion model for specific purpose is key.

Gaussian-plume models are best used for near-field applications where the steady-state meteorology assumption is most likely to apply (Mpanza *et al.,* 2020). The most widely used Gaussian plume model, the US-EPA Regulatory AERMOD model, which has been developed and endorsed by the AMS/EPA Regulatory Improvement Committee (AERMIC) (Hanna, Egan, Purdum, & Wagler, 1999). The AERMOD is a dispersion modelling system with three components, namely: AERMOD (AERMIC Dispersion Model), AERMAP (AERMOD terrain pre-processor), and AERMET (AERMOD meteorological pre-processor).

However, Gaussian Plume models can produce varying spatial wind fields due to topography or other factors cannot be included and its prediction uncertainty could be -50% to 200%. The accuracy relies on wind speeds in calm atmospheric conditions. The model requires good structuring to minimize total errors and the total uncertainty is summed up from a) the uncertainty due to errors in the model physics; b) the uncertainty due to data errors; and c) the uncertainty due to stochastic processes (turbulence) in the atmosphere.

Lee & Tchakerian (1995) used dispersion prediction models to determine that higher wind speed exceeding 6 m/s can initiate blowing dust in the Southern High Plains of the United States. However, Annegarn *et al*. (1991) suggested that the minimum speed of 4 m/s and above results in dust emission in the study and this disparity in wind speed predicted by these authors was due to the difference in the type of earth materials of the study area (Ogutonke *et al*., 2013). The study thus revealed that the levels of dust fallout at two sites were rather influenced by construction work within the areas, spontaneous equipment failure, and reprocessing of stabilized TSFs for fine gold extraction.

Ogutonke *et al.* (2013) employed a stepwise regression model to examine the contribution of meteorological parameters to dust fallout levels to determine frequencies of TSF dust episodes based on meteorological parameters within the Witwatersrand Basin, SA. The study revealed that TSF dust episodes within the study area were mainly influenced by mean relative humidity and wind speed, whereby seasonal variations were also considered.

Ngole-Jeme & Fantke (2017) study of ecological and human health risks associated with abandoned gold mine tailings contaminated soil in TSFs dust in the Witwatersrand Basin explored the use of SEtox, the UNEP-SETAC global consensus model for characterizing chemical emissions. This method has been key in assessing human toxicity and freshwater aquatic ecotoxicity impacts as suggested by Westh *et al*. (2015). The device combines multimedia environmental fate, multi-pathway exposure and potential negative effects associated with a chemical emission into the environment in a set of characterization factors (CFs) (Ngole-Jeme & Fantke, 2017). The study confirmed abandoned gold mine TSFs as contributing factors of ecological and human health risks due to metals and metalloid exposures emissions thereof. Furthermore, high concentrations of As, Cd, Co, and Ni in soil were suspected to present unacceptable risks to human populations including ecosystems nearby mining areas (Aucamp *et al*., 2000).

2.3.3. Dust Settling Velocity

Sánchez (2016) evaluated the average particle settling velocity inside a vortex using Computational Fluid Dynamics (CFD) which included development of computer algorithm that simulates the motion of the particles in the presence of a vortex and this was used to calculate the velocity. The dynamics of an isolated airborne particle of tailings blown by wind can be calculated by considering the particle dimensions (density, diameter, shape), the wind speed and the dimensions of the area from which it is propelled (Blight, 2004). A particle is assumed to be dragged and carried at a horizontal speed *g* equal to that of the wind, and to be falling at a vertical speed (*V*) given by Stokes' law. According to Stokes' equation (Equation 2.1. below), the gravitational force (*G*) acting downward on a free-falling sphere would be:

$$G = \frac{1}{6} \bullet \Pi \bullet d^3 (Ws - Wa) \bullet g$$ **(Equation 2.1)**

Where,

d = the geometric diameter of the sphere (m)

Ws = the density of the sphere (kg/m^3)

Wa = the density of the air (kg/m^3)

g = acceleration due to gravity (m/s^2)

2.3.4 Analytical Methods and Techniques

Methods of analyses have been employed to determine various characteristics of gold TSF dust worldwide. The four basic analytical techniques commonly used for elemental analysis are, namely, atomic absorption (AA), inductively coupled plasma-mass spectrometry (ICP-MS), ICP-optical emission spectroscopy (ICP-OES), and X-ray fluorescence (XRF). Each analytical technique can record the presence and abundance of individual elements across the bulk of the Periodic Table.

2.3.4.1 Atomic absorption (AA)

Atomic absorption spectrometry (AAS) can measure the elemental concentrations in various media, measures more than 70 elements and this Simplified AAS resembles a single beam spectrophotometer. The technique is based on four principles: a) the *source emits light* beam b) light passes through the *burner* c) the element activates to its atomic state before being focused upon the entrance slit of the *monochromator* d) selection of narrow wavelength interval and enters the detector slit (Perkel, 2012).

Steenkamp *et al*. (2005) used the adsorptive stripping voltammetry (AdSV) to determine the level of uranium concentrations in herbal remedies used within Gauteng, Limpopo, North West, and Mpumalanga Provinces of South Africa. The technique forms, adsorbs and accumulates uranium chelates with chloranil acid on the working electrode then records the stripping step current value. AdSV is widely reliable in uranium speciation studies, due to its high sensitivity levels and its capabilities of providing low detection limits down to parts per trillion (Wang *et al*., 1992; Steenkamp *et al*., 2005) unlike most analytical methods such as ICP-MS or AAS.

A combination of methods can be employed for several analyses. For the determination of U and other metals in waterborne and sediment, Winde *et al*. (2004) used the inductively coupled plasma optical emission spectrometry (ICPOES), with a lower detection limit of 2 mg/kg. To determine all other heavy metals in water, mass spectroscopy (ICPMS) was used while solid samples were analysed by atomic absorption spectroscopy (AAS). For the radioactive U concentration analysis in water samples, laser-phosphorescence (lower detection limit: 0.001 mg/l) was employed. The U concentrations as found in water and solid samples in different aqueous pathways (Winde *et al.,* 2004).

2.3.4.2 Inductively coupled plasma-mass spectrometry (ICP-MS)

In atmospheric deposition, inductively coupled plasma mass spectrometry (ICP-MS) has been popularly useful in determining elements trace and ultra-trace levels in all types of samples. Its usefulness has been proven to achieve best results due to high sensitivity, multi-element capability, wide linear dynamic range, high sample throughput, and ability to categorise between isotopes. The technique (Cubadda,

2007). Even though the modern ICP-MS systems can analyse most elements in the periodic table simultaneously at levels of 10 pg ml^{-1} with a mass resolution of <1 amu, its main limitation however, results in the formation of polyatomic interferences between atmospheric gases and matrix ions. ICP-MS can reach temperatures of up to 8000 K and can accommodate aqueous samples.

Candeias *et al*. (2014), used ICP-MS in identifying sources and assessing potential risk of exposure to heavy metals and hazardous materials in mining areas of the Central Portugal. Inductively coupled plasma atomic emission spectroscopy (ICP-AES) technique was successfully used by Malizia *et al.* (2012) to assess the concentrations of selected heavy metals (Cu, Zn,Mn, Pb, Cr, and Pd) in soil and plants. This revealed that the leaves of *Taraxacum officinale L.* and *Trifolium pratense L.* can accumulate Cu and *Urtica dioica L.* representing the vegetal species can accumulate the highest fraction of Pb.

Many South African studies also employed ICP-AES technique in detecting heavy metals in TSF soils and dust within the Witwatersrand Basin. Maseki (2013) studied the health risk of gold mine dust impacts on communities within the East Rand Gold operations which sampled soil material from East Rand Gold and Uranium Company (ERGO), East Rand Proprietary Mine (ERPM), Crown Gold Recoveries (CGR) and Durban Roodepoort Deep (DRD) TSFs. This was to establish the link between 20 um diameter particles and potential health effects on the immediate communities using ICP-MS to detect heavy metals of the TSF soil. It was established the exposure rates were within acceptable range required by the U.S. EPA for both adults and children (EPA, 2017).

ICP-MS has been used in the Witwatersrand for the determination of heavy metals accumulation and concentration in gold TSFs soils, and dust samples (Dudu *et al*., 2018). The method was also useful in determining mining and water pollution from the TSFs within the Central Rand goldfield of the Witwatersrand Basin by Tutu *et al*. (2011). Laser ablation-inductively coupled plasma-mass spectrometry (LAICP- MS) was preferable in analysing elemental components in gold grains from mapping of the grains on a grid pattern, with continuous ablation via successive line scans. This technique was tested to produce better distribution in heterogenous solid than spot analysis by Sanborn & Telmer (2003). Altigani *et al*. (2015) used this method for identification of elemental composition of gold mineralization in the Barberton Greenstone Belt, South Africa.

2.3.4.3 Inductively coupled plasma optical emission spectrometry (ICP-OES)

Okereafor *et al.* (2019) used inductively coupled plasma optical emission spectrometry (ICP-OES) for metal contamination assessment from TSFs dust within the nearby farming land of the East Rand (Ekurhuleni) in Gauteng. The study confirmed evidence of high heavy metal contamination in local soils due to previous gold mining activities (Okereafor *et al.,* 2019).

2.3.5 Metal Toxicity

In human health risk assessment studies, bioavailability analyses have been useful in determining human toxicity in relation to environmental pollution. To estimate the oral bioavailable fraction of soil-borne contaminants can be performed using a three-step approach, namely, (1) bio-accessibility, (2) transport across the gastric and intestinal

epithelia, and (3) the first pass effect (Kumpiene *et al.*, 2017). However, this approach can be dynamic and varies with time and space (Kumpiene *et al.*, 2017).

2.3.5.1 Metal bioavailability and bio-accessibility

Human health takes the highest priority in most risk assessment models, due to serious and aggravating factors triggered in numerous acute and chronic diseases (Duruibe *et al.*, 2007). Even though several studies on method validation and correlation between *in vitro* bio-accessibility and *in vivo* bioavailability have been performed (Marschner *et al*., 2006; Denys *et al*., 2012; Koch *et al*., 2013; Li *et al*., 2014; Juhasz *et al*., 2014; Bradham *et al*., 2015; Li *et al*., 2015; Ono *et al*., 2016), however reliability for human risk assessment is better validated by *in vivo* studies (Kumpiene *et al.*, 2017).

Yalala (2015) characterized gold TSF dust in the Witwatersrand to establish the mercury content, bioavailability and determine the associated health risks on the nearby communities of such structures. This was achieved using three (3) sequential extraction procedures, namely, modified BCR-the European Community Bureau of Reference, selective sequential procedure (SSE), and novel sequential extraction procedure (n-SEP)). The method was applied to determine the mobility, availability and persistence of mercury in urban dusts. The findings of this study revealed that mercury concentration decreased with distance away from the mine TSF This suggested that human exposure to Hg in dust via inhalation being greater than that via the gastric tract. The contamination assessment factor of the dust revealed TSF as the source of contamination and dust samples were classified as heavily enriched, very highly contaminated, and strongly polluted by mercury found in gold mine TSF.

2.3.5.2 Master Particle Sizer

Dust particle size distribution can be analysed using Malvern Particles Mastersizer 3000, which is the latest generation of the world's most widespread particle sizing instrument. Laser diffraction measures particle size distributions from 10nm up to 3.5mm, using the Mie Theory of light scattering. Large particles are measured at advanced focal plane detector design which can resolve very small diffraction angles. Sensitivity to sub 100 nm particles, scattering light at wide angles, is achieved using advanced optics and a powerful 10mW solid state blue light source (Malvernpanalytical, 2019). A range of particle size is measured through sequential combination with red and blue light sources as shown in Figure 2-4 below.

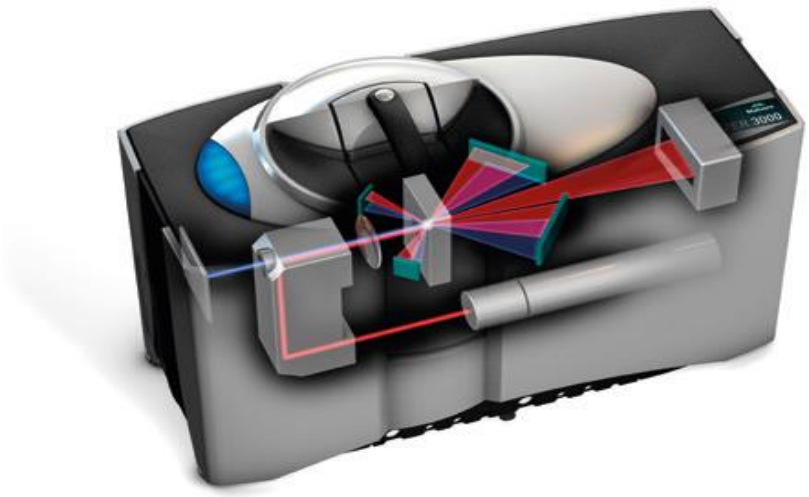

Figure 2-4: A typical Malvern Particle Mastersizer showing red and blue light sources scattering

Various techniques have been applied in studies of dust particle distribution in South Africa. Ngole-Jeme & Fantke (2017) used Malvern Mastersizer 2000 laser fitted with Hydro 2000G dispersion unit prescribed by Council for Geosciences (CGS, 2016) for

Au particle size composition in soil samples in three different areas of gold TSFs in Krugersdorp.

For the determination of non-occupational exposure to PM_{10} and PM_4 of crystalline silica in TSF dusts, Andraos *et al.* (2017) employed Aerodynamic Particle Sizer (APS Model 3321, TSI Inc Shoreview, MN), the Scanning Mobility Particle Sizer (SMPS Model 3080, TSI Inc.) and the Condensation Particle Counter (CPC Model 3772 TSI Inc.). This was connected to a Small-Scale Powder Disperser (SSPD Model 3433, TSI) linked to a computer software, Data Merge Software (DMS version 1.0.1 TSI) to produce single particle size distributions.

Silica quantified by MDHS method 101 and the crystalline silica in respirable airborne dusts, direct-on-filter analyses by infrared spectroscopy and X-ray diffraction. Crystalline silica (quartz) was the most dominant constituent in the dust, ranging from 73.14 ±4.90% to 87.09 ±3.70%, with high crystalline silica percentages in bulk samples, which concurred with the results for the Witwatersrand and Klerksdorp goldfields studies (Stanley, 1987; Malatse & Ndlovu, 2015). This enabled the health risk analysis using meteorological data, cancer and non-cancer characterization. The study suggested elevated ambient and personal crystalline silica levels in communities surround TSF in excess as compared to the international crystalline silica interim levels. Areas close to TSF showed higher PM_4 crystalline levels than distant sites (Andraos *et al*., 2017).

Various formulae were used to determine the particle size settling velocity in air; however, no suitable or accurate method has been approved under given environmental conditions (Farrel & Sherman, 2015).

2.3.5.3 Scanning Electron Microscopy (SEM)

The scanning electron microscope (SEM) is used to determine morphological, mineralogical and chemical characterization of the analytes and the technique involves an electron-optical instrument, which uses a source of electrons to illuminate the specimen. The newest Environmental Scanning Electron Microscope (ESEM) involves wet, dirty, oily, outgassing and samples as hot as 1 500 °C can be viewed (Tiedt & Pretorius, 2002). The technique involves acceleration of electrons are accelerated down the column and pass through a combination of electromagnetic lenses and apertures, producing various signals collected by appropriate detectors. The information is created and displayed in a form of an image (Tiedt & Pretorius, 2002).

As a valuable tool, the SEM can allow very fine detail to be resolved by offering a large depth of field, which is highly unlikely to achieve with an optical microscope. SEM can also be coupled with other detectors, which makes it a powerful analytical tool. However, if X-ray microanalysis is to be performed, probe currents of at least 10-10 amps is used for EDS and at least 10-8 amps (DustWatch, 2016). Where high-resolution secondary electron images are required, then a small probe size and short working distance should be used, limiting the current in the probe, creating noisy appearance of created images.

Adachi & Tainosho (2004) combined the use of field emission SEM (FESEM) with energy dispersive X-ray spectroscopy (FESEM/EDX) for the single particle analysis of metal particles. This was achievable since morphologies and individual chemical composition of the metal particles included have could not be thoroughly investigated by the (SEM) method only (Adachi & Tainosho, 2004). FESEM can analyse individual particles at high resolution due to its ability in providing narrower probing beams than that found in tungsten hairpin filament SEM, resulting in improved spatial resolution.

2.3.5.4 X-Ray fluorescence (XRF)

XRF spectroscopy technique is commonly used in analyzing the fluorescent X-Rays to gain information on the elemental composition of a sample material. Energy Dispersive XRF (EDXRF) and Wavelength Dispersive XRF (WDXRF), which differ primarily in the way the fluorescent X-Rays are detected and analysed (Malvernpanalytical, 2019). In WD-XRF), explained Ravi Yellepeddi, Marketing Director for Bulk Elemental Analysis at Thermo Fisher Scientific, the different X-ray wavelengths returning from a sample, which are signatures for each element, are separated and measured using a series of optics like white light with a prism. In energy-dispersive X-ray fluorescence (EDXRF), a solid-state detector measures the complete energy spectrum instead (Perkel, 2012).

Researchers such as Zaraz´ua-Ortega (2013) and Gao *et al*. (2017) used the total reflection X-ray fluorescence (XRF) technique to determine the concentrations of K, Ca, Ti, V, Cr, Mn, Fe, Ni, Cu, Zn, Rb, Sr, and Pb in Metropolitan Zone of Toluca Valley in Mexico. Atmospheric dust deposition was collected from six (6) urban sites in the using the epiphytic moss genera *Fabronia ciliaris*. This showed the dust source as the

industrial and urban areas, mainly due to the intense vehicular traffic and fossil fuel combustion (Gao *et al*., 2017).

Different methods and techniques were used for elemental analysis in gold TSF dust in the Witwatersrand. ContrAA 300 was used by Ngole-Jeme & Fantke (2017). XRF technique for the characterization of dust collected from the gold mining TSFs (Amodio *et al*., 2014; Yalala, 2015).

For the bulk chemical composition of the sample, XRF analysis was conducted using an ARL 9400XP+ Wavelength dispersive XRF Hitachi Spectrometer with a Cobalt tube, LiF200, LiF220, GER, AXO6 (a 50Å synthetic multilayer) and PET analysing crystals, with a flow proportional and scintillation detector supplied by United Scientific. The instrument is equipped with functionalities of WINXRF using the COLA algorithm with theoretical alphas deduced from fundamental parameters, for matrix correction of fused bead major elements as well as powder majors and trace element analysis of Cl, Co, Cr, V, Sc and S (Loubser & Verryn, 2008).

2.3.5.5 X-ray Diffraction (XRD)

X-ray diffraction (XRD) is based on constructive interference of monochromatic X-rays and a crystalline sample. X-rays are generated by a cathode ray tube, filtered to produce monochromatic radiation, collimated to concentrate, and directed toward the sample. The incident rays interact with the sample to produce constructive interference. The general relationship between the wavelength of the incident X-rays, angle of incidence and spacing between (Dutrow, 2018). The angle of incidence and

spacing between the crystal lattice planes of atoms in a sample is known as Bragg's Law (Equation 2.2 below**)**, expressed as:

$$(n\lambda = 2d \sin\theta) \qquad \text{Bragg's Law (Equation 2.2)}$$

Therefore, by using a spectrometer crystal to detect and quantify elements of interest based on the characteristic X-ray wavelengths produced by each element (Henry, 2018). Even though XRD has shown to be a powerful and rapid (< 20 min) technique for identification of unknown mineral and its data interpretation is relatively straight forward, homogeneous and single-phase material is best for identification of an unknown sample. However, the detection limit is ~ 2% of sample in a mixed materials and peak overlay may occur with worsened high angle reflections.

Results of mineralogical component assessments of the Witwatersrand TSF and mining dust in which XRD was employed, were recorded by various authors (Kamunda *et al*., 2016; Mpanza *et al*., 2020). XRD was found to reliable in confirming the dominance of quartz in aeolian ultrafine TSF dust from gold mines within the Witwatersrand (Yalala, 2015).

2.3.5.6 Neutron Activation Analysis (NAA)

Neutron Activation Analysis (NAA) is one of the most sensitive methods used to measure the concentration of trace amounts of many elements in a variety of sample types (Hamidatou *et al*., 2013). In NAA, a sample is bombarded with neutrons, resulting in the production of a radioactive isotope of the element of interest. Gamma rays emitted by the radioactive isotope are analysed, thus its usefulness in element identification i.e., qualitative analysis (Figure 2-5 below). The number of gamma rays

emitted is correlated to the number of atoms present in the sample, i.e., quantitative analysis (Hamidatou *et al*., 2013; Schmets *et al*., 2014).

This microanalytical method requires only a few milligrams of sample are required, hence it is valuable in examining lunar samples and artefacts, and in criminal investigations. NAA is a non-destructive technique, where analysis can be performed without destroying the sample. Multielement procedure involves more than 25 elements, providing simultaneous measurement for each in the sample.

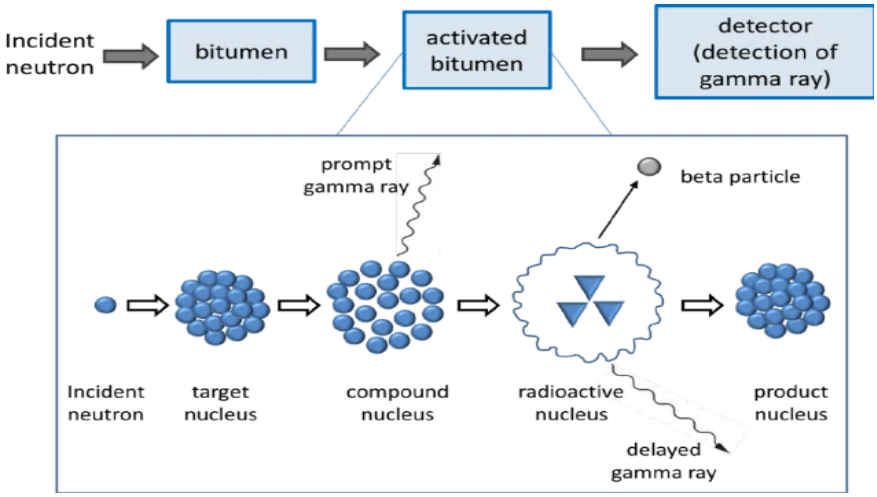

Figure 2-5: Schematic representation of Neutron Activation Analysis steps and illustration of the neutron capture process (Schmets *et al*., 2014)

The study of uranium concentrations in gold TSF dust by Dudu *et al*. (2018) employed HPGe well detector to analyse concentrations of radioactive elements of interest. GENIE 2000, Gamma Acquisition V.3.2.1 and Gamma Analysis Software V.3.2.3 were used for data acquisition. The study revealed higher mean concentration of Th (3.99 ±0.75) mg/kg than U (2.94 ± 0.68) mg/kg. The world average values for U and Th in soils were 2.64 mg/kg and 11.1 mg/kg respectively (Dragović *et al.* 2006) which suggested that Th concentration was below the world average whereas the U

concentration was proportional to the world's average. However, Papadopoulos *et al*., (2014) advised that the geochemical behaviour of the Th and U radionuclides is expected to be the same as they have similar distribution within the soils.

2.3.5.7 Visual impacts analysis

Various emperical studies have been published to examine landscape aesthetic values (Penning-Rowsell & Lowenthal 1986; Taylor, 1987). Grimm studied and quantified the visual impacts of windfarms on the natural landscape using the subjective (Psychophysical) and objective (Formal) models, through employing tools such as Global Positioning System (GPS), Geographic Information System(GIS), mapping and photomontage. Grimm (2009) maintained that landscape visual assessment was but one component within a broader discipline of landscape assessment.

GIS Mapping has effectively been used together with satellite thematic imagery (TERRA satellite ASTER images) and aerial photographs to visualize historical contamination of gold TSFs within the semi-arid and uranium mining region of the East Rand of Johannesburg (Sutton *et al.,* 2006). Identification of contamination hotspots from natural reef outcrops, historical spillages and wide-spread gold mining activities, and water-borne pathway for dissemination of pollutants (Naiker *et al*., 2003; Tutu *et al*., 2003; 2005 and Winde *et al*., 2004) were successfully achieved using ASTER and these could have remained undetected using only aerial photographs (Sutton *et al*., 2006). Further value-adding of this method include establishing standardized tool focusing on post-closure planning for environmental pollution clean ups and effective demonstration of compliance.

Focus and various methods from previous studies were used for analyzing visual assessments of wind turbines on landscape quality included: verbal questionnaires (V), photo-based questionnaires (P), questionnaires based on computer simulation (CS) and questionnaires filled in while viewing actual landscape (AL) (Molnarova *et al*., 2012). These methods were evaluated by experts, non-expert members of the public and through evaluation of pre-existing data.

2.3.5.8 Questionnaire and surveys

Collection of data is a combination of qualitative and quantitative approaches. Questionnaire explains meaning and is word based rather than numerical collection and analysis of data (David & Sutton, 2004). This includes structured, unstructured interviews, focus groups, one-on-one, observations, etc. Subjective feelings, values and attitudes, and is also advantageous where respondent's insight and understanding of a situation is required, based on their experiences of the subject matter being analyzed (Malhotra, 1996).

The questionnaire method was used by Molnarova *et al*. (2012), to determine the influence of physical attributes of landscape and introduction of wind turbines relating to the respondents' reaction on the perceived landscape within the European communities of the Czech Republic states. Possible distortion from verbal representations of visual elements were minimized using photographs as part of the questionnaire. Respondent reactions far exceed socio-demographic and attitudinal factors included residents and non-residents of the study area.

The method was also useful in establishing the sensitivity aspects of respondents relating to high aesthetic quality and acceptable of these structures in unattractive landscapes (Molnarova *et al*., 2012). This revealed that people living in proximity of highly intrusive structures such as wind turbines, e.g., males and highly educated, tended to be more critical of placement of such structures in high visual quality. People with positive attitude, on the other hand, perceived these structures on low visual quality as presenting an improvement opportunity. The method was recommended for public participation and worth using for improving public attitudes towards highly landscape proliferating structures.

Nkosi *et al.* (2016) established that children living near gold TSFs showed high dominance of asthma symptoms than those located further away. This was achieved using self-administered questionnaire of children residing in exposed areas of Gauteng and North West Provinces of South Africa, based on the International Study of Asthma and Allergies in Childhood (ISAAC) as suggested by Ellwood *et al*. (2005). Pocket electronic flow meter (Piko-1) was used to calculate Forced expiratory volumes in 1 second (FEV1) for each respondent. Concentrations of selected outdoor air pollutants and meteorological characteristics formed primary data of the analysis. However, one of the limitations of the study confirmed that no quantitative indoor air pollution exposure assessment was conducted; and only children living in smoke-free homes were included. Similar studies were conducted, linking dust exposures and health risk in adults over the age of 55 years, adolescents and school children (Nkosi *et al*, 2016; Nkosi & Voki, 2016; Nkosi, 2018, Wright *et al*., 2018).

Public perception study of the mine dust risk of the communities living nearby gold mine TSFs was conducted by Wright *et al.* (2014). This qualitative study, which was based on 5 focus groups with 62 participants of different ages and sex was carried out in the Witwatersrand Basin. While the study was useful in identifying community perception issues relating to mine dust, a comprehensive management plan was highly recommendable, incorporating all stakeholders.

2.3.5.9 Geographic Information Systems (GIS)

Orland (1994) established that GIS-based visualisation goes beyond the simple ability to discuss anticipated outcomes via traditional graphic tools and can visualise relationships across time and space. Orland (1994) moreover pointed out that extra flexible visualisation methods would enable users to select their own viewpoints and be free of weather, seasonal and other restrictions. Orland *et al*. (1995) later publicized that the coarse grain of data sources such as digital elevation models and remote sensed imagery make GIS most appropriate for large-scale, synoptic, views of resource issues used in visual analysis (Tveit *et al*., 2006).

2.3.5.10 Mapping tools, checklists and matrix

According to Mc Harg (1969) cited by Fuggle and Rabie (1992), overlays and mapping methods can identify both the social and natural processes as social values. These techniques include projective and reflective mappings, single and cumulative mappings, colour coded impact maps are useful in the visual analyses (Fels,1992).

Fisher (1995) analysed the effects of data errors on viewsheds calculated by GIS programs and showed that the calculations are extremely sensitive to small errors in

the data, and to the resolution of the data, errors in viewer location and elevation. Viewshed of the same data but with eight (8) different GIS programs can issue 8 different results making viewshed operation popular and reliable tool in visual analysis (Fisher, 991; 1992; 1993) and the optimization of the line-of-sight operation (De Floriani *et al*, 1994; Lee, 1991; 1994).

Visual Absorption Capability (VAC) technique presents the land's potential in absorbing the development changes without altering the landscape character. VAC considers vegetation, soil contrast, visual variety, topographical diversity and recover time. Low dense and patchy vegetated land provides minimal screening thus will have low VAC and high visual impact to the observer. The VAC technique is based on two groups of factors, firstly, physical changes caused by development features such as earthworks, buildings and structures, linear development (pipelines, etc.), outdoor recreation facilities and forest plantations. Secondly, the biophysical characteristics of the area, renewal potential of vegetation and the visual exposure of the area to observers (Amir & Gidalizon, 1990). VAC has been used so far in several regions with various geographical characteristics and was found to be effective and easy to apply.

2.3.5.11 Photographs

The use of photographs in preference surveys is an established substitute for the real landscape (Shuttleworth, 1980; Hull & Stewart, 1992) and their usefulness in showing respondents' visual stimulus have been studied by Scott & Canter (1997). Limitations were, however established in revealing the impact on the observer's perception from the image contents. Computer visualizations presented new opportunities for evaluation of landscapes under various scenarios (Daniel & Meitner, 2001), which

showed strong correlations between in-field assessments and landscape computer simulations (Bishop & Rohrmann, 2003).

Photographs were found to be useful in preference surveys by various authors (Shuttleworth, 1980; Hull & Stewart, 1992). Scott & Canter (1997) used photographs to show respondents' conceptualization landscape aspects to evaluate the visual stimulus or the place represented by the stimulus. However, photographs lack control on the observer's perception.

In South Africa, visibility maps have been widely used and this demonstrates the final visibility of design height, shape, side slope configuration, size and cover. Visibility maps can show surface topography within TSF location and its visible parts at a given point (ESRI, 2000:128) within certain buffer zones referred to as zone of visual influence (ZVI) or viewshed, visual envelope or visual basic (Rademeyer, 2007). Photographs were also used for visual analysis of the TSF landscapes in which the public was afforded a chance to express their visual preferences.

2.3.6 Risk Exposure Analyses and Assessments

2.3.6.1 Health risk analysis

Ojelede (2012) revealed that gold mine TSF dust poses potential risk on the immediate environment, including the health risk on the humans residing within close proximities of these areas. The study confirmed occurrences of smaller particle sized soils (i.e., PM_{10} and PM_5) which are thoracic and respirable respectively and potentially damaging to the human respiratory system causing various health problems. It was further confirmed that mineralogical characteristic of the sampled TSF dust being

dominated by quartz found in the respirable fraction (<PM_5) of the dust which exceeded the set limit for residential limit of 600 mg/m^2/day. Even though the samples were highly enriched with toxic heavy metals (Cr, As, Mo, Cd and U), however, these were below detection limits. Calculated heavy hazard quotient (HQ) and radioactive dose confirmed the value above 1 threshold (As and Cr) and mSva-1 (3,7 $mSva^{-1}$).

2.3.6.2 Radiation exposure risk analysis

The study by Kamunda *et al.* (2016) employed gamma spectroscopy to measure the activity concentrations of these radionuclides in TSF soil to determine radioactive hazards and NORMs of the study area. Activity concentrations of Uranium-238, Thorium-232, and Potassium-40 exceeded the recommended safe limits as suggested by GDARD (2012). The average values for the external hazard and the internal hazard from the mine tailings showed that the radiation hazard rates were unsafe and could pose a significant health risk to the population in the area (Kamunda *et al.,* 2016).

Airborne radiometric mapping surveys over mining areas were widely used by researchers, e.g., Coetzee (1995); Sutton & Weiersbye (2008), Tutu *et al*., (2003), which revealed that high gamma activities from immobile daughters of the Uranium decay series (^{226}Ra) from TSFs dust dispersion may have direct bearing adverse environmental pollution.

Kamunda *et al*. (2016) also conducted soil, water and plant analyses of the surrounding gold mining areas. A broad energy germanium (BEGe) detector with a relative efficiency of 60% and a resolution of 2.0 keV at 1332 keV gamma ray emission of ^{60}Co was useful in measuring the activity concentrations of NORMs. Version 3.1

RESidual RADioactivity (RESRAD) OFFSITE modelling program estimated cancer risk from NORMs for a hypothetical resident scenario.

Historically in South Africa, even though comprehensive studies confirmed tuberculosis (TB) cases due to silica exposure due from mine dumps from the occupational point of view (Cowie, 1994; Hnizdo & Murray, 1998; Ehrlich *et al*., 2006), recent studies also reported elevated ambient PM10 and PM4 crystalline silica levels in communities surrounding (non-occupational) gold mine TSFs (Andraos *et al*., 2018). Radiological assessments were used by Kootbodien *et al.* (2019), in which TB cases were diagnosed by radiological assessment rather than microbiological evidence. Furthermore, even though radiological assessment is considered a sensitive tool for pulmonary tuberculosis (PTB) screening (WHO, 2016) and recommended for PTB prevalence surveys, its usage was however, not recommended for TB specific chest radiographs (WHO, 2011; Kootbodien *et al*., 2019).

CHAPTER 3

In this chapter, research approach is introduced and defined, including sampling collection process, instrumentation, experimental procedures and surveys conducted. The chapter further discusses the methods followed for establishing the health, radiation and health risk analyses.

3. METHODOLOGY

3.1 Materials

Materials used for the deposited dust collection and samples filtering included the following:

- Solvents and reagents: 20% Si (Aldrich 99% pure).
- Pyrex low form graduated glass beakers (100ml, 150ml and 250ml), Serological and pasteur pipette glass, volumetric flasks (grade A, NS14), Vee Gee wide neck graduated Erlenmeyer flasks and plastic sterile petri dishes supplied by Chem Lab Supplies.
- Fine tip (2mm), Parrot Products low odour marker pen supplied by Waltons Stationery and DustWatch field book.
- CB 3000 (CB3000) chemical analytical microbalance scale (160g x0.001g) weighing to the 4th decimal of one gram or to 0.1 milligrams, SABS/NCRS approved (approval no. SA1422).
- Whatman Schleicher & Schuel wet strength (ash-less) filter papers supplied by Sigma Aldrich made by of 1506 quantitative hard filter paper medium fast, retention 4µm; thickness 0.15mm; weight 63 g/m^2, classification DIN 53 135-2b and of 47mm diameter, were used to collect the insoluble dust.

- Deschem Glass Vaccum Suction Filter Filtration Kit having 250ml Buchner Funnel 1000mL Conical Flask, Dermagrip latex nitrile gloves, chemical splash protection goggles and chattaway stainless steel spatulas supplied by Chem Lab Supplies.
- SH-2 hot plate Magnetic stirrer with dual control, 1 inch stir bar C3 -110 heat stainless steel top and stepless speeds ranging from 100 to 2000 RPM for premier support supplied by Masiye Laboratories.
- Commercially available domestic quality bleach (hypochlorite) solution of 3,50% and Milton (Sodium hypochlorite: 1.0% and Sodium chloride: 16.5%) manufactured by Incolabs, Parktown, South Africa.
- Pure steam distilled water supplied by Manicaa.

3.2 Instrumentation

3.2.1 Dust buckets monitors

The polypropylene buckets of 237.0 mm height, a lid with inside diameter of 175.0 mm were used for the analysis were protected by the Bocan Patent A98/0298 supplied by Burcap Plastics. The patent was used for rim protection and a double sealant lid to prevent leakages. The diameter used as the collection area was the outside diameter of 179.8mm.

3.2.2 X- ray diffractometer (XRD)

To determine the mineralogical component of the TSF dust samples, TD -2500 XRD, manufactured by Malvern Panalytical, UK, an X'Pert Pro XRD device with Co tube, was used. The device's specifications are shown in Table 3.1 below.

Backloading preparation method was used and front loading onto a zero-background silicon sample disc when the sample amount was too small, prepared by wet grinding with ethanol in a McCrone micronizing mill for between 5 to 10 min (Klug and Alexander, 1974; Buhrke *et al*., 1998; Loubser and Verryn, 2008). The samples were loaded onto a spinner stage inside the XRD identify a broad range material present in the samples. The powdered samples were scanned at the required 2θ angle ranges of 4 to 90 degrees (°C), with radiation filtering options of Fe^{-}, CoK, Ni, CuK or Mn^{-}. The phase identification and interpretation were done using PANalytical X'Pert Highscore plus software and ICDD database.

Table 3.1: XRD device specifications

Functionality item	**Description**
Start Position [°2Th.]	4.000
End Position [°2Th.]	110.000
Step Size [°2Th.]	0.0170
Scan Step Time [s]	100.6952
PSD Mode	Scanning
PSD Length [°2Th.]	2.12
Divergence Slit Size [°]	0.2500
Specimen Length [mm]	10.00
Measurement Temperature [°C]	25.00
Anode Material	Co
K-Alpha1 [Å]	1.54060
K-Alpha2 [Å]	1.54443
K-Beta [Å]	1.39225
K-A2 / K-A1 Ratio	0.50000
Generator Settings	40mA, 40kV

Sample analysis results were reflected in the monitor linked to the instrument. The reference relative peak intensities provide information on the phase composition of the sample, quantitative phase analysis of the crystalline and amorphous phases as well as the total amount of any added material in the sample.

3.2.3 X-ray Fluorescence (X-RF)

ARL 9400XP+ Wavelength dispersive XRF Hitachi Spectrometer with a Cobalt tube, LiF200, LiF220, GER, AXO6 (a 50Å synthetic multilayer) and PET analysing crystals, with a flow proportional and scintillation detector supplied by United Scientific. The instrument is equipped with functionalities of WINXRF using the COLA algorithm with theoretical alphas deduced from fundamental parameters, for matrix correction of fused bead major elements as well as powder majors and trace element analysis of Cl, Co, Cr, V, Sc and S and the Rhodium Compton peak ratio method was used for the other trace elements (Loubser & Verryn, 2008).

XRF PANalytical's Omnian method was used to determine approximate bulk-chemical compositions from XRF scans of most elements in the periodic table at relative errors of major elements of about 10 %, allowing for relative errors majors of about 2%. The bulk sample (9g) was prepared by drying, crushing to 10mm, riffle splitting and milling the sample in a tungsten carbide milling pot to ca. 80% below finely milled to 50 µm sized material to prepare the LOI 5g of a pressed powder which was dried at 105 °C. 1 g of sample was weighted directly into a platinum crucible and adding 5ml (50%) of aqueous HNO_3 solution. For sample oxidation, the solution was heated and dried on a hotplate at 110ºC (Weight 1) followed by addition of 6g of lithium tetraborate flux and fused at 1000°C (Weight 2). The fused bead was weighed to calculate the sample

mass before and after oxidation or the percentage loss on ignition (LOI) using Equation 3.1 below:

% LOI= [Weight$_1$ - Weight$_2$ ÷ Weight$_1$ – Weight $_{crucible]}$ x 100 (Equation 3.1)

`

The method used for the major elements analyses was adopted from H. Bennet and G. Olivier (1992) on fused beads. Samples of pre-roasted 1g and of 6g tetraborate ($Li_2B_4O_7$) flux were mixed in a 5% Au/Pt crucible and fused at 1000ºC in a muffle furnace automated fluxer (Beadmaster F-M4). A mouldable crucible was used to remove the bead for cooling and for the crucible bottom surface analysis to ensure complete melting of the bead.

The method suggested by Watson (1996) was adapted, using a saturated polyvinyl alcohol (40-88%) for binding and mixing in a zip-lock bag. 20 g of 75 µm powder is mixed with a few drops of polyvinyl alcohol and pressed at a pressure of 20 ton/cm^2 for two minutes in collapsible aluminium holders for mechanical support, using a polished piston, followed by drying at 110ºC before analysis.

Special sample preparation techniques were developed for non-routine materials from sulphide containing material to avoid solubility of sulphides in lithium borate fluxes and possible damage to the platinum ware (Lupon *et al*., 1997). This was achieved by simultaneous pre-oxidation and retaining quantitative SO4, by a thorough mixing of 0.5g sample with Lithium nitrate ($LiNO_3$) on a bed of (3g) $Li_2B_4O_7$ and covered with the remaining (3g) flux with theoretical alphas deduced from fundamental parameters, for matrix correction of fused bead major elements and trace element analysis of Cl, Co, Cr, V, Sc and S and the Rhodium Compton peak ratio method (Feather and Willis,

1976) was used for the other trace elements. The XRF results were used to validate the XRD results obtained (Fitton, G., 1997). Background and overlap corrections were calculated on a set of interference standards and stored in the calibration according to a method proposed by Willis and Duncan (1993) (Loubser& Verryn, 2008).

The XRF Spectrometer was calibrated with certified reference materials, specpure oxides and standards, *e.g.* Specpure AL2O3, AGV-1, BCR-1, BE-N, BHVO-1, BR, Specpure CaCO3, Specpure CaO, DR-N, FeCa (University of Pretoria, South Africa), FeSi, GA, GS-N, GSP-1, Specpure SiO2, JB-1, JG-1, Lithium tetraborate blank, MA-N, Mica-Fe, Mica-Mg, MRG-1, NIM-D (SARM 6), NIMG (SARM1), NIM-N (SARM4), NIM-P (SARM5), NIM-S (SARM2), PCC-1, SARM8, SARM9, SARM32, SARM34, SARM39, SARM40, SARM42, SARM44, SARM45, SARM46, SARM47, SARM49, SY-2, SY-3, UB-N, UREM3, UREM4, UREM7, W-2 (Govindaraju, K. 1984, Loubser and Verryn, 2008).

3.2.4 Master Particle Sizer

Malvern Particles Mastersizer 3000, manufactured by Malvern Panalytical was used, which is the latest generation of the world's most widespread particle sizing instrument. The technique uses the technique of laser diffraction to measure particle size distributions from 10nm up to 3.5mm. Sample dispersion is controlled by a range of wet and dry dispersion units, to ensure the particles are delivered to the measurement area of the optical bench at the correct concentration and in a suitable, stable state of dispersion with accurate and reliable particle size measurements. The analysis delivers verifiable particle sizing performance of 0.6% accuracy for polystyrene latex standard measurements and offers repeatability on polystyrene latex

standards better than 0.5%. Its recommended use includes reproducibility on polydisperse standards better than 1%, exceeding ISO 13320:2009 and USP recommendations.

The Malvern Particle sizer uses the two internationally accepted standards written on the use of diffraction: ISO 13320 (ref.9) and USP<429>(ref.10). Both standards require individual triplicate measurements of the individual sample laser. The technique ensures the coefficient of variation [COV, or (std dev/mean) *100] <3% at the D_{50} and < 5% at the D_{10} and D90 as required by the ISO 13320 requirements. The doubling effect occurs when the D_{50} of the material is less than 10µm, i.e. if D_{50} is measured to be 110µm, the expected D50 should be less than 120µm even with a maximum 10% error.

Mastersizer 3000 is equipped with log-spaced array detector of 0.015 to 144 degrees automatic alignment. The optics features include maximum of 4nW He-Ne (632.8Nm), nominal (10mW LED, 470Nm), reverse frontier or convergent beam lens arrangement and effective focal length of 300mm. Software packages include size detecting range of 10nm- 3.5 mm to a maximum of 100 size classes, 06% accuracy, repeatability better than 0.5% variation and reproducibility better than 1% variation. The device is equipped with manual wet dispersion units (Hydro EV, SM and SV), manual dry powder dispersion unit (Aero M), automated wet dispersion units (Hydro MV and LV) and automated dry powder dispersion unit (Aero S). Mastersizer 3000E carries special features for IQ/OQ validation, 21 CFR Part 11 support which assist with ER/ES compliance (Micron Scientific, 2018).

3.2.5 Scanning electron microscopy (SEM)

UOP. SKU: SW-70051-BS-UB100i Biological Binocular (weight 6.5kg) with 4 eye and a standard tight fitted lid, 47mm petri slides, a microscope fitted with a 10x eyepiece and objective lenses offering 4 x 10 x 40 magnifications. The device is manufactured and supplied by DustWatch. 5211 FFP2 disposable moulded EN particulate respirator mask (Honeywell Brand) with Willtech^{TM} valve, half-face seal and twin-stapled elastics supplied by hse Solutions.

The SEM-EDS analyses were conducted using UB100i Biological Binocular device with 4 eye magnifications settings for mineralogical assessments as shown in Figure 3-1 below. Samples were prepared in a standard tight fitted lid, 47mm petri slides. Microscanning was conducted through selection of a representative image for each sample. A graticule was used to determine all size fractions for the samples. This starts at 10 microns and allows for the d_{50} diameter of a samples for estimation. The photographs were taken at four magnifications depending on the requirements.

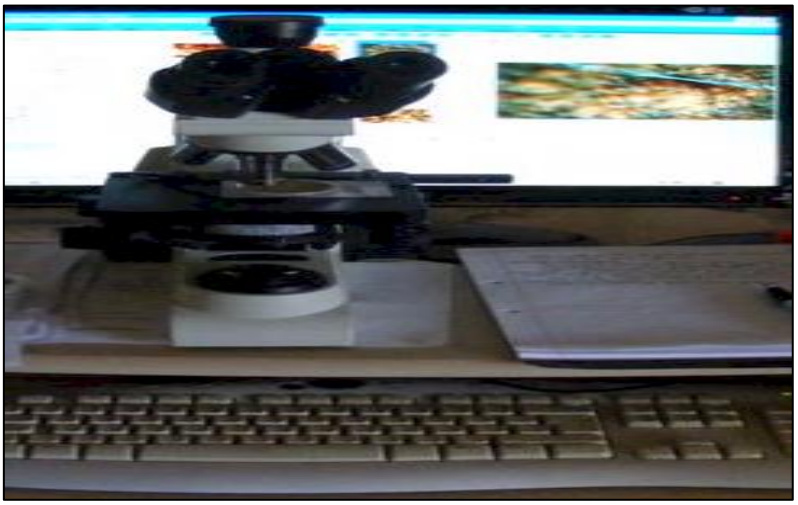

Figure 3-1: Microscope with eye piece and the optical camera

The Microscope has four magnification (mag) settings, 4x, 10x, 40x, and 100x as a field lens. The eye piece increases the magnification by 10x, and the camera increases it by 100 times (Figure 3-5). The camera is fitted to the top of the microscope and the eye piece magnification is not included. The total length of the graticule in the image below is 1mm from end to end. Each small line indicates a gap of 10 micron, each medium line is a gap of 50 micron and each long line is a gap of 100 micron. The sample is placed on Ideally samples should be in a standard tight fitted lid, 47mm petri slides for scanning and image selection. A graticule, with which can scan particle size of 10 µ and allowing for the d_{50} diameter was used to determine particles size fractions. The photograph of the sample was taken by the microscopic optical camera at four magnifications depending on the requirements of 1:400, 1:4000,1:1000 and 1:10000. Digitised images were further manipulated permitting viewing using polarised light and other means of illumination (DustWatch, 2016). The device is equipped with infinity corrected achromatic optical system which is ideally corrected over the field of view and produce crisp and clear images, thus making it the best choice for this analysis.

3.2.6 Visual risk analysis techniques

- Map indicating the location of the site and the nature of the surroundings, mainly depicted by 1:50 000 survey maps (Google Earth Pro 2020 using the Image Landsat/Copernicus, Data SIO, NOAA, U.S. Navy, NGA, GEBCO).
- Digital terrain model (DTM) showing topographical and cadastral information from the National Geo-spatial Information data supplied by the Department of Rural Development and Land Reform.

- Map imaging software: image © 2020 CNES/Airbus, © 2020 Esri Arc GIS, image ©2020 AfriGIS (Pty) Ltd and image ©2020 Maxar Technologies, Esri Arc QGIS (10.1) program files, 3D Analysist Extension.
- Canon EOS 1300D digital camera (of dimensions 129.0 x 101.3 x 77.6mm and weight Approx. 485g), with image sensor (Approx. 22.3 mm x 14.9 mm,18.0 megapixels and aspect ratio of 3:2), image processor (DIGIC 4+), lens (EF/EF-S equivalent to 1.6x the focal length of the lens), LCD monitor, flash (9.2 built-in) and focusing (TTL-CT-SIR with a CMOS sensor). The device was supplied by Camerawarehouse, Randburg, South Africa, is also equipped with Digital Photo Professional 4.4.0 (RAW Image Processing), Windows 10 / 8.1 / 8 / 7* and is battery charged).

3.2.6.1 Visual Analysis

The analysis was conducted as per Oberholzer (2008) combining various techniques following a 4-step approach discussed below:

- *Step 1: Administration of questionnaire on public perception environmental impacts of* TSF.

This was undertaken to analyse public perception of the visual impacts of TSF on their immediate environment from socio-economic, environmental, recreational, cultural and economic points of view. One of the interests of this study is to incorporate the public's perceptions and experience of the impacts of the TSF's within their environment. Thus, this study aimed to establish a) views, b) perceptions and c) truthfulness of the information of the study area.

- *Step 2: Site visits and photographic collection*

Site were visited to establish the extent of visibility of the TSFs as observed by the viewers, viewpoints, land use and roads infrastructure. Photographic views of the main viewpoints were taken and loaded onto GIS mapping (Rademeyer, 2007).

- *Step 3: Determining TSF zones of visual influence (ZVI) and visual absorption capacity* (VAC)

The ZVI considered the observer's or viewer's experience of the visual impact using visual exposure numerical ratings based on the observer's distance from the key viewpoints. These were rated using rating matrix showing severity, nature, extent, frequency and probability (Oberholzer, 2005).

- Step 4: Visual Risk Exposure

Visual Absorption Capability (VAC) was determined looking at the level of effectiveness of screening by topography and vegetation. Visual maps were created from Digital Terrain Model (DTM) of the study area using 5 km interval contours from the National Geo-spatial Information data supplied by the Department: Rural Development and Land Reform (DRDLR). The sites were plotted on the Google Earth Pro Map and superimposed on the DTM to select specific layers provided (WSP Environmental, 2019). The buffers were selected according to the distance of the TSF from the viewpoints (0-5km, 5-to 10km and beyond 10 km), creating VAC maps. Considering the site's biodiversity, landscape elevations and topographical features, zone of visual influence (ZVI) map was also created.

3.2.7 Radioactive elemental analysis

Coaxial high-purity germanium (HPGe) detector with a relative efficiency of 25.1%, peak to Compton ratio of 40.2:1 and a resolution of 2.3 keV at 1332 keV of 60Co shown in Figure 3.4 below. The detector was calibrated for energy and efficiency using

152Eu with an activity of (18.6±0.5) kBq. The activity concentration of 40K was determined directly from the gamma energy line of 1460.8 keV without sample irradiation. Gamma energy peaks of 277.6 keV and 312.2 keV from the decay of ^{239}Np and ^{233}Pa were used for the identifications of ^{238}U and ^{232}Th respectively.

Two High purity germanium detectors (HPGe) including: Broad energy germanium detector (including germanium crystal and all protection material), High voltage supply, Analog-to-digital converter (ADC), Pre-amplifiers, Amplifier, Nuclear Instrumentation Material (NIM), Multichannel Analyzer (MCA)

- Sample in cylindrical beaker (Including all materials used during sampling campaign, laboratory transfer and sample preparation)
- Global positioning system (GPS used to mark site during sampling campaign)
- Nitrogen cooling system
- Computer including Genie 2000 software and LabSocs mathematics simulation software for calibration
    - Calibration sources

The experiment was carried out in the Radio-analysis laboratory at the South African Nuclear Energy Corporation (NECSA), Pretoria, South Africa. The laboratory uses analytical methods which are documented in the Radio Analysis Quality Management System, based on ISO/IEC Standard 17025 (SANAS)- accreditation schedule T0111 (www.sanas.co.za). Three analyses were conducted: a) Gross Beta Analysis, b) Uranium and Thorium by neutron activation analysis and c) quantitative broad energy gamma analysis.

The analyses were conducted using a closed end coaxial high-purity germanium (HPGe) detector with a relative efficiency of 25.1%, peak to Compton ratio of 40.2:1 and a resolution of 2.3 keV at 1332 keV of 60Co shown in Figure 3-2 below. The detector was calibrated for energy and efficiency using 152Eu with an activity of (18.6 ± 0.5) kBq. The activity concentration of 40K was determined directly from the gamma energy line of 1460.8 keV without sample irradiation. Gamma energy peaks of 277.6 keV and 312.2 keV from the decay of ^{239}Np and ^{233}Pa were used for the identifications of ^{238}U and ^{232}Th respectively. Instrumentation used for this analysis are shown in Figure 3-2 below:

Photo 1

Photo 2

Figure 3-2: Photos 1-2 of the instrumentation at the NECSA Laboratories used for the radioactive analysis of the samples

The analytical methods for analysing dust samples were based on the Radio Analysis Quality Management System, as per the ISO/IEC Standard 17025 (SANAS)-accreditation schedule T0111. Three analyses were conducted: a) Gross Beta (**β)** Analysis, b) Uranium and Thorium by neutron activation analysis and c) quantitative broad energy gamma analysis. Application of the method requires the following steps: a) preparation a database of k0-NAA nuclear parameters, b) establishing the absolute detection efficiency of the used gamma ray spectrometers, c) determination of reactor

neutron spectrum parameters, and d) checking the accuracy of the obtained results via analysing some certified reference materials (Hamidatou *et al.*, 2012).

Samples were prepared and analyzed following a step approach detailed below as per the method suggested by Masok *et al*. (2017b). Each sample was marked with a unique identification number (sample ID), according to NECSA labelling system for traceability and taken to the laboratory. The samples were weighed and transferred into a separate metal drying pan and dried at a temperature of 105°C for 24h in a Labotech; model number MT 202 oven. This was then pulverized into a standardized fine power for good accuracy of analytical tools. Sub-sampling was done by transferring the standardized sample into a separate 500ml plastic container for gross **α** and beta activity measurement and gamma spectroscopy.

For the gross alpha and beta activity analysis, samples of 1.00±0.01 g each were weighed using weighing balance into the 25mm diameter planchette and compressed using a laboratory needle into a calibration matrix mixture. The samples were then in a petri dish and stored in a desiccator. By using Canberra supplied alpha/beta gas flow proportionality counter, Oxford Tennelec Series 5, gross (**α)** and (**β)** activity concentrations were analysed for each sample. Each sample was placed into a gas counting detector (a mixture of 90% argon and 10% methane), using a sample changer for 180 min. Elemental concentration analysis, specific activity (per unit mass) of ^{238}U, ^{232}Th and ^{40}K were expressed in *Bq.*kg^{-1} and converted into the sample elemental fraction (Masok *et al.,* 2017b).

As per the specifications by South African National Bureau of Standards (SABS), reference material was applied to determine the elemental constituents of the dust samples using irradiation and counting of the material under the same conditions as the samples. Blank samples were used for background measurements. Detection limits of sampling device considered the level of irradiation, decay, counting conditions and the blank from irradiation treatment and packing material. The detection limit provided the background under a gamma-ray peak, provided the gamma-ray background is the major interfering factor. The efficiency of the programmatic method is undeniable, but its accuracy and efficacy must be within acceptable error for the method to hold validity. The uncertainty value was calculated from the statistical counting process but not from standard deviation of the replicate sampling results (Masok *et al.,* 2017b).

3.2.8 TSF dust exposure Risk Analysis

Exposure analyses were conducted using data, namely, dust risk exposure, radiation risk exposure and health risk exposure.

3.2.8.1 TSF dust risk exposure analysis-dust settling velocity

Particles settling velocities were calculated using the distance of deposited settleable precipitant dust particles of various sizes to determine the extent at which these particles will travel away from the source, i.e., the TSF. Particle Settling Velocities (PSV) of particle sizes 1, 2.5, 5, 10, 30, 50, 80,100 and 84 µm were determined (DustWatch, 2019).

3.2.8.2 Radiation public exposure risk assessment

Radiation exposure risk assessment was conducted only focusing on atmospheric pathway exposure, limited at residential exposure resulting from environmental mining related sources such as TS's. Secondary data was used to compare the radioactive releases between TSF soil samples of two mining companies within the study area. Environmental conditions of the public were studied to establish various potential radiation sources of exposure based on primary community daily activities. This established inhalation and ingestion pathways (van Blerk & Potgieter, 2011a).

3.2.8.3 Human health exposure risk assessment

To determine the extent of dust, chemical composition, size and extend of contamination must be known. For this purpose, the enrichment factor (EF) and geo-accumulation indices (I*geo*) of the heavy metals found in the samples were determined using concentration analysis results.

3.2.8.4 Enrichment factor (EF)

The results of metal concentration were assessed for contamination using Enrichment Factor (EF) and Index of Geo-accumulation (I*geo*). EF calculation was achieved using the following equation 3.2 below:

$$\mathbf{EF = (C_X/C_{Fe})_{sample} \div (C_X/C_{Fe})_{crust}} \qquad \text{(Equation 3.2)}$$

In which,

- Fe(iron) is the selected natural element of reference;
- (C_X/C_{Fe}) sample is the ratio between concentration of the element "X" and that of Fe in the dust sample;

- $(C_X/C_{Fe})_{crust}$ is the ratio between concentration of the element "X" and that of Fe in unpolluted reference baseline.

3.2.8.5 Geo-accumulation index (Igeo)

The extent of heavy metal pollution in the selected precipitation dust samples was calculated using geo-accumulation index (I*geo*) proposed by Muller (1969) per Equation 3.3 below (Ntekim *et al*., 1993; Muller, 1981):

$$\mathbf{Igeo = \log2 (C_n/1.5B_n)} \qquad \text{(Equation 3.3)}$$

Where, Cn is the measured total concentration of the element ***n*** in the precipitant dust fraction in the sample, B***n*** is the average (crustal) concentration of element ***n*** in the Earth's Crust (background) and 1.5 is the lithogenic correlation factor compensating the background data.

3.2.8.6 Public Health Risk Exposure Experience questionnaire

A health risk exposure questionnaire was designed to determine the public dust experience from the residents' perspective, which was undertaken between July and September 2019. In this exercise, the focus was specifically on children of ages between 3 and 14 years, experiencing upper respiratory infections from inhalation of dust that could potentially be mining exposure related.

A set of health-related questions was designed looking at age, type of residence, medical condition, recreational activities, playing grounds condition of children within the targeted range. Letters requesting permission were sent to local Departments of Education, Department of Health, Health Centres, Clinics and schools within the study

area. Health specialists and teachers were approached requesting their participation in this study. Parents were also approached through one-on-one interviews, letters and via emails to collect information on their children's health related conditions targeted by this questionnaire. For comparison purposes, results from a mining area and non-mining area were used to establish any validations. However, responses were very poor, possibly due to perceived controversies on health issues relating to mines.

3.3 Sampling Protocol

3.3.1. Dust sampling

Dust sampling was conducted as per the American Society for Testing and Materials (ASTM D1739 1970) Standard Method for Collection and Analysis of Dust Fallout" (settleable particulates deposition dust). The method has been adopted as legal requirement in the South African National Environmental Management: Air Quality Act (Act 39 of 2004), National Dust Control Regulations of 2013 (NDCR 827, 2013). Precipitant dust samples were collected through single and directional precipitant dust bucket units attached/framed on a pole at a height of 2.2 m above the ground (DustWatch, 2016).

Precipitant dust samples were collected through single and directional precipitant dust bucket units attached or framed on a pole at a height of 2.2 m above the ground. For each site, the buckets were prepared by charging them with variable amounts of water, taking the expected evaporation that was likely to occur into account. The buckets were exchanged on a 30-day collection period over a period of 12 months to capture a full cycle seasonal variations and trends. A total of six (6) precipitant dust collection

sites [two (2) directional dust buckets and four (4) single buckets] were setup and a total of 114 samples were collected between June 2016 and July 2017.

3.3.2 Sample weighing and filtering

Under stable and well-ventilated laboratory conditions, 47mm filters were pre-weighed and placed into a marked petri dish. The contents of each bucket were filtered through the pre-weighed filters using a Buchner Funnel arrangement and care was taken to ensure that no dust was left in the buckets. Once the solid contents of the bucket were collected on the identified filter, it was left to dry in the open for a minimum of 24 hours. The filters were then weighed, and the masses were recorded with the initial masses of the filters.

3.3.3 Description of the study area

The site forms part of the West Wits Line Mines located within the Merafong City Local Municipality (MCLM) of the West Rand District Municipality (WRDM). Witwatersrand Basin is the world's largest gold and uranium mining basin in South Africa (shown in Figure 3-3 below).

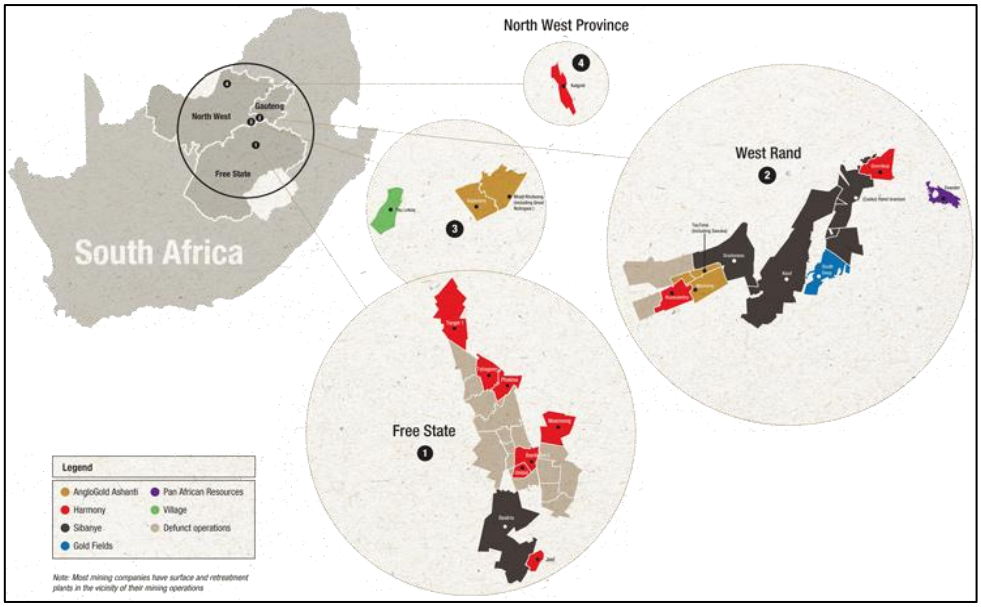

Figure 3-3: Witwatersrand Basin Gold mines locality map (Minerals Council South Africa, accessed on 23 August 2020)

The West Rand gold fields form part of the Witwatersrand Basin which is a gold reef stretching from the east (Germiston) to west (Randfontein) and comprise the Eastern Basin, the Central Rand Basin, the Western Basin, the Far Western Basin, the Klerksdorp, Orkney, Stilfontein and Hartbeesfontein (KOSH) Basins and the Free State gold mines as shown in Figure 3-4 below.

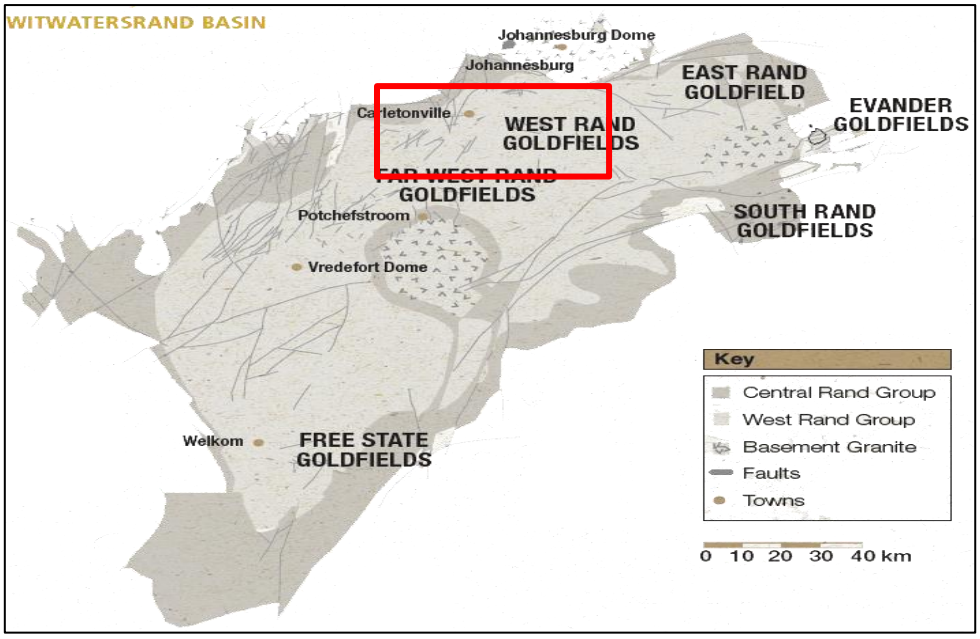

Figure 3-4: Map showing the West Rand Goldfields and the Far West Rand Goldfields (Minerals Council South Africa, accessed on 23 August 2020)

The reef dips south and stretches to West Wits Line then to the Free State goldfields. Gold mining on the West Wits Line contains of the biggest and richest mines in the entire Witwatersrand Basin (Robb, *et al,* 1997). There are seventeen mines in the Western Basin area, each with a different lifespan and impact on the groundwater resources of the area (Toens and Griffiths,1964; De Kock,1964; Lednor, 1986; Engelbrecht, 1986) as shown in Table 3.2 below.

Table 3.2: Mines forming the Western Basin Mining Area

West Rand Mine Lease Areas	West Wits Line Mine Lease Areas
1. East Champ D'Or	8. East Driefontein
2. Luipaardsvlei	9. West Driefontein
3. West Rand Cons (First Wesgold)	10. Blyvooruitzicht
4. Randfontein Estates (REGM)	11. Doornfontein
5. Western Areas N and S (WAGM)	12. Deelkraal
6. REGM Cooke	13. Elandsrandt
7. REGM Doornkop	14. Western Deep Levels
	15. Libanon (including Venterspost)
	16. Kloof
	17. Leeudoorn
18. Durban Roodepoort Deep (Shows Relationship to Central Rand Gold Mines)	

The Western and Far Western Goldfields Rand Mining areas are characterised by some of the oldest mining area which have been intensively mined and greatly disturbed in the region. Approximately six billion tonnes of mine waste have been generated since the beginning of mining in 1886 in the Witwatersrand Basin (GDARD, 2011). So far, approximately 270 tailings storage facilities (TSFs) have been commissioned, covering an area of about 180km^2 (Rösner *et al*., 2001). These resulted the legacy of TSFs, some of which have been covered by vegetation, while others are still exposed to wind and water erosion. Depending on the season and wind conditions, un-vegetated areas, uncovered mine TSFs dumps and paved areas contribute significantly to dust generation.

The West Rand District Municipality (WRDM) represents the jurisdiction area of the Western and Far West Rand Mining areas and is in the west of Gauteng Province. The area is formed by three local municipalities namely: Merafong City, Mogale City, Randfontein and Westonaria Local Municipalities and occupies about 4,095 km^2 size of land (WRDM IDP2017/2018). Merafong City Local Municipality (MCLM) is almost 163 157 hectares in extent, of which 32% is developed. The landscape of the study area is dominated by mining activities with protruding mine gears and mine residue deposits like waste rock dumps (WRD) and tailings storage facilities (TSFs). Formal and informal settlements exist, which include Carletonville CBD, Blyvooruitzicht, Deelkraal Elandsridge, Fochville, Khutsong, Mohaleshoek, Oberholzer and Wedela. Mine villages and mine residents form part of individual mine lease areas. The land use in the area comprises primarily of mining and agriculture activities take place on the outskirts of the area.

Sensitive environmental receptors include sensitive ridges with protected fauna and flora species, rivers such as the Elandsfontein, Vaarkenslaagte and the Wonderfonteinspruit drainage, which forms the main continuous discharge link between the mines in the area. The Wonderfonteinspruit Catchment Area is densely populated and there has been high dependency in using its water for recreation, spiritual rituals, domestic purposes, irrigation, watering of cattle and drinking purposes and consuming food planted within the area (Liefferink, 2015).

3.3.4 Topography

Prominent local structures which are protruding the landscape even from long distances include historic features such as the Danie Theron Monument, waste rock dumps, TSFs and mine headgears. The Gatsrand forms a prominent rocky ridge, rich in biodiversity, extending from east to west of the region and a distinct watershed within the area. Tourists' attraction spots such as Kraalkop Game Park with chalets are found in the area. The WRDM has elevation of between 1 473 m and 1 600 m above mean seal level, the highest elevation points are between 1 728 m and 1 856 m above mean sea level and the lowest points are between 1 217 m and 1 345 m. The average slope of the area is between 0 and 3% whereas the central and southern portions form areas of highest elevation (WRDM, 2010).

3.3.5 Meteorology

Climatic conditions, topography, natural and anthropogenic activities are key to the regional air quality (GPDACE, 1998). The pressure fluctuations and temperature inversions result in air movement and mixing affect pollution levels. The Gatsrand partly controls the level of air pollution either by providing a drainage pathway to

transport pollution from source to areas down gradient or acting as a barrier to pollution movement. The area's airshed allows for interaction of emitted pollutants or increase in concentration or extended period of suspended pollutants (WRDM, 2010).

The climate is characterised by highveld conditions, with relatively warm to hot summers, high rainfall and moderate to cool winters (with little or no rain). Data from the Krugersdorp Weather Station recorded rainfalls averaging between 4-138mm, with annual average precipitation of 736mm, occur mainly in summer from October to March, with the peak being in November-January. Air pollutants are thus washed down onto surface soils during this rainy period. Naturally occurring cycles of prolonged drought last for several years. Thunderstorms usually occur in the late afternoons during the summer months and extreme weather conditions in a form of hail and fog, rarely occur within the area. Annually, hail patterns occur on average 2 days during the year, while fog occurs on average 8 days (WRDM State of The Environment Report, 2005; WRDM, 2010).

3.4 Sampling Sites

3.4.1 Sampling sites selection criteria

The terrain, elevation, prevailing wind direction, location of tailings dump sources and residential areas were considered when the monitoring sites were selected. Each site is unique and the impact of the precipitant dust emanating from the mine TSF source is dependent on the following factors:

- The type of mineral being processed and
- The methods used.
- The local meteorology,

- Topography, and
- The zoning of the land surrounding the site.

Precipitant dust fallout monitoring stations were positioned within close proximities to mine TSF's, school premises, formal residential area, community centre, library and local hospital. Even though the main target was high precipitant dust fallout prone areas from TSFs, other gold mine related activities and processes contributed towards dust emission monitored. These are included and specified in Section 3.4.2 below.

3.4.2 Sampling sites locations (including coordinates)

Dust samples were collected at selected locations are shown in Figure 3-5 and described in Table 3.3 below.

Figure 3-5: Dust sample sites locations

Table 3.3: Sampling sites locations

Site No.	Site Name	Single (S)/ Directional (D) Bucket	Coordinates	Distance from TSF and direction	Other dust sources	Immediate environmental receptors
Site 1	**BLY**	**D**	**26°8'19.72" S; 27°22'37.17E**	Abandoned TSF 221,73 m, (W) Dormant TSF1-237,1m (NE) Dormant TSF2-104,88m (E)	Public road, E Dirt TSF roads Thatch roof harvesting	Local shopping complex 104,88m (E), Residential area 259,92 m, NE of TSF1
Site 2	**LES**	**D**	**26°25'17.92" S;** **27°22'25.13E)**	Dormant TSF-454, 51 m (NW)	Public road (E) Mine stockpiles and processing (NE)	Within hospital premises mine activities, W and SW Mine hostels.
Site 3	**P School**	S	**26°27'7.50" S;** **27°25'21.32" E**	Dormant TSF - 415,7 m (SE)	Abandoned waste rock dump- 1,39 km (W)	school premises, Public road (E), Old mine and TSF(N), Residential area (S)
Site 4	**S Centre**	S	**26°24'47.28" S; 27°22'33.45" E**	Abandoned TSF- 800 m(S)	Abandoned waste rock dump-	community center and residential area, school
Site 5	**WED LIB**	S	**26°28'6.86" S;** **27°22'44.55" E**	Active TSF- 1km (NE)	Mining activities	community library premises, residential, ridge
Site 6	**DEEL**		**26°27'30.01" S;27°19'30.37" E**	Active and dormant mine TSF's – km N, NE	Mining activities	Ridge (N), mine village

After calculating the dust fall rates, settleable dust samples trapped on the filter paper during the filtration process were prepared for laboratory analyses. This characterization included particle morphology (sizes, shapes, diameters), particle size distribution, chemical or elemental, radioactive elements and the mineralogical contents.

3.5 Statistical Analysis

Statistical Package for Social Scientists (SPSS) Software (1.0.0.1406, Windows, Mac, Linux) was used for the data analysis at 95% confidence interval. The ANOVA Test, non-parametric correlation (Kruskal Wallis and Spearman's Rho) tests were conducted. Descriptive and inferential statistics (regression), descriptive and inferential statistics (reliability and validity- Cronbanch alpha) and time series analyses, including Pearson Correlation Index.

3.6 Quality Assurance/ quality control performance

3.6.1 Deposition dust collection

The dust buckets were partly filled with distilled water, to which a 3,5% solution of hypochlorite was added to prevent the growth of algae. The buckets were exchanged on a 30-day collection period over a period of 12 months, between June 2016 and July 2017, to capture a full cycle seasonal variations and trends. Dust buckets were individually removed and sequentially replaced, using the labelled lid to seal the removed bucket and properly labelling the bucket.

To ensure that the buckets are free of contaminants prior every use, thorough cleaning with normal domestic use detergent [Sunlight Dishwasher (1 teaspoon) diluted in 1litre

of distilled water] and rinsed twice again with distilled water. Buckets and the lids were soaked with a commercial Milton (Sodium hypochlorite: 1.0% and Sodium chloride: 16.5%) sterilizing solution (1: 10 dilution) filled to a point up to the brim for at least 1 hour. The sterilising fluid was discarded and rinsed with the known sterile water and filled to the 1000ml (1 litre) level – no bleach or algaecide – and closed for transport to the sampling site. Buckets were only opened on site using sterilized screwdriver and placed on the dust monitoring unit. Once the sample has been collected after the sampling period, the dust buckets were immediately capped, labelled and transported in a cold box to the laboratory for filtration.

Laboratory equipment including vessels, flasks, funnels, spatulas and other glassware vessels were pre-cleaned by normal domestic use detergent and rinsed with tap water. Overnight soaking with 10% HNO3 followed by rinsing with tap water and then with deionised water (MΩ cm, Milli-Q Plus, Millipore) and storage in a cleaned zip lock polyethylene plastic bag (Yalala, 2015).

Dust collection buckets were transported in an upright position to prevent spillages. For dust filtering, initial desiccation was conducted in a dust free environment for a minimum of 24 hours to ensure complete drying out of all samples. Desiccated filters were placed on the balance and left to dry on the pan for about 60 seconds until the mass remained stable. The scales were zeroed, and the filters re-weighed twice and the average of three masses were recorded on the assessment sheet.

3.6.2 X-RF Methods

A blank and two certified reference materials were analysed with each batch of samples. Each tenth sample is run in duplicates and include own standards and duplicates in batches as per the International Association for Geoanalysts' GeoPT proficiency test suggested by Thompson (*et. al.*,1997). This requires a thrice annual geological analysis and statistical treatment with "z" values analyses results. Sample preparation errors were assessed by preparing a batch of unknows in the same process as unknowns to produce calibration curve setup at 20-30 standards and calculate limits of quantification.

CHAPTER 4

The chapter presents results obtained in this study.

4.1 RESULTS AND DISCUSSIONS

4.1.1 The Outcome Results of Experimental Analyses

Characterization of the precipitant dust was carried out to determine dust deposition rates, morphological, particle size distribution, radiological, mineralogical and elemental analyses. The specialist studies were also undertaken to assess the risks associated with dust and its constituents on the exposed public receptors as per this study's objectives:

4.1.2 Precipitant dust deposition rates for all sites

The results presented in Figure 4-1 below show that on average, Site 1 (BLY) recorded the highest dust deposition rates of 1165.5 mg/m^2/day, followed by Site 5 (Wed Lib) at 918 mg/m^2/day and these exceeded the regulated residential limit of 600 mg/m^2/day but below the non-residential (1200 mg/m^2/day) limit.

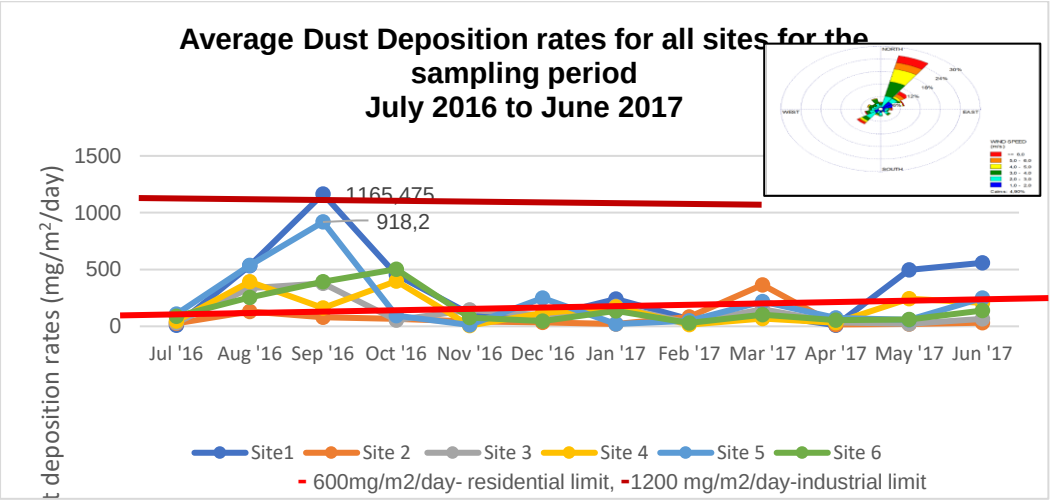

Figure 4-1: Average dust deposition rates for all sites (Sites 1-6) between July 2016 and June 2017

From Figure 4-1 above, it can be noted that both these exceedances occurred in the month of September 2016. This suggests that the predominant winds are predominantly north-easterly, and above 6m/s as suggested in the wind-rose inserted on the top right position in Figure 4-1 above. However, Sites 1 and 5 record the average lowest deposition of 10 and 12 mg/m^2/day in July and November 2016, respectively.

4.1.2.1 Four buckets (directional) sampling sites precipitant dust deposition rates

Site 1 (BLY) and Site 2 (LES) present the four buckets stations capturing precipitant dust from any of the main directions. The results are demonstrated in Figures 4-2. and 4-3 below.

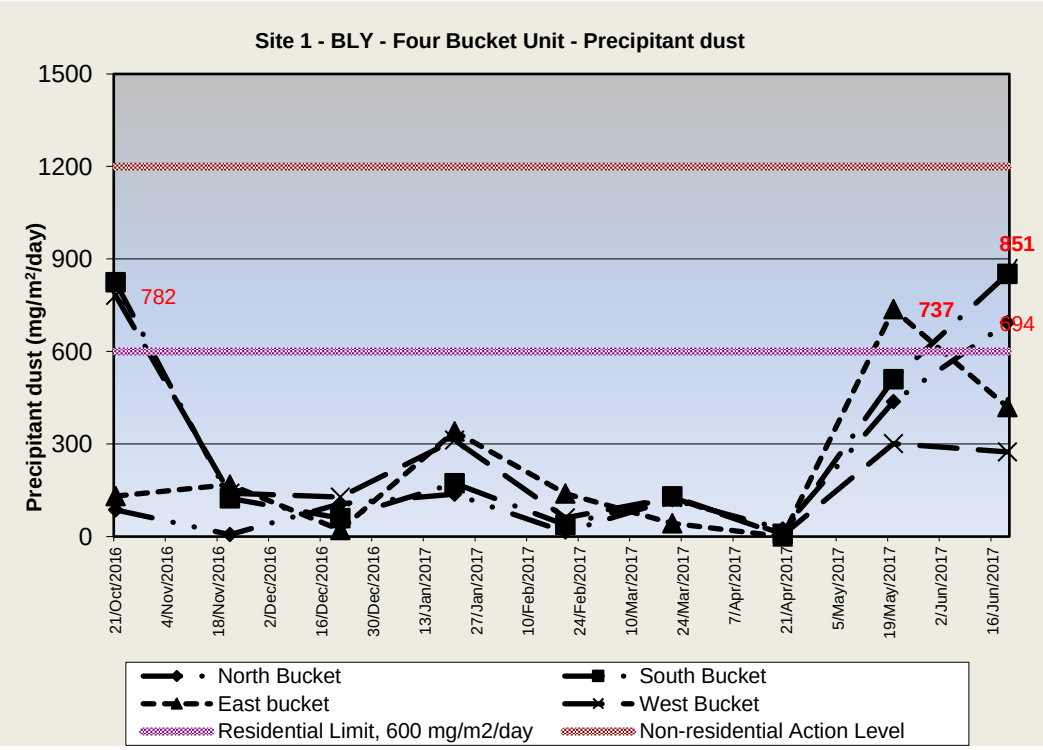

Figure 4-2: Settleable precipitation dust deposition rates representation for Site 1 between October 2016 and June 2017.

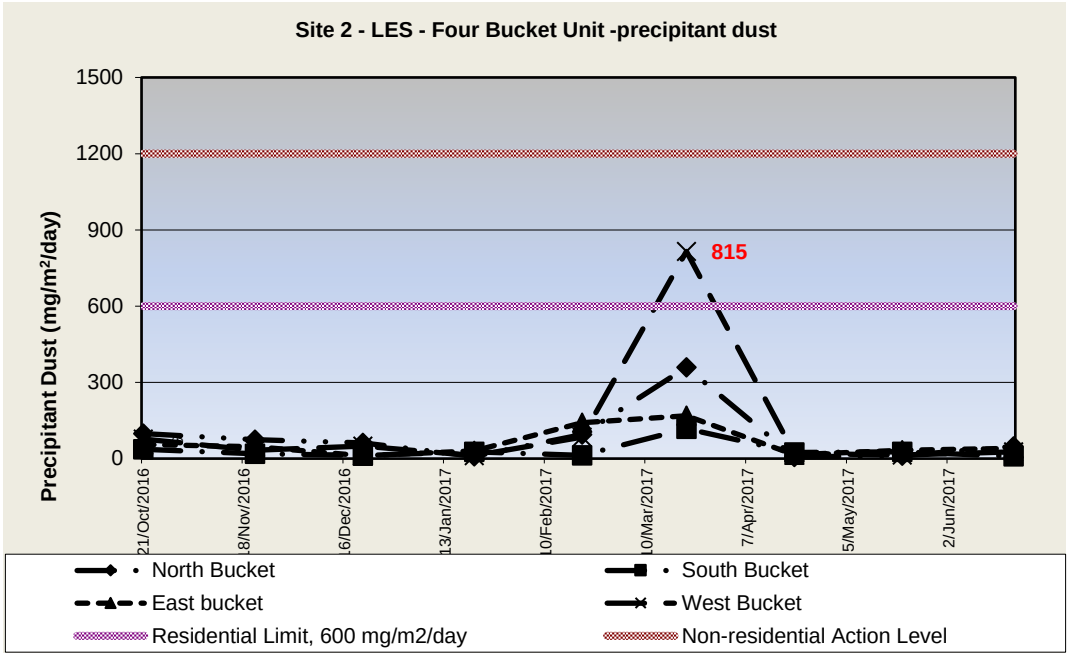

Figure 4-3: Settleable precipitant dust deposition rate for Site 2 during the period October 2016 and June 2017.

A comparative results analysis of the four-buckets sites, i.e., Site 1 and Site 2 as shown in Figures 4-2 and 4-3 above confirm that the precipitant dust deposition rates recorded at Site 1 coincided with the south-westerly to north-easterly winds in June 2017 and south-westerly winds measured on the 21 October 2016. Site 2 W recorded the only highest dust deposition rate of 815 mg/m^2/day predominantly from the west to the north, were measured in March 2017. This exceeds the residential limit of 600 mg/m^2/day, but below the non-residential limit of 1200 mg/m^2/day. The least dust deposition of 0 mg/m^2/day was recorded at Site 1E and Site 2S in April 2017 and June 2017 respectively.

4.1.2.2 Single dust buckets monitoring sites precipitant dust deposition rates

The results for Sites 3, 4, 5 and 6 in Figure 4-4 below show the highest dust deposition rates of 503, 398 and 205 mg/m^2/day at Sites 6, 4 and 5 respectively, collected between October and December months. The least deposition rates were recorded at

Sites 5 and 4 at 12 and 7 mg/m^2/day between November 2016 and February 2017. No exceedances were recorded at Sites 3, 4, 5 and 6 in terms of residential (600 mg/m^2/day) and non-residential (1200 mg/m^2/day) limits occurred within the sampling period. This was attributed to by the high rainfall events of within this period leading to high precipitation.

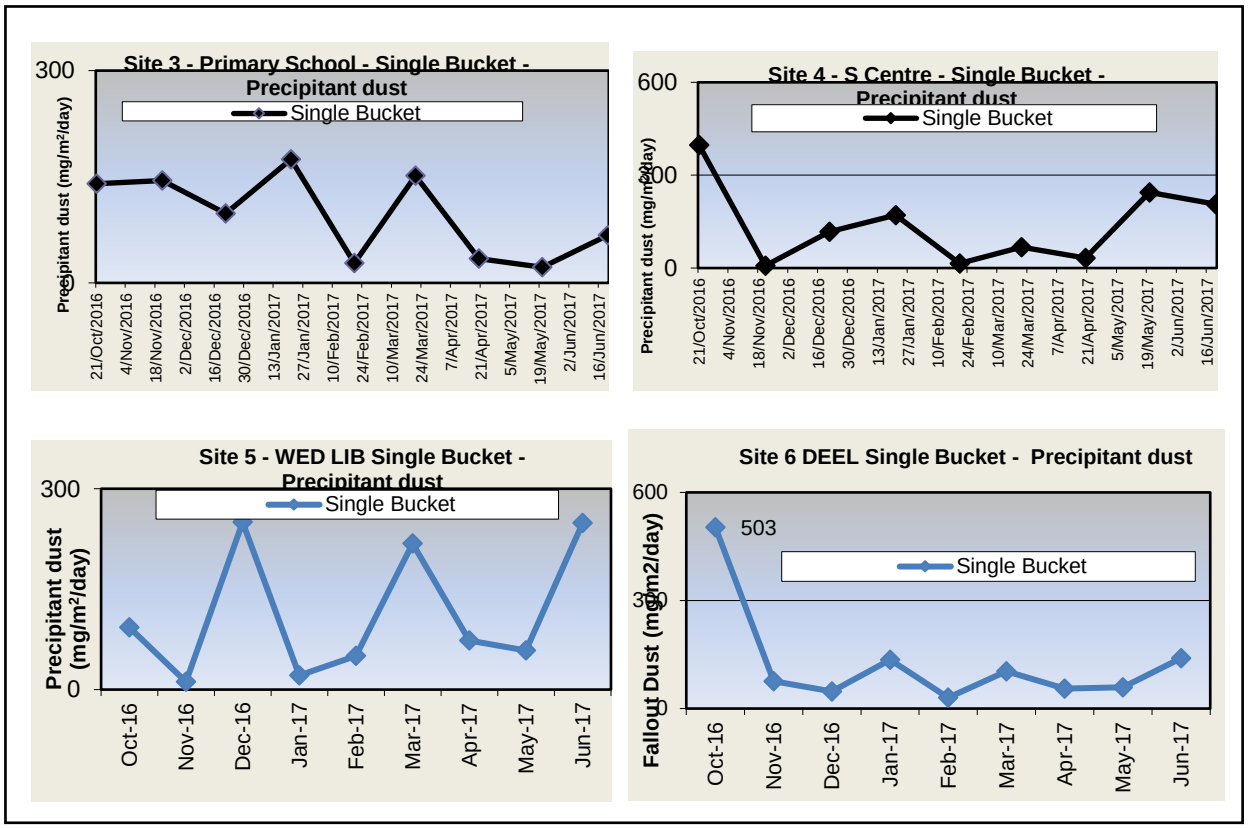

Figure 4-4 Single buckets precipitant dust deposition rates results for Sites 4,5 and 6 for the period October 2016 to June 2017

Within November 2016, Site 1 recorded the lowest dust deposition rate of 6 mg/m^2/day, below the average of 84 mg/m^2/day and Site 2 was within the average of 61 mg/m^2/day. Sites 1 and 2 are within the average deposition rates of 84 and 61 mg/m^2/day respectively.

4.1.2.3 Precipitant dust deposition rates per quarter

Quarter 3 2016 dust deposition rates results for four-dust buckets sites (Sites 1 and 2) and single dust buckets sites (Sites 3,4,5 and 6) are presented below in Figures 4-5 and 4-6.

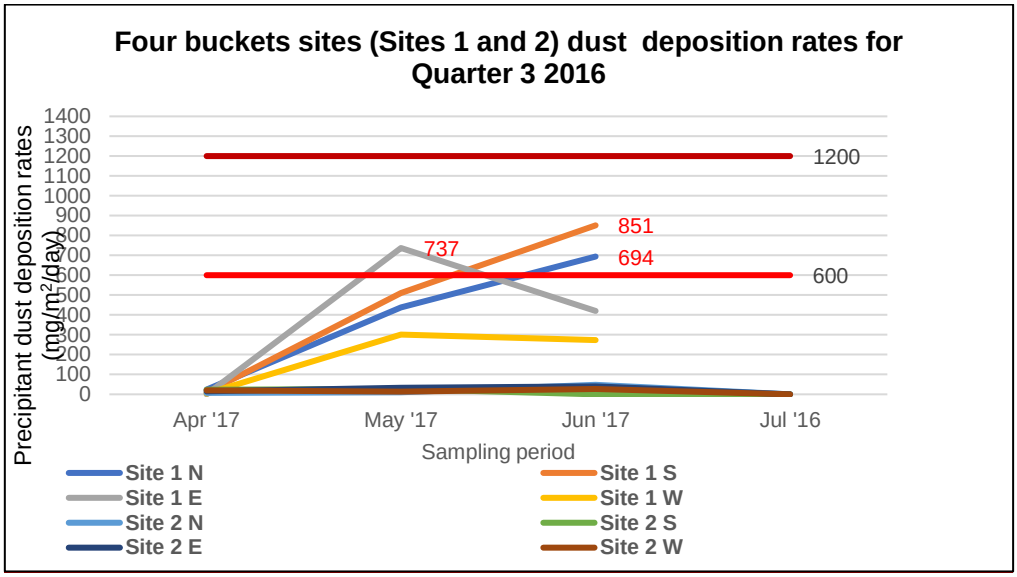

Figure 4-5: Quarter 3 2016 precipitant dust deposition rates for Sites 1 and 2

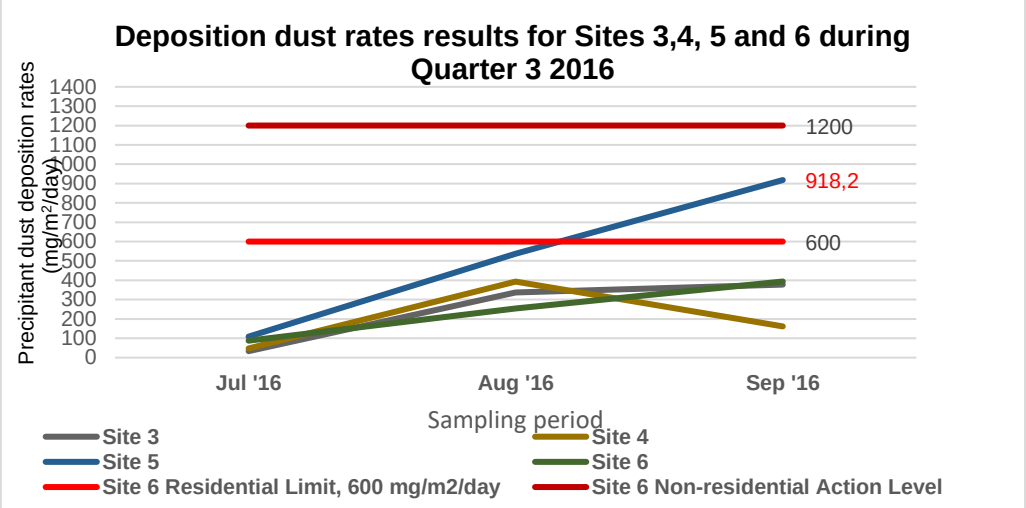

Figure 4-6: 1 Quarter 3 2016 precipitant dust deposition rates for Sites 3,4,5 and 6

The results in Figures 4-5 and 4-6 above confirm that for both single and the directional dust buckets sites, Sites 5, 1S, 1E and 1N show the highest precipitant dust deposition

rates of 918, 851, 737 and 694 mg/m^2/day respectively, exceeding the residential limit of 600 mg/m^2/day, but below the industrial limit of 1200 mg/m^2/day.

Quarter 4 2016 results confirm that the precipitant dust deposition rates at Site 1 exceeded the legal residential limit of 600 mg/m^2/day during October (Q4) of 2016 at 824 mg/m^2/day and 782 mg/m^2/day collected on the southern and western buckets, respectively. This suggests that the predominating winds were blowing from south westerly directions. Site 1 is located within the area of an unrehabilitated, high precipitant and abandoned dust depositing TSF. Of point to note, several complaints were raised by communities within the area due to the alleged dust exposures from the TSF which is located on the South Western part of the site. Notably, Site 2 records very low precipitant dust deposition rates during the period under observation as shown in Figure 4.5 above. Stockpiling activities from the mine located on the eastern part of Site 2 across the road which had ceased within the Q4 of 2016.

Within Q4 of 2016, Site 6 experienced the highest precipitant dust deposition rates contribution of 503 mg/m^2/day. Sites 4, 3 and 5 record precipitant dust deposition rates of 398 mg/m^2/day, 140 mg/m^2/day and 93 mg/m^2/day, respectively. However, in November 2016, Site 3 record the highest precipitant dust deposition rates of 144 mg/m^2/day, with Sites 6,5 and 4 recording the least precipitant dust deposition rates of 76 mg/m^2/day, 12 mg/m^2/day and 7 mg/m^2/day respectively. Precipitant dust deposition rates at all monitoring points around the study area are well below the legal limits (residential: 600 mg/m^2/day; and non-residential: 1200 mg/m^2/day) and no exceedances occurred. Even though this period has normally high rainfall occurrences in which precipitation is expected to be high thereby suppressing the dust, high precipitant dust deposition rates may be from other pollution sources within the area,

mainly mining related. Quarter 1 2017 precipitant dust deposition rates results for all sites are presented in Figures 4-7 and 4-8 below.

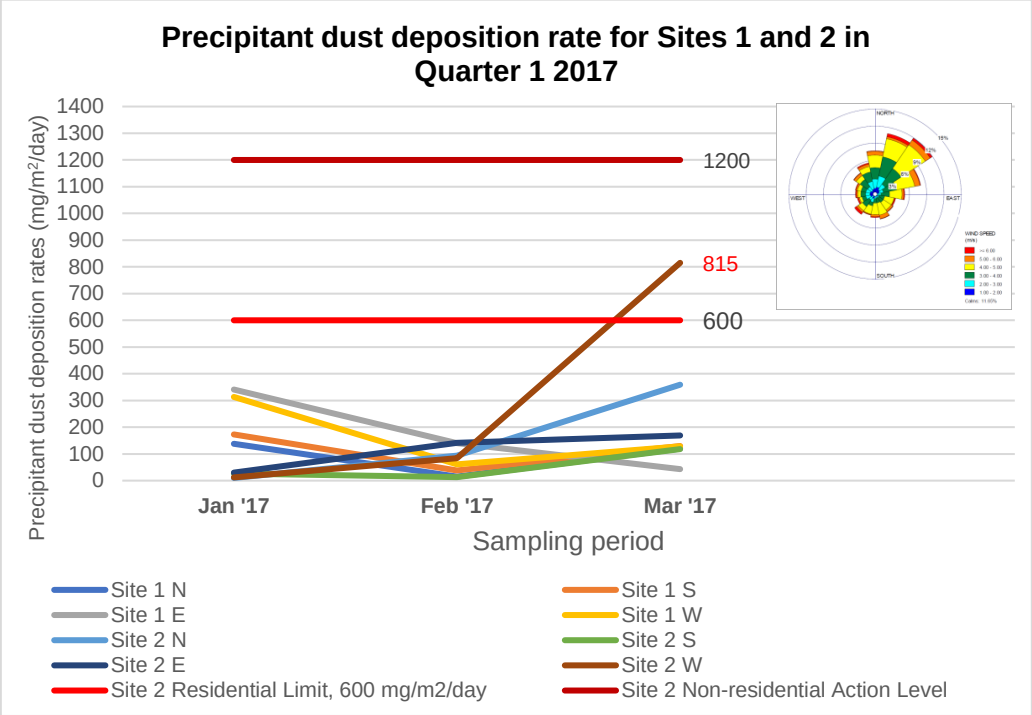

Figure 4-7: Precipitant dust deposition rates for Sites 1 and 2 for Quarter 1 2017

Precipitant dust deposition rates between January to March (Q1) of 2017 is concentrated around Site 2 at 815 mg/m^2/day (Figure 4-7). The monitoring station measured dust from the gold mine plant across the R500 Road., given that the prevailing wind direction is from the North-east and East (from the plant's direction), blowing dusty wind towards the site. Dominant activities taking place across the R500 Road located on the eastern direction from the site include transportation, processing and stockpiling of gold mine process material. Reclamation of the TSF to the immediate north-west border of Site 2 could also contribute to the dust deposition.

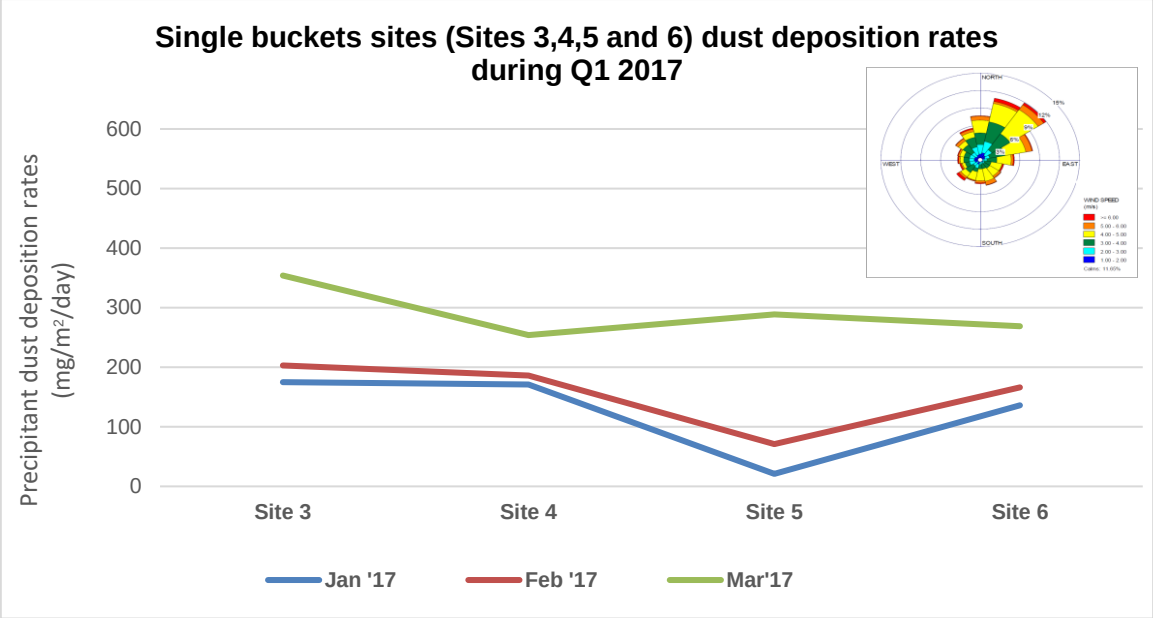

Figure 4-8: Precipitant dust deposition rates for Sites, 3,4,5 and 6 for Quarter 1 2017

Figure 4-8 above confirms that precipitant dust deposition rate in this quarter was well below the residential limit of 600 mg/m^2/day. Data confirmed that a small percentage of 3.1 % of strong winds were present and only 11.7 % of the recorded winds in this quarter were calm winds. Even though a high percentage of strong winds (29 % of winds between 4 m/s and 5 m/s) were recorded (AGA, 2017), a general decline in precipitant dust deposition rates for the quarter. Precipitation acts as an atmospheric cleansing mechanism, minimizing atmospheric pollutants and deter dust generation potentials.

A total of 417 mm of rainfall was recorded in the study area during January to March (Q1) of 2017. Within this quarter, the most dust from other sources in the area was deposited in the northern parts of the study area. The north-easterly winds dominated this area, indicate that the settleable precipitant dust deposition on the northern and eastern sides of all areas might either be from other sources or from storm events.

Immediate sources of directional dust could possibly come from surrounding mining activities such as reworking of the TSF's, road transportation of ore material, spillages and biomass burning from residential areas.

Although the site-specific nature of each of the sites and the variance in climatic conditions should be taken into consideration when the results are interpreted, the data does present one area where precipitant dust deposition rates increased, affecting the deposition rates at Site 1 and Site 3 located nearby the TSF dust sources. However, no exceedances were documented Q1 2017, except for Site 2 which experienced exceedance of 815 mg/m^2/day collected from the western bucket, exceeding the 600 mg/m^2/day residential limit. As the rainfall results are shown in Figure 4-8 above, low precipitant dust deposition rates could be from the rainfall events experienced between 21 and 28 December 2016, and 04 & 11 January 2017. Figures 4-9 and 4-10 below show the results of precipitant dust deposition rates during Quarter 2 2017.

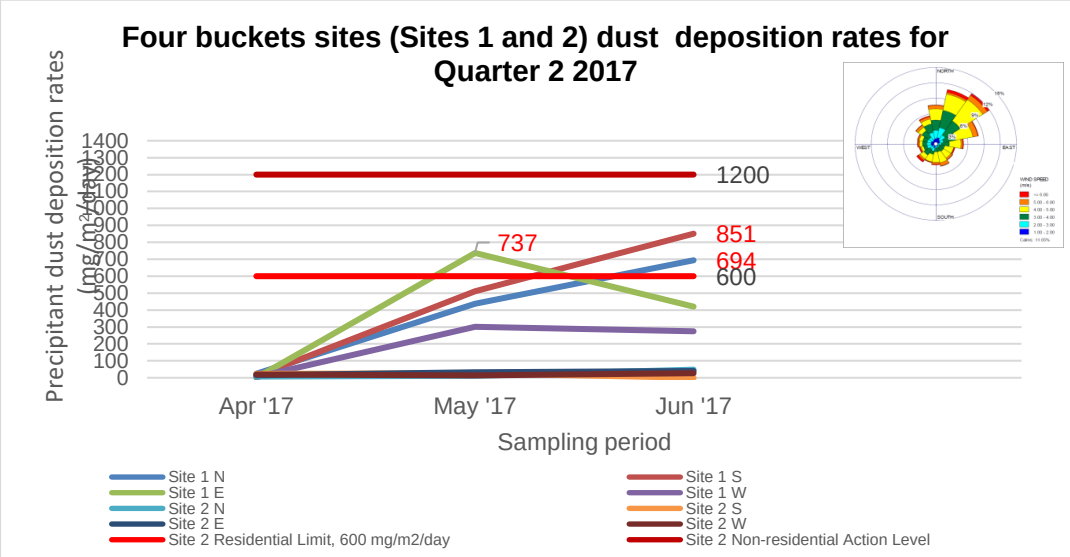

Figure 4-9: Precipitant dust deposition rates for Sites 1 and 2 for Quarter 2 2017

Figure 4.9 above confirms settleable precipitant dust deposition rates of 851 mg/m^2/day (June), 737 mg/m^2/day (May) and 694 (June) mg/m^2/day recorded at Site 1. These were beyond the residential limit of 600 mg/m^2/day, collected at the southern, eastern and northern buckets respectively (Figure 4.8). Even though the results for April 2017 show that almost no dust was collected in any of the buckets, yet the May and June results exceeded the residential limits, possibly due to several man-made factors and activities within the location of the dust collection station. Yet, recorded dust deposition rates for Site 2 ranged between 7 and 48 mg/m^2/day.

The reasoning behind such variance in dust deposition rates for Site 1 and Site 2 could be due to several factors both natural (metrological) and anthropological activities. Firstly, meteorological factors such as low winds could have contributed to the lower deposition rates results, e.g., low winds which normally occur during autumn season, i.e., from April to June (AGA, 2016; WeatherSA, 2019). Secondly, high deposition rates at Site 1 were not expected due to likely occurrences of low or calm winds (Scorgie and Sithole, 2002). At the time of this study, the site was not access-controlled, and dust collection could have been affected by grass harvesting activities taking place in very close proximities of the site, within 50 m of the site. Again, the Site1 is easily accessible by members of the community as they use the nearby footpath to walk between nearby residential areas and the shopping complex across the main road from the site.

Thirdly, the site is located within 100 m from the footprint of the TSF which was identified as a problem area in terms of dust deposition which drew a lot of community complaints in the area. Fourthly, the low results in April for both Sites 1 and 2 could

have been reduced by dust mitigation initiatives implemented by some of the mining houses within the area, probably, due to raised public complaints.

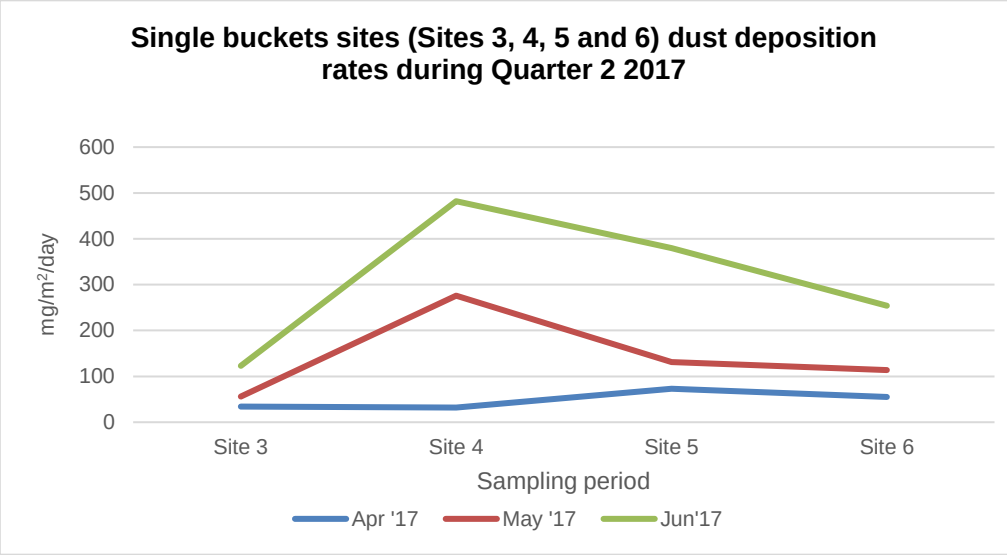

Figure 4-10: Precipitant dust deposition rates for Sites 3,4,5 and 6 for Quarter 2 2017

In Q2 of 2017, precipitant dust deposition rates for all sites were below the legal limits (residential: 600mg/m^2/day; and non-residential: 1200 mg/m^2/day) and no exceedances occurred for Sites 3,4,5 and 6.

The two greatest popular sources of pollutants in this area are vehicle entrainment over road surfaces and wind erosion of the TSFs (AGA, 2016). Due to mining gradually becoming inactive within the area, some TSFs have become either vegetated or remediated and some are no longer active, thus less of the material might not be exposed for wind erosion. Roads leading to and from these decommissioned TSFs are also no longer in use, thus vehicle entrainment impacts should be less where these roads are no longer in use (AGA, 2015). However, due to the recent reclamation of gold projects within the area from some of the inactive or dormant TSF's, liberation of dust gets re-emitted as the tailing's material gets exposed to wind power.

Due to the study area being in a predominantly mining area with related activities, such as trucking of mine process material, stockpiling, etc., this could worsen to the general precipitant dust deposition of the area. Other sources such as biomass burning and other stockpiled mine residues such as waste rock dumps are known to have cumulative effect to the overall precipitant dust deposition within the area (AgreenCo, 2015; DustWatch, 2016).

Strongest North and north-easterly winds of above 6 m/s dominate the wind field of the study area. Furthermore, day-night wind field switch resulted in an exchange from predominantly northerly and north-easterly winds to more frequent winds from the South West and north northeast. However, calm conditions occurred 1.6% of the time, with the average wind speed over the period calculated as 3.05 m/s. The resultant increase in wind speeds during the night-time conditions led to an increase in calms from 0.81% during the day to 2.02% during the night (Scorgie & Sithole, 2002; Airshed 2015).

Out of the four single buckets, July to August was the least dust deposition period, but Site 5 had the most deposition (918 mg/m2/day), followed by Site 6 with deposition of 88 and Site 4 (control site) being the least dust deposition site. Strong winds exceeding 6 m/s occurred most frequently during spring months (i.e., September, October and November). Calm conditions occurred most frequently during autumn months (February, March and April). Elevated lower wind speeds (0.5 – 2.1 m/s) occurred during autumn and winter months from the North East (AGA, 2017).

4.1.2.4 Seasonal variation of dust deposition rates

There are four seasons of weather in South Africa, namely, summer (December - February: DJF), autumn (March – May: MAM), winter (June – August: JJA), and spring (September – November: SON) (DEAT,nd) . Precipitant deposition dust rates for the period between July 2016 and June 2017 are expressed in Figure 4-11 below.

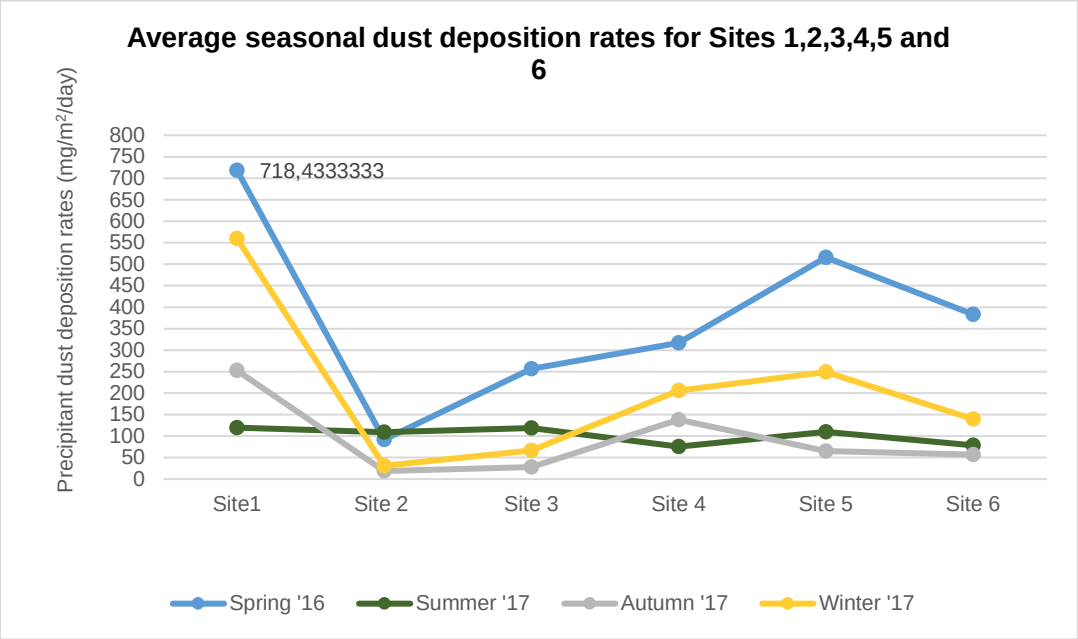

Figure 4-11: Average seasonal variation dust deposition rates for Sites 1,2,3,4,5, and 6

On average, in spring 2016 the dust deposition rates of 718.43, 516.16, 383.27, 317.30 and 256,37 mg/m^2/day occurred for Sites 1, 5, 6, 3 and 2 respectively. Only Site 1 recorded the average dust deposition rate of 718 mg/m^2/day, exceeding the residential limit of 600 mg/m^2/day. Spring represents the highest dust deposition period as the dust deposition for all sites and in all seasons, except for Site 2 (91 mg/m^2/day), which was below the average dust deposition for Site 2 (109 mg/m^2/day) in summer. Spring is characterised by dry and high wind speeds manifested by the highest dust deposition rates as the dry soils are exposed to erosion as shown in Figure 4-11 above.

These high dust deposition rates in 2016 spring were also noted in other studies within the area confirming elevated dust deposition rates occurrences due to low precipitation and high wind speeds (Mpanza, 2020). Lower wind speeds occur within May to August (winter period) while unstable tropospheric conditions were noted in summer and the prevailing winds could also come from different directions (Dudu *et al.,* 2013).

However, according to Scorgie & Sithole (2002), autumn and winter periods are characterised by high atmospheric stability with least wind speeds for dust generation, hence the least deposition rates shown in Figure 4-11 above. These strong winds exceeding 6 m/s normally also occur most frequently during spring months (i.e. September, October and November) as depicted in Figure 4-11 above. Other studies also confirmed that these elevated dust deposition rates are aggravated by the dominant north-westerly winds which mainly occur in the dry late-winter and early summer months when the surface of the mine dumps were still dry. In this period, contaminated soils are exposed by these prevailing winds, releasing dust laden with metals and metalloids distance away from the source (Van Alphen, 1999; Sterckeman *et al*., 2000; Scorgie & Sithole, 2004; Stafilov *et al*., 2010; Fernandez-Camacho *et al*., 2010; Taylor *et al*., 2010; Sanchez de la Campa *et al*., 2011, Yalala, 2015).

A representation of the wind meteorological conditions for the study area during the dust fallout monitoring period is shown in Figure 4-12 below.

Summer	**Autumn**
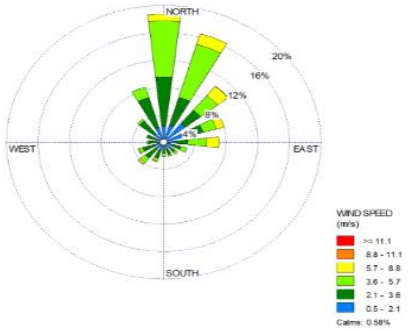	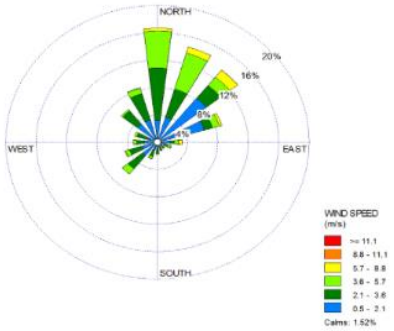
Winter	**Spring**
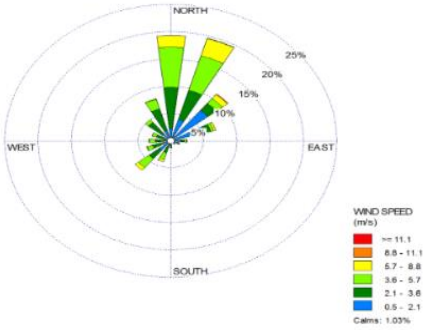	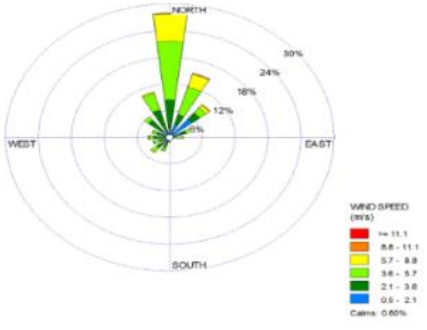

Figure 4-12: Seasonal windroses for the study area

The most dominating winds from the north and northeast and the strongest winds (>6 m/s) also emanated from these directions as noted in Figure 4-12 above. Calm conditions occurred 1.6% of the time, with the average wind speed over the period calculated as 3.05 m/s. Strong winds exceeding 6 m/s occurred most frequently during spring months and calm conditions occurred most frequently during autumn months. This increase in lower wind speeds (0.5 – 2.1 m/s) during autumn and winter months from the North East.

The lowest average deposition rates were recorded at Site 2 in autumn (18.875 $mg/m^2/day$) and winter (31 $mg/m^2/day$). This resulted from calm conditions occurring most frequently during autumn months (February, March and April). There was increase in lower wind speeds (0.5 – 2.1 m/s) during autumn and winter months (i.e. between Q1 and Q2 2017) from the north east (AGA, 2017).

During Autumn (February to April), even though the prevailing wind field was from the north and north-northeast, there is a distinct decrease in the frequency from these sectors with a slight increase of easterly flow supported by the wind roses in Figure 4.11 above. The wind field during the winter months (dry season-June to August) remains similar, with an increase in the occurrence of winds from the north and north-northeast during spring. Wind speed bears direct effects on dispersion of pollutants through dilution of pollutants by a factor proportional to the wind speed past the source. Secondly, mechanical turbulence, which increases mixing and dilution of pollutants, is created by the wind. Finally, a buoyant source (hot or cold) is likely to ‘bent over’ more at higher wind speeds, keeping it closer to its release height (Tiwary and Colls, 2010).

Summers are periods of low precipitant dust deposition due to precipitation, whilst winter periods present high precipitation dust occurrences due to dry conditions. High wind speeds with low humidity are likely to disperse pollutants into the ambient air (Dudu *et al., 2013*; Wright *et al.,* 2014).

4.1.2.5 Comparative analysis of dry season and wet season dust deposition rates results

The study area forms part of a subtropical climatic condition region which experiences summer rainfall amounts of 700 millimetres per year and is mainly concentrated during October to March as shown in Figure 4-13 below. Winter season takes place from May to August and is formed by a dry season, with rare and sporadic rains whereas **spring and autumn** are mild and sunny, occur in April and September. The rainfall pattern of the study area shown in Figure 4-13 below confirms high rainfall periods between November to March which are mainly wet seasons. Low rainfalls occur in from April to July and these are generally dry months of the year. Months of July and August are the windiest periods for this area.

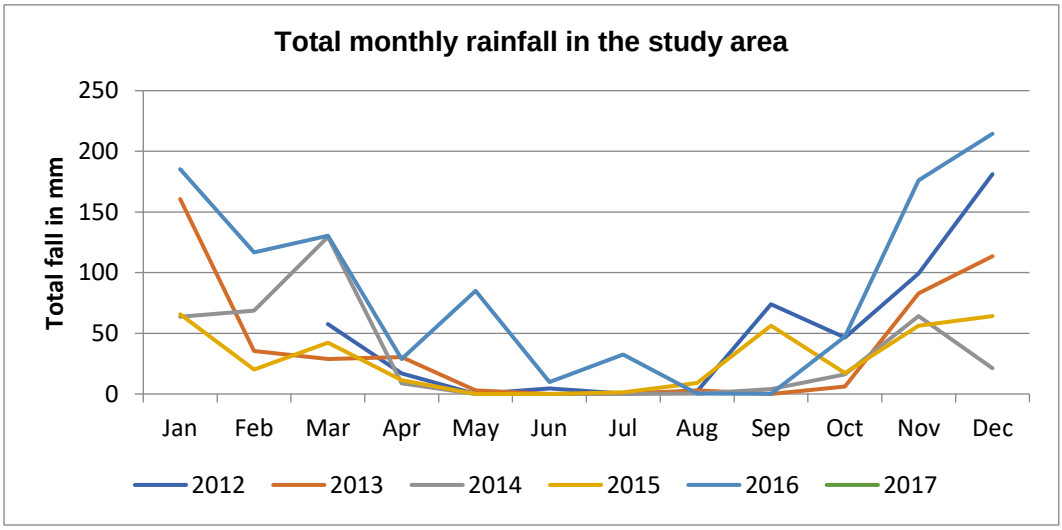

Figure 4-13: Regional rainfall patterns for the period 2012 to 2017 (AGA, 2017, WeatherSA, 2019)

The rainfall pattern of the study area shown in Figure 4-13 above confirms high rainfall periods from October to March making this the wet season of the year. Whilst low rainfalls occur in from April to July and these are generally dry months of the year, July and August are the windiest periods for this area (Annegarn *et al*., 2002; AGA, 2017). The data shows that the hottest temperatures occur in the summer months, between 13:00 and 15:00 in the afternoon. This is when the most evaporation of water from the mine waste material takes place and when the greatest risk of dust is present (AGA, 2015; WeatherSA, 2019).

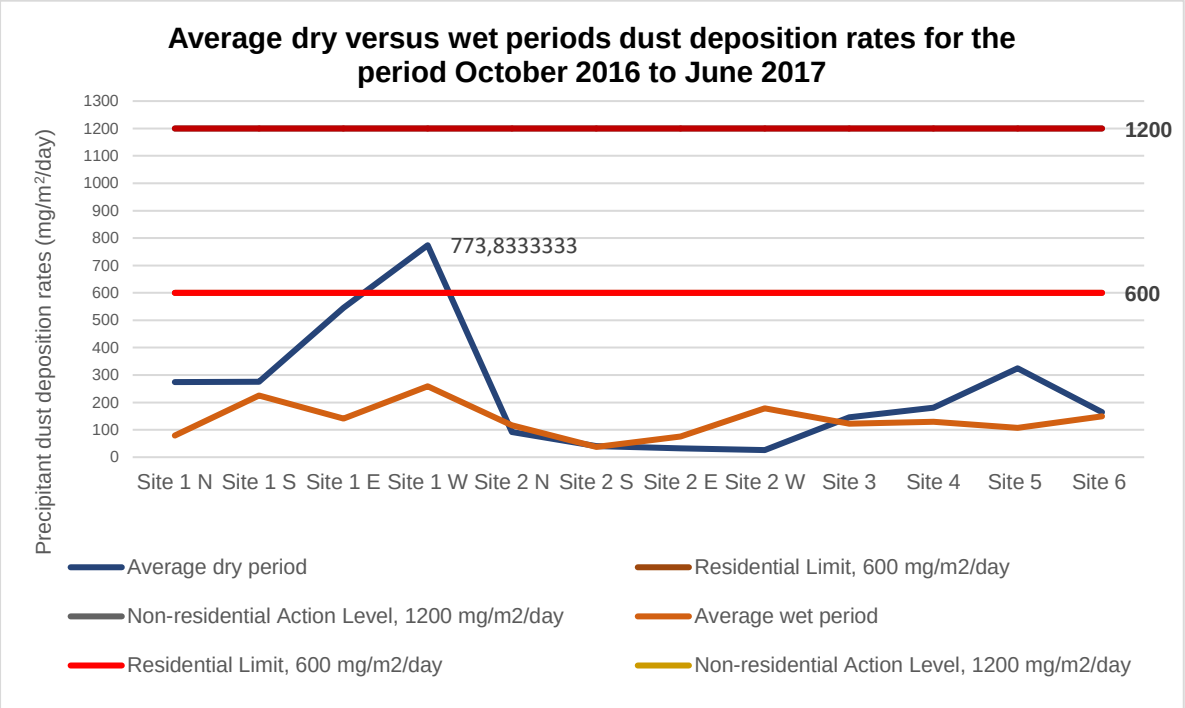

Figure 4-14: Comparison of the average dry and wet periods dust depositions

The results in Figure 4-14 above show that in the dry season (i.e. from April to September 2016), the average dust deposition at Site 1 W only exceeded the NDCR Residential Limit of 600 mg/m²/day (red trend line), recording 774 mg/m²/day. This occurred during the dry period when the average dust deposition rate across all sites within the dry period was calculated to be 135 mg/m²/day. The highest average over

the monitoring period of 774, 324 and 274 mg/m²/day at Sites 1W, 5 and 1N respectively. The lowest average value for the dust deposition monitoring network was recorded at 26, 37 and 116 mg/m²/day for dust bucket Sites 6, 2S and 2N respectively.

The wet period results recorded the highest dust deposition rates of 259, 225 and 178 mg/m²/day at Sites 1W, 1S and 2 W respectively. Within this period, the lowest recorded dust deposition rates of 38, 78 and 107 mg/m²/day at Sites 2S, 1N and 5 respectively. Lower reading within this period is contributed to by high rainfall patterns which present effective air pollution removal mechanism of atmospheric pollutants. Site 2 W recorded the lowest dust deposition of 4 mg/m²/day within the wet period (April 2017). This presents a transitional period from wet to dry season, characterised by low winds, even though the total average rainfall from October 2016 to March 2017 amounted to 145 mm.

The recorded dust deposition rates concurred with the results from other studies conducted within the study area confirming that the period from March to July (dry season) presents the lowest dust deposition whereas August to October months form windy season, with decreasing levels between November through February as this becomes the wet season. Rainfall patterns remain the most contributing factor of dust deposition rates. Autumn and winter dry months are also the time of greatest atmospheric stability and minimum wind speeds within the study area. The greatest wind erosion mainly occurs in early spring prior to the first rains and in summer, alternating wet and dry periods result with high winds and associated with thermal atmospheric turbulence (Scorgie & Sithole, 2002; Ogutonke *et al*., 2013).

4.2 Characterisation of TSF Dust Collected at Various Sites

The characterisation of TFS dust collected was done in terms of morphology, particle size distribution, radiological, chemical, and mineralogical components.

4.2.1 Scanning Electron Microscopy Analysis (Morphology)

Figure 4-15 below shows morphological images of the samples for Sites 1, 2, 3, 4, 5 and 6 for selected periods.

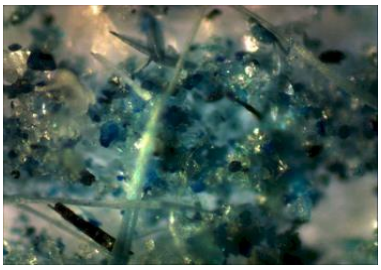

Image 1: Site 1 micro scans imaging showing tridymite thread in a sample within Q4 2016

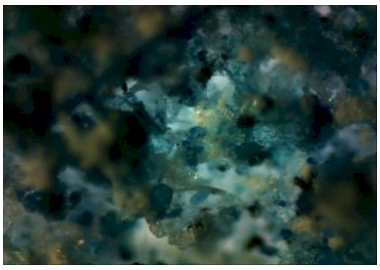

Image 2: Site 2 sample micro scans imaging showing traces of calcite crystalline aragonite for the period December 2016 and January 2017

Image 3: Site 3 The fine flakes which are clay bound and consist of fine d0,50 of 80 micron

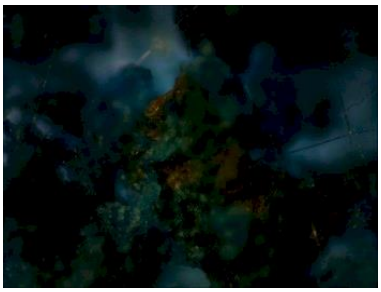

Image 5: Site 4 (S Centre) sample micro-scan imaging showing haematite material of the harder blue variety and rounded worn quartzite grits period January to March 2017

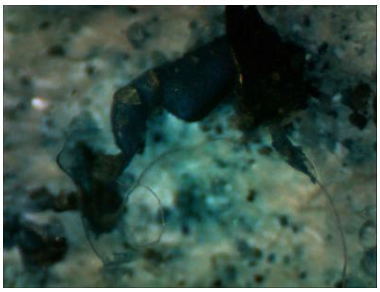

Image 7: Site 5 (WED LIB) sample micro scan imaging showing mostly fine round quartz during for the period January to March 2017

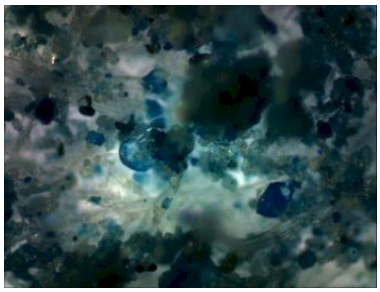

Image 8: Site 6 (DEEL) sample micro scan imaging showing rounded sandy worn and rounded particulates period January to March 2017

Figure 4-15: Particle size distribution for Sites, 1,2,3,4,5 and 6

Table 4.1 below provides the overall SEM analysis results per site, focusing on the original source of the mineral formations.

Table 4.1: Microscan Analysis Results of Sites 1,2,3,4,5 and 6

SITE	Quartz (sandy grits, quartzite, isolated, rounded, broken)	Pulverized roadway dust	Feldspar	Hematite (traces)	Clay (natural colloidal, traces, fine, isolated	Organic
Site 1	5-70% D50= 55-108 µm	10-15%	D50=38µm-70µm	D50 <59%µm	<6%, 30% D50= 63-73 µm	-
Site 2	10- 70% D50=37-200 µm	20% D50=69-118 µm	D50= 58µm	<2%	20-40% D50=63- 78 µm	-
Site 3	-	Traces	-	D50= 30-50 µm	Fine (>15%), D_{50}=70 µm)	fine evaporated viscous liquid crystalline material
Site 4	20-60%, D50=105-188 µm	40%, D50= 79µm	-	-	25% D50=53—61 µm	liquid or sap/ material anic crystals D_{50}=33 µm
Site 5	D50 = 105 µm	D50=55 µm	-	5%Fly high grit	10% liquid crystals D50=38µm	viscous red to orange liquid
Site 6	<5%, 70% D50 = 105 µm	Traces D50=55 µm	Fines <2%	-	10%	D50=38µm

Overall, samples for Sites 1,2,3,5, and 6 are predominantly made up of 5-70% quartz (rounded quartz, broken quartz and sandy grits) of size range (d50=37-200 µm) , haematite (<59%, d_{50}= 30-50 µm), pulverised roadway dust (10-40%, d50=63-79 µm), clay (6-40%, d_{50}=63-78 µm), felspar (<2%, d_{50}=30-58 µm), aluminium silicates 83 µm, viscous liquid crystalline (38 µm) and mica traces (only at Site 2E). Site 2W comprise

fine natural clays are always more prevalent during rainy season as acid rains and fine materials tend to become more plastic if there is some present feldspar to act as a catalyst. During dry periods such materials with coagulate, dry out and become more of a loamy topsoil. Further, components of the sample are of particles with sizes d_{50}=83µm, 79µm and 58µm of overall, topsoil and feldspar respectively. Site 3 sampled results for October and November 2016 shows fine evaporated viscous liquid crystalline material of organic origin. Of note, Site 6 sample detects sizes distribution $d0_{50}$ of 89µm, 88µm, 83µm, 78µm and 43µm, mainly from quartz, agricultural soil dust, overall, topsoil, and smoke carbon respectively. The smoke carbon reflecting a coal fired application is revealed in Site 2 W but at a very low content with agricultural soil dust at 45% and loamy topsoil 35% and pulverised roadway dust with rounded quartz traces also occurred. Particle size distribution d_{50} of 88 µm agricultural soil dust and 73 µm topsoil made up the sample constituents. The dust is almost all-natural ambient material rounded quartz grits 30% fine agricultural soil dust 20% and topsoils 35% with high organic debris and some calcrete material content evidence at Site 6.

4.2.2. Particle size distribution analysis results

A total of twelve (12) samples representing all sites were analyzed using the Malvern Instrument and the results are presented in Table 4.2 below.

Table 4.2: Average Particle Size Distribution for Sites 1,2,3,4, 5 and 6

Site Name	**Average particle size**	**% Particle content**				
Site 1 (BLY N)		**PM2.5**	**PM10**	**Size (site)**	**d50**µm **< 30 µm**	**d90**µm (limit 100-300µm)
	10	5.1	10.19254	14.5	61,3	299
Site 1 (BLY S)						
	10	3.6	7.249552	16.8	107	500
Site 1(BLY E)						
	10	5.2	10.3609	17.8	67,6	456
Site 1(BLY W)						
	10	2.0	4.038507	17.3	84,2	220
Site 2 (LES N)						
	10	3.6	7.249552	16.8	80,6	424
Site 2 (LES S)						
	10	5.1	10.19254	14.5	221	1030
Site 2 (LES E)						
	10	3.6	7.249552	16.8	60,3	194
Site 2 (LES W)						
	10	3.6	7.249552	16.8	55,4	175
Site 3 (School)						
	10	3.6	7.249552	16.8	230	602
Site 4 (S Centre)						
	10	3.6	7.249552	16.8	87,2	287
Site 5 (WED LIB)						
	10	5.1	10.19254	14.5	177	538
Site 6 (DEEL)						
	10	3.6	7.249552	16.8	199	650

Fine particles $PM_{2.5,}$ i.e., particles of size between 0.1 µm and 2.5 µm, which ranged between 0.0995 and 2.42 µm are recorded at Site 1E (N259 B), Site 2 N (N260), Site 2 E (N20B) and Site 2 W (N260C) whereas $PM_{2.5}$ ranging between 0,113 and 2.42 µm at Site 3 (N261), Site 5 (N263) and Site 6 (N264).

The overall particle size distribution for all sites ranged between 14,5 and 17,8 µm, with average PM $_{2.5}$ and PM_{10} of 4.35 and 8.7 µm respectively. According to Burton and Lundgren (1987), the percentage of total aerosol mass less than 10 micron varied

from about 50 to 90%, depending on the sampling location and sampling conditions. D_{50} for Sites 1,2,3,4,5 and 6 exceeded the expected particle size distribution of 30 µm. The highest D_{50} particle size 230 µm, 221 µm and 177 µm were detected at Sites 3, 2S and 5 respectively. The particle size collected is normally acceptable for the particle mass diameter. However, the D_{90} for Sites 1N (299 µm), 5 (287 µm), 1W (220 µm), 2E (194 µm) and 2W (175 µm) were within the expected range of 100 and 300 µm. The ideal number expected of less than 300 microns is acceptable contamination using this crude and non-specific test method, suggesting that the samples contained the normal for precipitant dust deposition size.

However, D_{90} for Site 2S (1030 µm), Site 6 (650 µm), Site 3 (602 µm), Site 5 (538 µm), Site 1S (500 µm), Site 1E (456 µm) and Site 2N (424 µm) exceeded expected for fallout dust levels (100µm with an upper error limit of 300 µm), and a localised dust source is likely to be the reason for elevated particles sizes being collected. Further, site in very close proximities to the source mainly result in course dust sample to be collected. Collected samples had larger particles in size and larger particulate had increased mass and this unit exceeded the non-residential action level of 1200_mg/m^2/day (DustWatch, 2016).

The results of this study suggest that the mean values of (475.5 µm) 75% in the samples collected were of coarser particle size ranged (100-300 µm), 130.15 (21%), whereas 4.35% and 8.72% of the particle size dust within the study area are of <2.5 µm and <10 µm, i.e. $PM_{2.5}$ and PM_{10} size fractions respectively. This concurs with Gruenewaldt *et al.* (2010), which noted small percentage of fine size fraction particles with mean values 5% and 13% (vol. %) in the <2.5 µm, and <10 µm size fractions, respectively.

Studies of TSF soil particles within the study area revealed that TSF1, TSF2 and TSF3 recorded values of D_{50} = 15, 21 and 68 µm respectively, confirming that the sampled data represent the finer components of the source, i.e. TSF soil collected as it got deposited to further areas away from the source. Settleable precipitant dust deposition rates in this area were largely contributed by TSF1 (89%) whereas daily and annual PM_{10} was mainly coming from the roads (36% and 52 % respectively) and other gold processing activities within the area (37% and 33% respectively) (Von Gruenewaldt *et al.,* 2010).

Comparatively, respirable and thoracic PM5 and PM10 component were evidenced in TSF source material of recent slimes, older slimes and sand at ranges (14–24 vol.%; 22–38 vol.%), (6–17 vol.%; 11–26 vol.%) and (1–8 vol.%; 2–12 vol.%), respectively (Ojelede *et al*., 2012). This explained the impact of improved gold processing technique, of the recent TSFs are characterized by finer particulate matter mainly due to advances in technology to finer milling and extraction of residual gold content, hence the reprocessing of old TSFs (Ojelede *et al*., 2012; Maseki, 2013; Yalala, 2015). Furthermore, the presence of coarse mode (1.0 to 10 µm) and giant suspended particle (GSP) modes in the airborne suspended particles shown in Figure 4-12 was a confirmation that their source was the tailings dams (Ojelede *et al*., 2012; Maseki, 2013; Oguntoke *et al.*, 2013; Yalala, 2015; DustWatch, 2016).

4.2.3 XRD-Mineralogical Analysis Results

The results of mineralogical contents of settleable precipitant deposition dust samples are shown in the below distributions shown in Figures 4-16 below showing quartz predominance at Site 1 as shown in Figure 4-16 below:

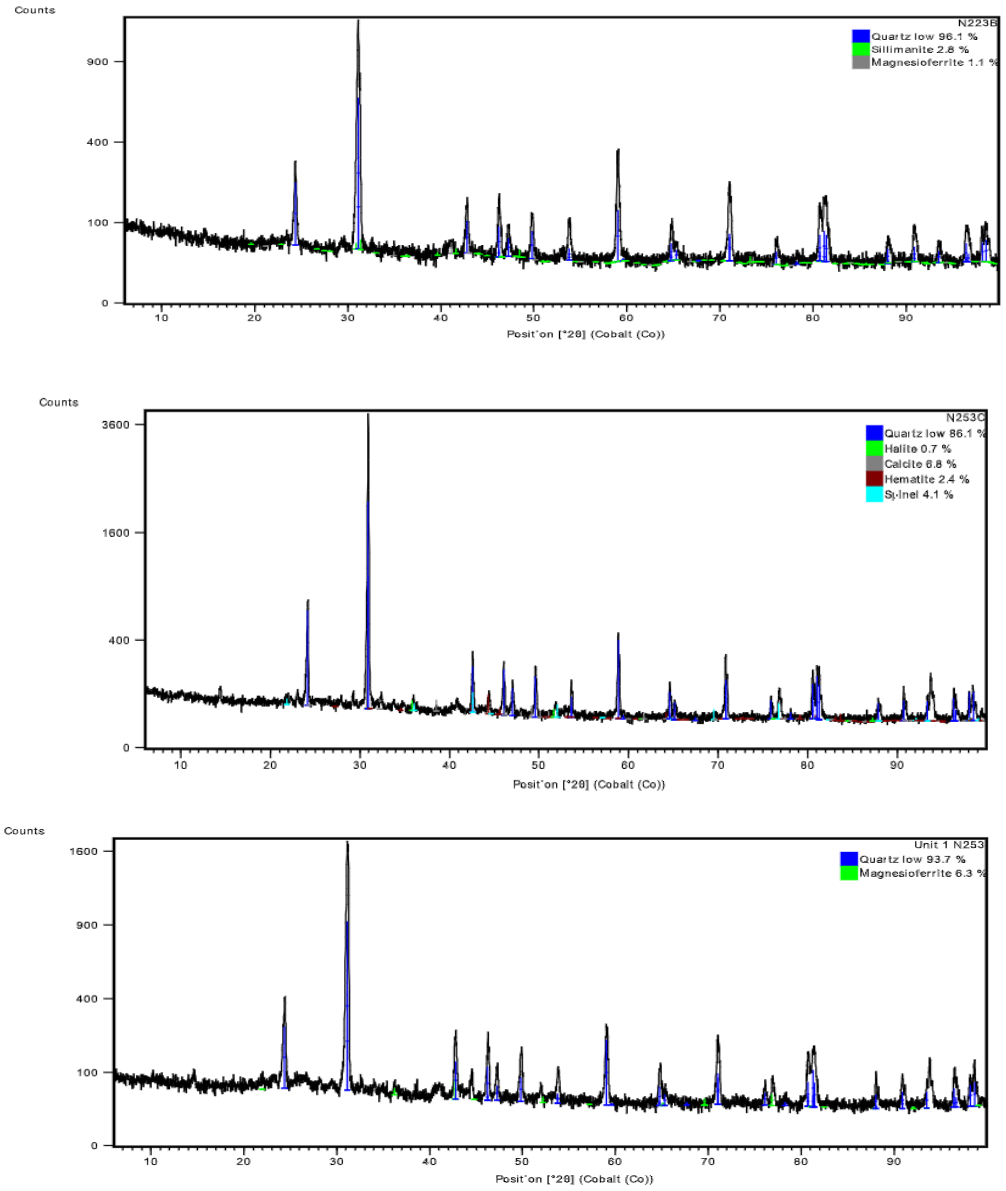

Figure 4.16: Results of mineralogical components (dominated by quartz) of the precipitant dust deposition samples at Site 1.

The results shown in Figure 4-16 above show that quartz predominately form larger constituents of Site 1 samples [Site 1E (N223 B), Site 1N (N253) and Site 1W (N253C)] which are 96%, 93,7 % and 86,1 % respectively. The average mineral composition for all sites samples is presented in Figure 4-17 below.

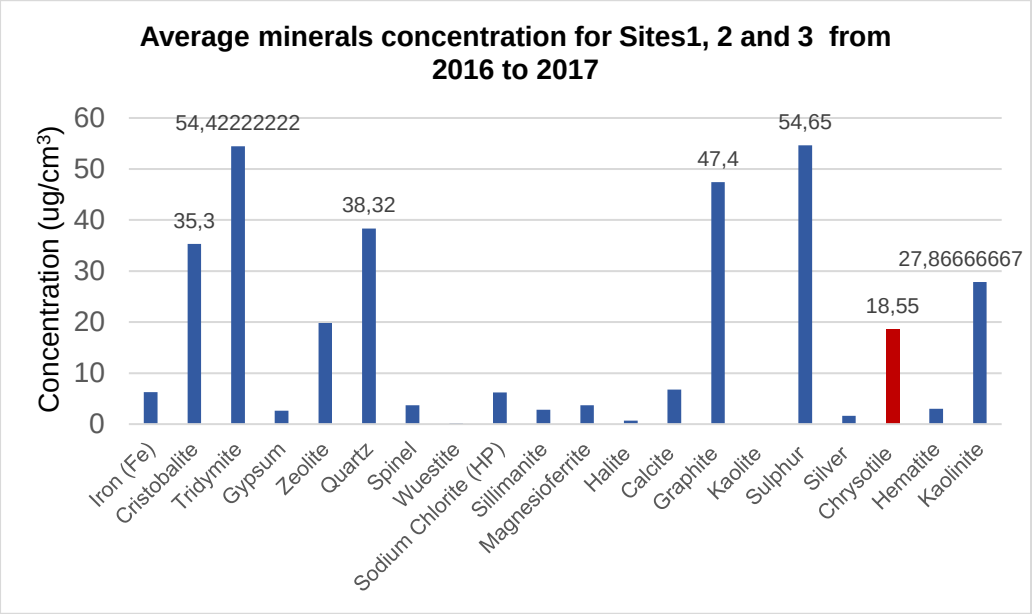

Figure 4-17: Average mineralogical composition of Sites 1,2, and 3 for 2016 and 2017

In this study, the average mineralogical components of all samples shown in Figure 4-17 above that sulphur (54,65%), tridymite (54,42%), graphite (47,4%), quartz (38,32%), cristobalite (35,3%) and chrysotile (27,87%) made up most of the precipitant dust. Chrysotile is associated with asbestosis occurrences in South Africa and its role in mesothelioma has been debated and documented for decades (Churg, 1988; Huncharek, 1994; Smith and Wright, 1996; Stayner *et al*., 1996; Egilman *et al*., 2003; McDonald, 2010; Phillips *et al*., 2012).

Comparatively, other studies of mineralogical composition of gold ore in the Witwatersrand confirmed occurrences of quartz (70-90%) (Liebenberg, 1956; Janisch,1986; Dudu *et al*., 2013; Maseki, 2013; Yalala, 2015, AGA,2016). The dominance of quartz confirms the original rock type material of the area (Yalala, 2015) and Archaean, quartz, veins and the pebble conglomerates reflect the most crucial gold minerals in the region (Frimmel and Minter, 2002; Maseki, 2013). However, sulphides only formed 1-2% of the reef conglomerate (Janisch,1986).

Table 4.3: XRD Results Showing Mineralogical Concentration (Ug/Cm3) Components of Dust, Tailings Material (Slurry), Pyrite Bearing Ore and TSF Soil

Site name	Iron (Fe)	Cristobalite	Tridymite	Gypsum	Zeolite	Quartz	Spinel	Wuestite	Sodium Chlorite (HP)	Sillimanite	Magnesioferrite	Halite	Calcite	Graphite	Kaolite	Sulphur	Silver	Chrysotile	Hematite	Kaolinite	Mica	Feldspar	Jarosite
School				0	66,9	21,2	5,5	0,2	6,2														
Bly E (A)						96,1				2,8	1,1												
Bly N (A)	0,7				61,6	31,1	6,6																
Bly W (A)						86,1	4,1					0,7	6,8						2,4				
Les S (A)			25,4		38,2	6,5	2,7							23,2					3,6				
Les N (A)						7,5								71,6			1,6	19,4					
Les E (A)	3,2				7,4	13,7	2,4									65,8				7			
Les W (A)	3,3				25,7	0,4	0,7									43,5				26,4			
Bly N (A)						93,7					6,3												
School (B)	51					26,9												17,7		50,2			
Bly N (B)	2,6	37,3	54,7	4,8	0,5																		
Bly S (B)	2,4	39,8	56,6	0,4	0,8																		
Bly E (B)	1	36,5	59,7	2,4	0,5																		
Bly W (B)	1,9	29,5	62,6	6																			
Les N (B)	2,9	28,6	58,5	0,2	9,7																		
Les S (B)	2,1	37	54,6	0,2	6,1																		
Les E (B)	0,7	36,8	57,8	4,4	0,3																		
Les W (B)	3,2	36,9	59,9																				
Heriotdale (a)						94.4																	
Joburg CBD (a)						90.8																	
Tailings material (d)				0,1		78.0																	3
Pyrite gold bearing ore (b)						74.0														2.0	1		1
TSF (c)				12		80.5														7.3	9,5	1	2,7

A=2016, B=2017; Yalala, 2015 (a); Tlowana et al., (2013) b; Nengovhela et al, (2006) c Rösner, (1999) (d)

With reference to Table 4.3 above, the result show that dust samples contained highest amount of quartz (26-96%) as compared to TSF soil (80.5%), tailings material (slurry) (78%) and pyrite bearing ore material (74%) (Yalala, 2015). Enrichment of minerals mainly depend on small particle size and large surface area (Madrid *et al*., 2008; Duong and Lee, 2009; Zhao *et al*., 2010; Duong and Lee, 2011; Luo *et al*., 2011; Zhao *et al*., 2011; Zverina *et al*., 2012; Yalala, 2015). The absence of pyrite (FeS_2) in the tailings material could result from oxidation over a period and the formation of secondary minerals like gypsum (CaSO4) and jarosite (KFe3(SO4) (OH)6) (Blight and Du Preez, 1997).

Several studies showed that 19% of all gold deposits have silver and conversely, 43% of all silver deposits have gold (Mindat, 2018; Yalala, 2015), hence traces of silver (1.6 µg/cm^3) were detected in Site 2 LES. The leaching and flotation process of gold extraction produces carbon and sulphide tailings hence the presence of sulphur in the sample indicates that the TSF may have contributed to the precipitant deposition (Fivas, 1988; Yalala, 2015).

Results obtained in this study shown traces of gypsum present at weight % of 18 µg/cm^3 at Sites 1 and 2. Gypsum was recognised as single crystals in an alunogen-bloedite matrix, sometimes covered by halite and chlorine dominated crystal matrix of the minerals confirmed salt evaporation processes as the source (Maya *et al.,* 2015).

Major oxides in the gold mine TSF dust sample are silica, magnesium oxide, alumina, sulphur trioxide, potassium oxide, calcium oxide, and haematite. In this study uranium was not detected by the XRD Analysis, however uranium oxide traces as gold

extraction by-product, are found in trace quantities (Sicelo, 2015), confirming the presence of sulphur, calcite, haematite and halite. Calcite is a rock-forming mineral with a chemical formula of $CaCO_3$, extremely commonly found worldwide in sedimentary, metamorphic, and igneous primary rocks. Carbon dioxide (CO_2), which is an important gas in Earth's environment and lithosphere serves as a greenhouse gas as it traps and holds heat near the surface of the planet. Calcite was only detected at Site 1W (N253C) at concentration of 6.8 µg/cm^3.

The lack of naturally occurring clay minerals, coupled with the current mineral assemblage, indicates that the source of the dust was probably from a gold TSF (Annegarn *et al*., 2010). Due to oxidation of tailings material resulted in the leaching out of trace metals to below detection limits in dust samples. However, other studies noted that mica, chlorite, chloritoid, pyrophyllite, clay, gypsum, pyrite, jarosite, pyrite, rutile, hematite, clinochlore, muscovite, and k-feldspar also occur as traces of mineral elements within the study area (Nengovhela *et al*., 2006; Ojelede, 2012; Tlowana *et al*., 2013).

4.2.4 XRF-Chemical Analysis Results

Total elemental analysis determined the following trace elements: Al. As, Ca, Cd, Co, Cu, Cr, Fe, Hg, Mn, Mo, Na, Ni, P, Pb, S, Ti, V and Zn are shown in Table 4.4 below:

Table 4.4: XRF Analysis Showing Total Elemental (Trace Elements Al, As, Ca, Cd, Co, Cu, Cr, Fe, Hg, Mn, Mo, Na, Ni, P, Pb, S, Ti, V And Zn) Concentration (µg/Cm3) Composition of Sites 1, 2 and 3 (Round Off)

Site ID	Ca	Ti	V	Cr	Mn	Ni	Cu	Zn	As	Mo	Pd	Cd	Sn	Hg	Tl	Pb	Fe	Na	Mg	Al	Si	S
Site 3[A]	15,4505	4,267	0,22	1,1885	1,9705	0,166	0,4045	11,1365	0,1165	n/a	0,2605	0,4265	n/a	0,029	0,0925	0,341	59,8065	2,192	6,5715	13,387	81,355	2,177
Site 1E[A]	13,8635	2,682	0,115	0,5625	1,4305	0,251	0,1525	1,5105	0,2145	n/a	n/a	0,1765	0,691	0,001	0,0315	0,502	62,1785	2,962	12,9615	17,734	266,661	0,304
Site 2 E[A]	5,2125	0,755	0,038	0,2465	0,3255	0,067	0,0565	0,9145	0,0555	0,0575	n/a	0,2485	n/a	n/a	0,0465	0,159	15,2725	0,968	3,9615	5,27	97,391	0,163
Site 1S[A]	8,6405	1,203	0,08	0,2945	0,6455	0,094	0,0755	0,7885	0,1065	0,0055	0,0435	0,2165	0,032	0,047	0,0015	0,218	24,9815	2,504	10,4485	15,639	129,776	0,246
Site 1N[A]	14,0065	2,389	0,121	0,5675	1,4095	0,211	0,1965	1,7205	0,2185	n/a	n/a	n/a	0,341	n/a	n/a	0,576	58,5845	3,225	13,8995	20,82	242,929	0,382
Site 1W[A]	12,5115	2,579	0,155	0,6155	1,5425	0,251	0,1715	2,4485	0,2655	n/a	n/a	0,1825	0,258	n/a	0,0445	0,637	70,4565	2,564	10,3455	15,219	271,681	0,318
Site 2S[A]	7,6445	1,578	0,095	0,4435	0,6345	0,079	0,1105	3,6095	0,1075	0,0625	n/a	0,0435	n/a	0,007	0,0465	0,309	28,9275	1,556	5,1035	10,569	85,093	0,234
Site 2N[A]	5,5745	1,133	0,082	0,3075	0,3165	0,035	0,1065	4,4195	0,0195	0,1175	0,0275	0,8135	0,194	0,018	0,0625	0,161	17,3905	1,605	4,0225	8,266	49,568	0,22
Site 2W[A]	3,6415	0,618	0,05	0,1665	0,1785	0,008	0,2255	0,8865	0,0465	n/a	0,6615	0,7105	0,338	0,005	0,0665	0,078	10,4755	0,826	2,2615	3,959	44,639	0,104
Site 3[B]	36,4255	2,27	0,14	1,0685	1,1005	0,103	0,5055	13,5385	0,0845	n/a	n/a	n/a	0,215	n/a	0,0625	0,302	38,1325	5,147	10,2875	17,098	122,373	0,513
Site 1N[B]	0,8175	0,059	0,028	0,0095	0,0225	0,002	n/a	n/a	0,0205	0,0735	n/a	0,4555	0,539	0,015	0,1045	0,051	0,6845	0,086	0,0925	0,246	1,261	n/a
Site 1S[B]	1,0595	0,071	0,014	0,0165	0,0385	n/a	n/a	0,0815	n/a	0,0755	n/a	0,2795	0,297	0,013	0,0185	0,026	1,0385	0,192	0,1395	0,32	1,751	n/a
Site 1E[B]	0,8905	0,053	0,003	0,0125	0,0105	n/a	n/a	0,0675	0,0025	0,0445	n/a	1,0565	0,764	0,048	0,1165	0	0,8105	0,139	0,1685	0,331	1,956	n/a
Site 1 W[B]	0,9735	0,042	0,039	0,0155	0,0285	0,005	n/a	0,0375	0,0025	0,0055	0,0075	0,4625	0,33	0,002	0,0775	0,067	0,5735	0,139	0,1575	0,24	1,236	n/a
Site 2N[B]	1,1865	0,121	0,012	0,0405	0,0235	n/a	n/a	0,0965	0,0375	n/a	n/a	0,5625	0,205	0,003	0,0995	0,034	1,4845	0,348	0,2155	0,535	2,485	n/a
Site 2 S[B]	0,8895	0,075	0,008	0,0305	0,0325	0,001	n/a	0,0325	0,0205	0,1075	n/a	n/a	0,291	n/a	0,0555	0,067	0,7685	0,288	0,1715	0,449	1,869	n/a
Site 1 E[B]	1,3145	0,156	0,027	0,0435	0,0475	n/a	n/a	0,2035	0,0095	0,1255	n/a	0,7245	0,547	0,037	0,0615	0,046	2,2135	0,006	0,2565	0,884	3,809	n/a
Site 2 W[B]	0,6615	0,045	0,015	0,0155	0,0075	n/a	n/a	0,0295	0,0105	n/a	n/a	0,8775	0,766	n/a	0,1085	0,021	0,6235	0,06	0,0905	0,286	1,292	n/a

A=2016 sample results; B=2017, Sample results n/a= not analysed

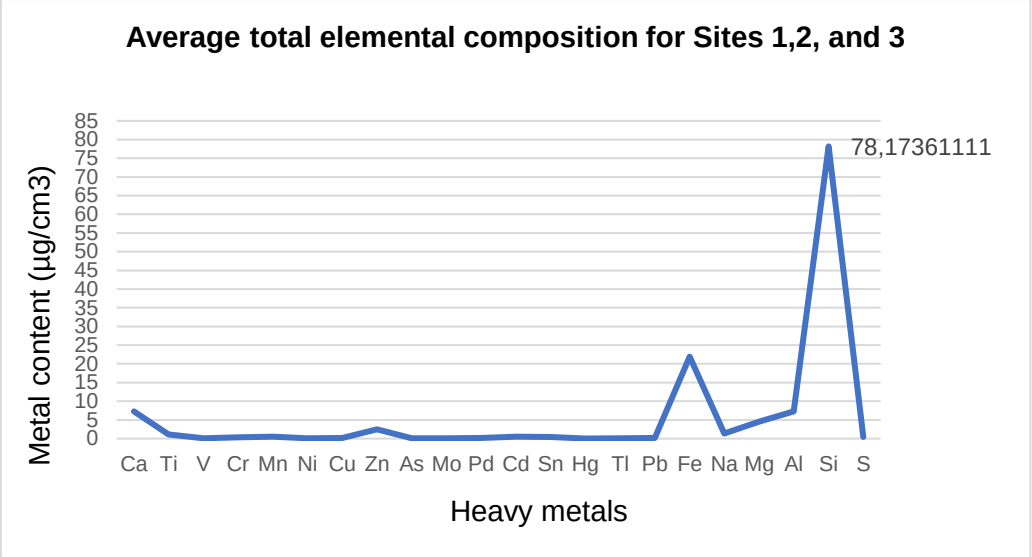

Figure 4-18: Average total elemental concentration composition for Sites 1,2, and 3

The results in Figure 4.18 above show that the principal elemental concentration of selected dust samples as: SiO_2 (21.2 – 96.8%), Al_2O_3 (0.5 – 72.4%), SO_2 (43.5-71.6%) and Fe_2O_3 (0.5–5.1%). In total, the average content of the sampled sites contained quartz (66.28%), silicates (60.3%), Al_2O_3 (20%), calcites (4.5%) and iron oxides (2.5%). The balance is formed by traces elements of arsenic, chromium, copper, manganese, nickel, potassium, and titanium oxides.

Site 3 (J045) recorded the highest S concentration (2 µg/cm^3) than the rest of the sampled sites. The major sulphide minerals in the mine waste materials are pyrite and pyrrhotite which are characteristically S carriers and based on this, sulphide oxidation is yielded by bacterial facilitation process (Tutu, 2008).

Site 3 samples were found to be higher than the other sites at Site 3 P SCHOOL (4 µg/cm^3), then Sites 1 E (2,7 µg/cm^3), W (2,6 µg/cm^3), N (2,3 µg/cm^3) and Site 3 (2,3 µg/cm^3) and Site 2 W having the least Ti concentration at 0.6 µg/cm^3.

Comparatively, results of the elemental formations of dust samples tested within the study area and Soweto residential areas located in close proximities to the gold mine TSF revealed high prevalence of SiO_2 in dust samples (Von Gruenewaldt *et al.,* 2010). Similarly, alumina-silicates form part of predominant quartz bonded to trace elements such as Al, As, Ca, Co, Cr, Cu, Fe, Hg, Mg, Mn, Ni, Pb, S, U, and Zn (Hallbauer & Von Gehlen, 1983; Janisch, 1986; Frimmel, 1997). However, Al, Ca, Fe, Mn and Si elements are mainly enriched in the dust as they are geologically inherent in the area (Yalala, 2015).

Major oxides of Ca found in the gold mine tailings sample are mainly silica, magnesium oxide, alumina, sulphur trioxide, potassium oxide, calcium oxide, and haematite (Malatse and Ndlovhu, 2015). Fe was detected in all samples at an average of 16.2 µg/cm^3, with the highest values at Sites 1 (W (N253C), E (N223B), Site 3 and Site1 N with the values of 70,5, 62,2 59,8 and 58,6 µg/cm^3 respectively. Fe is one of the main reagents used for gold extraction process for the liberation of gold particles as part of bio-oxidation of sulphide contained in refractory gold ores to increasing the gold yields (Fashola *et al.,* 2016).

Sites 1 (N253 C, N253 and N223 B) samples recorded the highest in Pb level of 0.64µg/cm^3, 0.60µg/cm^3 and 0.50µg/cm^3 respectively. It is possible that the TSF contributed to the lead concentrations in the soil, as it had a relatively high Pb-concentration, the measured concentrations are likely contributed by natural metal variation.

Lead, together with radon, can also form part of radioactive particulates (forming part of the Uranium decay chain) in the TSF can reach the environment and its highly carcinogenic character has been recorded as one of the major health concerns mainly in urban areas (Miller *et al*., 1998:465; AGA, 2015, Mpanza *et al*., 2020).

In this study, low concentrations of mercury were observed. Relatively, the mercury concentration in the Site 1 (N253 A) sample was higher than any of the other samples at 0.05µg/cm3, therefore indicating that contamination of the study area was not likely the dominant cause of the mercury contamination in the dust. Other studies recorded mercury concentration of (TSF2) (265 and 414 µg Hg kg^{-1}, respectively) at TSF2 (Lusilao, 2012), which is approximately 221,73 m from Site 1 (N253 A) and the next closest being Site 3 (J045), located approximately 415,7 m north west of the dormant TSF. Hence higher mercury detection at Sites 1 and 3 than all the sites (2,4,5 and 6).

Recent studies revealed higher mercury concentrations contamination in dust than sediments and soil samples due to high adsorption capacity of the small dust particle size fractions than in sediments metals and accumulation in soils (Ordonez *et al.*, 2002; Yalala, 2015). The source of mercury pollution in the study area confirmed to be the gold mining and related activities and these levels decrease with increased distance away from the source of pollution (mainly TSFs and pollution control dams) as it was observed the dust study within Johannesburg (Lusilao, 2012; Yalala, 2015).

4.2.5 Radiological analysis

Table 4-5 below presents the average radioactive elemental concentration from the radiological analysis of precipitant deposition dust samples from gold mine tailings storage facilities for Site 3 in July, August and September 2017.

Table 4.5: Average Radioactive Elemental Concentration (In Bq/Kg) Composition of Precipitant Deposition Dust Sampled In 2017.

Parameters	^{238}U	^{234}U	^{226}Ra	^{210}Pb	^{235}U	^{232}Th	^{228}Ra	^{228}Th	^{40}K	Gross alpha	Gross beta
AVE.	37,71	38,06	346,67	342,33	1,73	12,1	81	180	246,67	279	317,67
MIN	2,94	2,98	340	230	0,135	0	79	170	240	98	232
MAX	84,8	85,5	360	567	3,898	19,3	85	190	260	428	422
STD DEV	42,00	42,285	14,142	238,295	1,93	1,635	4,24	7,07	14,14	82,73	86,97
MEDIAN	25,4	25,7	340	230	1,166	17	79	180	240	311	299

Gross beta higher average concentration (317.67 Bq/kg) compared to gross alpha at 279 Bq/kg. ^{226}Ra, ^{210} Pb and ^{40}K had the highest activity concentration of 346.67 Bq/kg, 342.33 Bq/kg and 246.67 Bq/kg respectively whereas ^{235}U, ^{232}Th and ^{228}Ra record the lowest values. The order of the activity concentration recorded ^{226}Ra > ^{210} Pb > ^{40}K >^{228Th}>^{228} Ra>^{234} U>^{232}Th >^{235}U.

Dudu *et al*., (2018), however recorded that ^{232}Th had the least activity concentration and the maximum observed was for ^{40}K, following the order from the least to the highest as ^{232}Th < ^{238}U< ^{226}Ra < ^{40}K.

Studies of the TSF soil material within the study area, however established occurrences of other radioactive elements such as U-234 (421,376, and 465 Bq/kg),

Th-230 (421, 376 and 465 Bq/kg), Po-210 (560, 552 and 618 Bq/kg). U-235, Pa-231, Ac-227 and Ra-223 found in TSF soil had similar radio analysis elemental concentrations of (19,17 and 21 Bq/kg) each (Von Gruenewaldt *et al.,* 2010). Comparisons with study by Von Gruenewaldt *et al.* (2010) confirmed that the average radioactive elemental concentrations for Po-210, Ra-226 and U-238 were higher in TSF soils than in TSF dust at the concentrations of (576,67> 342,33) Bq/kg, (451,67> 346,67) Bq/kg and (413> 37,71) Bq/kg) respectively, the lowest being U-235Th-232 at (19> 1,733) Bq/kg and (25>0) Bq/kg respectively. However, Th-228 and Ra-228 concentrations in TSF dust were found to be higher than TSF soils at (180>30,33) Bq/kg and (81>31,33) Bq/kg.

Comparatively, the concentrations of the TSF soils were found to be higher than those of the TSF dust samples in Table 4-6 above taken by this study and this made sense based on the argument that concentration of point source pollution decreases with distance (Von Gruenewaldt *et al.*, 2010). This is since the precipitant dust gets blown away from the TSF source in its finer state and deposited at a distance away. For instance, U-238 values for dust for the three months, i.e. July, August and September were 82, 2.4 and 19.7 Bq.kg^{-1} respectively whereas the TSF soil showed 405, 373 and 461 Bq.kg^{-1}. Even though the period under observation is relatively a dry period, precipitant dust in July carried higher amounts of radioactive gross beta and alpha results. September and August detected the least concentrations, which could possibly be due to high winds generally occurring in August, causing the dilution of the radioactive concentrations in the dust (Van Blerk, 2016).

Kamunda *et al*. (2016) further confirmed that the average activity concentrations in Bq_kg_1 for Uranium-238, Thorium-232, and Potassium-40 from the mine tailings were found to be 785.3 ± 13.7, 43.9 ±1.0 and 427.0 ±13.1, respectively. On the other hand, the average activity concentrations in Bq_kg_1 for Uranium-238, Thorium-232, and Potassium-40 from the control area detected 17.0.1±0.4, 22.2±0.5 and 496.8±15.2, respectively (Kamunda *et al.,* 2016). This suggests that the U-238 TSF soil (785±13.7) > TSF dust-this study (37.71±42.00) > TSF (control area) (17.01±0.4) $Bq.kg^{-1}$. Th-232 results showed that TSF soil (43.9±1.0) > Control area (22.2±0.5) $Bq.kg^{-1}$ > TSF dust-this study (12.1±1.62) $Bq.kg^{-1}$. However, K-40 Control site (496.8±15.2 $Bq.kg^{-1}$) > TSF soil (427.0±13.1) $Bq.kg^{-1}$ > TSF dust -this study (246.67±14.14) $Bq.kg^{-1}$.

The activity concentration of ^{238}U, ^{232}Th and ^{40}K in soil samples from various studies around the world were averaged as 33, 45 and 420 Bq.kg-1, respectively (UNSCEAR, 2000) and compared as shown Table 4.6 below.

Table 4.6: Activity Concentrations (Bq.Kg-1) in Soil and Dust Sample Results (From This Study With Similar Studies From Other Countries Around The World)

Activity concentration in soil Bq/kg						
Country	**238 U**		**232 Th**		**40K**	
	Mean	**Range**	**Mean**	**Range**	**Mean**	**Range**
South Africa (★★)	37,71	2,94- 84,8	12,1	0- 19.3	246,67	240-260
South Africa (★)	413	373-461	25,33333	25-26	-	-
South Africa (**)	574.3	34.4-3681.6	49.4	20.5- 167.5	424.7	133.8-1177.0
Nigeria (++)	37	6-67	63	17-87	998	85-1565
Ghana (*)	29	-	25	-	582	-
Egypt (+)	37	6-120	18	2-96	320	29-650
Algeria (+)	30	2-110	25	2-140	370	66-1150
United States (+)	35	4-140	35	4-130	370	100-700
Romania (Uranium Area) (+)	57	-	31	-	486	-
China (+)	33	2-690	41	1-360	440	9-1800
India (+)	29	781	64	14-160	400	38-760
Japan (+)	29	259	28	2-288	310	15-990
Syrian Arab Republic (+)	23	10-64	20	10-32	270	87-780
Ireland (+)	37	8-120	26	3-60	350	40-800
Switzerland (+)	40	10-150	25	4-70	370	40-1000
Hungary (+)	29	12-66	28	12-45	370	79-570
Russian Federation (+)	19	0-67	30	2-79	520	100-1400
Greece (+)	25	1-240	21	1-190	360	12-1570
Portugal (+)	49	26-82	51	840	480	220-1230
World Average	33		45		420	

Legend: (+) UNSCEAR 2000 Report, * Darko, 2007; (★)Von Gruenewaldt *et al.* (2010); (++) Nasiru., 2013; (**) Kamunda *et al*, 2016; this study (★★)

Comparison analysis of the U-238, Th-232 and K-40 average activity concentrations in soil from the TSF (37.7 Bq/kg) dust from this study and other countries in the world

confirmed that U-238 is above the world average of 33 and on the same level with Nigeria “(37), Egypt (37) and Ireland (37). However, activity concentration Th 232 and K- 40 from this study (12.1 and 246 Bq/kg) are way below the world average of 45 and 420 Bq/kg respectively as shown in Table 4.7 above (modified from Kamunda, 2017).

4.3 Assessment of the Public Perception

4.3.1 Public perception of gold mine TSFs

This section presents descriptive statistics results from the data set on visual impacts of gold mine TSF’s around residential areas collected by means of a questionnaire comprises of 280 participants. The participants’ response on questions asked are that follow.

4.3.1.1 Population

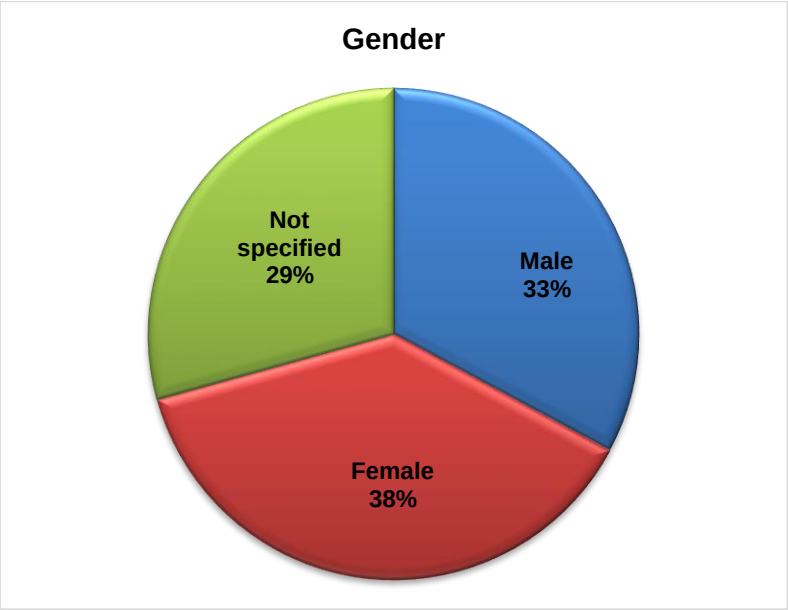

Figure 4-19: Gender of the participants

Figure 4-19 above confirms that 48% participants stay in Wedela, followed by 14% that stays in Carletonville and 11% in Fochville. 9% of participants reside in Elandsridge and 6% that stays in Mine Village or hostel less than 4% stays in Khutsong (3%), Potchefstroom, Blyvooruitzicht and Deelkraal (2% respectively), while none stays in Westonaria/Randfontein. 1% of participant's residence was not specified. The age group were 18-24 (27%), 25-29 (24%), 30-34 (11%), 35-39 (9%), 40-49 (17%), 50-59 (9%) and p≥ 60 (4%).

When gender was assessed by knowledge and understanding of environmental issues, the Pearson Chi square =58,0319; degrees of freedom = 22; and p value 0,000044 implies that there is a significant association between gender and knowledge and understanding of environmental issues. These results are resembled age of participants. The Chi-square results show that there is enough evidence to confirm that age of participants have a strong association to Knowledge and understanding of environmental issues, (Pearson Chi square = 457,968, degrees of freedom = 232 and *P* value = 0,0000). In terms of being knowledgeable of TSF's or mine dump of the participants, the results confirm basic knowledge (34%), intermediate knowledge and no knowledge (23% respectively). However, 13% of the participants have advanced knowledge and ≤ 8% did not specify their knowledge status.

In comparing age and the visual impacts, Molnarova *et al*. (2012) suggested that younger generation have lower sensitivity to the aesthetic impacts of high-rise structures such as wind turbines and TSFs' they are accustomed to such landscape types unlike the older generation.

4.3.1.2 TSFs impacts on the natural landscape

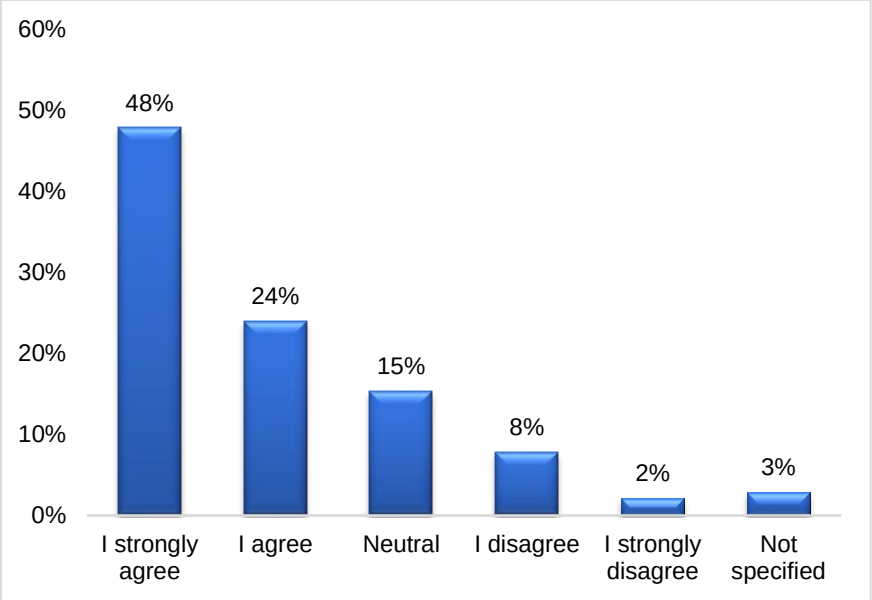

Figure 4-20: The results showing TSFs having negative impacts on the natural landscape

From Figure 4-20 above, the results show that the majority of 72% agree that TSF result in negative impacts to the natural landscape (where 48% strongly agree). Only 15% neither agree nor disagree with the statement and 10% disagree that TSF result in negative impacts to the natural landscape (where 2% strongly disagree). The 3% of participants did not comment on the statement.

4.3.1.3 Main TSF's visibility viewpoints

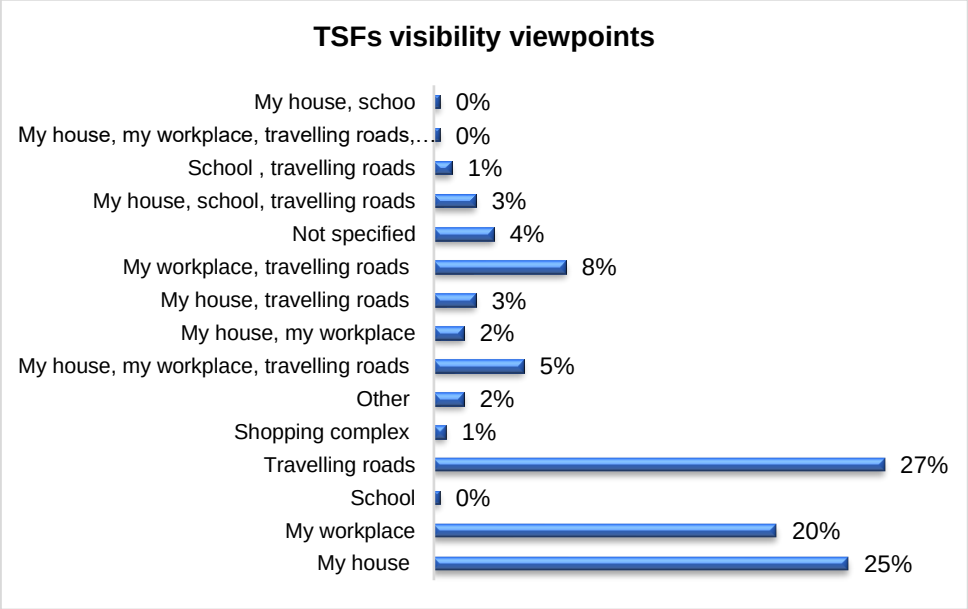

Figure 4-21: Participants' TSFs' visibility viewpoints

Whether they can see TSF's or not from the various viewpoints from travelling roads, houses, workplaces, school and workplace the results showed 27%, 25% and 20% respectively. Others (3-8%) can see TSF's from a combination of various locations as shown in Figure 4.21 above. 2% of participants that said they can see the TSFs from their houses and workplace while another 2% said they can see the TSFs from other places not listed in the questionnaire. Results also show that 1% said they can see the TSFs from schools and while travelling roads while another 1% from shopping complex.

4.3.1.4 Extent of TSF visibility

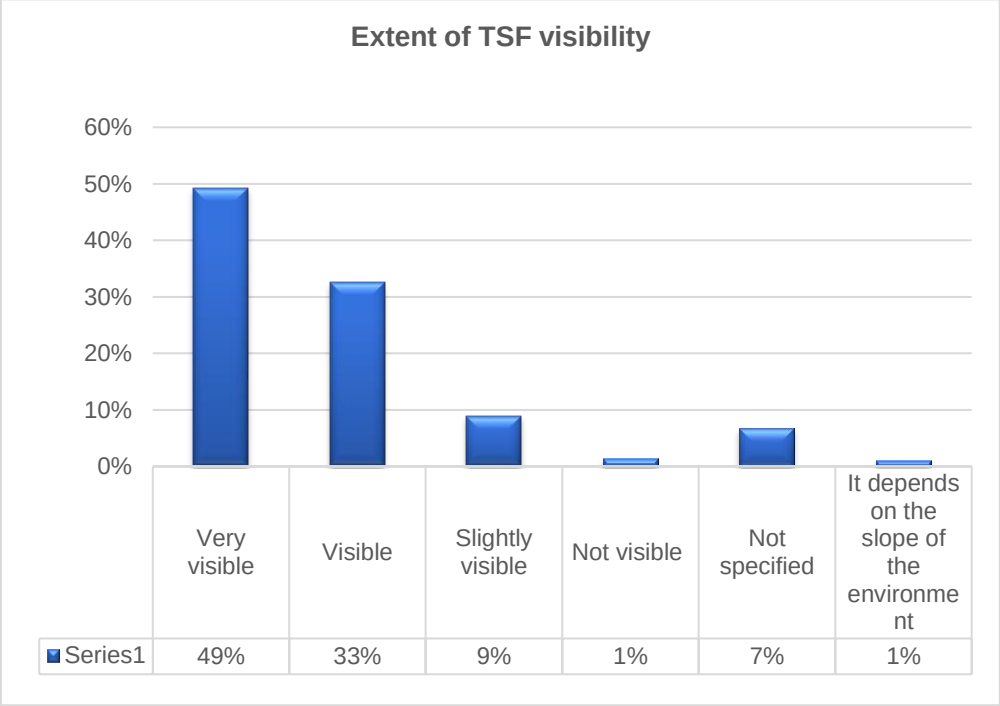

Figure 4-22: The extent of TSF visibility

Figure 4-22 above shows the participants' opinion of TSF's appearance against the natural landscape as very visible (49%), visible (33%), slightly visible (9%) and not visible (1%). While a further 1% of the participants indicated that the visibility of the appearance of the TSF against the natural landscape depends on the slope of the environment, 7% did not specify the visibility of the appearance of the TSF against the natural landscape from their point of view.

From the results, it can be confirmed that most participants said that TSF's are mostly visible all year round (75%), between July and September (17%) and 2% of the participants did not specify when TSF's are mostly visible. In terms of the participant's opinions on the most visually appealing environment, 37% prefers a natural landscape with no TSF's, followed by 28% of TSF's with trees planted around them, 16% trees

only and 10% TSF only. While 9% of participants said that it doesn't matter what the environmental setup consists of for it to look appealing to them, only 1% of participants did not specify the environmental setup that looks appealing to them. This could be based on fact that people with an experience of these structures within their environment see them as negatively impacting on the environment unlike people do not have an experience at all (Molnarova *et al*., 2012). Similar trends were noted by Bishop and Miller (2005) in contradiction to the findings by Eltham *et al*. (2008) who suggested that the acceptance of such structures and their perceived visual attractivity was significantly higher following their establishment rather than during the planning thereof.

Table 4.7: Descriptive statistical analysis of TSF's visibility versus seasonal conditions

		Frequency	Percent	Valid Percent	Cumulative Percent
Valid	1	30	3,0	11,4	11,4
	2	21	2,1	8,0	19,4
	3	59	6,0	22,4	41,8
	4	66	6,7	25,1	66,9
	5	80	8,1	30,4	97,3
	6	1	0,1	0,4	97,7
	8	6	0,6	2,3	100,0
	Total	263	26,6	100,0	
Missing	System	725	73,4		
Total		988	100,0		

From the results, the majority of 28% strongly agree that TSF's are more visible when the wind is blowing, followed by 26% who are neutral about when the TSF are more visible, then 23 % who agree that TSF's are more visible when the wind is blowing. From these results it is also seen that 12% of the participants strongly disagree that TSF's are more visible when the wind is blowing whereas 8% disagree. There are 2%

who did not specify their views on whether they agree or disagree that TSF's are more visible when the wind is blowing.

In total, 33 of 280 participants strongly disagree that irrespective of where you are, TSF are noticeable within their areas of location, 23 of 280 disagree, 73 of 280 are neutral 64 of 280 agree, 79 of 280 strongly agree, 1 of 280 specified other times of TSF visibility, 1 of 280 said that TSF's are more visible all year round.

4.3.1.5 TSF current management practices consideration

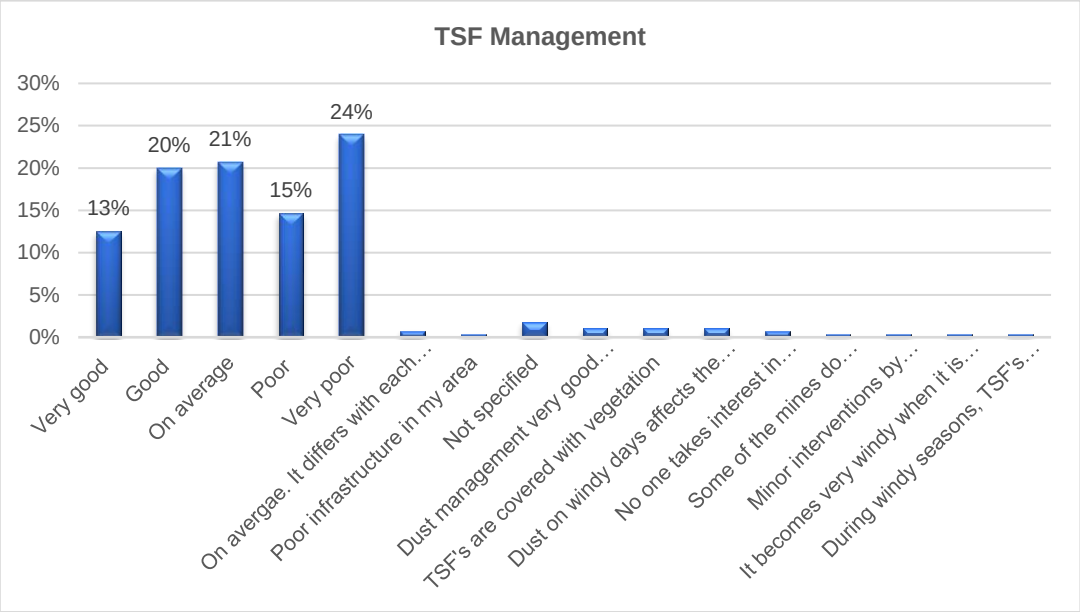

Figure 4-23: TSF management practices

From the results in Figure 4-23 above, 24% of the respondents believe that from the visual point of view, the current management of TSF within their area is very poor, 21% average, then 20% good and 15% poor. Furthermore, 13%mentioned very good management practices while 2% did not specify. The balance population confirm that this differs with time and they cannot generalise (1%), others mentioned that no one

takes interest in managing the TSFs in their area (1%), TSF's are covered with vegetation in their area (1%) and who said that in their area, dust management is very good and TSF do not pollute the environment (1%).

From the results, the majority of 36% said that the issue of visual impacts of TSF on the natural landscape can be best addressed by removing TSF and rehabilitating the environment. This is followed by 20% who said that the issue can be best addressed by investing in research and technology on various possible options and another 20% who said that the issue can be best addressed by planting trees around TSF's. 6% of the participants said that they will do nothing as they can live with having TSF's within their residential areas/environment while 5% said that they do not know what they can do to address the issue.

This concurs with the study by Bishop (2011) that high-rise structures are provoking when located in landscape located in high aesthetic quality such as ridges and can only be accepted provided they are limited in number and if they are not visible from settlements, viewpoints and the transportation network.

On the issue of mitigation of the visual impacts from TSFs, the results show that 3% of participants are of the opinion that the issue of visual impacts of TSF on the natural landscape can be best addressed by removing TSF's and rehabilitating the environment and by planting trees around TSF's. There are 1% who said that the issue can be best addressed by expanding the footprint of TSF's, another 1% said that it can be best addressed by considering more appropriate ways to prevent further developments of TSF's, another 1% said that it can be best addressed by planting

trees and investing in research and technology on various options, another 1% said that it can be best addressed by removing TSF's and they also said that TSF's should be well maintained because when on windy conditions TSF's are more visible. Further 1% suggested tree planting around TSF's and by investing in research and technology on various options. Another 1% suggested investing in research and technology and that growing certain plants and harvesting them would be an option on addressing the issue. Only 1% of participants confirmed that TSFs dust poses visibility during windy periods.

4.3.1.6 Significance of the visual impacts of TSF

The outcomes of the visual impact assessment in terms of the nature, severity, extent, frequency and probability using significance risk matrix, GIS mapping and photographs are presented in Figure 4-24 and Tables 4.8 below.

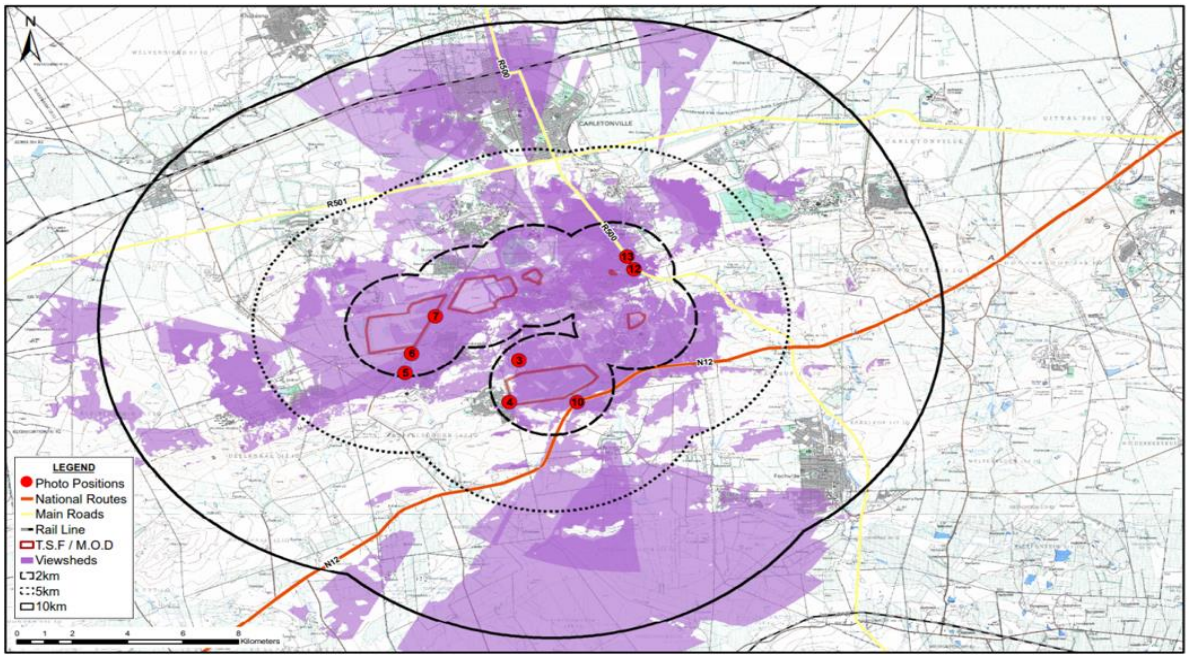

Figure 4-24: Map showing consolidated viewsheds, viewpoints and Zones of Visual Intrusion

The overall significance rating for the TSF's VIA is shown in Table 4.8 below.

Table 4.8 Summary of the overall Visual Impact Analysis Results using environmental risk assessment matrix (Oberholzer, 2005).

CRITERIA (INCLIDING REFERENCE FROM CHAPTER 3)	Significance rating										Impact description and results
	Consequence			Overall Consequence	Likelihood		Overall Likelihood	VIA Rating Risk/25	Risk		
	Severity	Duration	Extent		Frequency	Probability			Negative (-) Positive (+)	Low (L) / Low-Moderate (L-M)/Moderate-High (M-H) High (H)	References (Literature Review)	
Viewpoints Analysis (I)	3	3	3	**3**	3	2	**2,5**	**7,5**	**(-)**	**H**	Greyling (2001), Rademeyer (2007)	Highly visible from major roads N12, R500 and R501 Road, Danie Theron Monument presents one of the most predominant heritage sites, located on a koppie and forming the immediate southern boundary of the study area; Surrounding towns and residential areas of Carletonville, Fochville, Blyvooruitzich, Khutsong, Oberholzer, Mohale's Hoek and Wedela (H), Southdene, Kokosi,
Visibility (I & II)	2	1	2	**1,7**	1	2	**1,5**	**2,6**	**(-)**	**M**	Bishop (2011)	Protruding height of TSF's Partial screening by trees Noticeable from N12, R500 and R501 based on the number of road users. Undulating landscape. High dust emission during windy season (Figure 4.21)
Visual Exposure (IV)	2	1	2	**2,0**	3	3	**3,0**	**6,0**	**(-)**	**M-H**		Visual exposure decreases with increasing distance as indicated by a fading purple colour in the viewsheds (Figure 4.21).

CRITERIA (INCLIDING REFERENCE FROM CHAPTER 3)	Significance rating											Impact description and results
	Consequence			Overall Consequence	Likelihood		Overall Likelihood	VIA Rating Risk/25	Risk			
	Severity	Duration	Extent		Frequency	Probability			Negative (-) Positive (+)	Low (L) / Low-Moderate (L-M)/Moderate-High (M-H) High (H)	References (Literature Review)	
Visual Sensitivity of the Area (IV)	3	3	3	**3,0**	3	3	**3,0**	**9,0**	**(-)**	**M-L**	Ode and Fry, (2002) Ode *et al*. (2008)	Intrusion on sense of place and scenic value from mine infrastructure. Undulating topography Combination of disturbed natural features and very pristine due to recovery from severe historic impacts of mining.
Landscape Integrity	3	3	3	**3,0**	3	3	**3,0**	**9,0**	**(-)**	**L**		Dominance of mine infrastructure Retained natural integrity and preserved heritage sites.
Visual Absorption Capacity	3	3	2	**2,7**	3	3	**3,0**	**8,0**	**(-)**	**M-L**	Yeomans (1979) Amir and Gidalizon, (1990)	Trees from dust mitigation initiatives established screening/barrier. Vegetation planting on top of TSF's. Dense vegetation of the Gartsrand Ridge
Zones of visual influence	3	3	3	**3**	3	3	**3,0**	**9**	**(-)**	**H**	The Landscape Institute and the Institute of Environmental Management & Assessment (2013).	(Figure 4.21)

The findings as outcome were influenced by numerous factors, most importantly:

- The topography of the area on which the TSF's are located, and the surrounding area is undulating, with the Gatsrand Ridge forming a barrier between the north and the south of the region. The densely vegetation of the ridge act as a screen, minimizing the visibility, but maximizing the VAC of the TSF's from the viewpoints.
- The type of vegetation and the height thereof contribute towards the screening and blending in of the TSF's with the natural environment of the area. This also depends on the season. Minding of the discussion of public perception outcome of this study under Section 4.2 above, the TSF's are mainly visible when the wind is blowing.
- Surrounding developments such as numerous mining related infrastructure are cumulatively contributing towards the visual impact of these TSF's.
- Travel routes in and around the area both national and regional routes can be found around the study area. For instance, the N12 is a national route linking Johannesburg and Cape Town via Kimberley, a high number of travellers, including tourists use the road, some on a more frequent basis.

Given that the mining in the Witwatersrand was established in the early 1800's (Mineral Council South Africa, 2018), the TSF's are now considered part of the landscape or landmark of the area. Even though some of the TSF's are being remined to reclaim the residual gold, the visual impact does not necessarily disappear but merely transferred from one site to a new area where the new TSFs (mega dumps)

have been established. To make matters worse, the new dumps comprise of TSF material from several (TSF's) reclaimed within the area or operation.

Mega TSFs will result in more significant visual intrusion on the natural landscape as is currently the situation within the study area. Furthermore, this will negatively and cumulatively impact on the overall sense of place in the area and the visual sensitivity of the area. From this analysis is can therefore be suggested by this study that the TSFs are deemed to have the greatest impact on the landscape as compared to other mining related infrastructure.

4.4 Assessment of Gold TSF Dust Toxicity by Selected Heavy Metals

4.4.1 Contamination Assessment

Concentration of each heavy metal was used to determine the degree of enrichment, enrichment factor (EF) (Benhaddya & Hadjel, 2013; Nowrouzi & Pourkhabbaz, 2014) and the extent of accumulation, geo-accumulation (*Igeo*) or contamination, using the concentration data obtained from the laboratory analyses.

4.4.1.2 Enrichment factor

EF was calculated using the following formula in equation 4.1 below.

$$\mathbf{EF= (M/F_e)_{Sample} / (M/F_e)_{Background}} \quad \textbf{(}\text{Equation 4.1)}$$

Where, where (M/F_e) Sample is the ratio of metal and Fe concentrations in the sample, and (M/F_e) Background is the ratio of metal and F_e concentrations of the background (Mohsen Nowrouzi & Alireza Pourkhabbaz,2014; Yalala, 2015). Birch, 2003

established EF values using the criteria shown in Table 4.15 below: EF≤1 no enrichment, 1<EF<3 minor enrichment, 3<EF<5 moderate enrichment, 5<EF<10 moderate-to-severe enrichment, 10<EF<25 severe enrichment, 25<EF<50 very severe enrichment and EF>50 extremely severe enrichment.

The results in Tables 4.9 and 4.10 below above established that metals of “extremely severe enrichment” EF were sequentially evidenced in the dust samples as In>Pd>Ag>Au>Te>Sc>Pt>Sb>Br whereas Sn and Mo were “very severely enriched” metals in the sampled mine TSF dust, with EF valued at 35.2 and 33.2 respectively. The dust sample were “minor enriched” with trace metals according to the sequence Y>Zr>Cu> V>Nb>Si>Mg>Ga>Se. Detailed results are shown in Tables 4.9, 4.10 and 4.11 below.

Table 4.9 Enrichment Factor (EF) Classification of Heavy Metals in The Dust Samples Per Site for Sampling Period May to June 2016

Metal Enrichment for May -June 2016									
EF Classification **Birch (2003)**	**Site 1 N**	**Site 1 S**	**Site 1 E**	**Site 1 W**	**Site 2 N**	**Site 2 S**	**Site 2 E**	**Site 2 W**	**Site 3**
EF ≤ 1 **(No enrichment)**	Cr,Mn, Fe, Ni, As, Pb, S, Na, Co, Se, Br, Sr, Pd, Sn	Cr, Mn, As, Pb, S,Na, Co, Se, Br, Zr,Nb, Ag, Sn,Cs, W, Sb,Au, La, Ti, Tl	Cr, Mn, As, Pb, S, Na, Co, Se, Br,Nb, Pd, Ag,W, Sb, Ca, Cs, Te, La, Ti, Tl	Cr, Mn, As, Pb, S, Sc,Na, Co, Se, Br, Nb,Pd, Sn, W, Au, Ca, , Ti, Tl	K, P, Cr Mn, Fe, As, Pb, S, Na, Co, Se, Br, Sn, Sr, Nb, Ag, La, Au, W, Sb,Ti,Tl	K, Cr Mn, As, Pb, S, Na, Co, Se, Br, Sr, Y,Zr, Pd, Ce, Pt, Au, W,Sb, Ti, Tl	K, Cr, Mn, Br, Sr, Nb,Fe,As, Al, Pb, S, Na, Mg, V, Co, Se, W, Ca, La, Au, Ti, Tl	K, Cr Mn, As, Al, Pb, S, Na, Mg, Co, Se, Br, Rb, Sr, W, Sb, Au, Ca, Te,, La, Cs, Ti, TL	Cr, Mn, Sn, As, Pb,S,Na, Co,Se,Br,Sr,Zr, W, Ce, Ca, Te,La, Cs, Ti,Tl
1 < EF < 3 **(Minor enrichment)**	K, Fe, Sr, Zn, Zr,Ca	K, Fe, Al, Mg,V,Cu, Y,Ca	K, Fe,Mg, V, Sr, Zr	K, Fe, Al, Mg, V, Sr, La	Al, Mg, V, Cu, Y, Ca, La	Fe, Al, Mg, V, Cu, Ca, La, Cs	Cu	Fe, V, Y, Zr,Nb	K, Fe, Al, Mg, V, Nb, Ag
3 < EF < 5 **Moderate enrichment**	Al, Mg, V, Cu, Nb, Ag		Al, Cu, Y, Ce	Cu	Zr	Nb	Y	Cu, Ce	
36 **< EF < 10** **(Moderate-to-severe enrichment)**	Y			Ce	Si	Y, Ce	Ce	Si	Cu, Y
10 < EF < 25 **(Severe enrichment)**	Ce	Si, Ce		Y, Zr	Ce	Si,Zr, Sn	Si,Zr		Si
25 < EF < 50 **(Very severe enrichment)**		Zn					Zn	Zn	
EF > 50 **(Extremely severe enrichment)**	Zn, Si, Rb, Sb, Pt, Sc, In, Te	Rb, Pd, Pt, Sc, In, Te	Zn, Si, Rb, Pt, Au, Sc, In	Zn, Si, Rb, Sb, Pt, Sc, In, Te	Zn, Rb, Pt, Sc, In, Te	Zn, Rb, Ag, Pt, Sc, In, Te	Rb, Ag, Sn, Sb, Pt, Sc, In	Pd, Ag, Sn, Pt, Sc, In	Zn, Rb, Pd, Sb, Pt, Au, Sc, In

Table 4.10: Enrichment Factor (EF) Classification of Heavy Metals in The Dust Samples Per Site for Sampling Period July-August 2017

Metal Enrichment for July 2017									
EF Classification **Birch (2003)**	**Site 1 N**	**Site 1 S**	**Site 1 E**	**Site 1 W**	**Site 2 N**	**Site 2 S**	**Site 2 E**	**Site 2 W**	**Site 3**
EF ≤ 1 No enrichment	K, P,Cr,Mn, Fe, Ni, Zn, As,Cd, Si,Al, Pb, S, Na, Mg, V, Ga, Cu, Co, Se, Br, Sr, W, Sb,Ca, Pt, Au,Te, La, Ti, Tl	K, P, Cr, Mn, Fe, Ni, Zn, As, Cd, Si, Al, Hg,Pb, S,Na, Mg,V,Ga, Cu,Co, Se, Br, Sr,Nb, Pd, Sn, W, Sb, Cs, Pt, Au, Te, La, Ti, Tl	K, P, Cr, Mn, Fe, Ni, Zn, As, Cd, Si, Al, Hg, Pb, S, Na, Mg, V, Ga, Cu, Co, Se, Br, Sr, Y, Pd, Sn, Ca, Cs, Pt, Te, La, Ti, Tl	K, P, Cr, Mn, Fe, Ni, , Zn, As, , Cd, Si, Al, Hg, Pb, S, Na, Mg, V, Ga, Cu, Co, Se, Br, Rb, Sr,Zr, Ag, Sn, W, Sb, Ce, Au, Ca, Te, La, Ti, Cs	K, P, Cr Mn, Fe, Ni, Zn, As, Cd Si, Al, Hg, Pb, S, Na, Mg, V, Ga, Cu, Co, Se, Br, Rb, Sr,Zr, Ag, Pd, Sn, Sb, Ce, Ca,, Au, Te,Ti,Tl	K, P, Cr Mn, Fe, Ni, Zn, As, Cd Si, Al, Hg, Pb, S, Na, Mg, V, Ga, Cu, Co, Se, Br, Rb, Sr, Y,Zr, Pd, Ce, Pt, Au, Ca, Te, Ti, Tl	K, P, Cr Mn, Fe, Ni, Zn, As, Cd Si, Al, Hg, Pb, S, Na, Mg, V, Ga, Cu, Co, Se, Br, Sr, Zr,Pd, Ag, Sb, Pt, Cs, Au, Ca,Ti, Tl	K, P, Cr Mn, Fe, Ni, Zn, As, Cd Si, Al, Hg, Pb, S, Na, Mg, V, Ga, Cu, Co, Se, Br,Sb, Rb, Sr, Zr, Pd, Ag, Ce, Au, Ca, Te,, La, Cs, Ti, TL	P, Cr, Mn, Ni, Zn, As, Cd, Hg,Pb,S,Na,Ga, Co,Se,Br,Sr,Zr, Pd, W, Ag,Sn, Sb,Ce, Ca, Te,La, Cs, Ti,Tl
1 < EF < 3 Minor enrichment	Y, Ce, CS	Y, Zr	Zr, Nb, Ce	Nb	Y, La, Cs	La, Cs	Y, Nb, Ce, La, Cs	Y, Nb, W	K, Fe, Al, Mg, V
3 < EF < 5 Moderate enrichment	Zr	Ca		Y		Nb			Nb
< EF < 10 Moderate-to-severe enrichment		Ce	W						Y
10 < EF < 25 Severe enrichment					W				Si, Cu
25 < EF < 50 Very severe enrichment			Au			Sn, W	Sn, W	Sn	Au
EF > 50 Extremely severe enrichment	Rb,Ag,Sc,In,Te	Rb,Ag,Sc,In	Rb, Ag,Sb, Sc,In	Pd, Pt,Sc,In	Rb, Pt, Sc, In	Ag,Sb, Sc	Rb, Sc, In	Sb, Pt, Sc, In	Rb, Pt, Sc, In

Table 4.11: The Overall Enrichment for Samples of All Sites Confirm the Following Sequence from the Highest to the Least

Atomic No.	Elemental symbol	[] Precipitant dust (ppm)	[ ] Earth crust	Enrichment Factor (EF)	EF Rating
19	K	2,8975	26000	0,581	No enrichment
24	Cr	0,14747	15000	0,0512	No enrichment
25	Mn	0,2414	20000	0,0629	No enrichment
26	Fe	9,59317	50 000	1	
28	Ni	0,040799	15000	0,0142	No enrichment
30	Zn	0,91339	15 000	0,3174	No enrichment
33	As	0,02569	15 000	0,0089	No enrichment
48	Cd	0,010493	15 000	0,00365	No enrichment
14	Si	68,0545	27 7000	1,2805	Minor enrichment
13	Al	6,60763	81 000	0,42517	No enrichment
80	Hg	0,32666	15 000	0,1135	No enrichment
82	Pb	0,02495	15 000	0,00867	No enrichment
16	S	0,35541	15 000	0,12349	No enrichment
12	Mg	4,53551	20900	1,131063	Minor enrichment
23	V	0,03312	100	1,72623	Minor enrichment
29	Cu	0,4286	100	2,23388	Minor enrichment
27	Co	0,00043	20	0,112059	No enrichment
35	Br	0,00416	0,37	58,6	Extremely severe enrichment
42	Mo	0,00956	1,5	33,218078	Very severe enrichment
46	Pd	0,01277	0,0006	133115,539	Extremely severe enrichment
47	Ag	0,01655	0,07	12322,7552	Extremely severe enrichment
50	Sn	0,01484	2,2	35,1575889	Very severe enrichment
74	W	0,00112	1,1	5,30681	Moderate enrichment

Atomic No.	Elemental symbol	[] Precipitant dust (ppm)	[ ] Earth crust	Enrichment Factor (EF)	EF Rating
51	Sb	0,1529	0,2	398,46057	Extremely severe enrichment
56	Ba	0	500	0	No enrichment
78	Pt	0,00047	0,003	816,5532	Extremely severe enrichment
79	Au	0,00096	0,0011	5003,55982	Extremely severe enrichment
3	Li	0	20	0	No enrichment
20	Ca	4,43189	36 300	0,63634	No enrichment
21	Sc	3,95101	22	936,037637	Extremely severe enrichment
49	In	1,54698	0,049	164549,468	Extremely severe enrichment
52	Te	0,00295	0,005	3075,10448	Extremely severe enrichment
81	Ti	0,01294	4,4	15,3281402	Severe enrichment
83	Bi	0	0,048	0	No enrichment

Determination of elemental EF ratings are classified according to the following criteria:

Enrichment Factor Assessment Scale						
EF > 50	25 < EF < 50 Very severe enrichment	10 < EF < 25	36 < EF < 10	3 < EF < 5	1 < EF < 3	EF ≤ 1
Extremely severe enrichment	Very severe enrichment	Severe enrichment	Moderate to severe enrichment	Moderate enrichment.	Minor enrichment	No enrichment

Similar studies conducted detected the trace elements of Al, As, Ca, Cd, Co, Cu, Cr, Fe, Hg, Ni, Mn, Mo, Si, Ti, Pb, S, U, V, and Zn, and enrichment of Al, Ca, Fe, Mn, Ti, and Si detected in the tailings material, street dust and windblown dust (PM_{10} and PM_5 fractions) from man-made sources (Nengovhela *et al.,* 2006, Ojelede, 2012, Tlowana *et al*., 2013), while Al, Ca, Fe, Mn and Si elements are of geologic nature, thus naturally occurring.

Study by Maseki *et al*. (2013) showed the trend confirming gold mining TSF dust as being highly enriched with As, Pb, and Au. This was supported by Mpanza *et al*. (2020), further noting high enrichment of dust with Au, U and As exceeding the crustal average and ranging from 72-359, 30-82, and 33-317 respectively. This study, however, does not fully concur with these findings, noting EF Au=5004, as extremely severe enrichment and no enrichment from AS (EF=0.0089) and Pb (EF=0,00867) as shown in Table 4.11 above.

4.4.1.2 Geo-accumulation Index

Geo-accumulation index (*I*geo), which defines the extent of metal contamination was calculated using equation 4.2 below (Müller, 1981; Amato *et al*., 2009; Lu *et al*, 2009; Wei *et al.*, 2009; Škrbić & Mladenovic, 2010; Wei *et al*., 2010; Yalala, 2015):

$$\boldsymbol{Igeo = \ln Cn/1.5*Bn \text{ or } Log2\ (Cn/1.5\ Bn)} \qquad \text{(Equation 4.2)}$$

Where, **Cn** is the measured total concentration of the element **n** of the dust sample, **Bn** being the concentration of element **n** in the Earth's Crust at the lithogenic correlation factor of **1.5** in the background data. Table 4.12 below provides the results of metal contamination (Igeo) analysed in this study.

Table 4.12: Geo-Accumulation of Heavy Metals in Dust Samples

Atomic No.	Element	Elemental Conc. (ppm)	[ ]Abundance crust	Igeo value	Igeo Rating
19	K	2,8975	26000	16,55948663	Extremely contaminated
15	P	0,11064	15000	13,87268197	Extremely contaminated
24	Cr	0,14747	15000	10,52620578	Extremely contaminated
25	Mn	0,24144	20000	11,65248649	Extremely contaminated
26	Fe	9,59317	50000	18,2866856	Extremely contaminated
28	Ni	0,04079	15000	8,672071697	Extremely contaminated
30	Zn	0,826265	15000	13,01238884	Extremely contaminated
33	As	0,02427	15000	7,923030298	Extremely contaminated
48	Cd	0,30495	15000	11,574357	Extremely contaminated
14	Si	68,0545	277000	23,58318261	Extremely contaminated
13	Al	6,60763	81000	18,44480469	Extremely contaminated
80	Hg	0,001524	15000	3,929790998	Heavily contaminated
82	Pb	0,02386	15000	7,898450233	Extremely contaminated
16	Si	0,19745	15000	10,94727165	Extremely contaminated
11	Na	1,32037	28300	14,6044942	Extremely contaminated
12	Mg	4,53551	20900	15,94751761	Extremely contaminated
23	V	0,03312	100	1,142740172	Uncontaminated to moderately contaminated
31	Ga	0,002942	19	-4,746022025	Uncontaminated
29	Cu	0,04286	100	1,514669349	Uncontaminated
27	Co	0,0043	20	-4,124482031	Uncontaminated
34	Se	0,00088	0,05	-15,05709945	Uncontaminated

Atomic No.	Element	Elemental Conc. (ppm)	[ ]Abundance crust	*Igeo* value	*Igeo* Rating
35	Br	0,00416	0,37	-9,928566081	Uncontaminated
37	Rb	0,03387	0,3	-7,205776298	Uncontaminated
38	Sr	0,03361	370	3,051453313	Heavily contaminated
39	Y	0,02186	30	-1,193634694	Uncontaminated
40	Zr	0,13356	190	4,080453011	Heavily contaminated
41	Nb	0,00684	20	-3,454822365	Uncontaminated
42	Mo	0,00956	1,5	-6,708773666	Uncontaminated
46	Pd	0,01277	0,0006	-17,57881004	Uncontaminated
47	Ag	0,01655	0,07	-10,33848874	Uncontaminated
50	Sn	0,01484	2,2	-5,521824075	Uncontaminated
74	W	0,00112	1,1	-10,24974453	Uncontaminated
51	Sb	0,01529	0,2	-8,938158379	Uncontaminated
56	Ba	0	500	0	Uncontaminated
58	Ce	0,05651	68	1,35715034	
78	Pt	0,00047	0,003	-20,02083591	Uncontaminated
79	Au	0,00096	0,0011	-20,43792124	Uncontaminated
20	Ca	4,43189	36300	16,7106415	Extremely contaminated
21	Sc	3,95101	22	5,856690616	Extremely contaminated
49	In	1,54698	0,049	-4,306582396	Uncontaminated
52	Te	0,00295	0,005	-16,63388802	Uncontaminated
57	La	0,00446	34	-3,306240234	Uncontaminated
55	Cs	0,00451	4,4	-6,240115828	Uncontaminated

Atomic No.	Element	Elemental Conc. (ppm)	[ ]Abundance crust	*Igeo* value	*Igeo* Rating
22	Ti	0,1294	0,048	-7,915874762	Uncontaminated
81	Tl	0,00311	363000	9,555777818	Extremely contaminated
83	Bi	0	363000	0	Uncontaminated

Even though K, P, Cr, Mn, Ni, Zn, As, Cd, Al, Hg, Pb, Si, Na, Co, Rb, Sr, Li, Ba, Ca, La and Tl were depleted and not enriched as per Table 4.12 above, these were found to be extreme contaminants of the dust samples as shown in Table 4.12 above. The results of this study show the order of metal contamination as follows: Si>Al>Ca>K>Mg>Na>P>Zn>Mn>Cd>Si>Cr>Tl>Ni>As>Pb>Sc>Hg. Interestingly, the results showed both extremely severely enriched and extremely contaminated with Sc as only metal depicted.

Si, as one the largest and most important class of minerals and make up approximately 90% of the Earth's crust they are also the most popularly gold mining induced (Yalala, 2015). Even though the TSF dust samples are not enriched with Si, extreme contamination surfaced in the results, in the following sequence Si>Al>Fe>Ca>K>Mg. Statistical nonparametric correlation analysis of heavy metals found in the sample as shown in Table 4.13 below.

Table 4.13: Pearson correlation between elements in PM25 dust samples from the study area

	K	P	Cl	Ca	Ti	V	Cr	Mn	Co	Ni	Cu	Zn	Ga	Ge	As	Se	Br	Rb	Sr	Y	Zr	Nb	Mo	Pd	Ag	Cd	Sn	Sb	I	Au	Hg	Pb	Fe	Mg	Al	Si	S
K	1,000																																				
P	.846**	1,000																																			
Cl	-0,055	0,445	1,000																																		
Ca	.950**	.877**	0,118	1,000																																	
Ti	.961**	.832**	-0,127	.938**	1,000																																
V	.856**	.805**	0,045	.878**	.851**	1,000																															
Cr	.945**	.888**	0,082	.961**	.960**	.883**	1,000																														
Mn	.957**	.808**	-0,082	.944**	.961**	.891**	.949**	1,000																													
Co	-0,500	-0,500	0	-0,500	-0,500	1.000**	-1.000**	-0,500	1,000																												
Ni	.922**	0,512	-.803**	.883**	.933**	.872**	.864**	.949**	0	1,000																											
Cu	0,358	0,564	0,000	0,612	0,442	.673*	.636*	0,406	0	0,292	1,000																										
Zn	.828**	.955**	0,373	.912**	.870**	.858**	.925**	.838**	-1.000**	0,532	0,515	1,000																									
Ga	.649*	.695*	0,084	.582*	.582*	.635*	.660*	.667*		0,280	0,033	0,572	1,000																								
Ge	0,128	0,111	0,183	0,163	-0,035	0,018	0,109	0,009	-1.000**	0,005	0,595	-0,091	0,137	1,000																							
As	.864**	.629**	-0,109	.793**	.894**	.784**	.821**	.871**	-0,500	.906**	0,236	.658**	.625*	-0,015	1,000																						
Se	0,419	0,497	-0,316	0,275	0,132	0,491	0,252	0,180		0,290	0,866	0,198	0,564	0,700	-0,109	1,000																					
Br	0,335	0,418	0,378	0,075	0,075	0,226	0,151	0,176		-0,319	0,200	0,050	0,607	0,343	0,144	0,000	1,000																				
Rb	.846**	.620*	0,006	.833**	.912**	.912**	.851**	.938**	1.000**	.900**	.733*	.681*	0,614	0,203	.929**	0,564	0,176	1,000																			
Sr	.911**	.714**	-0,127	.890**	.896**	.873**	.905**	.945**	-1.000**	.960**	0,333	.729**	0,594	0,136	.851**	0,655	0,151	.881**	1,000																		
Y	.753**	.548*	-0,405	.708**	.795**	.565*	.772**	.759**	-1.000**	.847**	0,261	.514*	0,400	0,242	.853**	0,323	0,036	.792**	.871**	1,000																
Zr	.895**	.596*	-0,082	.851**	.934**	.890**	.868**	.943**	0	.948**	0,309	.679**	0,525	0,098	.984**	0,667	-0,050	.956**	.939**	.842**	1,000															
Nb	-0,033	0,219	0,214	0,041	0,033	0,088	0,103	-0,028	0	-0,055	0,452	0,154	-0,176	.728*	0,073	-0,324	0,257	0,217	0,123	0,181	0,200	1,000													
Mo	-0,091	-0,015	-0,400	-0,128	0,176	-0,182	0,158	-0,012	0	-0,505	0,600	0,201	-0,257	-0,427	-0,046	-0,100	-0,500	-0,381	-0,092	-0,038	-0,286	0,573	1,000												
Pd	0,400	0,500	0,200	0,400	0,400	0,300	0,300	0,400	0	0,400	0,600	0,500	0,105	-0,200	0,700	-1.000**	1.000**	1.000**	0,000	0,700	0,400	0,400	0,000	1,000											
Ag	-0,190	0,096	0,500	-0,095	-0,238	0,167	-0,262	-0,286	1.000**	0,100	0,500	0,179	0,000	-0,600	-0,162	-0,400	0,500	-0,600	-0,487	-0,643	-0,371	-0,500	-0,543		1,000										
Cd	-.604*	-0,372	0,150	-.646**	-.646**	-.604*	-.595*	-.714**	-0,500	-.705*	0,095	-0,481	-0,403	0,256	-.829**	0,257	0,450	-.804**	-.660*	-.649*	-.797**	0,188	0,268	-0,100	0,679	1,000									
Sn	-0,354	-0,433	-0,517	-0,389	-0,332	-0,282	-0,441	-0,371	0,500	0,006	0,393	-0,415	-0,622	0,086	-0,337	-0,143	0,275	-0,155	-0,165	-0,066	-0,145	0,146	0,072	0,200	0,600	0,364	1,000								
Sb	-0,643	-0,559	0,400	-0,607	-0,643	-0,214	-0,571	-0,643	0	-0,771	0,500	-0,429	0,400	0,657	-0,342	0,200	1.000**	0,300	-0,429	-0,234	0,800	0,464	-0,319	-0,500	-0,500	-0,029	-0,300	1,000							
I	-1.000**	-1.000**		-1.000**	-1.000**	-1.000**	-1.000**	-1.000**	0	0	0	-1.000**	-1.000**	1.000**	-1.000**	0	0	-1.000**	-1.000**	0	-1.000**	0	-1.000**	0	0	1.000**	1.000**		1,000						
Au	0,071	0,144	-1.000**	0,214	-0,071	0,714	-0,234	0,143	0,500	0,200	0	0,600	-0,500	-0,357	-0,234	-0,200	0	0,000	-0,400	-0,536	-0,500	-0,564	-0,300		1.000**	-0,543	-0,086	0,000		1,000					
Hg	-0,021	0,172	0,095	-0,035	-0,007	-0,189	-0,098	-0,056	1.000**	0,119	-0,371	0,018	-0,127	-0,212	-0,269	0,029	.812*	-0,382	-0,049	-0,114	-0,418	-0,721	0,072	0,300	0,086	0,350	-0,018	-.896*	1.000**	0,000	1,000				
Tl	-.496*	-0,236	0,109	-.491*	-.501*	-0,331	-0,468	-.612**	0,500	-0,506	0,563	-0,243	-0,153	0,293	-.628**	0,371	0,096	-0,435	-.550*	-0,429	-0,421	0,221	0,043	0,100	0,563	.736**	0,451	0,286	1.000**	-0,036	0,091				
Pb	.919**	.770**	-0,064	.864**	.902**	.917**	.888**	.931**	0,500	.959**	0,297	.793**	.589*	0,060	.894**	0,518	0,000	.899**	.926**	.737**	.965**	0,109	-0,192	0,400	-0,143	-.732**	-0,386	-0,018	-1.000**	0,360	-0,245	1,000				
Fe	.942**	.821**	-0,109	.938**	.981**	.837**	.944**	.948**	-0,500	.960**	0,370	.868**	0,519	-0,097	.885**	0,060	-0,092	.886**	.920**	.802**	.960**	-0,011	0,067	0,400	-0,095	-.650**	-0,318	-0,643	-1.000**	-0,071	-0,028	.882**	1,000			
Na	.882**	.765**	0,227	.907**	.872**	.798**	.883**	.865**	-0,500	.883**	0,406	.801**	0,474	0,259	.832**	0,156	-0,201	.789**	.829**	.692**	.851**	0,106	-0,216	0,300	-0,262	-.672**	-0,490	-0,143	-1.000**	-0,143	-0,161	.872**	.877**			
Mg	.965**	.789**	0,073	.928**	.924**	.792**	.896**	.911**	-0,500	.913**	0,127	.772**	0,477	0,085	.854**	0,419	-0,008	.754**	.884**	.736**	.873**	-0,019	-0,073	0,300	-0,190	-.621*	-0,346	-0,679	-1.000**	0,071	0,007	.895**	.930**	1,000		
Al	.938**	.793**	0,118	.932**	.936**	.773**	.914**	.895**	-1.000**	.894**	0,273	.804**	0,456	0,096	.849**	0,132	-0,075	.749**	.862**	.761**	.855**	0,088	0,049	0,300	-0,190	-.596*	-0,293	-0,750	-1.000**	-0,286	0,070	.855**	.940**	.979**	1,000	
Si	.899**	.741**	0,027	.878**	.907**	.734**	.868**	.880**	-1.000**	.911**	-0,067	.752**	0,481	-0,090	.864**	0,132	-0,176	.745**	.880**	.801**	.890**	-0,116	-0,085	0,300	0,000	-.639*	-0,293	-0,714	-1.000**	-0,286	0,042	.844**	.944**	.955**	.959**	1,000	
S	.867**	0,491	-0,533	.976**	.867**	.915**	.952**	.879**	0	.766**	0,612	0,588	0,402	0,595	.648*	0,866	0,429	.817**	.745*	0,588	.673*	0,143	-0,400	-0,200	-1.000**	-0,381	0,179	-0,500	0	0	0,257	.733*	.794**	.661*	.733*	0,455	1,000

The values in bold indicate the strongest correlations where R>0.5, whereas R<0.1 signifies the weakest correlations.

4.5 Determination of TSF Dust Zones of Influence Using Settling Rates and Deposition Distance Away from the Source

4.5.1 Particle settling rates and terminal velocity

Wind induced dust deposition can occur from the source and travel thousands of kilometres in the atmosphere to a small local confined source, thereby impacting on sensitive receptors (Ravi *et al.,* 2011). Determination of transportation and deposition of windblown dust from mine TSF's is therefore vital for establishing exposure risks in neighbouring communities (Stovern *et al.,* 2016). In this study, particles settling velocity based on Stokes Law (Equation 2.1) and the drag force (Equation 3.3) were used to calculate the distance of individual particle dust deposition.

This was used to calculate the deposition distances of different particle sizes from TSF's of different heights within the area and the results are shown in Tables 4.14 to Table 4.16 below:

Table 4.14: Particle Settling Rate Versus the Time Taken for the Particle to Reach the Ground

	Mean	Med.	Std. Dev.	Min.	Max.	Percentiles			
	Valid						25	50	75
Settling Rate	69	0,36	0,20	0,47	0,00	1,42	0,01	0,20	0,62
Time	69	53465,02	230,34	139698,4	24,65	523831,6	72,2	230,34	5238,32

The results of the nonparametric correlations from the Spearman's rho analysis showed higher terminal setting velocity rates mean value (0.36 m/s) than the median (0,20 m/s) of the dust particles, with ***p***=0.00<0001≤ 0.005, which suggests a statistically significant, negative correlation between "settling rate" and "time for particle to reach the ground". There is a statistically significant, negative relationship between "settling rate" and "time for particle to reach the ground", since the ***p***-value < 0.05.

Table 4.15: TSF Height Versus Distance at which the Particle Travelled Before Reaching the Ground

	N	**Mean**	**Std. Deviation**		**Cohen's d Effect sizes**		
				Welch p-value	**35**	**40**	**45**
35	21	56722,31	155368,95	0,118		0,32	0,32
40	24	386542,21	1044682,25				0,04
45	24	434859,98	1175267,53				

Results of one-way ANOVA Test as per Table 4.15 above shows a correlation between TSF height and distance at which the particle travelled before reaching the ground confirmed a Welch ***P***-value of 0.118, in which ***P***-value > 0.005. This suggest that there is no statistically significant difference in the mean dust deposition distance between the three heights above ground categories (30, 40, 45). This resulted from a large variability in the data, and this differs according to the Cohen' d effects size of the practical significance.

Table 4.16 Particle Size Distribution Versus Distance Travelled Away from the Source

Size of particle (µm)	N	Mean	Median	Std. Dev.	Min.	Max.	Percentiles		
							25	50	75
1		2803469,13	2473649,23	1800518,51	931256,18	5238316,02	1018561,45	2473649,23	4801789,68
2.5	9	422169,47	372502,47	266060,72	130375,87	838130,56	158313,55	372502,47	698442,14
10	9	26385,59	23281,40	16628,80	8148,49	52383,16	9894,60	23281,40	43652,63
30	9	3022,69	2667,08	1904,97	933,48	6000,93	1133,51	2667,08	5000,77
50	9	1160,23	1023,73	731,20	358,31	2303,40	435,09	1023,73	1919,50
80	9	517,20	456,35	325,95	159,72	1026,80	193,95	456,35	855,66
100	9	363,67	320,89	229,20	112,31	722,00	136,38	320,89	601,67
840	9	159,62	140,85	100,60	49,30	316,90	59,86	140,85	264,08

Table 4.16 above containing the results of nonparametric statistical techniques using Kruskal-Wallis Test showing the ***P***-value of 0.00<0.001 in which ***P***-value <0.005, confirm a statistical significance difference in the distance travelled between the different sizes of particle. This suggests that the larger the particle size, the shorter the distance travelled away from the source. Ultrafine particles (PM<2.5 µm) are lighter, and they can therefore travel for longer distance away from the source.

The results presented in Tables 4.14, 4.15 and 4.16 above confirmed that particles' sizes terminal settling velocities remain constant irrespective of the height from which they fall, speed and deposition distance at which they land on the ground. Table 4.16 above confirmed that for the same velocity, particle size of 1 µm and less (finer) will travel to a greater distance whereas a particle sizes of 840 µm (coarser) will be deposited within a shorter distance. It is also evident that the particles from higher the TSF will travel longer distances than from the shorter TSF's in a bouncing movement.

The height to which particulate is lifted depends on air turbulence, temperatures, humidity, density and thermals which can be encountered.

Comparative analysis of distances travelled by precipitant dust particle sizes of 1, 2.5, 10, 30, 50, 100 and 840 µm at velocities of 2, 5 and 10m/s, dispersed from heights of 30, 40 and 45 meters TSFs. Tables 4.14, 4.15 and 4.16 above suggest that in a worst scenario, finer particles size (µm) travelling at 2m/s from the TSF height of 35, 40 and 45 m can be deposited at 130, 149 and 167 kms respectively reaching sensitive receptors within such distances. In the same breath, 10 µm particle can be deposited at residential area located 10.5 km away from a 45 m high TSF. It can also be speculated that an individual located within a residential area located within less than 700m of a mine TSF complex of maximum height of 45 m can be exposed to a dust cluster comprising a suite of particle size ranging from 1 and 840 µm through inhalation, dermal and ingestion pathways.

Within the study area, close residential areas, clinics/hospitals, schools and other areas public importance are located as close as within 1km away from mine TSF's as described in Chapter 3 which are potentially exposed to the dust particles depicted in Tables 4.14, 4.15 and 4.16 above. For instance, Wedela residential area is located within very close proximities of the mine TSF's which are within 1 to 5km distance in the eastern, north-east, north and western directions.

Study by Blight (2008) confirmed that a particle of 0.006 mm diameter would travel 100 times as far (i.e., 69 km) while one having the D_{50} diameter of 0.13 mm, would travel about 147 m. These theoretical distances are compatible with observations of sand and dust blown from TSFs. The layer of sand on the leeward slopes of TSFs showed that sand-size particles are carried tens of metres by the wind, whereas it is

common experience that fine dust can be carried downwind for tens of kilometres. It was further found that sand of particle size 0.13 mm diameter would travel approximately 200-300m, silt (0.06 mm) will reach 700-1000m whereas a clay particle size of 0.006 mm would travel further than 100km away from the source (AgreenCo, 2012). Thus, similarities are picked up in the trends from the results of this study compared to the above-mentioned studies.

4.6 Determination of Risks Exposures Sensitive Receptors within Close Proximities of the Mine TSFs

4.6.1 Public risk exposure assessment

Radiological risk exposure and health risk assessments were conducted to determine typical exposure public considering soil, biota, water, and air exposure pathways as suggested by Scavina *et al.* (2012). However, this study only focuses on the risks associated with air exposure pathway.

4.6.2.1 Radiological public risk exposure

With reference to Sections 2.12.2 and 3.8.2, the results present the findings established during radiation exposure analysis of this study.

4.6.2.1.1 Radiation Elemental Concentration of TSF soil Material

Analysis of secondary data results of the radionuclide elemental concentrations in the TSF soil samples from two gold mine TSFs conducted by van Blerk are presented in Table 4.17 below. Comparison of radionuclides from material from two mining companies within the area are shown in Table 4.17 below.

Table 4.17: Radionuclides for TSF Soil Material at Mine 1 and Mine 2 Sites (Van Blerk 2015; 2016)

Radionuclide	MINE 1 TSF's			MINE 2 TSF's				
	TSF 1	TSF 2	TSF 3	All	TSF D4	TSF D3	TSF D2	TSF D1
	Bq.kg^{-1}							
U-238	405	373	461	522.0	108.0	166.0	912.0	930.0
U-234	421	376	465	60.6	60.6	166.0		
Th-230	421	376	465	60.6	60.6	166.0	912.0	930.0
Ra-226	430	455	470	512.0	111.0	127.0	946.0	871.0
Pb-210	560	552	618	710.0	181.0	136.0	1200.0	1030.0
Po-210	560	552	618	710.0	181.0	136	1200.0	1030
Th-232	26	25	25	25.4	15.4	15.7	30.8	39.8
Ra-228	26	25	43	36.3	9.5	0.0	39.3	57.2
Th-228	35	26	30	24.6	17.2	19.6	25.3	37.9
-235	19	17	21	24.0	5.0	7.7	42.0	42.8
Pa-231	19	17	21	-	-	-	-	-
Ac-227	19	17	21	-	-	-	-	-
Ra-223	19	17	21	24.6	17.2	19.6	25.3	37.9

4.6.2.2 Atmospheric Pathway Results

Study results from secondary data confirmed that maximum activity of 71 Bq g^{-1} were measured in the inhalable fractions of sources material and east-west gradient of radioactivity across the Witwatersrand were found. Calculated annual exposure dose through inhalation pathway was estimated at 3.7 mSv, with the derived environmental default concentration of PM10 aerosol particles taken at 40 µg m^{-3}, based on doses above 1 mSv limit recommended by the International Commission on Radiological Protection for the public (van Blerk 2015; Van Blerk, 2016).

The calculated dose of 3.7 mSv, was above average radiation to world population of 2.4. mSv a^{-1} and above 1 mSv a^{-1} exposure limit recommended by ICRP for the public (ICRP, 1991). The alpha and beta activities amongst the samples analysed ranged from less than 4.5 to 70 Bq g^{-1} and 1.9 to 27 Bq g^{-1} respectively. The maximum activities found in the analysed samples were in the western section of the study

domain, Carletonville (55 Bq g^{-1}) and Westonaria (7 Bq g^{-1}). Majority of the samples have activities less than 16 Bq g^{-1}(van Blerk 2015, 2016).

4.6.2.3 Public Activity Analysis

This assessment identifies one or more groups of people whose habits, location, age or other characteristics expressed in Table 4.18 below that would cause them to receive a higher dose than the rest of the exposed population as suggested by van Blerk (2015). The Residential Exposure Condition (REC) is done to evaluate the radiological consequences to members of the public residing in both formal and informal residential areas surrounding the areas of Wedela, Fochville, Khutsong, Mohaleshoek, Carletonville Central Business District (CBD), Deelkraal, Elandsrand and Southdene. The main contributor to a total effective dose is expected to come from the atmospheric and associated secondary pathways (van Blerk & Potgieter, 2011b). This, however, extends to boundaries outside these areas as the study area only forms part of the regional mining area in which TSF's mostly form part of the landscape.

Table 4.18: Public Activity Assessment

Community	Class of exposure conditions (e.g. formal residential, informal residential, industrial/mining)	Daily activities
Mine Residences	Mining	All the residents are employed and during their shifts they are underground. When they are off duty, many residents spend time outside socialising or doing chores like washing, gardening, etc.
Carletonville Town	Formal, urban	Target population mainly include mine employees travelling from Carletonville CBD for work. They get exposed to radiation sources for the period of the work shift which is on average between 8 and 12 hours per day.
Deelkraal, Oberholzer, Elandsridge, South Dene, Blyoor village	Formal, urban	Mainly recreational, play area with outdoor play equipment where children can play, fishing, swimming and braai around the dam
Farming Community	Formal, rural	The farmers and their workers spend most of the day outside, busy with farming activities and activities such as maintenance, new projects and development.
MohalesHoek Informal Settlement	Informal, mining	Given the high levels of unemployment in the community, many people are at home during the day. Some people would sit outside and socialise.
Wedela	Formal, mining	Mostly people spend outside, some women doing things like fetching wood, gardening or cooking outside. Small children spend a lot of time playing outside. Employed people spend less time outside, unemployed people will walk and sit outside. Some people hunt in the fields around the township and some religious activities also take place outside.
West Wits Village	Formal, mining	Most people are at work during the day and not many people have been observed outside. In some gardens there were garden workers. Some of the houses are quite large with very big gardens and they have facilities like a private swimming pool, tennis court, lapa and outdoor braai area. Based on the sports clubs and outdoor facilities, it is most likely that people spend more time outside over weekends.
Fochville, Kokosi, Greens Park	Formal, urban	This area comprises formal residential area with Fochville CBD forming the hub of businesses, shops and offices. Kokosi is a township area closer to a more upper class Fochville which comprises formal houses with community-based facilities such as churches, schools, clinics, etc. Most people in this area are unemployed and they spend time outside performing chores with children playing outside. However, some community members are mainly employed by the mines and own small businesses within the surrounding area.

4.6.2.4 Hazard identification

For Hazard Identification, it was assumed in a worst-case scenario that the members of the immediate community of study area are continuously exposed to the dust. These include mothers looking after small children at home, petrol attendants and convenient store workers within close proximities to one of the sites (Site 1), school children at one of the monitoring sites within the school (Site 3), and community care-based centre (Site 4), exposed to the concentrations of PM_{10} and metals in air as determined by the monitoring and analyses of the short-term PM samples.

4.6.3 Health Risk Exposure

For the health risk assessment, it was assumed that the respondents of the public health risk exposure experience questionnaire are a representation of the population targeted by this study in terms of comparing the mining (exposure) and non-mining (non-exposure) area. The target population is mainly children aged between 3-15 years (Nkosi *et al*., 2017).

Assessment of health risks associated with inhalation of windblown particulates (dust) from the TSFs within the study area was done according to Strydom *et al*., (2014) and using the World Health Organisation (WHO, 2005) equations as implemented by van Niekerk *et al*., (2014).

4.6.3.1 Enrichment Factors (EF)

Enrichment facts were calculated by first determining the concentration of all metals as a measure of the magnitude and variation of these elements as discussed in Section 4.3.1 above.

4.6.3.2 Results of population health risk questionnaire

The results of the health assessment questionnaire administration confirm that the learners' participation in the survey are predominantly blacks (62%), followed by coloured (22%), then white (10%) and then Indians (6%). The sample comprised 54% female compared to compared 46% of their male counterparts. Figures 4-25 to 4-33 below show the results of the health risk questionnaire.

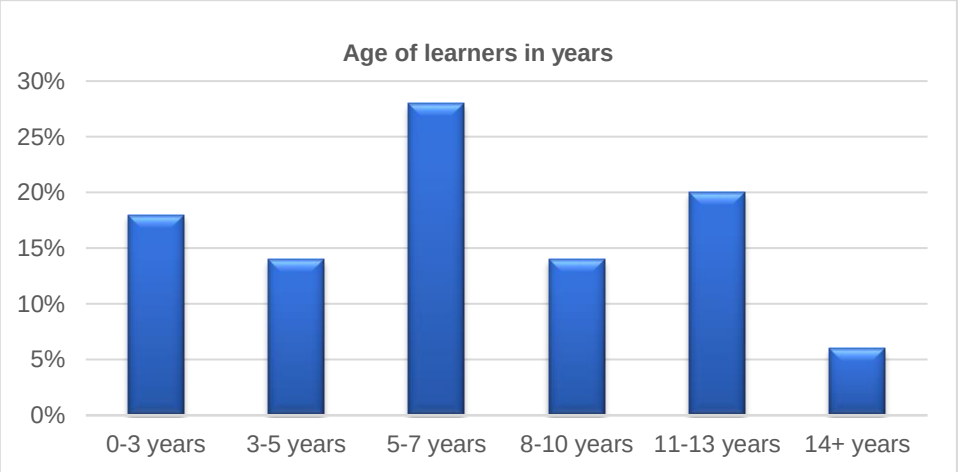

Figure 4-25: Age in years of learners

Results show that most respondents learners fall within the 5-7 years' age bracket (28%), followed by 11-13 years' age bracket (20%), then 0-3 years' age bracket (18%). 14% of learners fall within 3-5 years' age bracket and 8-10 years' age bracket each, respectively. The last 14% of learners who responded to the survey are aged 14 years and above. Furthermore, a greater percentage in crèche (22%), followed by Grade 1 (14%), then Grade 8 and Grade 3 forming 12% each. Grade R learners makes 10% of the total learners who responded while Grade 7 and Grade 4 makes 7%, each. 4% of learners are in Grade 6 and 2% of learners are in Grade 5.

4.6.3.2.1 Residential location of exposure

In terms of respondent's location, the results of respondents are shown in Figure 4-26 below.

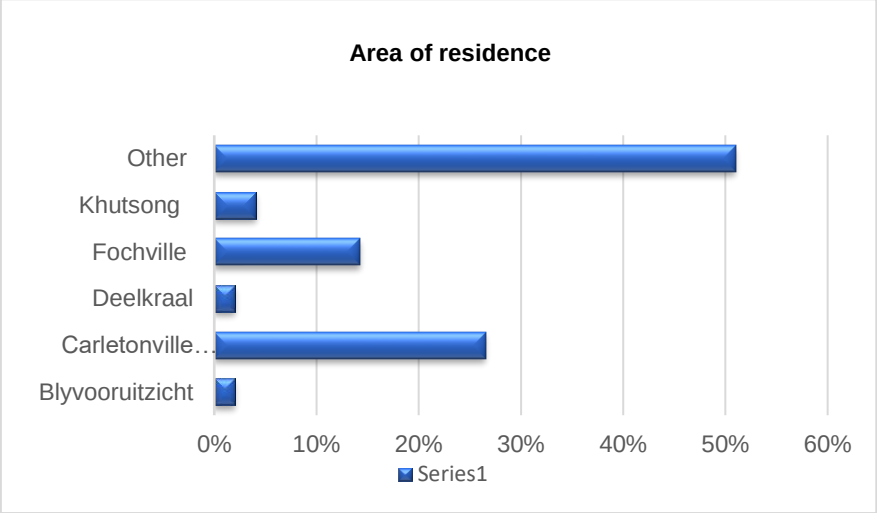

Figure 4-26: Area of residence

The results show that a greater percentage of learners comes from other places of residents outside the study area (51%), of which some are mining areas (exposure areas) and others are not (non-exposure areas). This is followed by Carletonville CBD (27%), then Fochville (14%), Khutsong (4%) while learners residing at Deelkraal and Blyvooruitzicht makes 2% of total respondents for each area.

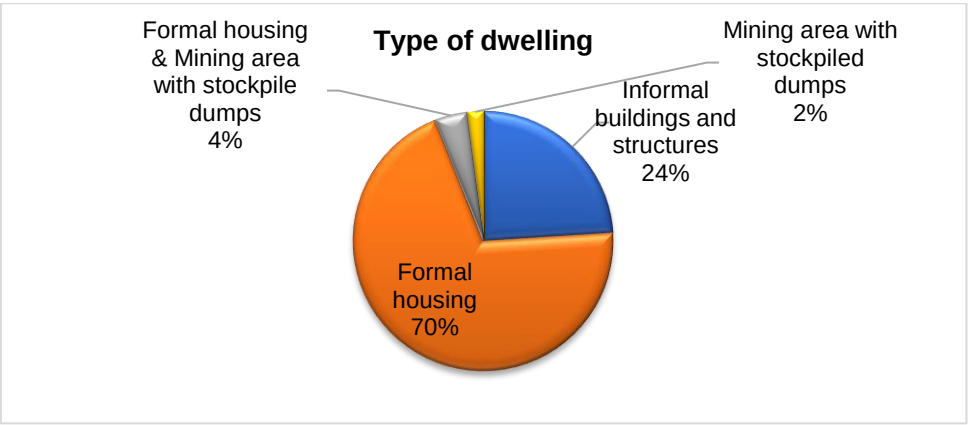

Figure 4- 27: Type of residential dwelling

The results show in Figure 4.27 above that 70%, 24%, 4% and 2% of learner respondents resides in formal houses, informal buildings and structures, formal housing and mining areas with stockpile dumps and in mining areas with stockpile dumps respectively. Types of residential dwellings which learner respondents reside in are formal houses made up of bricks and cement (72%), followed by informal houses made up of corrugated steel (26%), then fabricated structures made up of steel or wood (2%).

From the results the most daily time spent by the leaners playing outside are 1 to 3 hours (52%), followed by 4 to 6 hours (32%) then 0 to 1 hour making (16%) of the total number of learner respondents. Playing grounds conditions of the respondent learners were made of concrete lining or paved yard and playgrounds (20%), open field with a combination of bare soils, with grass, concrete lined or paved, paved with grass (18%), open field with bare soils (16%); open field with grass, concrete lined or paved (16%) and another who are attend schools with open field with grass (16%). Others include open field with bare soils (12%), grass (8%) and bare soil only (6%). The balance comprises of open filled with bare soils, with grass, concrete lined or paved, paved with grass and open field with grass; concrete lined or paved of 2% each.

4.6.3.2.2 Source of prevailing dust exposure

The results show that the source of prevailing dust is from playing on unlined grounds and playing on unlined school grounds, vehicle travelling on close by roads, dust blowing within the area towards the school including from mining activities at 21% each. (11%) of learners said that the prevailing dust comes from mining activities while another 11% said it comes from dust blowing within the area towards the school. Less

than 9% of the leaners confirmed a combination of blowing dusts, mining activities, vehicle travelling on bare soils and industrial activities.

4.6.3.2.3 Absenteeism due to respiratory infections or illness

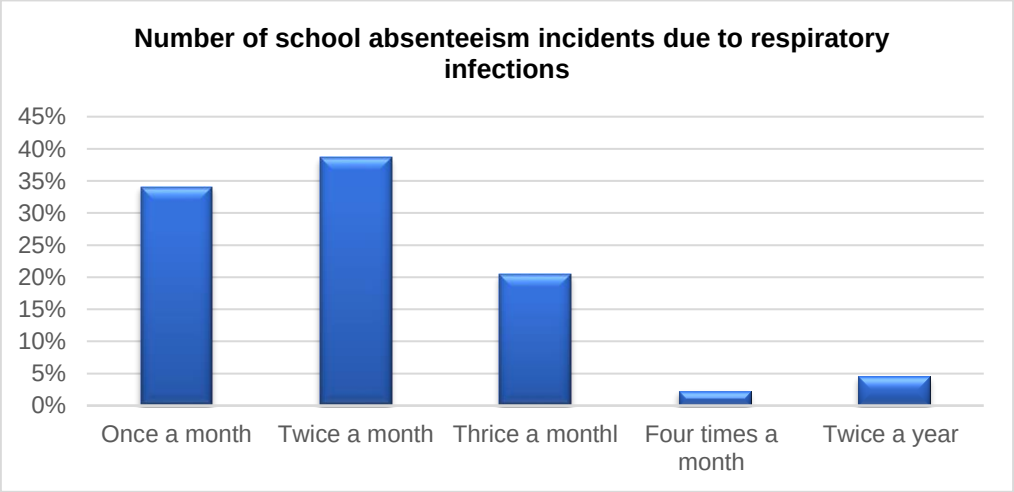

Figure 4-28: Number of absenteeism incidents due to respiratory infections or illness

It is evident from Figure 4.28 above that the majority of 39% learners are absent from school twice a month due to respiratory infections or illness, followed by 34% once a month, and those absent thrice a month (20%). While 5% of learners are absent from school twice a year and only 2% stays absent from school four times in a month.

Results also show in Figure 4-29 below that the dominant respiratory infections or illnesses experienced are runny nose (12%), while a combination of persistent cough, sneezing and runny nose, and persistent cough and runny nose (7%) each symptom are also experienced. Other symptoms of a combination of the above including skin irritation, hair loss, vomiting and runny, asthmatic attack, breathlessness, fever and wheezing (2-5%).

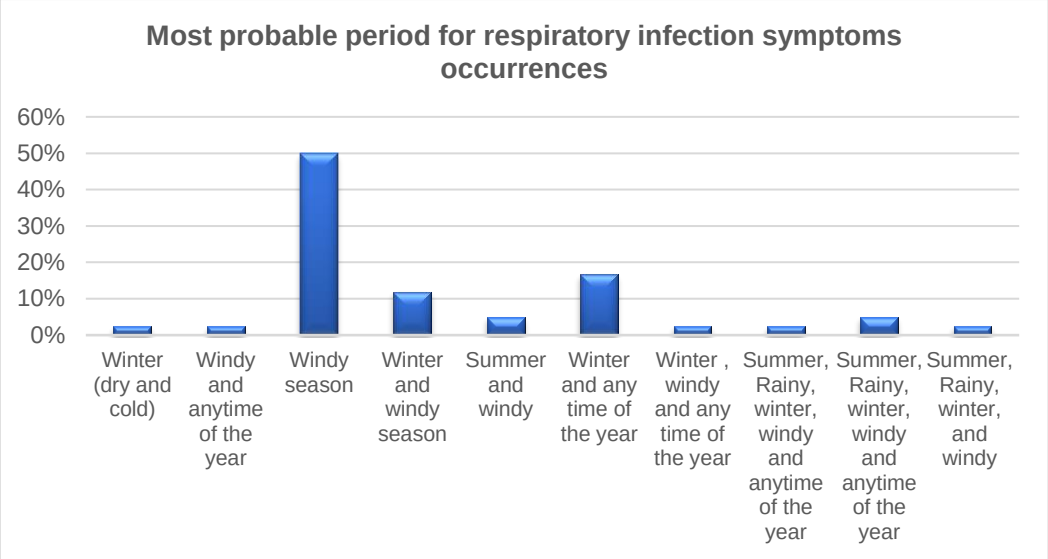

Figure 4-29: When do these symptoms occur

Figure 4-29 above shows that 50% of learners suffer from runny nose experience the symptoms windy season, followed by 17% who experience the symptoms during winter and any time of the year, 12% who experience the symptoms during winter and windy season and another 5% who experience the symptoms during summer and windy season. While 7% of learners experience the symptoms during summer, rainy, winter, windy season and at any time of the year, a total of 6% experience these symptoms in winter, in windy season, in cold weather and any time of the year.

4.6.3.2.4 Length of symptoms

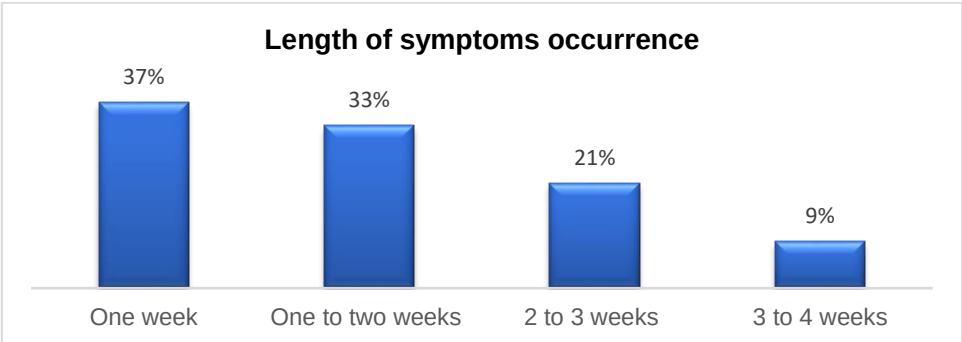

Figure 4-30: How long does the child stay away from school per incident

While on average, 37% of the learners experience these symptoms and stay one (1) week away from school per incident, only 9% stay 3 to 4 weeks away from school per incident, as shown in Figure 4-30 above.

4.6.3.2.5 Learners' health conditions upon TSF dust exposure

In relation to the learners' health conditions due to exposures to TSF dust, the results are shown in Figure 4-31 below.

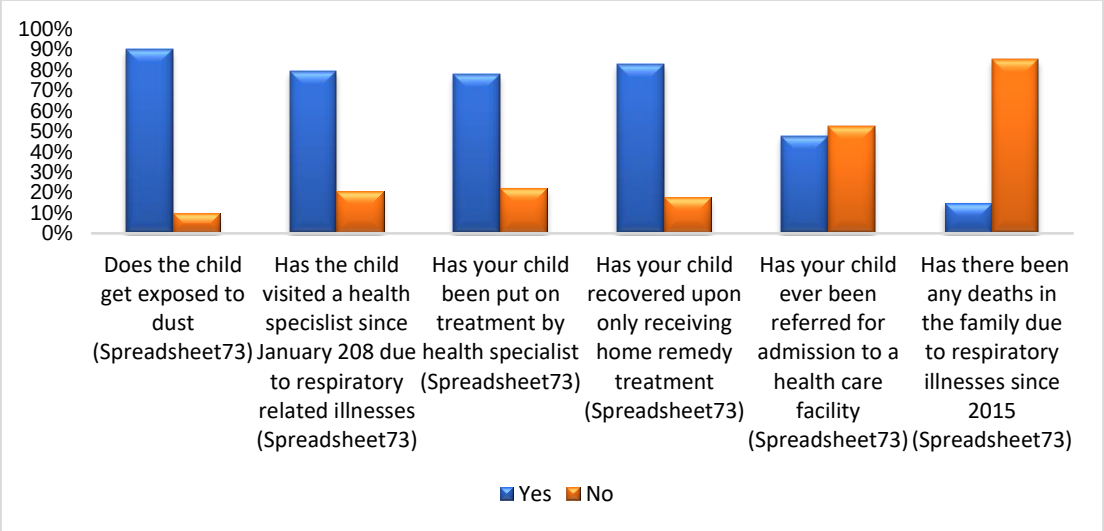

Figure 4-31: Learners' health conditions upon TSF dust exposure

Results of learners' health conditions shown in Figure 4-31 show that 15% of families confirmed death in their families due to respiratory illnesses since 2015 while 85% mentioned none. 48% the children were referred to a health care facility while 52% said no. 83% of families said that their child recovered upon only receiving home remedy treatment while 17% showed no recovery following home remedy treatment. The results further show that 78% of the parents said that their child has been put on

treatment by health specialist as opposed to 22%. It is also evident that 80% of the children visited a health practitioner since January 2008 due to respiratory related illnesses, while 20% said they haven't. In addition, 90% of the families said that their child gets exposed to dust while 10% said they don't.

4.6.3.2.6 Learners' dust exposure

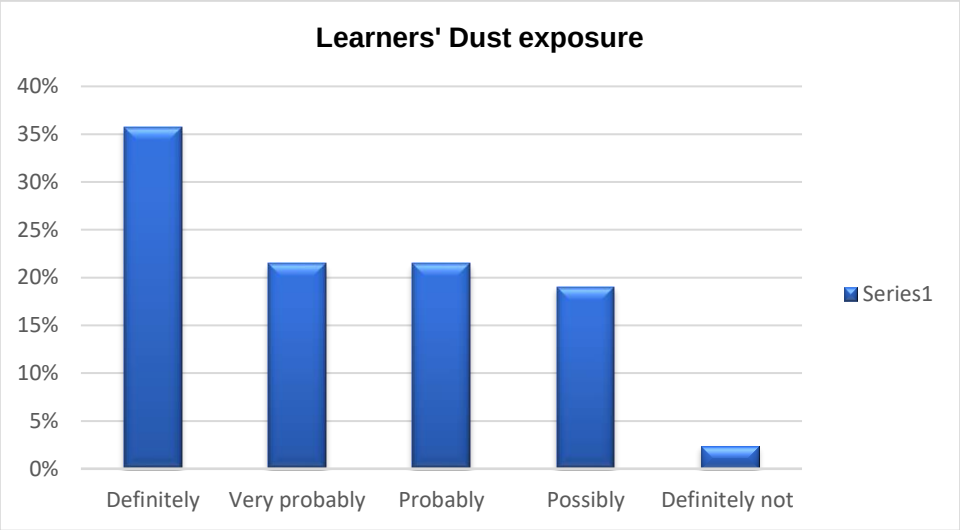

Figure 4- 32: Do you think dust exposure from the mine dumps is a concerning issue in your child's area of residence or schooling.

Parents were asked whether dust exposure from mine TSF is concerning in their areas of residence, play and schooling, as shown in Figure 4-32 above. The levels of responses confirmed (36%), probably (42%), possibly (19%) and (19%) not.

Chi-square results on the level of association between Dust exposure and symptoms are shown in Table 4.19 below.

Table 4.19: Chi-square results between association between dust exposure and symptoms

Source of the prevailing dust	**Chi-Square**	**df**	**p-value**
Type of residence	36,8523	28	0,1221
Type of family dwelling	34,067	28	0,1987

Time child spend outside playing	42	28	0,0433
Child getting exposure to dust	5,33	14	0,9806

From Table 4.19 above, there is no association between dust and where the prevailing dust come from since ***P***-values >0.05, therefore not enough evidence exists to show association between dust and the source of prevailing dust. Similarly, there is no association between dust and type of residence, no association between dust and type of family dwelling and no association between dust and child getting exposure to dust. However, strong association exists between dust and time child spend outside playing confirmed by ***P***-values < 0.05, and therefore enough evidence exists to show the association between dust and time child spend outside playing.

The results show that there is an association between dust exposure and the number of absenteeism due to respiratory infections or illness as there is enough evidence to show association (***P***-value < 0.05). There is no association between dust and symptoms that a child suffers from. However, Nkosi *et al.* (2017) confirmed a significant difference of indoor respirable dust in the classroom between exposed (0.17 $mg.m^3$, located at 1–2 km from gold mine dumps) versus unexposed (0.01 $mg.m^3$, located at distances above 5km or more from the mine dumps) children with asthma at each school ($p < 0.001$) (Nkosi et al., 2015; 2016). This suggested significant detrimental effect of indoor respirable dust in exposed schools on children with asthma, as they were significantly higher than the unexposed schools, in the absence of environmental exposure standards for children with asthma.

The results of this study establish the link between dust and when the symptoms occur. However, no association exists between dust and whether the child visited a health specialist since January 2015 due to respiratory related illnesses. There is no association between dust and whether the child ever been referred for admission to a health care facility. The results further show that there is no association between dust and whether there have been any deaths in the family due to respiratory illnesses since 2015. Similarly, no association is established between TSF dust exposure and how people think dust exposure from the TSF is a concerning issue in their child's area of residence or schooling.

With reference to the study by Mpanza (2020), it was established that TSFs within the study area contained both fine and coarse material of which 60% are of inhalable and respirable dust fraction range. This also suggested an annual SiO_2 exposure level exceeding 3 μg/m³ for respirable crystalline silica posing a health threat for communities residing within 2 km of the TSFs. Makgae (2011) and Maseki (2013) established TSFs as the source of radioactivity risk for numerous mining residential areas of the study area.

CHAPTER 5

5. CONCLUSION

5.1 General conclusions

This study established that on average the highest total precipitant dust deposition occurs in spring season as reflected in the results at Sites 1 and 5 at 1165 and 918 mg/m^2/day respectively, exceeding the residential limit of 600 mg/m^2/day set out in terms of the South African National Dust Control Regulations of 2013 (NDCR 827, 2013). These predominantly dry and high-speed north-eastern winds specifically occurred during September 2016 (windy period) with low precipitation levels.

In total, the average content of the sampled sites contained quartz (66.28%), silicates (60.3%), Al_2O_3 (20%), calcites (4.5%) and iron oxides (2.5%). The cause for concern is the fact that once silica dust is inhaled it could permanently damage the lungs, increasing the risk of contracting TB (Murray, 2016). The balance is formed by trace elements of arsenic, chromium, copper, manganese, nickel, potassium, and titanium oxides, which make up main components of gold mine extraction process and its by-product tailings material.

The mineralogical characteristic of the TSF dust confirms 27,87% occurrence of chrysotile and this is associated with asbestosis as confirmed by studies in South Africa. This should pose a health concern as it was found out in this study that the average mineralogical components of all samples confirmed that sulphur (54,65%), tridymite (54,42%), graphite (47,4%), quartz (38,32%), cristobalite (35,3%) and

chrysotile (27,87%) made up most of the precipitant dust. Chrysotile is associated with asbestosis occurrences in South Africa.

Microscan analysis validated the above results confirming a predominance of gold TSF dust by 5-70% quartz (rounded quartz, broken quartz and sandy grits) of size range (D_{50}=37-200 µm), haematite (<59%, D_{50}= 30-50 µm), pulverised roadway dust (10-40%, D_{50}=63-79 µm), clay (6-40%, d_{50}=63-78 µm), felspar (<2%, d_{50}=30-58 µm), aluminium silicates 83 µm, viscous liquid crystalline (38 µm) and mica traces detected only at Site 2E.

This study confirms that gold mine TSF dust samples are laden with metals of "extremely severe enrichment", with EF were sequentially evidenced as In>Pd>Ag>Au>Te>Sc>Pt>Sb>Br whereas Sn and Mo "very severe enriched" metals in the TSF dust samples, with EF valued at 35.2 and 33.2 respectively and extremely contaminated elements sequentially with

Si>Al>Ca>K>Mg>Na>P>Zn>Mn>Cd>Si>Cr>Tl>Ni>As>Pb>Sc>Hg.

Similarly trace elements were detected by other studies within the study area which established high enrichment of Al, Ca, Fe, Mn, Ti, and Si detected in the TSF material, street dust and windblown dust (PM_{10} and PM_5 fractions) from man-made sources. Even though the dust samples were not enriched with Si, extreme contamination surfaced in the results of this study, in the following sequence Si>Al>Fe>Ca>K>Mg, with Si being one of the largest and most important class of minerals that are both naturally occurring and the most popularly gold mining induced.

The precipitant dust further contains highly radioactive radionuclides originating from gold ore bearing rock material mined underground in the Witwatersrand Basin goldfields. Gross beta higher average concentration of 317.67 Bq/kg and gross alpha at 279 Bq/kg were detected in the radio-analysis of the precipitant dust samples. ^{226}Ra, ^{210} Pb and ^{40}K had the highest activity concentration of 346.67 Bq/kg, 342.33 Bq/kg and 246.67 Bq/kg respectively whereas 235 U, 232 Th and 228 Ra recorded the lowest values. The order of the activity concentration recorded ^{226}Ra > ^{210} Pb > ^{40}K > ^{228}Th > ^{228} Ra > ^{234} U > ^{232}Th > ^{235}U. This study confirms higher Th-228 and Ra-228 concentrations in TSF dust at (180>30,33) Bq/kg compared to TSF soils (81>31,33) Bq/kg, making TSF dust radioactive.

Based on the visual analysis results, TSF structures within the study are visible from travelling roads, houses, workplaces, school and workplace the results showed 27%, 25% and 20% respectively and they are very visible (49%), visible (33%), slightly visible (9%) and not visible (1%) according to the respondents within the study area. Even though the visibility is the most evident throughout the year (75%), these structures are also visible between July and September (17%), when the wind is blowing. This was also verified by the numerical risk assessment (Table 4.9) and specific zones of influence shown in Figure 4.20.

These could be due to the current management practises which are very poor (24%), on average (21%) and poor (15%). However, 20% and 13% are in views of good and very good management practices respectively, as some of these structures are vegetated to reduce the visual intrusion on their viewpoints from the public. From the results, the majority of 36% said that the issue of visual impacts of TSF on the natural

landscape can be best addressed by removing TSF and rehabilitating the environment. This practise is supported by Bishop (2011) that high-rise structures such as TSFs are provoking when located in landscape located in high aesthetic quality such as ridges and they become acceptable provided they are not visible from settlements, viewpoints, and the transportation network.

The results of the nonparametric correlations from the Spearman's rho analysis showed a statistically significant, negative relationship between "settling rate" and "time for particle to reach the ground", since the ***p***-value is smaller than 0.05 (i.e., p-value=0.00<0001). There is no statistically significant difference in the mean dust deposition distance between the three heights above ground categories (30, 40, 45). This study also suggests that particles' sizes terminal settling velocities remain constant irrespective of the height from which the particles fall, speed and deposition distance at which they land on the ground. This is inclusive of fine and very fine particle sizes of PM1 and PM2.5.

For the same velocity, particle size of 1 µm (finer) will travel to a greater distance whereas a particle sizes of 840 µm (coarser) will be deposited within a shorter distance. It was also evident that the particles from higher the TSF will travel longer distances than from the shorter TSF's in a bouncing movement. The height to which particulate is lifted depends on air turbulence, temperatures, humidity, density and thermals which can be encountered. On contrary to other studies suggesting that communities residing closer to the TSFs as sources are at high health risk exposures due to inhalation of particles compared to far distant residents, this study has verified that using particle settling velocity calculations confirming that it is the finer particles

that travel longer distances. The study thus suggests possible health risks from TSF on far distant communities away from the TSFs than those closer to the source. However other factors such as dilution, temperature inversions and prevailing wind direction may also contribute towards the level of exposures to communities located at far distances from the TSFs.

Main finding of this study with regards to health exposure perspective is that even though most learners (70%) reside in formal housing made up of bricks and cement, they get exposed to dust from mainly mine TSF and vehicular movement as they spend time playing outside. This was confirmed by a strong association between dust and time child spend outside playing. Such exposures mainly occur during windy seasons and in wintertime. As a result, these learners experience respiratory related illnesses not less than three times a month making them absent from school for one (1) week or more per incident. This is confirmed by an association between dust number of absenteeism due to respiratory infections analysis. This study, therefore, confirmed that from precipitant dust deposition characterisation analyses conducted including the heavy metals and radionuclides characteristics, public exposure of both exposure and non-exposures of the gold mine TSF dust is evident with possible health effects. Furthermore, the lighter particles can travel over a long distance as suggested by Yalala, (2015) Nkosi, (2018) and Mpanza *et al.,* (2020).

5.2 Study limitations and knowledge gaps

5.2.1 Limitations during undertaking of the visual analysis

Determining visual resources and visual impact analysis is a subjective process. Evaluating a landscape's visual quality can be complex, as assessment of the visual

landscape applies mainly qualitative standards. This study is based on assessment techniques and investigations that are limited by time and budgetary constraints applicable to the type and level of assessment undertaken, in this case a baseline assessments studies and to some extent, secondary data that was available at the time of this study. The radiological public exposure analysis could not be conducted as this was outside the scope of this study.

Only a questionnaire was administered in the health risk exposure study, due to lack of technical resources to conduct a very comprehensive epidemiological study supported by advanced specialised software models by highly qualified personnel. This also requires consideration of scenarios of both cancerous and non-cancerous conditions studies over an extended period considering trends.

5.3 Recommendations

Public exposure to gold mine TSF dust can be inclusive of other sources within the study area. Whilst this is a sensitive matter to address, it could have long-term significant detrimental effects on the gold mining industry, the public and authorities in the region post mine closure. It is therefore imperial that a closer look be taken into the issue to facilitate its effective management by all relevant parties. This study therefore recommends that a detailed comparative epidemiological analysis study should be undertaken to further investigate, e.g., other underlying factors such as historic exposures, of both exposure and non-exposure communities for comparisons. While health risks associated with gold mine TSF dust exposures are highly probable, these are equally preventable, provided control measures are enforced and monitored in South Africa as these have successfully been managed by intensely gold mining

countries such as Australia. The onus further lies with ex-miners to also ensure regular check-ups on their health status for proper controls.

The visual impact assessment presents one of the environmental impacts that are less explored but gradually being incorporated in the environmental assessments' studies, and only done when imposed by authorities during individual project approval process. There is sensitive landscape, including environmental features within the study area that are detrimentally impacted because of the anthropogenic activities of mining which some might be permanent and irreversible. Knowledge base from the data this study could contribute towards raising awareness on protection of the natural environment features by the local public as long-term custodians of the environment post mine closure.

There should be an endeavour in marrying the technical scientific research and active public involvement as these are currently conducted in silos, creating mistrust between various role players and lack of cooperative approach in mitigating environmental legacies post mine closure.

Results of this study could also assist the public, municipality, and the provincial governments (WRDM and DMRE) for comparisons of the status of the air quality moving towards rehabilitation, closure, and post closure of the mines in this study area. Data generated from this study will be useful for inclusion in the revised and updated environmental information in the local and national standards relating to limits of exposure of heavy metals of focus in inhalable fraction of particulate matter specifically for the study area. This could also be useful to the mines on comparative basis to their

existing data to encourage companies which are making efforts in managing issues relating to public exposure to continue and improve on such initiatives. Further, the data could be used to raise awareness to those industries within the area not managing these risks and impacts due to their potential long-term effects on the public.

REFERENCES

Abdul-Wahab, S. and Marikar, F. (2012). The environmental impact of gold mines: Pollution by heavy metals. Open Eng., **2**: 304–313.

Abello, R.P., Bernaldez, F.G. and Galiano, E.F. (1986). Consensus and contrast components in landscape preference. Environment and Behaviour, **18**: 155.

Adam, T.P. and Stassen K.R. (2013). The differences in perception of radiological risks: lay people versus new and experienced employees in the nuclear sector.

Agency for Toxic Substance and Disease Registry (ATSDR). (2003b). Toxicological Profile for Mercury U.S. Department of Health and Humans Services, Public Health Humans Services, Centers for Diseases Control. Atlanta.

Africa Stockpiles Programme. (2009). Annual Report (July 2008-June 2009). Africa Stockpiles Programme. www.africastockpiles.net.

Agency for Toxic Substances and Disease Registry (ATSDR). (2005). Public Health Assessment Guidance Manual. (2005 Update).
http://www.atsdr.cdc.gov/hac/phamanual/
appg.html (Accessed date: 3 November 2016).

Agency of Natural Resources, Department of Environmental Conservation. (1998). Air Toxics Report. http://dec.vermont.gov/content/air-toxics-report, Accessed date: 2 August 2016.

Agrawal, A. (2012). Toxicity and Fate of Heavy Metals with Particular Reference to Developing Foetus. Advances in Life Sciences 2012, 2(2): 29-38 DOI: 10.5923/j.als.20120202.06

Ait-Khaled, N., Odhiambo, J., Pearce, N., Adjoh, K.S., Maesano, I.A., Benhabyles, B., Bouhayad, Z. (2007). Prevalence of symptoms of asthma, rhinitis and eczema in 13- to 14-year-old children in Africa: The International Study of Asthma and Allergies in Childhood Phase III. Allergy. **62**: 247–258.

Akabzaa, T.M. (2000). Boom and Dislocation: A Study of the Social and Environmental Impacts of Mining in the Wassa West District of Ghana; Third World Network, Africa Secretariat: Accra, Ghana, 2000.

American Thoracic Society (ATS). (1997). Adverse effects of crystalline silica exposure: American Thoracic Society Committee of the Scientific Assembly on Environmental Occupational Health. Am. J. Res. Critic. Care Med., **155**: 761–765.

Amir, S. and Gidalizon, E. (1990) Expert based Method for the Evaluation of Visual Absorption Capacity of the Landscape. Journal of Environmental Management, **30**: 251-163.

Anderson, L.M., Mulligan, B.E., Goodman, L.S. and Regen, H.Z. (1983) Effects of sounds on preferences for outdoor settings. Environment and Behaviour, **15**: 539-566.

Anderson, H.R., Ruggles R, Pandey, K.D., Kapetanakis, V., Brunekreef, B., Lai, C.K.W., Strachan D.P. et al., 2010. Ambient particulate pollution and the world-wide prevalence of asthma, rhinoconjunctivitis and eczema in children: phase One of the International Study of Asthma and Allergies in Childhood (ISAAC). Occup Environ Med., **67**: 293–300.

Andraos. C., Utembe, W., Gulumian, M. (2018). Exceedance of environmental exposure limits to crystalline silica in communities surrounding gold mine tailings storage facilities in South Africa, Science of The Total Environment, **619–620**: 504-516.

Annegarn, H.J., Surridge, A.D., Hlapolosa, H.S.P., Swanepoel, D.J.D.V., Horne, A.R. (1991). Review of 10 years of environmental dust monitoring at Crown Mines. J Mine Vent Soc S Afr., **44** (3):46.

Annegarn Environmental Research. (2007). Crown Gold Recoveries Quarterly Dust Monitoring Report for DRD (July – September 2007). Rand burg: Annegarn Environmental Research (Pty) Ltd (now SGS Environmental).

Annegarn, H.J., Scorgie, Y., and Sithole, J. (2002). Dust monitoring and mitigation on surface gold tailings reclamation. Proceedings of Surface Mining 2002 – Modern Developments for the New Millennium. South African Institute for Mining and Metallurgy, Johannesburg. 103–109.

Annegarn, H. J. (2006). Implications of the new Air Quality Act for the residential built environment. Environ. Manage. **1** (3): 18–21.

Annegarn, H. J., Surridge, A. D.; Hlapolosa, H. S. P.; Swanepoei, D. J. D. V.; and Horne, A. R. (1991). A review of 10 years of environmental dust monitoring at Crown Mines. Journal of the Mine Ventilation Society of South Africa, **44**, (3): 46.

Annegarn, H.J. and Sithole, J. (2002). Dust monitoring and mitigation on gold tailings reclamation. In Proceedings of the Mine Ventilation Society Symposium: Occupational Health “Impact Prevention and Aftermath Strategies”, Pretoria, South Africa, 28 February–1 March 2002; CSIR: Pretoria, South Africa, 2002: 13.

Annegarn, H.J., Zucchiatti, A., Sellschop, J.P.F., Booth-Jones, P. (1987). PIXE characterization of airborne dust in the mining environment. Nucl Instrum Meth B. 1987; **22** (1–3): 325– 330.

Appleton, J. (1975). Landscape evaluation: the theoretical vacuum. Transactions of the Institute of British Geographers, **66**: 120-123.
Appleton, J. (1996). The Experience of Landscape. 2nd edition. Chichester: Wiley. 282.

Arriaza, M., Cañas-Ortega, J.F., Cañas-Madueño, J.A. and Ruiz-Aviles, P. (2004). Assessing the visual quality of rural landscapes. Landscape and Urban Planning, **69** (1), 115–125.

Arthur, L.M. (1977). Predicting scenic beauty of forest environments: some empirical tests. Forest Science, **23**: 151-160.

Arthur, L.M., Daniel, T.C. and Boster, R.S. (1977). Scenic assessment: an overview. Landscape Planning, **4**: 109-129.

Aucamp, P. and van Schalkwyk, A. (2003). Trace element pollution of soils by abandoned Gold mine tailings, near Potchefstroom, South Africa", Bulletin of Engineering Geology and the Environment, **62**: 123–134.

Bell, S. (1999). Landscape: Pattern, Perception and Processes. E& FN Spon, London.

Bell, S. M. and Morse, S. (2005). Delivering sustainability therapy in sustainable development projects. Journal of Environmental Management, **75** (1): 37-51.

Bell, M.L., Zanobetti, A. and Dominici, F. (2013). Evidence on vulnerability and susceptibility to health risks associated with short-term exposure to particulate matter: a systematic review and meta-analysis. Am J Epidemiol., **178** (6): 865–76.

Bergin, J. and Price, C. (1994). The travel cost method and landscape quality. Landscape Research, **19**: 21-23.

Bhagia, L., (2009). Non-occupational exposure to silica dust in vicinity of slate pencil industry, India. Environ. Monit. Assess. **151** (1–4): 477–482.

Bhagia, L., (2012). Non-occupational exposure to silica dust. Indian J. Occup. Environ. Med., **16** (3): 95–100.

Bishop, I.D. and Hulse, D.W. (1994). Prediction of scenic beauty using mapped data and geographic information systems. Landscape and Urban Planning, **30:** 59-70.

Bishop, I.D. and Hulse, D.W. (1994). Prediction of scenic beauty using mapped data and geographic information systems. Landscape and Urban Planning, **30** (1–2): 59–70.

Bishop, I.D. (1996). Comparing regression and neural net-based approaches to modelling of scenic beauty. Landscape and Urban Planning, **34** (2): 125–134.

Bishop, I.D., Wherrett, J.R. and Miller, D.R. (2000). Using image depth variables as predictors of visual quality. Environment & Planning B: Planning & Design, **27** (6): 865–875.

Bishop, I.D. and Rohrmann, B. (2003). Subjective responses to simulated and real environments: a comparison. Landscape and Urban Planning, **65**: 261-277.

Blight, G.E. and Caldwell, J.A. (1984). The abatement of pollution from abandoned gold residue dams. J. S. Afr. Inst. Min. Metall., **84**: 1–9.

Bobbins K. and Trangoš G. (2018). Mining landscapes of the Gauteng City-Region. GCRO Research Report # NO. 07. ISBN: 978-0-620-74637-3

Bowker, L.N. and Chambers, D.M. (2015). The Risk, Public Liability, and Economics of Tailings Storage Facility Failures.

Bowker, L.N. and Chambers D.M. (2017). In the dark shadow of the supercycle tailings failure risk & public liability reach all-time highs. Environments. **4**: 75.

Brabyn, L. (1996). Landscape Classification using GIS and National Digital Databases. Landscape Research, **27:** 277-300.

Bourassa, S.C. (1990). A paradigm for landscape aesthetics. Environ. Behav. **22**: 787–812.

Briggs, D.J. and France, J. (1980). Landscape Evaluation: A comparative study. Journal of Environmental Management, **10**: 263-275.

Brown, G. (2004). Mapping spatial attributes in survey research for natural resource management: methods and applications. Society and Natural Resources, **18** (1): 17-39.

Brush, R.O. and Shafer, E.L. (1975). Application of a Landscape-Preference Model to Land Management. In Landscape Assessment: Values, Perceptions and Resources (eds. Zube, E.H., Brush, R.O. and Fabos, J.G.),168-181, Halstead Press.

Buchecker, M., Hunziker, M. and Kienast, F. (2003). Participatory landscape development: Overcoming social barriers to public involvement. Landscape and Urban Planning, **64** (1–2): 29–46.

Bugai D., Kozak M.W., van Blerk J.J. and Avila R. (2014). Paper presented at EU NORM 2 Conference, Prague, Czech Republic, June 17-19, 2014.

Buhyoff, G.J. and Riesenmann, M.F. (1979). Experimental manipulation of dimensionality in landscape preference judgements: a quantitative validation. Leisure Sciences, **2:** 221-238.

Buhyoff, G.J. and Wellman, J.D. (1980). The specification of a non-linear psychophysical function for visual landscape dimensions. Journal of Leisure Research, **12:** 257-262.

Buhyoff, G.J., Miller, P.A., Roach, J.W., Zhou, D. and Fuller, L.G. (1994). An AI Methodology for Landscape Visual Assessments. AI Applications, **8**: 1 - 13.

Buhyoff, G.J., Miller, P.A., Hull, R.B. and Schlagel, D.H. (1995). Another look at expert visual assessment: validity and reliability. AI Applications, **9:** 112-120.

Bureau of Land Management (BLM). (1980). Visual resources management program. U.S. Dept. of Interior, Washington, D.C.

Burmil, S., Daniel, T.C., Hetherington, J.D. (1999). Human values and perceptions of water in arid landscapes. Lands. Urban Plann., **44**: 99–109.

Candeias C., Melo R., Paula P.F., Ferreira da Silva E., Salgueiro A.R. and Teixeira J.P. (2013). Heavy metal pollution in mine-soil-plant system in S. Francisco de Assis - Panasqueira mine (Portugal). Appl. Geochemistry., **44** (4): 1–12.

Carls, E.G. (1974). The effects of people and man-induced conditions on preferences for outdoor recreational landscapes. Journal of Leisure Research, **6**: 113-124.

Carlson, A.A. (1977). On the possibility of Quantifying Scenic Beauty. Landscape Planning, **4** (1): 131–172.

Cassar, L. F. (2010). A landscape approach to conservation: Integrating ecological sciences and participatory methods. Msida: International Environment Institute.

Kampa, M. and Castanas, E. (2008). Human health effects of air pollution. Environmental Pollution Volume, **151** (2): 362-367. https://doi.org/10.1016/j.envpol.2007.06.012.

Centre for Development Support (CDS). (2004). Proposals for the utilisation of redundant mine infrastructure for the benefit of local communities. CDS Research Report, LED and SMME Development, 2004(1). Bloemfontein: University of the Free

State (UFS). A review of the distribution of particulate trace elements in urban terrestrial environments and its application to considerations of risk.

Charlesworth, S., De Miguel, E. and Ordóñez, A. (2011). A review of the distribution of particulate trace elements in urban terrestrial environments and its application to considerations of risk. Environ Geochem Health, **33**: 103–123. https://doi.org/10.1007/s10653-010-9325-7.

Chen, H., Goldberg, M.S. and Villeneuve, P.J. (2008). A systematic review of the relation between long-term exposure to ambient air pollution and chronic diseases. Rev. Environ. Health., **23** (4): 243–297.

Chevrel, S., Courant, C., Cottard, F. and Coetzee, H. (2003). Very high-resolution remote sensing and GIS modelling in multiscale approach of a mining related environmental risk analysis in urbanised areas: Example of the Witwatersrand goldfield, East Rand, South Africa. In Proceedings of the 4th European Congress on Regional Geoscientific Cartography and Information for Spatial Planning and Information for Spatial Planning, Regione Emilia-Romagna, Bologna, Italy, 17–20

Chevrel, S, Croukamp, L, Bourguignon, A and Cottard, F. (2008). A Remote Sensing and GIS Based Integrated Approach for Risk Based Prioritization of Gold Tailings Facilities — Witwatersrand, South Africa, in A Fourie, M Tibbett, I Weiersbye & P Dye (eds), Proceedings of the Third International Seminar on Mine Closure, Australian Centre for Geomechanics, Perth, 639–650.

Churchyard, G.J., Ehrlich, R., Water Naude, J.M., Pemba, L., Dekker, K., Vermeijs M., White N.J. and Myers J. (2004). Silicosis prevalence and exposure-response relations in South African goldminers. Occup Environ Med., **61**: 811–816.

Cocco, P. (2003). The long and winding road from silica exposure to silicosis and other health effects. Occup Environ Med., **60**:157–158.

Colls, J. (2002). Air Pollution – Second Edition, Spon Press, ISBN 0-20347602-6, UK.

Collier, J., and Collier, M. (1986). Visual anthropology: Photography as a research method. Albuquerque: University of New Mexico Press.

Conrad, E., Christie, M., Fazey, I. (2011). Understanding public perceptions of landscape: A case study from Gozo, Malta. Applied Geography, 159-170.

Cooper, A. and Murray, R. (1992). A structured method of landscape assessment and countryside management. Applied Geography, **12:** 319-338.

Crofts, R.S. (1975). The landscape component approach to landscape evaluation. Transactions of the Institute of British Geographers, **66**: 124-129.

Crofts, R.S. and Cooke, R.U. (1974). Landscape Evaluation: A comparison of techniques. Occasional Papers, no 25, Department of Geography, University College London.

Csavina, J., Field, J., Taylor, M.P, Gao, S., Landázuri, A., Betterton, A.E. and Sáez, E. (2012). A review on the importance of metals and metalloids in atmospheric dust and aerosol from mining operations. Science of the Total Environment, **433:** 58–73.

Curtis, M. (2009). Mining and tax in South Africa: Costs and benefits. www.curtisresearch.org. http://www.curtisresearch.org/SAfrica.MiningTax.Feb09.Curtis.pdf.

Council for Geoscience South Africa (CGSA). (2014). Selected active mines. http://www.geoscience.org.za/images/stories/selectedactivemines.gif (accessed 20 September 2014).

D'Amato, G., Liccardi, G., D'Amato, M. and Cazzola, M. (2002). Outdoor air pollution, climatic changes and allergic bronchial asthma. Eur Respir J., **20**: 763–776.

Daniel, T.C. 1990. Measuring the quality of the natural environment e a psychophysical approach. American Psychologist, **45**: 633-637.

Daniel, T.C. and Boster, R.S. (1976). Measuring Landscape Aesthetics: The Scenic Beauty Estimation Method. Research Paper RM-167. USDA Forest Service, Fort Collins.

Daniel, T.C. and Meitner, M.J. (2001). Representational validity of landscape visualizations: the effects of graphical realism on perceived scenic beauty of forest vistas. Journal of Environmental Psychology, **21:** 61-72.

Daniel, T.C. (2001a). Aesthetic preferences and ecological sustainability in: Forests and Landscapes: Linking ecology, sustainability and aesthetics. (Eds. Sheppard S. & Harshaw H.). IUFRO research series Vol 6: 15–29. CABI Publishing, Wallingford.

Daniel, T.C. (2001b). Whither scenic beauty? Visual landscape quality assessment in the 21st century. Landscape and Urban Planning, **54** (1–4): 267–281.

Daniel, T.C. and Vining, J. (1983). Methodological Issues in the Assessment of Landscape Quality. In Behaviour and the Natural Environment (eds. Altman, I. and Wohwill, J.), Chapter 2, 39-83, Plenum Press.

Davidson, R.J. and Sole, M.J. (2007). The major role played by calcium in gold plant circuits. The Southern African Institute of Mining and Metallurgy, 2007. SA ISSN 0038–223X/3.00 +0.00.

Davies, T.C. and Mundalamo, H.R. (2010). Environmental health impacts of dispersed mineralization in South Africa. Journal of African Earth Sciences, **58**: 652–666.

Davies, M. (2004). ‘World experience with tailings stacking’, AMEC Earth and Environmental (ed.), Presented at CONRAD Tailings Seminar, Alberta Research Council.

Dearden, P. (1980). A Statistical Technique for the Evaluation of the Visual Quality of the Landscape for Land-use Planning Purposes. Journal of Environmental Management, **10**: 51 - 68.

Dearden, P. (1984). Factors influencing landscape preferences: An empirical investigation. Lands. Plann. **11:** 293–306.

Dearden, P. (1985). Philosophy, theory, and method in landscape evaluation. Canadian Geographer, **29**: 263-265.

Department of Environmental Affairs (DEA). (2011a). Development, Operation and Management of a National Ambient Air Passive Sampling Campaign. Department of Environmental Affairs, Pretoria.

Department of Environmental Affairs (DEA). (2011 b). State of Air Quality Governance Report. Department of Environmental Affairs, Pretoria.

Department of Environmental Affairs (DEA). (2011 c). Baseline Survey on Government-Owned Air Quality Monitoring Network (AQMN). Department of Environmental Affairs, Pretoria.

Department of Agriculture and Rural Development (GDARD). (2011). Feasibility Study on Reclamation of Mine Residue Areas for Development Purposes: Phase II Strategy and Implementation Plan, Technical report no. 788/06/01/2011, Gauteng.

Department of Environmental Affairs and Tourism (DEAT). (2006). State of the environment Outlook. Pretoria: DEAT.

Department of Environmental Affairs and Tourism. Full technical report on climate trends and scenarios for South Africa. https://www.environment.gov.za/sites/default/files/docs/climate_trends_scenarios.pdf (accessed on 02 March 2021).

Deloitte Global Services Limited. Tracking the Trends (2014). https://www2.deloitte.com/tw/en/pages/energy-and-resources/articles/Tracking-Trends-2014.html (accessed on 02 March 2021).

DiClemente, R.J. and Jerrold M.Jackson J.M. (2017). Learn more about Health Risk. Risk Communication in International Encyclopaedia of Public Health (Second Edition), 2017.

Dlamini L.Z.D. and Sifiso Xulu S. (2019). Monitoring Mining Disturbance and Restoration over RBM Site in South Africa Using Land Trendr Algorithm and Landsat Data. Sustainability 2019, 11, 6916; doi:10.3390/su11246916 www.mdpi.com/journal/sustainability.

Dockery, D.; Pope, C.A. (1994). Acute respiratory effects of particulate air pollution. Annual. Rev. Public Health, **155**: 107–132.

Dockery, D.W. (2001). Epidemiological evidence of cardiovascular effects of particulate air pollution. Environmental Health Perspective, **109**: 483–486.

Dudu, V.P., Mathuthu, M. and Manjoro, M. (2018). Assessment of heavy metals and radionuclides in dust fallout in the West Rand mining area of South Africa. Clean Air J., **28**: 42–52.

Durand, J. (2012). The impact of gold mining on the Witwatersrand on the rivers and karst system of Gauteng and North West Province, South Africa. J Afr Earth Sci., **68**: 24–43.

Dunn, M.C. (1976). Landscape with photographs: testing the preference approach to landscape evaluation. Journal of Environmental Management, **4**, 15-26.

Ernst & Young Global Limited. Business Risks Facing Mining and Metals (2015–2016). Available online: http://www.ey.com/Publication/vwLUAssets/EY-business-risks-in-mining-and-metals-2015-2016- new/$FILE/EY-business-risks-in-mining-and-metals-2015-2016-new.pdf

Environmental Protection Agency (EPA). (2017). Update for Chapter 5 of the Exposure Factors Handbook Soil and Dust Ingestion. National Center for

Environmental Assessment Office of Research and Development U.S. Environmental Protection Agency Washington, DC 20460.

Fashola, M. O. Ngole-Jeme, V. M., and Babalola, O. O. (2016). Heavy Metal Pollution from Gold Mines: Environmental Effects and Bacterial Strategies for Resistance. International Journal of Environmental Research and Public Health, **13**(11): 1047. Retrieved 2 22, 2021, from https://mdpi.com/1660-4601/13/11/1047/htm.

Feather, C.E. and Koen, G.M. (1975). The mineralogy of the Witwatersrand reefs. Mineral Science and Engineering, **7**: 89–224.

Federation for a Sustainable Environment. (2010). Annual report on the past year's activities. Rivonia, Johannesburg. 51 pp.

Federation for a Sustainable Environment (FSE). (2017). Tour of the West Rand Goldfields case studies. http://www.fse.org.za/index.php/mining/item/543-tours-of-west-rand-gold-fields. Accessed 19 May 2017.

Frimmel, H.E. and Minter W.E.L. (2002). Recent developments concerning the geological history and genesis of the Witwatersrand gold deposits, South Africa. Integrated Methods for Discovery: Global Exploration in the Twenty-First Century. Goldfarb, R.J. and Nielsen, R.L. (eds). Special Publication, vol. 9. Society of Economic Geologists: 17–45.

Gao, J., Tao Yue, T., Zuo P., Liu, Y. Tong, L., Wang, C., Zhang, X. and Qi S. (2017). Current Status and Atmospheric Mercury Emissions Associated with Large-Scale Gold Smelting Industry in China. Aerosol and Air Quality Research, **17**: 238–244.

Gauteng Department of Agriculture Conservation and Environment (GDACE) (2009). Gauteng Province Air Quality Management Plan. Final Report, January.

Gauteng Department of Agriculture and Rural Development (GDARD). (2002). Conceptual Study on Reclamation of Mine Residue Areas for Development Purposes; Rep No. 4250074879: 118; North West University: Potchefstroom, North West Province, South Africa, 2009. Guidelines for Landscape and Visual Impact Assessment', Spon Press.

Gauteng Department of Agriculture and Rural Development (GDARD). (2012). Mine Residue Areas Strategy and Implementation Plan.

Gielen, M.H., van der Zee, S.C., van Wijnen, J.H., van Steen, C.J. and Brunekreef, B. (1997). Acute effects of summer air pollution on respiratory health of asthmatic children. Am. J. Respir. Crit. Care. Med., **155**(6): 2105–2108.

Goldberg, M.S., Burnett, R.T., Stieb, D.M., Brophy, J.M., Daskalopoulou, S.S., Valois, M.F. and Brook, J.R. (2013). Associations between ambient air pollution and daily mortality among elderly persons in Montreal, Quebec. Sci. Total. Environ., 931–942.

Gobster, P.H. (1999). An ecological aesthetic in forest landscape management. Landscape journal **18** (1): 54–64.

Grange, G. H. (1973) The control of dust from mine dumps.

Gruehn, D. (2006). Landscape Planning as a Tool for Sustainable Development of the Territory — German Methodology and Experience. In: Vogtmann, H. & Dobretsov, N. (eds.). Environmental Security and Sustainable Land Use — with special reference to Central Asia (pp. 297–307). Dordrecht: Springer Netherlands.

Gruehn, D. (2010). Validity of landscape function assessment methods — a scientific basis for landscape and environmental planning in Germany. The Problems of Landscape Ecology, 28, 191–200.

Gwaze, P. and Mashele, S.H. (2018). South African Air Quality Information System (SAAQIS) mobile application tool: bringing real time state of air quality to South Africans. Department of Environmental Affairs, Pretoria. http://dx.doi.org/10.17159/2410-972X/2018/v28n1a1.

Harrison, R.M. and Yin, J. (2000). Particle matter in the atmosphere: which particle properties are important for its effects on health? Science of the Total Environment, **249**: 85–101.

Harvard Law School International Human Rights Clinic. (2016).The cost of gold: Environmental, health, and human rights consequences of Gold Mining in South Africa's West and Central Rand. Cambridge: Harvard College.

Hattingh, RP., Lake, J., Boer, RH., Aucamp, P. and Viljoen C. (2003). Rehabilitation of contaminated gold tailings dam footprints. WRC No 1001/1/03. Water Research Commission, Pretoria, South Africa.

Hattingh, J.M. and van Deventer P.W. (2004). The effect of the chemical properties of tailings and water application on the establishment of a vegetative cover on Gold Tailings Dam. Report WRC. Report No 899/1/04. Pretoria, RSA.

HB 436. (2004). Risk Management Guidelines, Companion to AS/NZS 4360:2004, Standards Australia.

Hnizdo, E. and Vallyathan, V. 2003. Chronic obstructive pulmonary disease due to occupational exposure to silica dust: a review of epidemiological and pathological evidence. Occup. Environ. Med. **60**: 237–243.

Hockings, P. (Ed.). (1995). Principles of visual anthropology. New York: Mouton de Gruyter.

Hoet, P.H.M., Bruske-Hohlfeld, I., and Salata, O.V. (2004). Nanoparticles – known and unknown health risks. Journal of Nanobiotechnology, **2** (12):15. DOI:10.1186/1477-3155-2-12.

Hnizdo E. (1994). Risk of silicosis in relation to fraction of respirable quartz. Am J Ind Med., **25** (5): 771–772. http://dx.doi.org/10.1002/ajim.4700250517.

Hnizdo, E. and Vallyathan, V. (2003). Chronic obstructive pulmonary disease due to occupational exposure to silica dust: a review of epidemiological and pathological evidence. Occup. Environ. Med., **60** (4): 237–243.

Hnizdo, E., Murray, J., Sluis-Cremer, G.K. and Thomas, R.G. (1993). Correlation between radiological and pathological diagnosis of silicosis: An autopsy population-based study. Am J Ind Med., **24** (4): 427–445. http://dx.doi.org/10.1002/ajim.4700240408.

Homer, P.M. and Kahle, L.R. (1988). A structural equation test of the value–attitude–behaviour hierarchy. J. Person. Soc. Psychol., **54**: 638–646.

Hu, X., Zhang, Y., Luo, J.U., Wang, T., Lian, H., and Ding, Z. (2011). Bioaccessibility and health risk of arsenic, mercury and other metals in urban street dusts from a mega-city, Nanjing, China. Environmental Pollution, **159**: 1215–1221.

Hu, X., Zhang, Y., Ding, Z., Wang, T., Lian, H., Sun, Y. and Wu, J. (2012). Bioaccessibility and health risk of arsenic and heavy metals (Cd, Co, Cr, Cu, Ni, Pb, Zn and Mn) in TSP and PM2.5 in Nanjing, China. Atmospheric Environment, **57**: 146–152.

Hull, R.B., Buhyoff, G.J. 1984. Individual and group reliability of landscape assessments. Landscape Planning, **11** (1): 67–71.

Hull, B., Buyhoff, G. and Cordell, H. (1987). Psychophysical models: An example with scenic beauty perceptions of roadside pine forests. Landscape Journal, **6** (2): 113–122.

Hull, R.B. and Revell, G.R.B. (1989). Issues in sampling landscapes for visual quality assessments. Landscape and Urban Planning, **17**, 323-330.

Hull, R.B. and Stewart, W.P. (1992). Validity of photo-based scenic beauty judgments. Journal of Environmental Psychology, **12**: 101-114.

Humby, T. (2013). 'Environmental Justice and Human Rights on the Mining Wastelands of the Witwatersrand Gold Fields', Revue generale de droit, University of Ottowa.

Institute for Health Metrics and Evaluation (IHME). Findings from the Global Burden of Disease Study (2017). Seattle, WA: IHME, 2018.

International Atomic Energy Agency (IAEA). (2012). Management of radioactive waste from the mining and mining of ores. International Atomic Energy Agency, Vienna.

International Council on Mining & Metals (ICMM), (2016). Review of Tailings Management Guidelines and Recommendations for Improvement.

International Agency for Research on Cancer (IARC). (2013). Outdoor air pollution a leading environmental cause of cancer deaths, Press release no 221, Lyon. www.iarc.fr/en/mediacentre/ iarcnews/pdf/pr221_E.pdf

Jaishankar, M.; Mathew, B.B.; Shah, M.S.; Murthy, K.T.P. and Gowda, S.K.R. (2014). Biosorption of few heavy metal ions using agricultural wastes. J. Environ. Pollut. Hum. Health, **2**: 1–6.

Jaishankar, M., Tseten, T., Anbalagan, N., Mathew, B.B., Krishnamurthy, N. and Beeregowda, K.N. (2014). Toxicity, mechanism and health effects of some heavy metals. Interdiscip Toxicol., **7** (2): 60–72. **doi:** 10.2478/intox-2014-0009.

Jan, A.J., Azam, M., Kehkashan, S.K., Ali, A., Choi, I., and Rizwanul H. Q.M. (2015). Heavy Metals and Human Health: Mechanistic Insight into Toxicity and Counter Defense System of Antioxidants. Int. J. Mol. Sci., **16**: 29592–29630; doi:10.3390/ijms161226183.

Kaltenborn, B.P. and Bjerke, T. (2002). Association between environmental value orientations and landscape preferences. Landscape and Urban Planning, **59**: 1–11.

Kaplan, R. (1985). The analysis of perception via preference: a strategy for studying how the environment is experienced. Landscape Planning, **12**: 161-176.

Kaplan, R. and Kaplan, S. (1989). The experience of nature, a psychological perspective. Cambridge University Press, Cambridge.

Kaltenborn B.P. and Bjerke T. (2002). Landscape and Urban Planning 59 (2002) 1–11.

Khumalo, T. (2017). State of Air Report and National Air Quality Indicator, presentation given at the 12th Air Quality Governance Lekgotla, 2-3 October 2017, Sandton.

Knight, D.H., Ehrlich, F.J. anfd Churchyard, G. (2013). The changing epidemiology of silicosis in South African gold mining - an industry wide study. University of Cape Town/ International SOS, Cape Town, South Africa; LSTMH, London, United Kingdom; Aurum Health Institute, Johannesburg, South Africa. Occup. Environ.Med. 10.1136/oemed-2013-101717.78.

Kneen, M.A., Ojelede, M.E. and Annegarn, H.J. (2015). Housing and population sprawl near tailings storage facilities in the Witwatersrand: 1952 to current. S. Afr. J. Sci. https:// doi.org/10.17159/sajs.2015/20140186.

Kootbodien, T., Iyaloo, S., Wilson, K., Naicker, N., Kgalamono, S., Haman, T., Mathee, A. and Rees, D. (2019). Environmental Silica Dust Exposure and Pulmonary Tuberculosis in Johannesburg, South Africa. Int. J. Environ. Res. Public Health, **2019** (16): 1867. https://doi.org/10.3390/ijerph16101867.

Koenig, J.Q. (2000). Health Effects of Ambient Air Pollution: How Safe is the Air we Breathe. Kluwer Academic Publishers.

Krause C.L. (2001). Our visual landscape Managing the landscape under special consideration of visual aspects.

Krause, R. D. and Snyman, L. G. (2014). Rehabilitation and mine closure liability: An assessment of the accountability of the system to communities. Johannesburg: Centre for Applied Legal Studies, University of Witwatersrand.Assessment of Methods for Determining Bioavailability of Trace Elements in Soils: A Review, Pedosphere, Volume 27, Issue 3, 2017, Pages 389-406, ISSN 1002-0160, https://doi.org/10.1016/S1002-0160(17)60337-0. (https://www.sciencedirect.com/science/article/pii/S1002016017603370).

Lacy, H. (2005). Closure and rehabilitation of tailings storage facilities, M Adams (ed.), Ch. 15, Developments in Minerals Processing, Elsevier.

Lacy, H. and Barnes, K. (2006). Tailings Storage Facilities; Decommissioning Planning is vital for successful closure. In Mine Closure 2006. Eds. Fourie and Tibbett. Center for Land Rehabilitation and Australian Centre for Geomechanics. Perth, Australia.

Lawyers for Human Rights. (2017). Blyvooruitzicht Mine Village: the human toll of state and corporate abdication of responsibility in South Africa. FIDH January 2017 / N° 687a.

Liebenberg-Enslin, H. (2014). A Functional Dependence Analysis of Wind Erosion Modelling System Parameters to Determine a Practical Approach for Wind Erosion Assessments. Ph.D. Thesis, University of Johannesburg, Johannesburg, South Africa, May 2014.

Liebenberg-Enslin, H. Air Quality Baseline Assessment for West Wits. (2014). Available online: https://www.airshed.co.za//Downloads/Publications/#Dispersion%20Modelling (accessed on 5 March 2019).

Liefferink, M. (2009). Comments on GDARD'S feasibility study on reclamation of mine residue areas for development purposes. The federation for a Sustainable Environment. South Africa.

Liefferink, M. (2011). Assessing the past and the present role of the National Nuclear Regulator as a public protector against potential health injuries: the West and Far West Rand as case study. New contree: Journal Of Historical And Human Sciences For Southern Africa **62**: 125-153.

Liefferink, M. and Liefferink, S.L. (2014). Current reclamation of historical uraniferous tailings dams and sand dumps–exacerbating the mess or minimizing the mining footprint? Case studies within the Witwatersrand goldfields. In: Merkel, JB, Alireza, A (eds) Uranium-past and future challenges, Freiberg: Springer, 387–400.

Liefferink, S. L. (2015). Determining attainable ecological quality requirements for the Upper Wonderfonteinspruit Catchment, based on human community requirements : the case of Bekkersdal. Retrieved 2 22, 2021, from https://repository.nwu.ac.za/handle/10394/15364.

Liefferink, M. (2019). 'Selected extracts from South Africa's environmental legislation: challenges with the management of gold tailings within the Witwatersrand gold fields and case studies', in AJC Paterson, AB Fourie & D Reid (eds), Proceedings of the 22nd International Conference on Paste, Thickened and Filtered Tailings, Australian Centre for Geomechanics, Perth: 53-67, https://doi.org/10.36487/ACG_rep/1910_0.04_Liefferink.

Lippmann, M. and Chen, L.C. (2009). Health effects of concentrated ambient air particulate matter (CAPs) and its components. Crit Rev Toxicol., **39**: 865–913.

Liu, J. and Lewis, G. (2014). 'Environmental toxicity and poor cognitive outcomes in children and adults', Journal of Environmental Health, **76**:130-138.

Lothian, A. (1999). Landscape and the philosophy of aesthetics: Is landscape quality inherent in the landscape or in the eye of the beholder? Landscape and Urban Planning, **44**(4), 177–198.

Lund, B.O., Miller, D.M. anfd Woods, J.S. (2017). Studies on mercury (II) induced H_2O_2 formation and oxidative stress in vivo and in vitro in rat kidney mitochondria. Biochem. Pharmacol., **45**: 2017–2024.

Madalane, T. (2012). The obligation to rehabilitate mining areas: post mining activities.

Makua, M. P. and Odeku, K.O. (2017). Harmful mining activities, environmental impacts and effects in the mining communities in South Africa: a critical perspective. Environmental Economics (open access), **8**(4): 14-24. doi:10.21511/ee.08(4).2017.02.

Malatse, M. and Ndlovu, S. (2015). The viability of using theWitwatersrand gold mine tailings for brickmaking. J. South. Afr. Inst. Min. Metall., **115** (4): 321–327.

Malta Environment and Planning Authority. (2004). Landscape assessment study of the Maltese Islands. Available from. http://www.mepa.org.mt/lpgstructureplanreview#Landscape Last Accessed 22.10.10.

Matooane, M., J. J., Ooisthuizen, R. and Binedel, M. (2004). Vulnerability of South African Communities to Air Pollution. CSIR, South Africa.

McConnell, R., Islam T., Shankardass, K. (2010). 'Childhood incident asthma and traffic-related air pollution at home and school', Environ Health Perspect., **118**:1021–6.

Maddison, D. (1997). A Meta-analysis of Air Pollution Epidemiological Studies, Centre for Social and Economic Research on the Global Environment, London, University College London and University of East Anglia.

Martins, J.J. (2014). A critical evaluation of the challenges facing dust management within gold mining regions of South Africa [MSc thesis]. Potchefstroom: North-West University.

Maseki, J. (2013). Risk assessment of inhaled and ingested airborne particles in the vicinity of gold mine tailings : case study of the Witwatersrand Basin. Retrieved 2 22, 2021, from https://ujdigispace.uj.ac.za/handle/10210/8693.

Maseki, J. (2017). Health risk posed by enriched heavy metals (As, Cd, and Cr) in airborne particles from Witwatersrand gold tailings. J. S. Afr. Inst. Min. Met., **117**: 663–669.

Maseki, J., Annegarn, H.J., and Spiers, G. (2017). Health risk posed by enriched heavy metals (As, Cd, and Cr) in airborne particles from Witwatersrand gold tailings. The journal of the Sothern African Institute of Mining and Metallurgy, **117.** http://dx.doi.org/10.17159/2411-9717/2017/v117n7a8.

Mathuthu, M., Kamunda, C., and Madhuku M.M. (2016). Modelling of Radiological Health Risks from Gold Mine Tailings in Wonderfonteinspruit Catchment Area, South Africa. Int J Environ Res Public Health, **13** (6): 570. Published online 2016 Jun 7. doi: 10.3390/ijerph13060570 PMCID: PMC4924027.

Kamunda, C.; Mathuthu, M. and Madhuku, M. (2016). Health Risk Assessment of Heavy Metals in Soils from Witwatersrand Gold Mining Basin, South Africa. Int. J. Environ. Res. Public Health, **13**: 663. https://doi.org/10.3390/ijerph13070663.

Kamunda, C. (2017). Human health risk assessment of environmental radionuclides and heavy metals around a gold mining area in Gauteng Province, South Africa. http://hdl.handle.net/10394/25382

Kamunda, C., Mathuthu, M. and Madhuku, M. (2017). Determination of Radon in Mine Dwellings of Gauteng Province of South Africa using AlphaGUARD Radon Professional Monitor. J Environ Toxicol Stud, **1**(1) doi http://dx.doi.org/10.16966/jets.107.

Marticorena, B. (2014) Dust Production Mechanisms. In: Knippertz P., Stuut JB. (eds) Mineral Dust. Springer, Dordrecht. https://doi.org/10.1007/978-94-017-8978-3_5.

Minerals Council of Australia. (1996). Tailings storage facilities at Australian gold mines, Submission to the Senate Environment, Recreation, Communication and the Arts References Committee, Canberra, Australia.

Ming-Ho, Y. (2005). Environmental Toxicology: Biological and Health Effects of Pollutants, Chap. 12, CRC Press LLC, ISBN 1-56670-670-2, 2nd Edition, Boca Raton, USA.

Mining Association of Canada. (2011). A Guide to the Management of Tailings Facilities, Second Edition.

Minnitt, R.C.A. (2014). Sampling in the South African minerals industry. School of Mining Engineering, University of the Witwatersrand, Johannesburg, South Africa. © The Southern African Institute of Mining and Metallurgy, ISSN 2225-6253.

Moeng, K. (2019). Community perceptions on the health risks of acid mine drainage: the environmental justice struggles of communities near mining fields. Environ Dev Sustain., **21,** 2619–2640. https://doi.org/10.1007/s10668-018-0149-4.

Mhlongo, S.E. and Amponsah-Dacosta F. (2016). A review of problems and solutions of abandoned mines in South Africa, International Journal of Mining, Reclamation and Environment, **30** (4): 279-294, DOI: 10.1080/17480930.2015.1044046.

Mhlongo, S.E., Amponsah-Dacosta, F. and Kadyamatimba, A. (2020). Appraisal of Strategies for Dealing with the Physical Hazards of Abandoned Surface Mine Excavations: A Case Study of Frankie and Nyala Mines in South Africa. Minerals, **10:** 145. https://doi.org/10.3390/min10020145.

Molnarova, K., Sklenicka, P., Stiborek, J., Svobodova, K., Salek, M. and Brabec, E. (2011). Visual preferences for wind turbines: Location, numbers and respondent characteristics. Applied Energy, **92**: 269–278.

Morakinyo, O.M., Adebowale, A.S., Mokgobu, M.I. (2010). Health risk of inhalation exposure to sub-10 µm particulate matter and gaseous pollutants in an urban-industrial area in South Africa: an ecological study BMJ Open, **7:** 13941. doi: 10.1136/bmjopen-2016-013941.

Moreno, M.E., Acosta-Saavedra, L.C., Meza-Figueroa, D., Vera, E., Cebrian, M.E., Ostrosky-Wegman, P. and Calderon-Aranda, E.S. (2010). Biomonitoring of metal in children living in a mine tailings zone in Southern Mexico: A pilot study. Int. J. Hyg. Environ. Health., **213**(4):252–258.

Morrison-Saunders, A., McHenry, M.P., Sequeira, A.R., Gorey, P., Mtegha H.and Doepel D. (2016). Integrating mine closure planning with environmental impact assessment: challenges and opportunities drawn from African and Australian practice, Impact Assessment and Project Appraisal, **34** (2): 117-128. DOI: 10.1080/14615517.2016.1176407 To link to this article: https://doi.org/10.1080/14615517.2016.1176407.

Mpanza, M. and Moolla, R. (2019). The assessment of the external costs of dust fallout in Blyvooruitzicht Gold Mining Village. In Proceedings of the VII National Association for Clean Air (NACA) Conference, Protea Hotel by Marriot|Stellenbosch|Technopark|Western Cape, Cape Town, South Africa, 3–4 October 2019; National Association of Clean Air: Centurion, South Africa; Pretoria, South Africa, 2019.

Nahar, S.N., Schmets, A.J.M. and Scarpas, A. (2015). Determining Trace-elements in Bitumen by Neutron Activation Analysis Naicker, K.; Cukrowska, E.; McCarthy, T. Acid mine drainage arising from gold mining activity in Johannesburg, South Africa and environs. Environ. Pollut., 122: 29–40.

Naicker, K., Cukrowska, E. and McCarthy, T.S. (2003). Acid mine drainage arising from gold mining activity in Johannesburg, South Africa and environs. Environ Pollut., **122**: 29–40.

National Cancer Institute, 'Definition of premature death -NCI Dictionary of Cancer Terms', https://www.cancer.gov/publications/dictionaries/cancer-terms/def/premature-death, accessed on 2018-07-06 15:38:38.

National Nuclear Regulator Act No 47 of 1999, viewed 26 March 2019.

National Nuclear Regulator. (2007). Radiological Impacts of the Mining Activities to the Public in the Wonderfontein Spruit Catchment Area, report TR-RRD-07-0006.

National Nuclear Regulator. (2015a), Remediation Criteria and Requirements, position paper 0018.

National Nuclear Regulator. (2015b), Plan for the Remediation of Contaminated Sites, report: PLN-SARA-15-012.

Nelson, G., (2013). Occupational respiratory diseases in the South African mining industry. Glob. Health Action 6, 19520. https://doi.org/10.3402/gha.v6i0.19520.

National institute of occupational safety and health (NIOSH). (1994). Manual of analytical methods. Method 7602, Silica Crystalline by IR.

Nkosi, V., Wichmann, J. and Voyi, K. (2015). Mine dumps, wheeze, asthma, and rhinoconjunctivitis among adolescents in South Africa: any association? International Journal of Environmental Health Research, **25** (6): 583-600. DOI: 10.1080/09603123.2014.989493.

Nkosi, V., Wichmann, J. and Voyi, K. (2015). Acute respiratory health effects of air pollution on asthmatic adolescents residing in a community in close proximity to-mine dump in South Africa: Panel study. International Research Journal of Public and Environmental Health, **3** (11): 257-269, November 2016 Available online at http://www.journalissues.org/IRJPEH/ http://dx.doi.org/10.15739/irjpeh.16.032.

Nkosi, V., Wichmann, J. and Voyi, K. (2015). Chronic respiratory disease among the elderly in South Africa: any association with proximity to mine dumps?. Environ Health **14:** 33. https://doi.org/10.1186/s12940-015-0018-7.

Nkosi V. (2015). Association between mine dumps and health impacts.

Nkosi, V. and Kuku Voyi K. (2016). Reliability of an adult respiratory symptom questionnaire in a community located near a mine dump in South Africa: pilot study,

Southern African Journal of Infectious Diseases, **31**: (3): 103-105, DOI: 10.1080/23120053.2016.1156318.

Ngole-Jeme, V.M. and Fankte, P. (2017). Ecological and human health risks associated with abandoned gold mine tailings contaminated soil. PLoS ONE 12(2): e0172517. doi: 1371/journal.

Norris, G., Young-Pong, S.N., Koenig J.Q., Larson, T. V., Sheppard, L. and Stout, J.W. 1999. An association between fine particles and asthma emergency department visits for children in Seattle. Environ. Health. Perspect., **107** (6):489–493.

Oberholzer, B. (1994). Visual and Aesthetic Assessment Techniques in Integrated Environmental Management. Unpublished paper for CSIR workshop.

Oberholzer, B. (1998). Visual Guidelines for Communication Masts. Unpublished report for Cape Metropolitan Council.

Oberholzer, B. (2005). Guideline for involving visual & aesthetic specialists in EIA processes:
Edition 1. CSIR Report No ENV-S-C 2005 053 F. Republic of South Africa, Provincial Government of the Western Cape, Department of Environmental Affairs & Development Planning, Cape Town.

Ode, A., Fry, G, Tveit, M.S., Messager, P. and Miller, D. (2008). Indicators of perceived naturalness as drivers of landscape preference. Journal of Environmental Management, **90**: 375-383.

Ode, A., Tveit, M. S., and Fry, G. (2008). Capturing landscape visual character using indicators: touching base with landscape aesthetic theory. Landscape Research,**33** (1): 89-117.

Okereafor U., Makhatha E., Mekuto L. and Mavumengwana V. (2019). Dataset on assessment of pollution level of selected trace metals in farming area within the proximity of a gold mine dump, Ekurhuleni, South Africa.

Ojelede, M.E., Annegarn, H.J. and Kneen, M.A. (2012). Evaluation of aeolian emissions from gold mine tailings on the Witwatersrand. Aeolian Res., **3** (4): 477–486. http:// dx.doi.org/10.1016/j.aeolia.2011.03.010.

Oelofse, S.H.H.; Cobbing, J. and Hobbs, P. (2014). The Pollution and Destruction Threat of Gold MiningWaste on the Witwatersrand—A West Rand Case Study. Available online: http://www.anthonyturton.com/assets/my_documents/my_files/983_SWEMP.pdf (accessed on 3 April 2019).

Ojelede, M.E. (2012). Risk assessment of atmospheric emissions from gold mine tailings on the Witwatersrand. PhD thesis, University of Johannesburg,South Africa.

Olalde, M. (2015). The haunting legacy of South Africa's gold mines. Yale Environment 360. http://e360.yale.edu/features/the_haunting_legacy_of_south_africas_gold_mines. Accessed 13 April 2016.

Oguntoke, O., Ojelede, M.E. and Annegarn, H.J. (2013). Frequency of mine dust episodes and the influence of meteorological parameters on the Witwatersrand area, South Africa. Int J Atmos Sci., **3** (4): 602–611. http://dx.doi.org/10.1155/2013/128463.

Ogwuegbu, M.O. and Ijioma, M.A. (2003). Effects Of Certain Heavy Metals On The Population Due To Mineral Exploitation. In: International Conference on Scientific and Environmental Issues In The Population, Environment and Sustainable Development in Nigeria, University of Ado Ekiti, Ekiti State, Nigerian, 8-10.

Oguntoke, O. and Annegarn, H.J. (2014). Effectiveness of mediation in the resolution of environmental complaints against the activities of gold mining industries in the Witwatersrand region. Clean Air J., **24** (2): 17–23.

Oosthuizen, M.A., John, J. and Somerset, V. (2010). Mercury exposure in a low income community in South Africa. South Africa Medical Journal, **100**: 366-371.

Oosthuizen, M. Wright, C.Y., Matooane,M. and Phala, N. (2015). Human health risk assessment of airborne metals to a potentially exposed community: a screening exercise. Clean Air J., **25** (1): 51–57.

Öhlander, B., Müller, B., Axelsson, M. and Alakangas, L. (2007). An attempt to use LA-ICP-SMS to quantify enrichment of trace elements on pyrite surfaces in oxidizing mine tailings. J. Geochem. Explor., **92**: 1–12.

Orland, B., Weidemann, E., Larsen, L. and Radja, P. (1995). Exploring the relationship between visual complexity and perceived beauty. Imaging Systems Laboratory, Department of Landscape Architecture, University of Illinois at Urbana-Champaign. Internet page: http://imlab9.landarch.uiuc.edu/projects/compleximages/complexity.html.

Oriyomi O., Oluwayemi O., Muideen G., Adejoke O. and Oluwaseun. A. (2016). Chemical speciation of some heavy metals and human health risk assessment in soil around two municipal dumpsites in Sagamu, Ugun State, Nigeria, Chemical Speciation & Bioavailability, **28** (1-4): 142-151.

Pacyna, EG, Pacyna, J.M. and Steenhuisen, F. (2006). Global anthropogenic mercury emission inventory for 2000. Atm Env., **40**: 4048–4063.

Pacyna, E. G., Pacyna, J. M., Sundseth, K. Munthe, J. Kindbom, K., Wilson, S., Steenhuisen, F. and Maxson, P. (2010). Norwegian Institute for Air Research, 2027 Kjeller, NorwayGlobal emission of mercury to the atmosphere from anthropogenic sources in 2005 and projections to 2020. Atmospheric environment, **44**, (20): 2487-2499.

Palmer, J.F. (1983). Visual Quality and Visual Impact Assessment. In Social Impact Assessment Methods (eds. Finsterbusch, K., Llewellyn, L.G. and Wolf, C.P.), Chapter 13: 268-283, Sage Publications.

Palmer, J. F. (2004). Using spatial metrics to predict scenic perception in a changing landscape: Dennis, Massachusetts. Landscape and Urban Planning, **69** (2-3), 201-218.

Palmer, J.F. (2004). Using spatial metrics to predict scenic perception in a changing landscape: Dennis, Massachusetts. Landscape and Urban Planning, **69**: 201-218.

Palmer, J.F. and Hoffman, R.E. (2001). Rating reliability and representation validity in scenic landscape assessment. Landscape and Urban Planning, **54**, 149-161.

Paschoa, A.S., Wrenn, M.E., Jones, K., Cholewa, M. and Carvalho, S.M. (1984). Elemental Composition of Airborne Particulates in Uranium Mining and Milling Operations, 8th Conference on the Application of Accelerators in Research and Industry; Brookhaven National Lab.: Upton, NY, USA, 1984.

Penning-Rowsell, E.C. (1982). A public preference evaluation of landscape quality. Regional Studies, **16**: 97-112.

Perko, T., Adam, B. and Stassen, K.R. (2015). The differences in perception of radiological risks: lay people versus new and experienced employees in the nuclear sector, Journal of Risk Research,**18**:1,40-54.

Phillips, A. (2005). Landscape as a meeting ground: Category V protected landscapes/seascapes and world heritage cultural landscapes. In J. Brown, M. Beresford, & N. Mitchell (Eds.), The protected landscape approach: Linking nature, culture and community (19-36). Gland: Island Press.

Phillips, A. (2011). Applying a mathematical model of sustainability to the rapid impact assessment matrix evaluation of the coal mining tailings dumps in the Jiului Valley, Romania.

Phillips, C.O. (2011). Radiological Status of Tudor Shaft Informal Settlement. Letter to the Mogale City Local Municipality, 18 January 2011: 1.

Piketh, S., Annegarn, H., and Tyson, P. (1999). 'Lower tropospheric aerosol loadings over South Africa: The relative contribution of aeolian dust, industrial emissions, and biomass burning', J. Geophys. Res.-Atmos., **104**: 1597–1607.

Pope III, C.A. and Dockery, D. W. (2006). Health effects of fine particulate air pollution: lines that connect. Journal of Air and Waste Management Association, **56**: 709–742.

Popescu, F. (2009). Ambient air quality measurements in Timisoara. Current situation and perspectives, Journal of Environmental Protection and Ecology, **10** (1).

Popescu, F. and Ionel, I. (2010). Anthropogenic Air Pollution Sources, Air Quality, Ashok Kumar (Ed.), ISBN: 978-953-307-131-2, InTech, Available from: http://www.intechopen.com/books/airquality/anthropogenic-air-pollution-sources.

Prosser, J. (1998). Image-based research: A sourcebook for qualitative researchers. London: Falmer.

Poswa, T.T. and Davies, T.C. (2017). The Nature and Articulation of Ethical Codes on Tailings Management in South Africa. Geosciences, 7: 101. https://doi.org/10.3390/geosciences7040101.

Pukkala, T., Kellomäki, S. and Mustonen, E. (1988). Prediction of the amenity of a tree stand. Scandinavian Journal of Forest Research, **3**: 533–544.

Rademeyer, B., Wates, J.A., Bezuidenhout, N., Jones, G.A., Rust, E., Lorentz, S., van Deventer, P.W, Pulles, W. and Hattingh,J. M. (2006). A preliminary decision support system for the sustainable design, operation and closure of metalliferous mine residue disposal facilities. WRC Project No. 15551/1/06. Water Research Commission, Pretoria, RSA.

Rapant, S., Dietzová, Z. and Cicmanová, S. (2006). Environmental and health risk assessment in abandoned mining area, Zlata Idka, Slovakia. Environ. Earth Sci., **51**:, 387–397.

Ramos, B. and Panagopoulos, T. (2004). The use of GIS in visual landscape management and visual impact assessment of a quarry in Portugal. Proceedings of the 8th International conference on Environment and Mineral processing. Ostrava, Tzech Republic, **1**: 73-78.

Ribe, R.G. (1989). The aesthetics of forestry: what has empirical preference research taught us? Environmental Management **13**: 55–74.

Rice M.B., Ljungman P.L., Wilker E.H. et al., (2015). 'Long-term exposure to traffic emissions and fine particulate matter and lung function decline in the Framingham heart study', Am J. Respir Crit Care Med, **191**: 656–64.

Robb, L.J. and Meyer, F.M. (1995). The Witwatersrand basin, South Africa, geological framework and mineralization processes. Ore Geology Reviews, **10** (2): 67–94.

Rösner, T. (2001). A preliminary assessment of pollution contained in the unsaturated and saturated zone beneath reclaimed gold-mine residue deposits. Report no. 797/1/01. Pretoria: Water Research Commission.

Rösner, T., Boer, R., Reyneke, R., Aucamp, P. and Vermaark, J. (2001). A preliminary assessment of pollution contained in the unsaturated and saturated zone beneath reclaimed gold-mine residue deposits, Water Research Commission, report no. 797/1/01.

Rossouw, A., Furniss, D.G., Annegarn, H.J., Weiersbye, I.M., Ndolo, U., Cooper, M. (2009). Evaluation of a 20–40-year-old mine tailings rehabilitation project on the Witwatersrand, South Africa. Proceedings of the Fourth International Conference on Mine Closure, Mine Closure.

Roth, M. and Gruehn, D. (2016). Visual Landscape Assessment for large areas — using GIS, internet surveys and statistical methodologies in participatory landscape planning for the Federal State of Mecklenburg-Western Pomerania, Germany Royal College of Physicians (RCP), 2016, Every breath we take: The lifelong impact of air pollution, Report of a working party, London.

Rundell, K.W., Hoffman J.R., Caviston, R., et al. (2007). Inhalation of ultrafine and fine particulate matter disrupts systemic vascular function. Inhal Toxicol., **19**: 133–40.

Sardar, K., Ali, S., Hameed, S., Afzal, S., Samar, F. S., Shakoor, M.B., Bharwana, S.A. and Tauqeer, H.M. (2013). Heavy Metals Contamination and what are the Impacts on Living Organisms, 2013. Greener Journal of Environmental Management and Public Safety, **2** (4): 172-179.

Satarug, S.; Garrett, S.H.; Sens, M.A. and Sens, D.A. (2011). Cadmium, environmental exposure, and health outcomes. Cienc. Saude Coletiva, **16**: 2587–2602.

Schimmer, C. and van Deventer, P.W. (2018). Baseline status of microbial activity on gold tailings facilities in South Africa, Applied Soil Ecology, Volume 123, 2018, Pages 355-374, ISSN 0929-1393, https://doi.org/10.1016/j.apsoil.2017.10.020.

Schnell, I., Potchter, O, Yaakov, Y. et al. (2016). Human exposure to environmental health concern by types of urban environment: the case of Tel Aviv.Environ Pollut., **208**: 58–65

Schnelle, K.B. and Brown, C.A. (2002). Air pollution control technology handbook, CRC Press, ISBN 0-8493-9588-7, Boca Raton. Florida

Schrader, A. and Winde, F. (2015). Unearthing a hidden treasure: 60 years of karst research in the Far West Rand, South Africa. South African Journal of Science, **111**: 1-7.

Schroeder, H. and Daniel, T. (1981). Progress in predicting the perceived scenic beauty of forest landscapes. Forest Science, **27** (1): 71–80.

Scott, M.J. and Canter, D.V. (1997). Picture or place? A multiple sorting study of landscape. Journal of Environmental Psychology, **17**: 263-281.

Schofield, S.J., Winde F., Albrecht C., Kielkowski D., Liefferink, M. et al. (2014). Health effects in populations living around uraniferous gold mine tailings in South Africa: Gaps and opportunities for research. Cancer Epidemiology; New York, **38**, (5): 628-32.

Seiderer, T., Venter, A., Van Wyk, F., Levanets, A. and Jordaan, A. (2017). Growth of soil algae and cyanobacteria on gold mine tailings material. S. Afr. J. Sci., **113** (11/12), Art. #2016-0384, 6 pages. http://dx.doi.org/10.17159/ sajs.2017/20160384.

Sharma, V., and Padma Singh.P. (2015). Heavy Metals Pollution and its Effect on Environment and Human Health. International Journal of Recent Scientific Research, **6** (12): 7752-7755.

Shafer, E.L. and Richards, T.A. (1974). A Comparison of Viewer Reactions to Outdoor Scenes and Photographs of Those Scenes. USDA Forest Service Research Paper NE-302. Northeastern Forest Experimental Station, Upper Darby, PA.

Shafer, E.L., Hamilton, Jr., J.F. and Schmidt, E.A. (1969). Natural landscape preferences: a predictive model. Journal of Leisure Research, **1**: 1-19.

Shafer, E.L. and Tooby, M. (1973). Landscape preferences: an international replication. Journal of Leisure Research, **5**, 60-65.

Shirinde J, Wichmann J, Voyi K. (2014). Association between wheeze and selected air pollution sources in an air pollution priority area in South Africa: a cross-sectional study. Environ Health., **13**:1–12.

Shuttleworth, S. (1980a). The use of photographs as an environment presentation medium in landscape studies. Journal of Environmental Management, 61-76.

Shuttleworth, S. (1980b). The Evaluation of Landscape Quality. Landscape Research, **5**, 14 - 20.

Sim˜oes M.R., Fiorim J., de Batista P.R, Fioresi M., Rossoni L., Stefanon I., Alonso M.J., Salaices M., and Vassallo D.V. (2012). Toxic Effects of Mercury on the Cardiovascular and Central Nervous Systems. Hindawi Publishing Corporation Journal of Biomedicine and Biotechnology, **2012**: 1-11.

Smith, K.R., Bruce, N. et al. (2014). 'Millions dead: How do we know and what does it mean? Methods used in the comparative risk assessment of household air pollution', Annual Review of Public Health, **35**:185-206.

Smith, K.S. and Huyck, H.L.O. (1999). An overview of the abundance, relative mobility, bioavailability, and human toxicity of metals. Reviews in Economic Geology, Volumes 6A and 6B. The Environmental Geochemistry of Mineral Deposits Part A: Processes, Techniques, and Health Issues Part B: Case Studies and Research Topics published by the Society of Economic Geologists, Inc. (SEG) 1999 Www.segweb.org/store/SearchResults.aspx?Category=REV06-PDF_Stamps AE. 1999. Demographic effects in environmental aesthetics: A meta-analysis. Journal of Planning Literature, **14**:125–175.

Soriano A., S. Pallarés S., Pardo F., Vicente A. B., Sanfeliu T., and J. Bech J., "Deposition of heavy metals from particulate settleable matter in soils of an industrialised area," Journal of Geochemical Exploration, **113**: 36–44.

South Africa. (1996). The Constitution of the Republic of South Africa. Pretoria: Government Printer.

South Africa. (1998). National Environmental Management (Act 107 of 1998). Government gazette. 19519. 27 November 1998. Pretoria: Government Printer.

South Africa. (2002). Mineral and Petroleum Resources Development (Act 28 of 2002). Government gazette. 26254. 10 October 2002. Pretoria: Government Printer.

South Africa. (2004). Mineral and Petroleum Resources Development Regulations. 2004. Government gazette. 26275. 23 April 2004. General notice no. R527. Pretoria: Government Printer.

South Africa. (2013). Mineral and Petroleum Resources Development Amendment Bill. 2013. Government Gazette. 36523. 31 May 2013. Pretoria: Government Printer.

Statistics South Africa. http://www.statssa.gov.za/ (accessed 5 May 2018).

Sutton, M.W, Weiersbye, I.M., Galpin, J.S. and Heller, D. (2006). A GIS-Based History of Gold Mine Residue Deposits and Risk Assessment of Post-Mining Land-Uses on the Witwatersrand Basin, South Africa. Mine Closure 2006 – Andy Fourie and Mark Tibbett (eds) © 2006 Australian Centre for Geomechanics, Perth, ISBN 0-9756756-6-4.

Sutton, M.W. and Weiersbye, I.M. (2007). South African legislation pertinent to gold mine closure and residual risk. In: A.B. Fourie, M. Tibbett and J. Wiertz (eds), Mine

Closure 2007, Proceedings of the 2nd International Mine Closure Seminar, Santiago. pp. 89–102

Sutton, M.W. and Weiersbye, I.M. (2008). Land use after mine closure – risk assessment of gold and uranium mine residue deposits on the Eastern Witwatersrand, South Africa. In: Fourie, AB, Tibbett, M, Weiersbye, IM, Dye, PJ (eds) Proceeding of the Third International Conference on Mine Closure, Mine closure, 14–17 October 2008, Johannesburg, South Africa. Perth: Australian Centre for Geomechanics. 363–373.

Statistics South Africa (StatsSA). (2014). Mortality and causes of death in South Africa: Findings from death notification, Statistical release P0309.3, Statistics South Africa, Pretoria

Stovern, M., Felix, O., Csavina, J., Rine, K.P., Russell, M.R., Jones, R.M., et al. (2014). Simulation of windblown dust transport from a mine tailings impoundment using a computational fluid dynamics model. Aeolian Res., **14** (1):1–10.

Svobodova, K., Sklenicka, P., Molnarova, K. and Salek, M. (2011). Visual preferences for physical attributes of mining and post-mining landscapes with respect to the sociodemographic characteristics of respondents. Ecological Engineering, **43**: 34– 44.

Tahvanainen, L., Tyrväinen, L., Ihalainen, M., Vuorela, N. and Kolehmainen, O. (2001). Forest management and public perceptions – visual versus verbal information. Landscape and Urban Planning, **53**: 53–70.

Tahvanainen, L., Tyrväinen, L. and Nousiainen, I. (1996). Effect of afforestation on the scenic value of rural landscape. Scandinavian Journal of Forest Research, **11**: 397–405.

Terradellas, E., Slobodan Nickovic S., and Xiao-Ye Zhang, X. (2015). Airborne Dust: A Hazard to Human Health, Environment and Society.

The World Bank. (2016). Armenia: Strategic Mineral Sector Sustainability Assessment. 106237.

Theunissen, N.H. and van Deventer, P.W. (2001). Rehabilitation on gold slimes dams: Quo vadis. Conference on environmentally responsible mining in South Africa. Chamber of mines of SA. **1**. Johannesburg.

Thienpont, J.R., Korosi, J.B., Hargan, K.E., Williams, T., Eickmeyer, D.C., Kimpe, L.E., Palmer, M.J., Smol, J.P. and Blais, J.M. (2016). Multitrophic level response to extreme metal contamination from gold mining in a subarctic lake. Proc. R. Soc. B 283: 20161125. http://dx.doi.org/10.1098/rspb.2016.1125.

Thomas, N., Calderón, L., Senick, J., et al. (2019). Application of Three Different Data Streams to Study Building Deficiencies, Indoor Air Quality, and Residents' Health, **154** Rutgers University: 281-295.

Tlotleng, N., Kootbodien, T., Wilson, K., Made, F., Mathee, A., Ntlebi, V., Kgalamono, S., Mokone, M., Du Preez, K. and Naicker, N. (2019). Prevalence of Respiratory Health Symptoms among Landfill Waste Recyclers in the City of Johannesburg, South Africa. Int. J. Environ. Res. Public Health, **16**: 4277.

Tsiouri, V., Kakosimos, K.E., and Kumar, P. (2014). Concentrations, sources and exposure risks associated with particulate matter in the Middle East Area - a review. Air Qual Atmos Health, **8**: 67–80.

Turšiˇc, J.; Radi´c, H.; Kovaˇceviˇc, M.; Veber, M. (2008). Determination of Selected Trace Elements in Airborne Aerosol Particles Using Different Sample Preparation. Arch. Ind. Hyg. Toxicol., **59**, 111–116.

Turton, A. (2008a). High Confidence Study of Children Potentially Affected by Radionuclide and Heavy Metal Contamination Arising from the Legacy of Mine Water Management Practices on the Far West Rand of South Africa. Short Title – Tooth Fairy Project. Council for Scientific and Industrial Research, 1-20.

Turton, A. (2008b). Water and Mine Closure in South Africa: Development that is sustainable? On-Line Development 2008 'Water and Development'. www.sidint.org.

Tutu, H., McCarthy, T. and Cukrowska, E. (2008). The chemical characteristics of acid mine drainage with particular reference to sources, distribution and remediation: The Witwatersrand Basin, South Africa as a case study. Appl. Geochem., **23**: 3666–3684.

Tveit, M., Ode, A. and Fry, G. (2006). Key concepts in a framework for analysing visual landscape character. Landscape Research, **31**: 229-255.

Tyrväinen, L., Silvennoinen H. and Kolehmainen, O. (2003). Ecological and aesthetic values in urban forest management. Urban For. Urban Green. **1**: 135–149

Ulrich, R.S., 1979. Visual landscapes and psychological well-being. Landscape Research, **4**, 14-23.

Ulrich, R.S. (1986). Human responses to vegetation and landscapes. Landscape and Urban Planning, **13**: 29-44.

Ulrich, R.S. (1993). Biophilia, biophobia, and natural landscapes. In: Kellert, S.R., Wilson, E.O. (Eds.), The Biophilia Hypothesis. Island Press, Washington, DC, 73–137.

Ulrich, R.S., Simons, R.F., Losito, B.D., Fiorito, E., Miles, M.A. and Zelson, M. (1991). Stress recovery during exposure to natural and urban environments. J. Environ. Psychol., **11**: 201–230.

United States. (2013). Abandoned mine lands. Bureau of Land Management http://www.abandonedmines.gov/ep.html. Accessed on 22 Nov 2013.

United States EPA. (2009). United States Environmental Protection Agency, Air Emission Sources, November 04, 2009, http://www.epa.gov/air/emissions/index.htm, 2009. www.intechopen.

United States Environmental Protection Agency. (2009). Risk Assessment Guidance for Superfund Volume I: Human Health Evaluation Manual (Part F, Supplemental Guidance for Inhalation Risk Assessment).

United States Environmental Protection Agency. (2011). Exposure Factors Handbook. 2011 Edition (Final). U.S. Environmental Protection Agency, Washington, DC (EPA/600/R- 09/052F).

US EPA. (2011a). Exposure factors handbook (final edition). United States Environmental Protection Agency, Washington, DC. EPA/600/R-09/052F. https://cfpub.epa.gov/ncea/risk/recordisplay.cfm?deid=236252 [Accessed 29 August 2016].

US EPA. (2011b). Risk assessment guidance for superfund. Part A: Human health evaluation manual; Part F, Supplemental guidance for inhalation risk assessment, vol. I. United States Environmental Protection Agency, Washington, DC. https://www.epa.gov/risk/risk-assessment-guidancesuperfund-rags-part-f [Accessed19 July 2017].

US Environmental Protection Agency. (2017). Soil and Dust Ingestion, Update for Chapter 5 of the Exposure Factors Handbook. National Center for Environmental Assessment. EPA/600/R-17/384F September 2017.

Utembe, W., Faustman, E.M., Matatiele, P. and Gulumian, M. (2015). Hazards identified and the need for health risk assessment in the South African mining industry. Hum Exp Toxicol., **34** (12): 1212-1221

Unwin, K.I. (1975). The relationship of observer and landscape in landscape evaluation. In Transactions of the Institue of British Geographers, **66**: 130-133.

Van Blerk, J.J. (2002). Analysis of a post-closure safety assessment methodology for radioactive waste disposal systems in South Africa.

Van den Berg, A.E., Vlek, C.A. and Coeterier, J.F. (1998). Group differences in the aesthetic evaluation of nature development plans: A multilevel approach. Journal of Environmental Psychology, **18**: 141–157.

Van Deventer, P.W., Hattingh, J.M. and van Wyk, S.J. (2004). Soil quality parameters and specifications for sustainable rehabilitation of mine waste. 3rd International mining and Industrial Waste Conference. Johannesburg, South Africa.

Van Deventer, P.W. (2006). An all-Inclusive approach to mine tailings Rehabilitation, Southern African institute of Mining and Metallurgy, Conference, Johannesburg, South Africa.

Van Deventer, P.W., Hattingh, J.M. and Bloem, A.A. (2008). Some Rehabilitation issues on Witwatersrand gold Tailings Dams. 4th IMIWM Conference 2008 – Proceedings – Rustenburg, South Africa.

Van Deventer, P.W. (2009). Holistic approach for rehabilitation and mine closure. Report and lecture notes. North West University, Potchefstroom, South Africa.

Viljoen, M. (2009). The life, death and revival of the central Rand Goldfields. World Gold Conference 2009, The Southern African Institute of Mining and Metallurgy.

Wade, G. (1982). The relationship between landscape preference and looking time: a methodological investigation. Journal of Leisure Research, 14, 217-222.

Wade, P.W. and Van Tonder, D.M. (2006). Sustainable Development through mining. Regional Closure Strategy for the KOSH Goldfield. Council for Geoscience.

West Rand District Municipality. (2011). Emission Inventory for 2011. Report No. uMN014-12.

West Rand District Municipality: Air Quality Management By-Laws No. 147 Provincial Gazette Extraordinary, 31 May 2012.

West Rand District Health Council Area (WRDCA) Health Care Plan 2018/2019-2020/2021.

West Rand District Municipality. Integrated Development Plan (IDP) 2016/17 to 2020/21.

Williams, D.R. (1995). Mapping Place Meanings for Ecosystem Management. A Technical Report Submitted to the Interior River Basin Ecosystem Management Project, USDA Forest Service, Washington.

Williams, D.R., Patterson, M.E., Roggenbuck, J.W. (1992). Beyond the commodity metaphor: examining emotional and symbolic attachment to place. Leisure Sci. 14, 29–46.

Williams, D.J. (2005). Placing covers on soft tailings, chap. 17, B. Indraratna and J. Chu (eds.) Ground Improvement — Case Histories, Elsevier. 491–512.

Williams, D.J. (2002). Engineering closure of an open pit gold operation in a semi-arid climate, International Journal of Surface Mining and Reclamation, Special Edition on Mining and the Environment, 35–50.

Williams, D.A. and Jones, H. (2005). Tailings storage facilities. Developments in Mineral Processing,**15**: 729–751.

Willis, K.G. and Garrod, G.D. (1993). Valuing Landscape: a Contingent Valuation Approach. Journal of Environmental Management, **37**: 1-22.

Wichmann, J., Wolvaardt, J.E., Maritz, C. and Voyi, K.V.V. (2007). Household conditions, eczema symptoms and rhinitis symptoms: relationship with wheeze and severe wheeze in adolescents living in the Polokwane Area, South Africa. J Asthma, **44**: 659–666.

Winde, F. (2010). Uranium pollution of the Wonderfonteinspruit, 1997-2008 Part 2: Uranium in water - concentrations, loads, and associated risks. Water SA, **36** (3): 257-278.

Winde, F., Stoch, E.J., Erasmus, E. and Schrader, A. (2011). Desktop Assessment of the Risk for Basement Structures of Buildings of Standard Bank and ABSA in Central Johannesburg to be Affected by Rising Mine Water Levels in the Central Basin, final report, volumes I-III, submitted by Mine Water Research Group, North West University, Potchefstroom Campus, 267.

Winde F. (2013). Uranium pollution of water – a global perspective on the situation in South Africa. Inaugural lecture. February 2013 ISBN 978-1-86822-629-0.

Winde, F. and Erasmus, E. (2015). Assessing risks associated with the flooding of mine voids on underground infrastructure and water resources in and around Johannesburg (South Africa). https://link.springer.com/chapter/10.1007/978-3-319-11059-2_24.

World Commission on Dams. (2000). Dams and Development: A New Framework for Decision Making.

World Health Organization (WHO). (2000). Addressing the Links Between Indoor Air Pollution, Household Energy and Human Health. Based on the WHO-USAID Global Consultation on the Health Impact of Indoor Air Pollution and Household Energy in Developing Countries (Meeting Report).

World Health Organization (WHO). (2000). Guidelines for air quality, World Health Organisation, Geneva.

World Health Organisation (WHO). (2013). Review of Evidence on Health Aspects of Air Pollution – REVIHAAP Project, World Health Organisation, Bonn, www.euro.eho.int/_data/assets/ pdf_file/0004/193108/REVIHAAP-Final-technical-report-finalversion. pdf/.

World Health Organisation (WHO). (2016), Ambient air pollution: a global assessment of exposure and burden of disease, World Health Organisation, Geneva.

Wright, K. B. (2005). Researching Internet-based populations: advantages and disadvantages of online survey research, online questionnaire authoring software packages, and Web survey services. Journal of Computer-Mediated Communication, **10** (3): 260-272.

Wright, C., Matooane, M., Oosthuizen, M.A., Phala, N. (2014). Risk perceptions of dust and its impacts among communities living in a mining area of the Witwatersrand, South Africa. Clean Air J., **24** (1): 22–27.

Yalala, B. N. (2015). Characterization, bioavailability and health risk assessment of mercury in dust impacted by gold mining. Retrieved 2 22, 2021, from http://wiredspace.wits.ac.za/handle/10539/20168.

Yu, K. (1995). Cultural variations in landscape preference: comparisons among Chinese sub-groups and Western design experts. Lands. Urban Plann., **32**: 107–126.

Zuckermann, M., Ulrich, R.S. and McLaughlin, J. (1993). Sensation seeking and reactions to nature paintings. Person. Ind. Differ., **15**: 563–576.

Zube, E.H., Brush, R.O., Fabos, J.G. (Eds.). (1975). Landscape Assessment: Values, Perceptions, and Resources. Dowden, Hutchinson and Ross, Stroudsburg, PA.

Zube, E.H., Sell, J.L. and Taylor, J.G. (1982). Landscape perception: research application and theory. Lands. Plann., **9:** 1–33.

Zube, EH**.** (1984). Themes in landscape assessment theory. Landscape Journal, **3**: 104–109.

Zube, E.H., Pitt, D.G. and Evans, G.W. (1983). A lifespan developmental study of landscape assessment. J. Environ. Psychol., **3**: 115–128.

Zube, E.H., Simcox, D.E. and Law, C.S. (1987). Perceptual Landscape Simulations: History and Prospects. Landscape Journal, **6** (1): 62–80.